66th Annual Technical Conference & Exposition

St. Louis, Missouri

The Investment Casting Institute would like to thank the following companies who have sponsored the

66th Technical Conference & Exposition

GATEWAY TO THE FUTURE

thank you

AUTOWAX INCORPORATED

AUTOWAX INC.

AUTOMATED WAXROOM TECHNOLOGIES GROUP

Cronimet Specialty Metals USA, Inc.

paramelt

experience. performance.

AVALON

PMI PRECISION METALSMITHS

WHERE THE FUTURE IS TAKING SHAPE

Autowax, Inc. Booth 322

Cronimet Specialty Metals USA, Inc. Booth 231

Paramelt Booth 212

The Investment Casting Institute would like to thank the following companies who have cast the awards for the

66th Technical Conference & Exposition.

ARISTO CAST
INVESTMENT CASTING

Artcast inc

Aristo-Cast, Inc.
7400 Research Drive
Almont, MI 48003
USA
ph. (810) 798-2900
fax (810) 798-2730
www.aristo-cast.com

Artcast, Inc.
14 Armstrong Avenue
Georgetown, Ontario L7G 4R9
CANADA
ph. (905) 877-5455
fax (905) 877-0205
www.artcast.com

The Investment Casting Institute would like to thank the following Member companies for their educational support and promotion of the industry. Two scholarships are being offered in honor of the following individuals:

Larry Blum of Aristo-Cast

Hank and Laurie Harvey

The Investment Casting Institute would like to thank the following individuals who ran for the 2019 Board of Directors election.

Thank you to the following candidates listed below who have been nominated to fill the Regular Member openings on the Board of Directors:

Russell Gallagher
Bescast, Inc.

Sonny Tran
Fenico Precision Castings, Inc.

Thank you to the following candidates listed below who have been nominated to fill the Affiliate Member opening on the Board of Directors:

Bill Fricker
Paramelt

Julie Markee
Key Process Innovations

Keith Orlebeck
Intrepid Automation

The Investment Casting Institute would like to thank the following advertisers who have placed ads in INCAST Magazine and INCAST News.

Thank YOU FOR YOUR SUPPORT

Air & Energy Systems, Inc.
Ajax TOCCO Magnethermic
ALD Vacuum Technologies, Inc.
Aristo-Cast, Inc.
Armil C.F.S., Inc.
ASK Chemicals, LLC
B&L Information Systems, Inc.
Blasch Precision Ceramics, Inc.
Buntrock Industries, Inc.
Cannon-Muskegon Corp.
Consarc Corporation - PV/T, Inc.
Core-Tech
Davis Alloys Manufacturing, LLC
Eagle Engineered Solutions, Inc.
Electralloy
Ergoflex, Inc.
Fireline, Inc.
Fuge Technology, Ltd.
Goff, Inc.
Gradient Lens Corp.
Inductotherm Corp.
Industrial Ceramic Products, Inc.
Kittyhawk Products
Kyanite Mining Corp.
LECO Corp.
MAGMA Foundry Technologies
Metsch Refractories, Inc.
MPI, Inc.
Nutec Bickley
O'Fallon Casting
Pacific Kiln & Insulations Co.
Paramelt
Pillar Induction
Pressure Technology, Inc.
Ransom & Randolph
REMET® Corporation
SECO Warwick (Retech)
SELEE™ Advanced Ceramics®
Shell-O-Matic, Inc.
Stoner Inc.
Synchro ERP, Ltd.
TPM, Inc.
Vulcan Engineering Co.
VA Technology, Ltd.
voxeljet America, Inc.
Westech Wax Products, Inc.
Zircar Refractory Composites, Inc.

INVESTMENT CASTING INSTITUTE

MISSION STATEMENT

The Investment Casting Institute will market the investment casting industry and support its members by facilitating professional, academic, educational, and technical interests, and will provide a forum for advancement in technology and product quality for customers and manufacturers, while promoting free trade, fair competition, and adhering to U.S. laws and regulations regarding commerce and industrial trade.

GENERAL RULES OF ANTITRUST COMPLIANCE

The following rules are applicable to all ICI activities and must be observed in all situations and under all circumstances, without exception or qualification other than as noted below:

1. Neither the ICI nor any committee, conference or activity of the ICI shall be used for the purpose of bringing about, or attempting to bring about, any understanding or agreement, whether written or oral, formal or informal, expressed or implied, among competitors with regard to prices, terms or conditions of sale, discounts, tying provision or purchase of a good or service with another, exclusive dealing arrangements, distribution, volume of production, allocation of territories or customers, restrictions on non-deceptive advertising, or credit of suppliers, customers or competitors or any understanding or agreement which could be perceived as restraining competition.

2. No ICI activity or communication shall (a) include discussion, survey, or action, for any purpose or in any fashion of costs, prices or pricing methods, rebates or other price discrimination, production quotas or other limitations on either the timing or volume of production or of sales; (b) take any action likely to raise prices or reduce quantity or quality of goods available, or (c) involve allocation of territories or markets or customers in any way. “Communication” includes but is not limited to electronic communications, such as emails, test messages, faxes, blog or web posts and/or social media posts.

3. No ICI committee shall undertake any activity, which involves exchange or collection and dissemination among competitors, of any information regarding prices, pricing methods, costs of production, or of sales or distribution or individual company statistics of any kind, without first obtaining the advice of legal counsel, provided by ICI, as to those proper and lawful methods by which these activities may be pursued.

4. No ICI activity or communication shall include any discussion or action which may tend to or may be construed as an attempt to prevent any person or business entity from gaining access to any market or to any customer for goods or services, or to prevent or boycott any supplier, competitor, customer, or other entity from obtaining, accessing, or selling a supply of goods or otherwise purchasing or distributing goods or services freely in the market.

5. No ICI activity or communication shall include any discussion or action which might be construed as an agreement or understanding to refrain from purchasing any raw materials, equipment, services or other supplies from any supplier.

6. Neither ICI nor any committee thereof, shall make any effort to bring about the standardization of any product or method of manufacture, credentialing, listing or certification of any product or program for the purpose of preventing the manufacture or sale of any product not conforming to a specified standard or which would tend to have the overall affect of either lessening competition or resulting in a degree of price stabilization.

7. No person or company shall be commercially disparaged nor shall any ICI Member make statements that are reasonably likely to have a negative reputational impact on another so as to exclude that person or company from ICI membership or participation in any ICI activity where such exclusion is designed to or may impair such person's or company's ability to compete effectively in the investment casting industry.

8. In conducting ICI committee meetings, the chairman thereof shall prepare and follow a formal agenda which shall be provided to all committee members prior to the meeting; else it shall not be considered. Agenda items listed as “Any Other Business: shall be prohibited. Minutes of each meeting shall be distributed to all persons who attended such meetings. Approval of the minutes shall be obtained from the membership of the committee at its next meeting. Copies of the minutes shall be transmitted to the headquarters staff.

9. ICI speakers and authors of conference papers shall be informed of the need to comply with ICI's antitrust policy in the preparation and presentation of their papers and addresses.

10. In informal or social discussions at the site of an ICI meeting (whether such meetings are conducted in-person or via telecommunications services), which are beyond the control of its officers and chairmen, all representatives are expected to observe the same standards of personal conduct required of ICI in its compliance with these antitrust guidelines. Members are reminded that even actions or discussions occurring outside of the U.S. may still be subject to federal antitrust laws. In addition, copies of the foregoing Antitrust Policy Statement and General Rules of Antitrust Compliance will be included in registration packets and will also be printed in the ICI Committee Directory. The Board may from time to time require all members to sign an acknowledgement that each member has read and understood these Rules of Antitrust Compliance.

ANTITRUST POLICY STATEMENT OF THE INVESTMENT CASTING INSTITUTE

The Investment Casting Institute (ICI) is a trade and technical association of investment casting foundries (and their suppliers) where castings of metal are made.

The ICI is organized to promote the common interests of the investment casting industry. The ICI is not intended to become, and will not become, involved in the competitive business decisions of its members, nor will it take any action which would tend to restrain competition in the investment casting industry.

Nevertheless, it is recognized by the Board of Directors of ICI that the Institute itself, as well as its varied activities, could be regarded by some as a forum or opportunity to promote anti-competitive conduct. For this reason, the Board of Directors promulgates this statement of policy to make clear its unequivocal support for the policy of competition served by federal and state antitrust laws, as well as its uncompromising intent to comply strictly in all respects with those laws.

In addition to stating the ICI's firm commitment to the principle of competition served by antitrust laws, the ICI also wishes to advise that the penalties which may be imposed upon both ICI and its individual and corporate members involved in any violation of such laws are now so severe that prudent business judgment demands that every effort be made to avoid any such violation. In addition to injunctions and other equitable remedies, violations of the Sherman Act, such as price-fixing, are felony crimes for which individuals may now be imprisoned for up to ten (10) years and fined up to one million dollars ($1,000,000.00), and corporations can be fined up to 100 million dollars ($100,000,000.00) for each offense, or twenty percent (20%) of affected commerce. The Department of Justice has recently obtained fines of up to five hundred million dollars ($500,000,000.00). Under the Sherman Act, state Anti Trust law, the Federal Trade Commission Act and Robinson-Patman Act, treble (triple) damage claims based on the amount of gain or loss by private parties (including class actions) for antitrust violations are extremely expensive to litigate and can result in judgments of a magnitude which could destroy the ICI and seriously affect the financial interests of its members. This includes attorney's fees and "joint and several liability" where one may be liable for an entire Judgement even though their role in the antitrust violation was rather small.

It is the responsibility of every member of the ICI to be guided by ICI's policy of strict compliance with antitrust laws in all ICI activities. It shall be the special responsibility of ICI officers, directors and committee chairmen to ensure that this policy is known and adhered to in the course of activities pursued under their leadership.

To assist the ICI staff and all its officers, directors and committee chairmen in recognizing situations which may raise the appearance of an antitrust problem, the Board will as a matter of policy furnish to each of such persons copies of ICI's General Rules of Antitrust Compliance. The ICI will also make available general legal advice when questions arise as to the manner in which the antitrust laws may apply to the activities of the ICI or to any committee thereof.

Antitrust compliance is the responsibility of every ICI member. If you have any questions or information concerning potentially anti-competitive conduct, please contact the Board's Executive Committee orally, in writing and even anonymously. Alleged violations of the ICI General Rules of Antitrust Compliance or of this policy statement will be vigorously investigated and reviewed with due process pursuant to the by-laws of the ICI; violations may result in revocation of membership in ICI and removal from any ICI office.

PRELIMINARY AGENDA

SUNDAY, OCTOBER 27, 2019

3:00 p.m. - 6:00 p.m. **REGISTRATION – St. Louis Union Station Hotel Lobby**
6:00 p.m. - 7:30 p.m. **WELCOME RECEPTION – Grand Hall (Hotel Lobby)**

MONDAY, OCTOBER 28, 2019

8:00 a.m. - 8:10 a.m. **WELCOME INTRODUCTION **** 66th Technical Conference & Expo 2019**
Grand Ballroom: D / E / F

8:10 a.m. – 9:00 a.m.	**Tim Sullivan,** *ICI Director* *Hitchiner Manufacturing* **Russ Rosmait,** *ICI Academic Advisor* *Pittsburg State University,*	**Annual Awards Ceremonies - Scholarships, Casting Contest, Member Emeritus, Hall of Honor & Innovator of the Year**
9:00 a.m. – 9:10 a.m.	**Joseph E. Fritz,** *ICI Executive Director* *Investment Casting Institute*	**ICI Updates**
9:10 a.m. - 10:10 a.m.	**Krister Ungerbock**	**Keynote Address: The Secret Sauce for Success In Business – and in Life**
10:10 a.m. – 10:30 a.m.	**BREAK**	
10:30 a.m. – 11:30 a.m.	**Julie Markee,** *ICI Director* *Key Process Innovations* **Chris Whitehouse** *Ceradyne, Inc. – A 3M Company* **Booth 113**	**Paper No. 1** Panel Discussion: Mold Dryness and its Impact on Shell Strength
11:30 a.m. – 12:00 p.m.	**Erich Knoespel** *Artcast, Inc.*	**Paper No. 2** How it's Made: School of Fish Art Casting
12:00 p.m. - 1:00 p.m.	**LUNCH - Grand Ballroom: A / B / C**	
1:00 p.m. - 1:30 p.m.	**Steven Ashlock** *Kyanite Mining Corp.* – **Booth 332**	**Paper No. 3** How it's Made: Premium Grade Virginia Mullite
1:30 p.m. – 2:15 p.m.	**Gavin Dooley** *REMET UK, Ltd.* – **Booth 201**	**Paper No. 4** Analysis of Surface Tension of Materials to Improve Coating Performance of Wax Coating
2:15 p.m. – 3:00 p.m.	**Sam Duncan** *Ransom & Randolph* – **Booth 213**	**Paper No. 5** A Comprehensive Analysis of Viscosity Measurements
3:00 p.m. – 6:00 p.m.	**Expo - Midway West**	

TUESDAY, OCTOBER 29, 2019

8:00 a.m. - 8:10 a.m.	**WELCOME INTRODUCTION **** 66th Technical Conference & Expo 2019 – Day 2** **Grand Ballroom: D / E / F**	
	Nip Singh, *ICI Director* *S&A Consulting Group LLP*	**Process Control Standards Update**
8:10 a.m. - 8:55 a.m.	**Aaron Phipps** *MPI, Inc.* – **Booth 312**	**Paper No. 6** Culture and Employment Strategies for Forward Thinking Companies
8:55 a.m. - 9:25 a.m.	**Evan Letourneau** *MAGMA Foundry Technologies* – **Booth 131**	**Paper No. 7** Eliminating Shrinkage Porosity in a Complex Investment Cast Part
9:25 a.m. – 10:10 a.m.	**Robert Zebick** *Atlantic Casting & Engineering* **Brian Began** *Foseco* – **Booth 108**	**Paper No. 8** An Investment Casting Foundry Experience in Improving Degassing and Grain Refining in Molten Aluminum Alloys
10:10 a.m. - 10:30 a.m.	**BREAK**	
10:30 a.m. - 11:15 a.m.	**Will Jeffs** *Castings Technology International* – **Booth 342**	**Paper No. 9** Massive Shells and Castings in Reactive Alloys from a Highly Customized Facility……Finally.
11:15 a.m. - 12:00 p.m.	**Phil Geers** *Blasch Precision Ceramics* – **Booth 226**	**Paper No. 10** Improving Thermal Conditions and Reducing Process Costs for Core Setters in Aerospace and IGT Applications
12:00 p.m. – 1:00 p.m.	**LUNCH - Grand Ballroom: A / B / C**	
1:00 p.m. - 1:30 p.m.	**Victor Okhuysen** *Cal Poly Pomona University*	**Paper No. 11** Analysis of 17-4 AND 15-5 Alloy Data from Investment Casting Trials
1:30 p.m. - 2:15 p.m.	**Dan Z. Sokol** *Renaissance Services – PERFECT-3D Division* – **Booth 324**	**Paper No. 12** Enhanced Investment Casting Quality Using 3D-Printed Ceramic Filters
2:15 p.m. – 3:00 p.m.	**Michael Kugelgen** *MK Technology GmbH* – **Booth 321**	**Paper No. 13** Innovation & the Race to Space
3:00 p.m. - 6:00 p.m.	**EXPO – Midway West**	
6:30 p.m. - 8:00 p.m.	**EVENING RECEPTION - Grand Hall (Hotel Lobby)**	

WEDNESDAY, OCTOBER 30, 2019

8:00 a.m. - 8:05 a.m. **WELCOME INTRODUCTION **** 66th Technical Conference & Expo 2019 – Day**
Grand Ballroom: D / E / F

8:05 a.m. – 8:50 a.m. **Jacob Lehman, CMfgE**
Pittsburg State University
Paper No. 14
3D Printed Inserts and Mold Cavities that Can Be Used for Producing Wax Patterns

8:50 a.m. – 9:35 a.m. **Rahul Alreja**
VJ Technologies Inc. – **Booth 334**
Paper No. 15
Autonomous Quality Control: The Future is Now

9:35 a.m. – 10:20 a.m. **Aaron Meyer**
Wisconsin Precision Casting Corporation
Paper No. 16
An Evaluation of Using a Low-Cost 3D Printer for Prototype Investment Casting Patterns

10:20 a.m. – 10:35 a.m. **BREAK**

10:35 a.m. – 11:20 a.m. **Ben Wynne**
Intrepid Automation – **Booth 144**
Paper No. 17
Digitization & Automation of the Process of Printing Patterns for Investment Casting

11:20 a.m. – 12:05 p.m. **Tom Mueller**
Mueller Additive Manufacturing Solutions
Paper No. 18
Improvements in the Burnout Process for Printed Patterns

12:05 p.m. - 12:10 p.m. **Adjournment**

12:30 p.m. **Board bus for tour of O'Fallon Casting – Midway West, 20th St. Exit**

SPEAKERS

Krister Ungerbock **Keynote Speaker**
Motivational Speaker
Premiere Speakers Bureau
109 International Drive, Suite 300
Franklin, TN 37067
Phone: (615) 261-4000

Julie Markee **Paper No: 1**
Managing Director
Key Process Innovations
2110 N.W. 379th Street
La Center, WA 98629
Phone: (360) 975-8110

Chris Whitehouse **Paper No: 1**
Engineer Specialist
Ceradyne, Inc. – 3M Company
510 Midway Circle
Midway, TN 37809
Phone: (423) 422-4802

Erich Knoespel **Paper No: 2**
Additive Technologies Specialist
Artcast, Inc.
14 Armstrong Avenue
Georgetown, Ontario L7G 4R9 Canada
Phone: (905) 877-5455

Steven Ashlock **Paper No: 3**
Director of Research & Technology
Kyanite Mining Corp.
30 Willis Mt. Plant Lane
Dillwyn, VA 23936
Phone: (434) 983-2043

Gavin Dooley **Paper No: 4**
Group Technical Director
REMET UK Ltd.
44 Riverside II, Sir Thomas Longley Rd.
Rochester, Kent ME2 4DP UK
Phone: (44) 1634-226240

Sam Duncan **Paper No: 5**
Product & Application Engineer
Ransom & Randolph
PO Box 1570
Maumee, OH 43537
Phone: (419) 865-9497

Nip Singh **Process Control Standards Update**
Consulting Partner & CEO
S&A Consulting Group LLP
2573 Butterwing Road
Cleveland, OH 44124
Phone: (216) 593-0050

Aaron Phipps **Paper No: 6**
VP of Manufacturing & Engineering
MPI, Inc.
165 Smith Street
Poughkeepsie, NY 12601
Phone: (845) 471-7630

Evan Letourneau **Paper No: 7**
Project Engineer
MAGMA Foundry Technologies, Inc.
10 N. Martingale Road, Suite 425
Schaumburg, IL 60173
Phone: (847) 969-1001

Robert Zebick **Paper No: 8**
Director of Facilities & Engineering
Atlantic Casting & Engineering
810 Bloomfield Avenue
Clifton, NJ 07012
Phone: (973) 779-2450

Brian Began **Paper No: 8**
Applications Manager
Foseco
20200 Sheldon Road
Brook Park, OH 44142
Phone: (440) 826-4548

SPEAKERS

Will Jeffs **Paper No. 9**
Technical Development Manager
Castings Technology International
Brunel Way Catcliffe
Rotherham, S60 5WG UK
Phone: (44) 11421-58300

Phil Geers **Paper No: 10**
Sr. Molten Metal Market Manager
Blasch Precision Ceramics, Inc.
580 Broadway
Albany, NY 12204
Phone: (518) 436-1263

Victor Okhuysen **Paper No: 11**
Professor of Ind. & Mfg. Engineering
Cal Poly Pomona University
3801 West Temple Ave. Bldg. 17-2643
Pomona, CA 91768
Phone: (909) 869-2698

Dan Z. Sokol **Paper No: 12**
Managing Partner
Renaissance Services – Perfect 3D Div.
1 Herald Square
Fairborn, OH 45324
Phone: (937) 322-3227

Michael Kugelgen **Paper No: 13**
General Manager
MK Technology GmbH
Robert-Koch-Str. 11
D-53501 Grafschaft, Germany
Phone: (49) 2225-8887-0

Jacob Lehman **Paper No: 14**
Associate Professor
Pittsburg State University
1701 South Broadway
Pittsburg, KS 66762
Phone: (620) 235-4375

Rahul Alreja **Paper No: 15**
Director of Global Sales & Marketing
VJ Technologies
89 Carlough Road
Bohemia, NY 11716
Phone: (631) 589-8800

Aaron Meyer **Paper No: 16**
Project / Process Engineer
Wisconsin Precision Casting Corp.
300 Interchange North
Lake Geneva, WI 53147
Phone: (262) 248-4461

Ben Wynne **Paper No: 17**
CEO
Intrepid Automation
7867 Dunbrook Road, Suite A
San Diego, CA 92126
Phone: (858) 354-8983

Tom Mueller **Paper No: 18**
President
Mueller Additive Manufacturing Solutions
13830 Foxwood Drive
New Berlin, WI 53151
Phone: (224) 548-2191

SPEAKER BIOGRAPHIES

Krister Ungerbock..... Keynote Address
Motivational Speaker
Groundbreaking leadership lessons don't come easily. Krister Ungerbock grew his software company 3,000% - from a small team in St. Louis to hundreds of employees in 8 countries. Chart-topping employee engagement ratings of 99.3% led to 5 consecutive annual Top Workplace Awards. His experience is global - Krister has done business in 40 countries, built businesses in 6, and lived in 3. Now a retired tech CEO at age 42, and the world's first Leadership Archaeologist, he travels to all corners of the Earth (so you don't have to) to discover hidden, powerful leadership secrets. Krister's groundbreaking leadership approach "cracks the code" to employee engagement, increased profitability, and faster growth: Better bosses. What's the simplest, most practical way to build better bosses - or become one? Upgrade your language of leadership. As Krister says, "The easiest way to change how we lead is to change our words."

Julie Markee.....Paper No: 1
Managing Director – Key Process Innovations
Julie Markee is an expert in helping manufacturing companies to achieve extraordinary results. Her focus on people, process, and priorities increases performance, productivity, and profitability. Julie's projects generate high return on investment for her clients so they can improve quality and increase capacity without any capital expenditure. She has presented on numerous topics focused on helping PIC foundries remove variability from their process, including her patented shell monitoring system. Julie is a member of the Investment Casting Institute's Board of Directors, the chair of the Publications Committee, and leads the Education subcommittee tasked with updating the ICI Process Control Class.

Chris Whitehouse.....Paper No: 1
Engineer Specialist – Ceradyne, Inc. – a 3M Company
Chris Whitehouse, Engineer Specialist, is pleased to be serving Ceradyne 3M and their fused silica customers. Chris has over 17 years' experience in investment casting. Currently designing flour and additive packages to help optimize investment casting slurries and shell systems, bringing greater value and profitability to our customers in new and unique ways.

Erich Knoespel.....Paper No: 2
Additive Technologies Specialist – Artcast, Inc..
Erich Knoespel is a Project Coordinator and the Additive Technologies Specialist at Artcast, Inc., a family-run fine art foundry in Georgetown, Ontario. Erich has been around the art and foundry industries for his entire life, but he has been working full time at the foundry since 2013. Erich took the ICI Industry Certification Course back in 2014 successfully receiving a light grey polo shirt. Erich's role in the foundry has grown out of a passion for experimentation which has been an asset when working with artists and suppliers looking to explore the use of additive technologies for casting. Using digital sculpting and design applications, Erich designed the ICI casting contest medallion which Artcast has won two of to date for the fine-art category of the annual ICI Casting Contest.

Steven Ashlock…..Paper No: 3
Director of Research & Technology – Kyanite Mining Corp.
Steven Ashlock has worked for 5 years on the research and development of investment casting materials and refractories. He currently serves as the Director of Research and Technology for Kyanite Mining Corporation. Steven has experience in materials analysis, characterization, and testing, slurry design and control, casting procedures, and industrial processes. He has written several papers for the investment casting and refractories industries that primarily focus on the impact that raw material choices have on the performance of the end part, with an aim to reduce downtime and scrap. Steven graduated with a B.S. in Ceramic Engineering from the Missouri University of Science and Technology. He is a member of the ASTM Committee on Refractories, the UNITECR planning board, an Associate Member of The Refractories Institute, and is currently the Vice Chair of the Refractories Ceramics Division of the American Ceramics Society.

SPEAKER BIOGRAPHIES

Gavin Dooley…..Paper No: 4
Group Technical Director – REMET UK Ltd.
Gavin studied Mechanical and Manufacturing Engineering in Trinity College Dublin, Ireland and a PhD from the University of Birmingham, UK. Gavin's PhD was entitled "Shell Improvements for the Investment Casting of Orthopaedic Implants". He has gained over 5 years investment casting experience as a process and materials engineer within a medical device foundry before joining REMET in 2016. He is currently studying for a Masters in Management with the Open University. Gavin co-ordinates global R&D activities on new products, testing and customer technical service.

Sam Duncan…….Paper No: 5
Product & Application Engineer – Ransom & Randolph
Sam Duncan is the Product & Application Engineer for Ransom & Randolph in the ceramic shell division. In this role, he provides technical support to foundries so that they can improve and streamline their processes in order to achieve their desired results. He started with R&R after graduating from Penn State University in 2018 with a Bachelor's Degree in Materials Science and Engineering. With only a year in the industry under his belt, he is still learning about the ins and outs of investment casting, but aims to improve with each challenge that comes his way.

Nip Singh ……Process Control Standards Update
Consulting Partner & CEO – S&A Consulting Group LLP
Nipendra (Nip) Singh has been an affiliate member of ICI for more than 28 years. He is also member of ICI Board of Directors representing affiliate members and working/chairing many key committees for the welfare of Investment Casting in general and both Affiliate and Regular members. Nip has almost 40 years of experience in the high technology aircraft engine components manufacturing business including nearly 20 years with Rolls Royce , General Electric and TRW/PCC Corporations. Since 1991 Nip is Consulting Partner and CEO of S&A Consulting Group LLP, Cleveland, USA.

Aaron Phipps……..Paper No: 6
VP of Manufacturing & Engineering – MPI, Inc.
Aaron Phipps is the VP of Manufacturing & Engineering for MPI, Inc. Aaron is the son of founder Bruce Phipps and has been with the company in an official capacity since 2010. In truth, Aaron has been in and around the investment casting industry his entire life. Aaron has an engineering degree from Rochester Institute of Technology. He currently teaches the wax section of the Certification Course for the Investment Casting Institute. He presented a paper at the 2015 ICI Technical Conference entitled, "Current Problems in the Wax Room and How they are Best Overcome," and also presented at the EICF World Conference in Paris a paper entitled, "Overcoming Common Wax Injection Problems: The First Step toward Automation." He sits on the Advisory Board of the New Paltz School of Science and Engineering, receiving this year's award for invaluable contributions to the school's Internship Program. Prior to joining MPI in an official capacity, Aaron worked at A.W. Bell in Australia as a product engineer and in the Bio Medical industry. After joining MPI, Aaron has worked his way through MPI taking on key roles including product and automation engineering, process engineering, establishing a training curriculum, department manager, VP of Sales and Service and now VP of Manufacturing and Engineering. After working in all phases of engineering, Aaron took over the MPI Technology Center as manager, overseeing critical areas of the business including pattern production services, demonstrations, process validation, testing and operator/engineer training. The Technology Center is MPI's state-of-the-art facility where engineering, innovation and R&D intersect to create real-world solutions to customer's wax room challenges without having to interrupt their production. MPI has experienced explosive growth over the past 5 years, having doubled in size. Aaron has been an instrumental contributor to this growth as a talented problem solver who effectively collaborates with customers and vendors alike to develop solutions for a wide array of challenges.

Evan Letourneau……Paper No: 7
Project Engineer – MAGMA Foundry Technologies, Inc.
Evan Letourneau is a Project Engineer at MAGMA Foundry Technologies Inc., a software company that is committed to casting excellence and achieves this through its casting process simulation tool MAGMASOFT®. Evan is a recent graduate from the University of Wisconsin – Madison, where he received a degree in Materials Science and Engineering with a focus on metallurgy. He was first exposed to foundry through the campus AFS chapter, which he went on to lead for two years. Evan entered the industry at an internship with Signicast, a steel investment casting foundry in WI. There Evan worked on reducing scrap through gating modification. He moved on to do failure analysis on castings and weldments in the materials lab at Oshkosh Corporation in WI during a co-op. After finishing his final year of school, Evan began working at MAGMA Foundry Technologies Inc., where he has worked for five months.

SPEAKER BIOGRAPHIES

Robert Zebick……..……..……Paper No: 8
Director of Facilities & Engineering – Atlantic Casting & Engineering
Robert Zebick is the Director of Facilities & Engineering, at Atlantic Casting & Engineering in Clifton, NJ. Robert began his foundry career at Atlantic in November 1989 as a Process Engineer. Robert graduated from Stevens Institute of Technology in Hoboken, NJ, with a bachelor's degree in Mechanical Engineering. His first exposure to a foundry is still locked in his memory as "one of the coolest things ever", and after almost 30 years, Robert still enjoys the challenging and dynamic nature of the investment casting process, and the industry as a whole. After 6 years gaining valuable non-ferrous foundry exposure at Atlantic, Robert took the opportunity to expand his knowledge base in the foundry of an orthopedic implant manufacturer, Biomet, where he functioned as Manufacturing Engineer, and later Engineering Manager. Robert returned to Atlantic in 2011 as a Director. Robert enjoys being an active member of the ICI, and has participated as an instructor in the Process Control Course. This will be Robert's first time speaking at the ICI conference.

Brian Began ……Paper No: 8
Applications Manager - Foseco
Brian Began is an Application Manager, Non-Ferrous Metal Treatment, at Foseco in Cleveland, OH. Brian started with Foseco in February 1998 and has worked in a variety of roles. Brian Began graduated from Case Western Reserve University (CWRU) with a bachelor's degree in Materials Science and Engineering. His experiences within the foundry industry include CWRU's experimental foundry and cooperative education assignments at both Ford Motor Company's Cleveland Casting Plant and Element Materials Technology (formerly Climax Research Services) in Wixom, MI. Brian completed his MBA in April 2007 and an additional specialization in Finance in August 2007 from the Graduate School at Ashland University. Brian is the immediate Past Chairman for the AFS Aluminum Division Committee and has held numerous roles within both the AFS Aluminum Division and the CAC-Ohio AFS chapter structure since 2001. Brian was the recipient of the 2011 AFS Glenn Stahl Service Award for service to the aluminum industry. Brian has published in *Modern Castings, AFS Transactions* and *INCAST Magazine*. Brian has also presented on various topics at various AFS, NADCA chapter meetings, casting congresses and specialty conferences. Brian last spoke at the ICI conference in 2017.

Will Jeffs ..... Paper No: 9
Technical Development Manager – Castings Technology International
During over 35 years at Cti, Will has become renowned globally for his practical knowledge and experience in all aspects of high alloy manufacture and the application of ceramic moulding processes for both conventional and reactive alloys in a wide range of manufacturing facilities. Will was educated in the original "steel city" of Sheffield at the Hallam University, where he studied "extractive Metallurgy" and has hands on operating experience of all elements of casting manufacture, in addition to managing Cti's in-house casting operations for many years and was a key member of the team that developed the Replicast® process. In his current role, Will is responsible for promoting licenses for all Cti technologies, transferring relevant know-how and providing ongoing support. With this huge experience of continuously pushing the shell making boundaries, the latest developments at Cti, with AMRC Castings represent the latest developments in massive shell manufacture.

Phil Geers ……..……..Paper No: 10
Sr. Molten Metal Market Manager – Blasch Precison Ceramics, Inc.
Phil Geers, Sr. Molten Metal Market Manager has been with Blasch Precision Ceramics since 2001. Phil has 30 years of technical and engineering sales experience implementing ceramic and mechanical components into process equipment and industrial applications. He holds B.S. in Business and Marketing from SUNY Empire State College.

SPEAKER BIOGRAPHIES

Victor Okhuysen.....Paper No: 11
Professor of Industrial & Manufacturing Engineering – Cal Poly Pomona University
Dr. Okhuysen has held jobs in academia and industry. He has been a Professor of Industrial and Manufacturing Engineering at Cal Poly Pomona since 1998. Prior to his academic career he held various positions in the Metal Casting industry the last of which was as Engineering Manager at CMI-Tech Cast Foundry in Myerstown, PA. In his academic career Dr. Okhuysen has taught multiple courses in areas related to Manufacturing, Materials and Industrial Engineering. He has had multiple research projects, typically in partnership with industrial entities and some sponsored by government agencies. He has many articles and presentations in the area of Metal Casting. As a Professor, he has won several awards including the 2015 Outstanding Academic Advisor from the College of Engineering, the Outstanding Faculty Award from the Veteran's Resource Center and the Distinguished Professor Award from the American Foundry Society and the Foundry Educational Foundation. Dr. Okhuysen has also held administrative positions. In academia, he was Co-Chair of the Graduation Initiative with the goal to improve students' academic performance and graduation rates and in industry as Engineering Manager. Dr. Okhuysen obtained his Bachelor's Degree in Materials Engineering from Cal Poly San Luis Obispo in 1992, MS and PhD in Industrial Engineering from Penn State University in 1995 and 1998 respectively.

Dan Sokol …….....Paper No: 12
Managing Partner – Renaissance services – Perfect 3D Division
Dan Z. Sokol is the Managing Partner of Renaissance Services Inc. He is involved in leading large technology integration projects for automotive and aerospace companies such as General Motors, Lockheed, and PCC. Dan has most recently been the technical lead for various projects focused on the improvement of investment casting, which involves the 3D-printing of ceramic cores, filters, and molds. He was the technical leader and principal investigator on additive manufacturing development efforts sponsored by the Air Force and Defense Logistics Agency. Dan has also successfully managed efforts funded by the National Institute of Standards and Technology, Missile Defense Agency, and the National Science Foundation. Dan has received multiple patents for software and engineering systems. He has published over thirty technical papers and he was recently awarded the Society of Automotive Engineers Excellence in Presentation Award. He was also a finalist for the Ernst & Young Ohio Entrepreneur of the Year award. Dan received a BS in Industrial & Systems Engineering and a BS in Computer Sciences from the Ohio State University, and an MBA from the University of Dayton.

Michael Kugelgen.....Paper No: 13
General Manager – MK Technology GmbH
Michael Kügelgen, General Manager of MK Technology GmbH, worked from 1987 in the company "International Aerospace Technologies" as the leader of the development and production for Unmanned Air-Vehicles, UAV's. In 1993 he started with his own Engineering Office Kügelgen & Partner in Bonn. His major activities were construction and consulting services in the aviation sector, as well as general construction services worldwide. In early 1997 after the implantation of a feasibility study in the field of Rapid Prototyping / Rapid Tooling, Michael Kügelgen decided to build up beside the consultant work his own production to develop appropriate machines. Meanwhile, MK Technology GmbH is a modern production facility and has its own training centre. Apart from the standard programme customized systems are also available. Michael Kügelgen with his company MK Technology GmbH has won twelve innovation prices and awards in the field of Rapid Prototyping and holds several patents.

Jacob Lehman.....Paper No: 14
Associate Professor – Pittsburg State University
Jacob Lehman is an Associate Professor in the department of Engineering Technology at Pittsburg State University in Pittsburg, Kansas. He teaches Manufacturing ETECH courses, including Manufacturing Methods, Computer Aided Manufacturing, Casting Design and Simulation and has been at PSU for over 10 years. Mr. Lehman holds a Master's Degree in Engineering Technology and has spent time working for Honeywell FM&T and ETCO Specialty Produces.

SPEAKER BIOGRAPHIES

Rahul Alreja ..... Paper No: 15
Director of Global Sales & Marketing – VJ Technologies
Recently named to Stony Brook University's *Forty Under 40,* Rahul Alreja is the Director of Global Sales & Marketing at VJ Technologies, a leading provider of x-ray inspection solutions for quality control in a wide range of industries throughout the world. Author of several technical papers, Rahul has been invited around the world to speak on next-generation advances in the field of non-destructive testing as VJT constantly pushes the boundaries of what's considered possible and bring advanced technology, robotics, automation, and computer/machine learning to a variety of industries, specifically targeting quality control and product flow. Rahul is also a co-founder and Chief Strategy Officer for Psocratic, a behavioral AI company looking at stress mitigation via corrective actions on an individual level, while driving enhanced performance out of teams. Rahul holds MBAs from Columbia University and London Business School, is a member of Young Presidents' Organization (YPO), and serves on the Advisory Board for the Grainger Institute for Engineering at the University of Wisconsin, Madison.

Aaron Meyer ..... Paper No: 16
Project / Process Engineer – Wisconsin Precision Casting Corp.
Aaron Meyer has been with Wisconsin Precision Casting since 2011 as a Project/Process Engineer, responsible for implementing both production and prototype parts into the investment casting process as well as troubleshooting and providing technical support. He has experience with several different prototype pattern products, including SLA, PMMA, and printed sand. Aaron has a BS degree in mechanical engineering from Michigan Technological University.

Ben Wynne..... Paper No: 17
CEO – Intrepid Automation
Ben Wynne is passionate about all things additive, having developed low cost 3D Print concepts for Hewlett Packard, driving 3D scanning technology into consumer products and facilitating the purchase of David Laserscanner by HP Inc. He experienced first hand the limitations of using additive for production during his time as CTO at Wiivv Wearables. Since then he worked alongside the other founding members of Intrepid to start the Advanced R&D lab for 3D Systems in San Diego, ultimately developing the Figure 4 platform. Ben and the team believe that Investment Casting combined with additive patterns are the future of metal part production.

Tom Mueller..... Paper No: 18
President – Mueller Additive Manufacturing Solutions
Tom is the founder and president of Mueller Additive Manufacturing Solutions, a consulting company focusing on metal casting applications of additive manufacturing. He has been involved in 3D printing applications for more than 30 years. He led the first beta site for stereolithography at Baxter Healthcare in the late 80s. He then went on to found two 3D printing service companies. One of those companies, Express Pattern, was sold to 3D Systems. He worked for 3D Systems as Director of Business Development focusing on metal casting applications and later for Voxeljet as Director of Metal Casting applications. Tom has published more than 50 technical papers and journal articles related to 3D printing applications. He holds BSME and MSME degrees from the University of Illinois and an MBA from the Sloan School of Management at MIT.

INVESTMENT CASTING INSTITUTE

Mold Dryness & Its Impact on Shell Strength

Julie Markee – Key Process Innovations
Chris Whitehouse – Ceradyne, Inc. – A 3M Company

66TH TECHNICAL CONFERENCE
&
EXPO 2019

Paper № 1

Panel Discussion: Wax vs Mold Surface Dryness

Julie Markee

1.0 OVERVIEW

At the 2018 ICI Fall Technical Conference, three foundries presented various papers around shell drying. As a result of the questions and discussion, it was decided to have another panel discussion around this same topic. In this panel, we will look at the effect of intra-coat drying on shell strength and the difference between the moisture level on the mold surface versus the wax surface. In addition, DePuy will present an update on their project to increase shell room throughput by reducing final dry time. This specific paper explores the difference in moisture between the wax and mold surfaces during the drying process.

2.0 BACKGROUND

During the shell dipping process, liquids from the slurry are absorbed into the shell. In the initial layers, the liquids are wicked back to the wax surface. However, in the later coats, absorption is based on shell thickness, slurry viscosity, immersion time in the tank and shell permeability.

Immediately after dipping, the temperature of the mold drops due to the latent heat of evaporation. Provided there is sufficient airflow, the temperature of the mold decreases and approaches the wet bulb temperature. When the surface is no longer saturated with water, the evaporation rate slows to the point where the convective heat transferred from the room to the mold exceeds the temperature decrease due to evaporation. At this point, the temperature of the mold starts to rise. A mold is considered dry when its temperature reaches 2-3°F from ambient.

During the drying process, liquids move to the surface of the mold in two different stages as described in the 1996 paper presented by Leyland [1]. During the first stage, the rate of evaporation is independent of the moisture content. In the second stage, the rate of evaporation is dependent on the capillary network within the mold. Since the liquids absorbed into the shell must move to the surface of the mold, it is often assumed that the last area of the mold to dry is closer to the mold surface.

Understanding the moisture profile throughout the mold is the first step in determining the level of dryness needed prior to applying the next dip or dewaxing the mold. Once this is understood, a foundry will be able to establish a level of mold dryness needed to produce a mold which can survive the remaining steps in the investment casting process.

3.0 EXPERIMENTAL

3.1 Slurry and Mold Building

For this test, a basic 120/200 slurry with small particle binder was built. No latex was used. The slurry was mixed with a lightning mixer overnight and was adjusted to a viscosity of 20 seconds as measured on a Zahn EZ #5 cup. Each mold received 7 layers, two layers with fine sand and five layers with coarse sand.

Mold dryness was measured using Key Process Innovation's kpi-dry™ system. This system has two digital sensors which measure temperature and relative humidity and are protected by a waterproof, breathable membrane. One sensor was placed at the wax surface and the second sensor was placed at the mold surface. Just prior to applying each dip, the second sensor was moved to the mold surface.

3.2 Mold Set-Up

A tree and sprue were assembled, and two identical parts were attached to the sprue. The sensors were placed facing inward towards the sprue in an area that would be the hardest area to dry.

Figure 1: Mold Set-Up

3.0 RESULTS AND DISCUSSION

3.1 Room Environment

Shell drying was performed in a small room with an oscillating fan. The room temperature was controlled to 71 ±2°F and relative humidity target was 38%. Room temperature, humidity and air flow were measured using an anemometer.

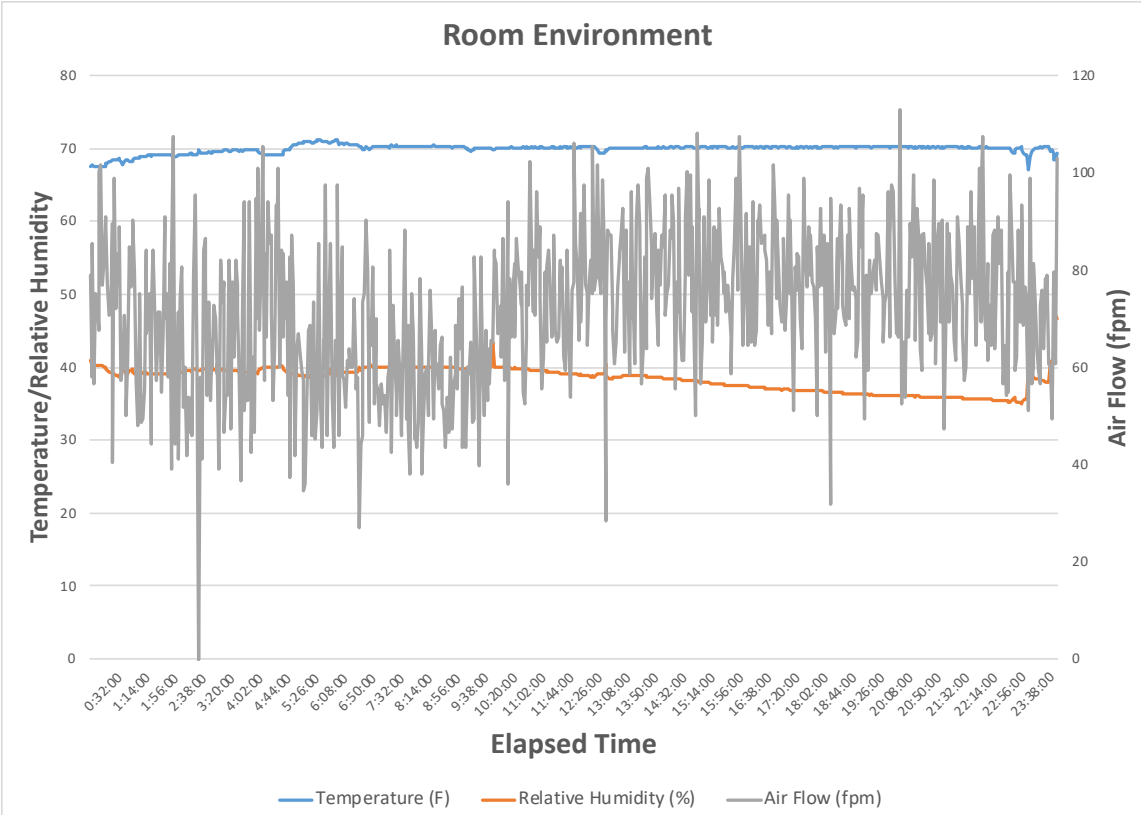

Figure 2: Drying Room Environment for Initial Test

3.2 Initial Test Data

Both temperature and relative humidity of the mold were measured during the dipping and drying process. The mold was dipped once the sensor located on the shell surface reached 65% relative humidity.

As described above, after dipping, the temperature of the mold decreases and approaches the wet-bulb temperature. Throughout the test there was approximately a 4°F difference in temperature between the wax and mold surfaces.

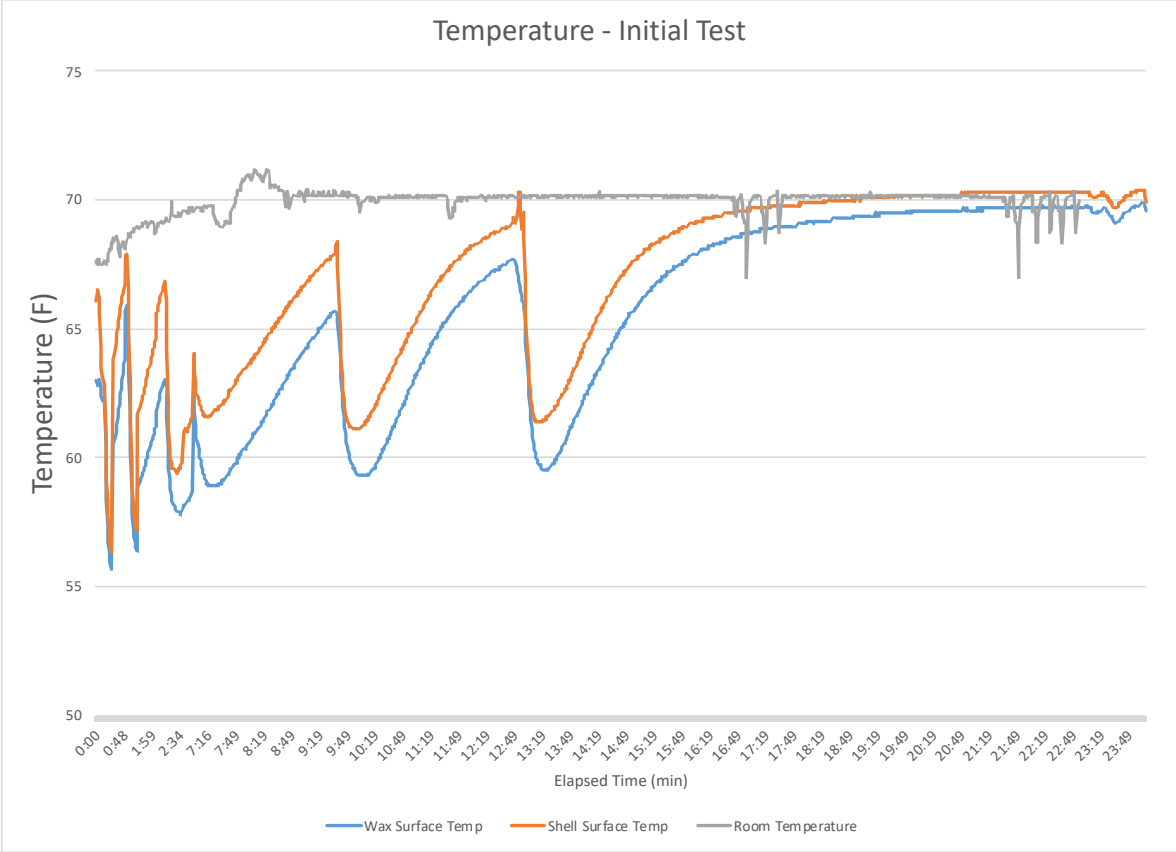

Figure 3: Comparison of Wax and Shell Surface Temperature

After dipping, relative humidity of the mold will climb towards 100% and as it dries, the RH will fall towards ambient. In the chart below, the expected trend is observed on the shell surface, but it is clear that the wax surface is not achieving the same level of dryness. As more layers are applied, the difference in relative humidity between the two surfaces increases.

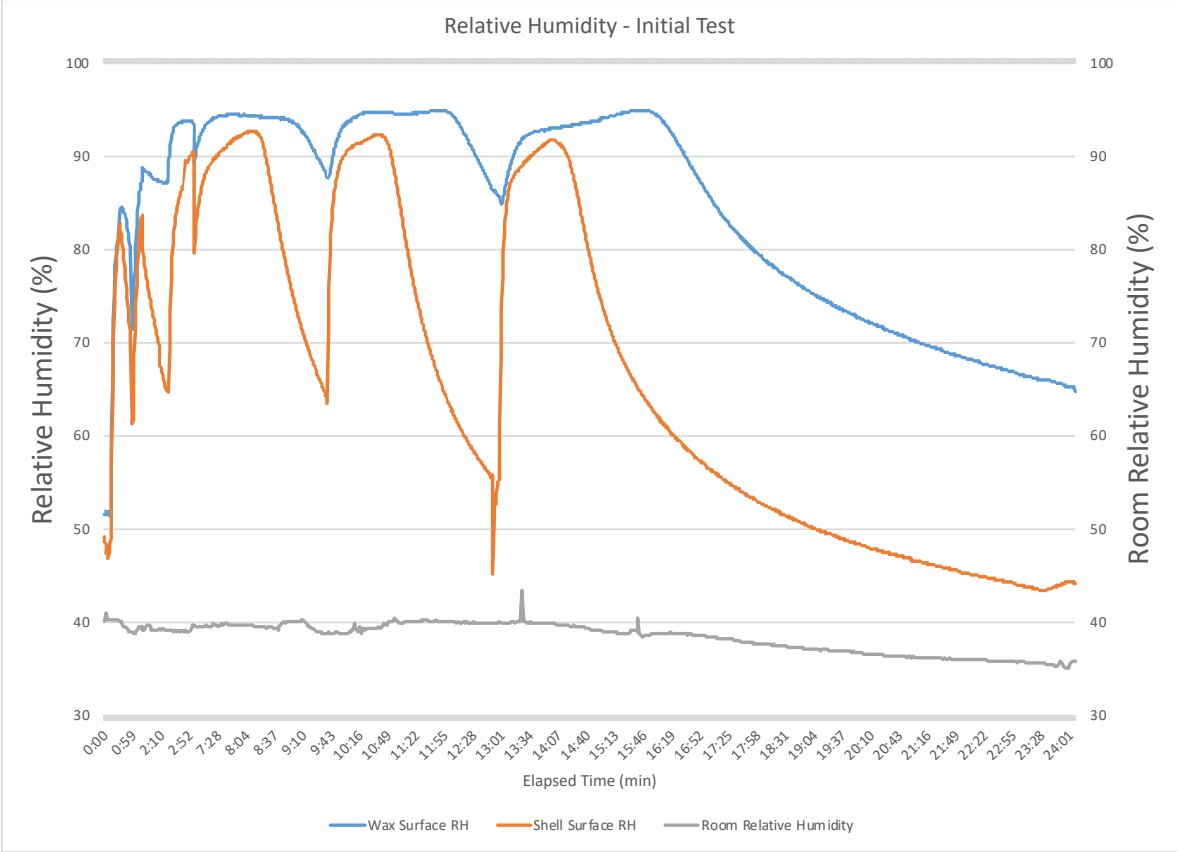

Figure 4: Comparison of Wax and Shell Surface Relative Humidity

It is interesting to note that for the second and third coats on the wax surface, the relative humidity climbs after the mold is dipped, falls slightly and then increases again. This could be the intersection of soak back of the liquids to the wax surface and moisture moving to the surface of the mold. Meaning the moisture at the wax surface is moving to the mold surface causing the relative humidity to drop and then the moisture being absorbed by the shell due to soak back replaces the removed moisture.

This curve has not been observed in prior kpi-dry™ tests. This could be a result of a couple of factors. First, the sampling rate for this test was reduced to 1 reading per minute, where typically it is recommended that readings be taken every 5-10 minutes. Second, according to the sensor manufacturer, the response time of the temperature and relative humidity sensor is approximately 5 minutes with an air velocity of 1 m/s or approximately 200 ft/min. In reviewing the room environmental conditions, it was noted that the air flow averaged approximately 80 ft/minute.

In order to test this out, the test was repeated but this time, the air flow was increased to approximately 225 ft/minute. The sampling rate remained constant at one reading per minute.

3.3 Second Test

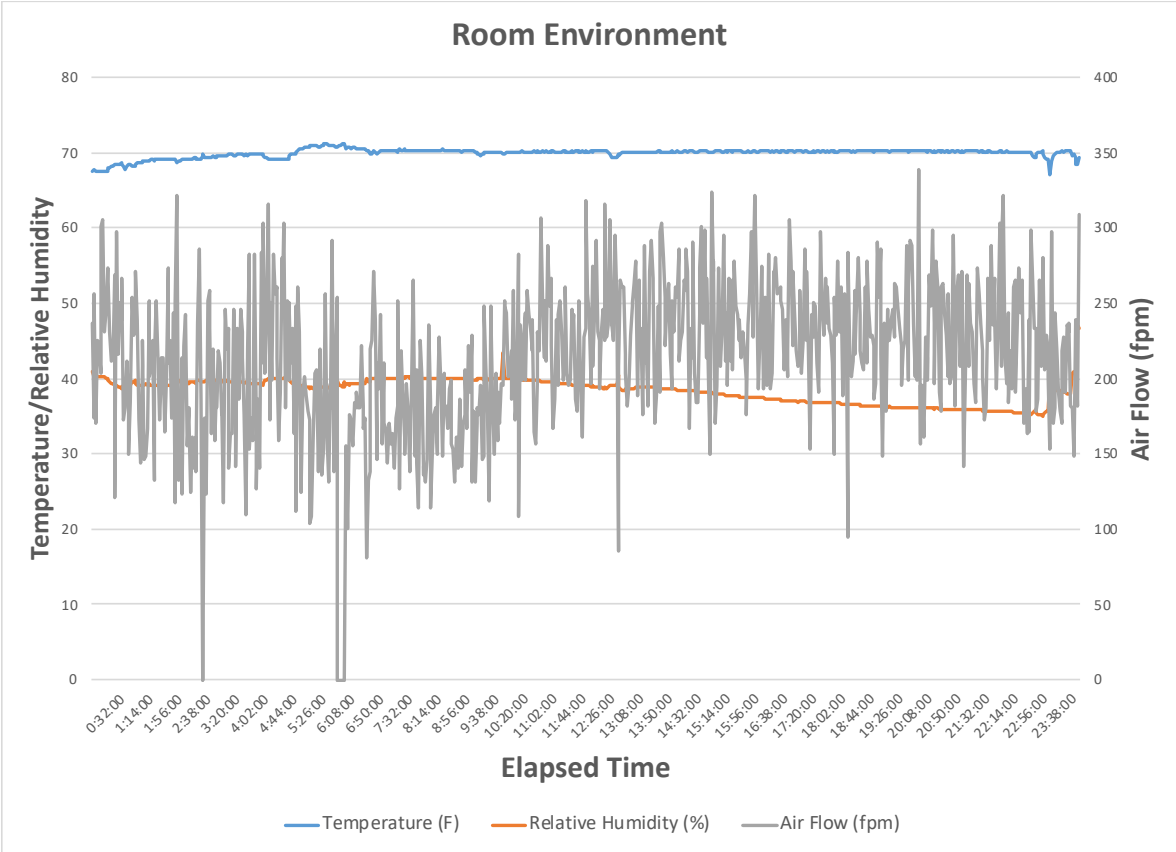

Figure 5: Room Environmental Conditions for Second Test

For this test, only 4 coats were applied the first day and the remaining 3 coats were applied the second day. While these aren't ideal conditions, it did highlight some differences in drying.

The temperature profile between the wax and shell surface was much closer, averaging approximately 1.5 °F which could be attributed to the higher air flow. As discussed in previous papers on mold drying, sufficient air flow is needed to remove moist air from the surface of the mold. This provides a gradient that allows moisture from within the mold to migrate to the surface.

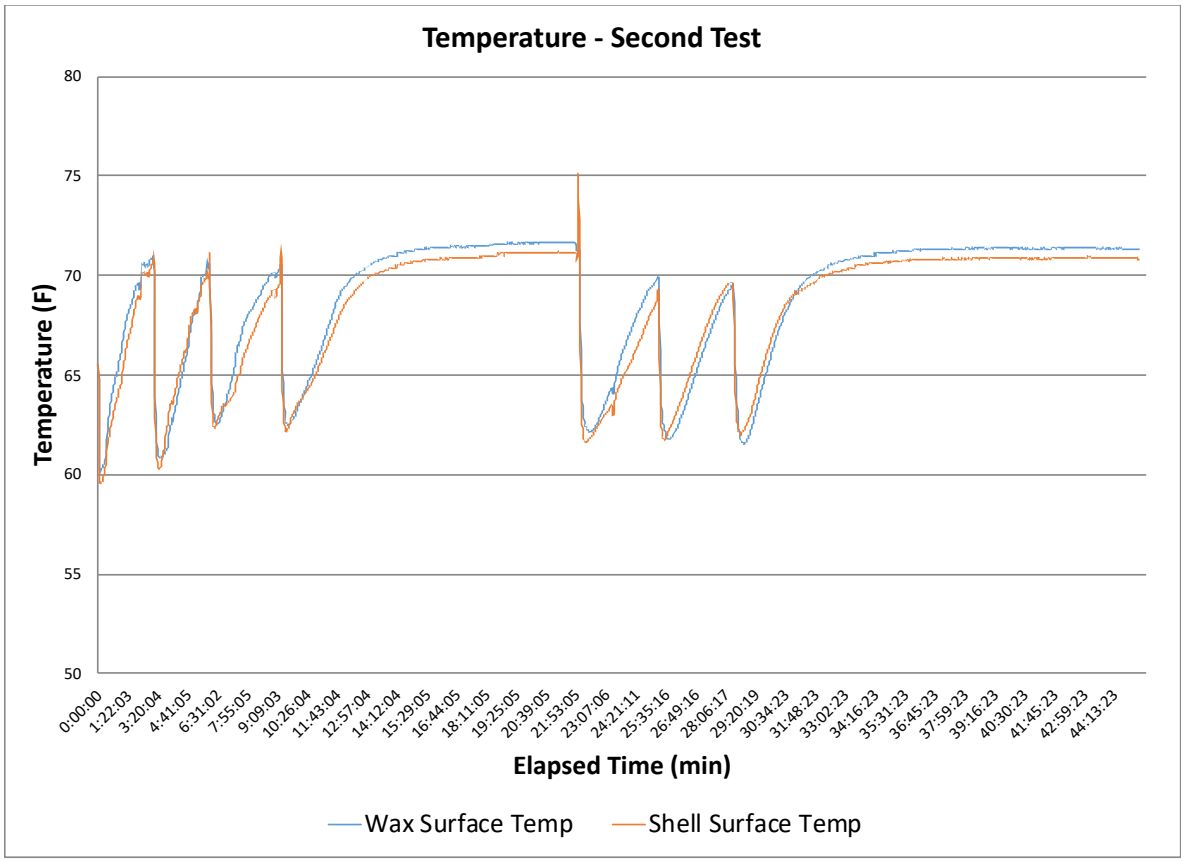

Figure 6: Comparison of Wax and Shell Surface Temperature for Second Test

The relative humidity chart showed a smoother curve in the earlier coats which could also be attributed to the increased air flow. It also shows that the level of dryness between the two surfaces, as measured by relative humidity, is much closer. This is not surprising as airflow is a key variable for mold drying.

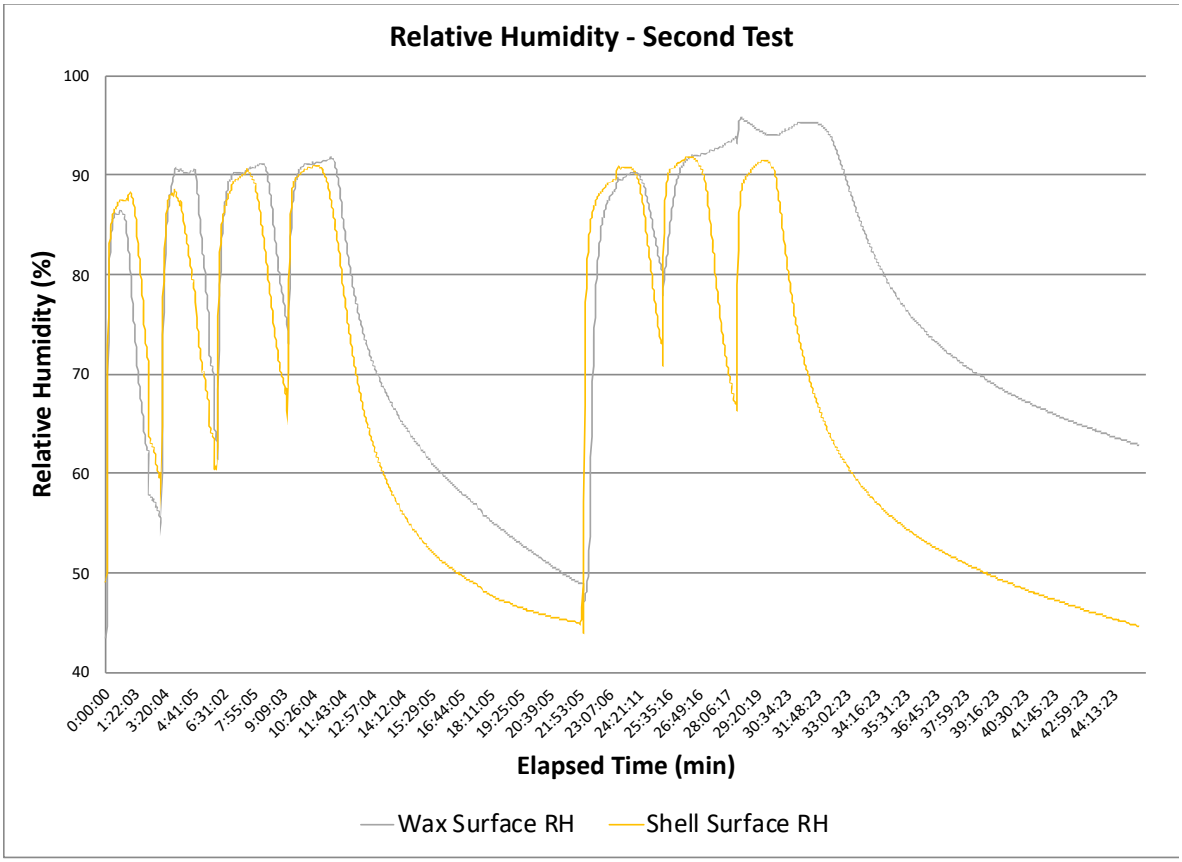

Figure 7: Comparison of Wax and Shell Surface Relative Humidity

The chart also shows that after 4 dips were applied, the mold dried approximately 12 hours which allowed the moisture between the wax and mold surfaces to nearly equilibrate. However, as the remaining coats were applied, the difference in the relative humidity between the two locations continued to increase. And after 16 hours of final dry time, the relative humidity at the wax surface was much greater than the shell surface.

Now that there is a test that measures moisture at the wax and mold surfaces, the next step is to create a profile of dryness on the wax and shell surface and then correlate this to mold strength, ideally measured around the mold's ability to survive the dewax process.

4.0 CONCLUSIONS:

4.1 The wax surface has a higher level of moisture, as measured by relative humidity than the mold surface.

4.2 The amount of air flow can impact the difference in the temperature and relative humidity between the wax and mold surface.

4.3 Further testing is needed to determine the level of dryness needed at the wax or mold surface to ensure the optimal strength of the mold.

5.0 REFERENCES:

1. S. Leyland, et.al. "Implementation of a Water Based shell Mould Investment Casting Process," 9th Annual World Conference on Investment Castings, 1996, pp: 23.
3. J. Snow, et.al. "Shell Drying- Water Based", 46th Annual Technical Meeting of the Investment Casting Institute, 1998, pp 8:1-30.
4. J. Markee, "A New Method for Measuring Dryness During the Shell Building Process," 59th Annual Technical Meeting of Investment Casting Institute, 2012.

DePuy Synthes Foundry Final Dry Time Analysis Using KPI Dry

Case Study, September 2019

DePuy Synthes: Robert Tella
Wayne Gayford

Key Process Innovations: Julie Markee

At Johnson and Johnson's DePuy Synthes Raynham branch, the foundry manufactures castings of knee and hip replacement product parts. In the shell-making process, the final dry room is a temperature and humidity regulated room where parts go to dry after their final dip in the slurry. Out of 176 total hangers in the shell room, 47 are located in the final dry room. This puts a ceiling limit for capacity and creates an issue if it is full when more product needs to be moved in to meet dry time specifications.

The goal is to reduce the minimum dry time specification in the DePuy foundry final dry room to increase capacity and move product through the room faster. Visually, it seems that the molds are dry sooner than the minimum dry time specification suggests. However, a study is needed to determine when the mold is actually dry and ready to move on. After discussing with Key Process Innovations, DePuy decided to use the KPI-Dry^{TM} unit as the method for measuring dryness. If the data from multiple trials shows consistent duration to reach a target relative humidity (RH) value and temperature, then the data can be used to support a change in dry time specification.

In last year's study, the humidity and temperature trends showed variation in dryness in different areas of the mold. It also showed the evaporation of the molds taking a little longer than expected, as shown by the temperature trends. As the water from the wet slurry evaporates off the mold, the temperature increases until there is nearly no water remaining. At this point, the temperature plateaus at the ambient temperature. After investigating the reasons for the longer rate of evaporation, it was found that there was poor airflow in the final dry room. In some areas, there was virtually no airflow at all. Airflow is necessary for mold drying as it removes moisture in the air surrounding the mold. The more saturated the air is with water, the fewer water molecules can be absorbed by the air. Therefore, the mold will dry faster if the air surrounding it is drier. To improve airflow, and therefore improve drying, three large barrel fans were installed in the final

dry room. One main goal of this year's study is to see how the addition of the fans affect mold drying through measurement of relative humidity and temperature.

Location Number	Avg air speed before new fans (fpm)	Avg air speed with new fans (fpm)	Max air speed change (fpm)
1	83	35	-48
2	92	132	40
3	2	70	68
4	2	109	107
5	47	83	36
6	92	90	-2
7	17	234	217
8	64	139	75
9	93	140	47
10	59	547	488

Table 1. Average air speed (1-minute interval) comparison of 10 chosen locations in the final dry room, from before and after the addition of the fans.

Location Number	Max air speed with original fans (fpm)	Max air speed with new fans (fpm)	Max air speed change (fpm)
1	144	129	-15
2	134	245	111
3	67	148	81
4	83	146	63
5	101	129	28
6	138	154	16
7	82	373	291
8	83	180	97
9	167	201	34
10	113	763	650

Table 2. Maximum air speed (1-minute interval) comparison of 10 chosen locations in the final dry room, from before and after the addition of the fans.

From looking at Table 1 and Table 2, it is clear that the addition of the fans helped the airflow in the final dry room significantly. It is also apparent that some locations get better airflow than others, which unfortunately adds variability to each mold's dry time since the conveyors do not

move constantly. All in all, the overall airflow was increased, with some areas seeing nearly a 10x improvement in air speed. On a side note, at Location 1 it was discovered that an existing fan was not working which may explain the reduction in air movement.

DePuy used four data loggers which allows for eight locations on the mold to be measured at one time in a trial. In order to expand on last year's study, four sensors were used on the wax surface and four sensors were placed on the shell surface, in the same locations for the same product type. The chosen locations are representative of what is believed to be the best- and worst-case scenarios based on a combination of mold geometry, and location on the product tree. The best-case scenario, or area believed to dry fastest, is on the patella because it is the area on the part most exposed to airflow. Furthermore, due to fan placement, the outer-half of the mold should receive more airflow than the inner-half of the mold, and so parts on the outer-half are considered best-case as well. The worst-case location, or area believed to take longest to dry, is in the box because it is subject to the least amount of airflow since it is hidden within other features of the geometry and more likely to trap moisture. Additionally, sensors were placed on parts configured on the middle row of the mold, since the airflow may be blocked from parts above and below them. Hence, the worst-case scenario is the location of the box of the part in the middle row, on the inner-half of the mold.

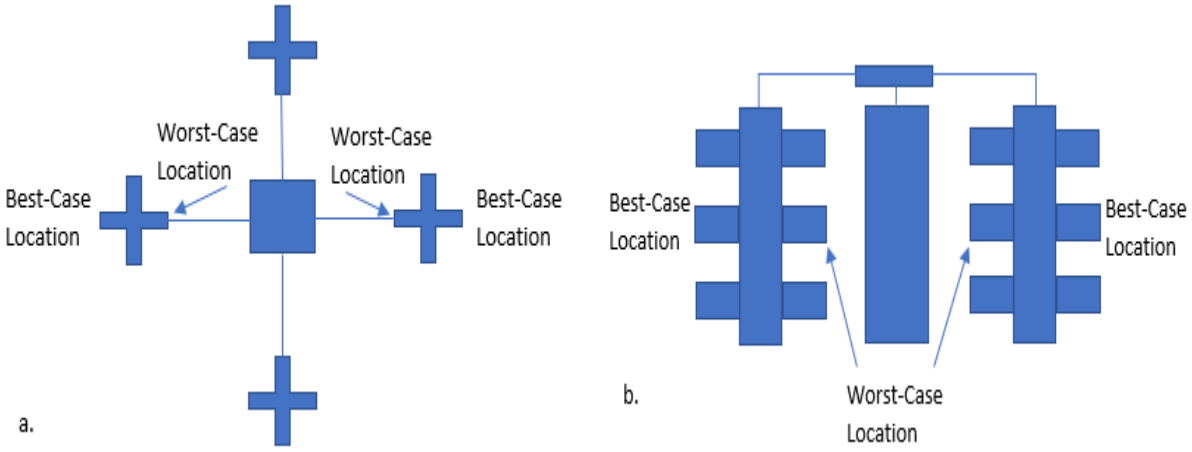

Figure 1. Image "a" represents the configuration of a 4-mold assembly from the top view. Two sensors, one for the box and one for the patella, were placed at each best-case (outer half) and worst-case (inner half) location. Image "b" represents the configuration of the same 4-mold assembly from the side view.

To understand how the shell is drying throughout all the layers, sensors were placed at the wax surface and shell surface. Figure 2 shows the measurements taken at the wax surface last year, and Figure 3 shows the measurements taken at the wax surface this year after the installation of the new fans in the final dry room.

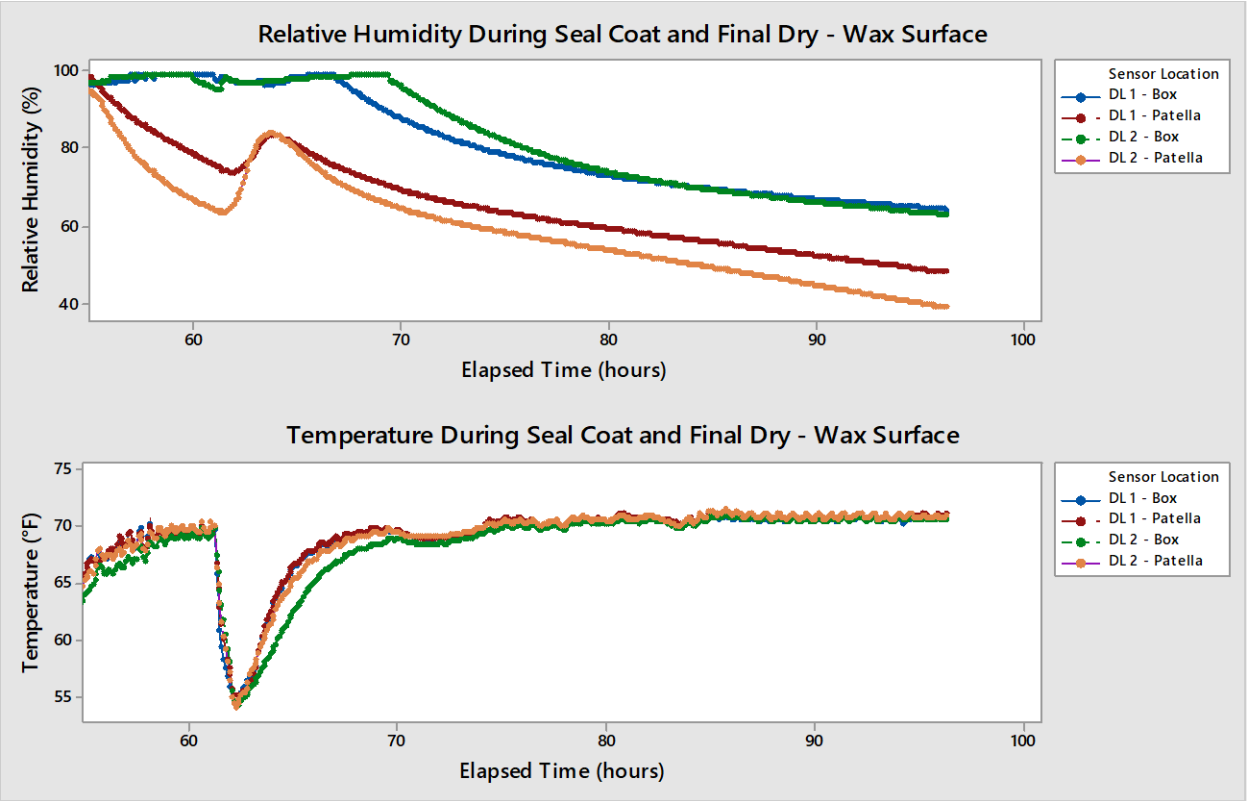

Figure 2. The relative humidity and temperature readings at the wax surface during and after the application of the final coat of slurry, before the installation of the new fans in the final dry room.

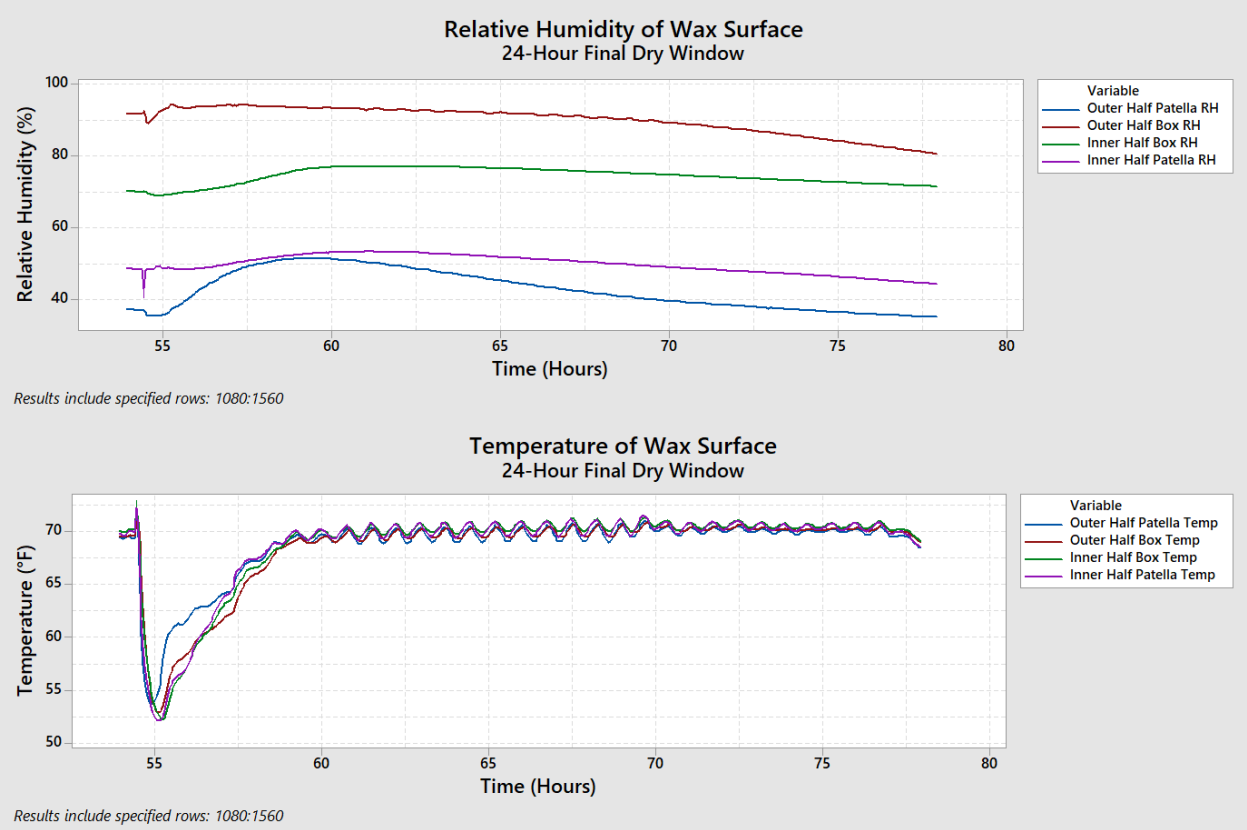

Figure 3. The relative humidity and temperature readings at the wax surface during and after the application of the final coat of slurry, after the installation of the new fans in the final dry room.

The trends in the temperature of Figure 3 show that all four locations reach the ambient temperature faster and more consistently than those of Figure 2. More specifically, the temperature plateaued about 3 hours sooner on the wax surface after the addition of the fans. This suggests the improvement in airflow led to a significant change in the rate of mold drying.

One surprise that came with the study was the inconsistency in relative humidity (RH). The outer half of the mold, considered to be the best-case scenario for drying, had the highest RH in the box location (>80% in the entire 24-hour window) and the lowest RH in the patella location (≤50% in the entire 24-hour window). The patella data improved from last year's data, while the box data worsened. In terms of the inner half of the mold, considered to be the worst-case scenario for drying, the box had lower RH than the outer-half and the patella had higher RH than the outer-half.

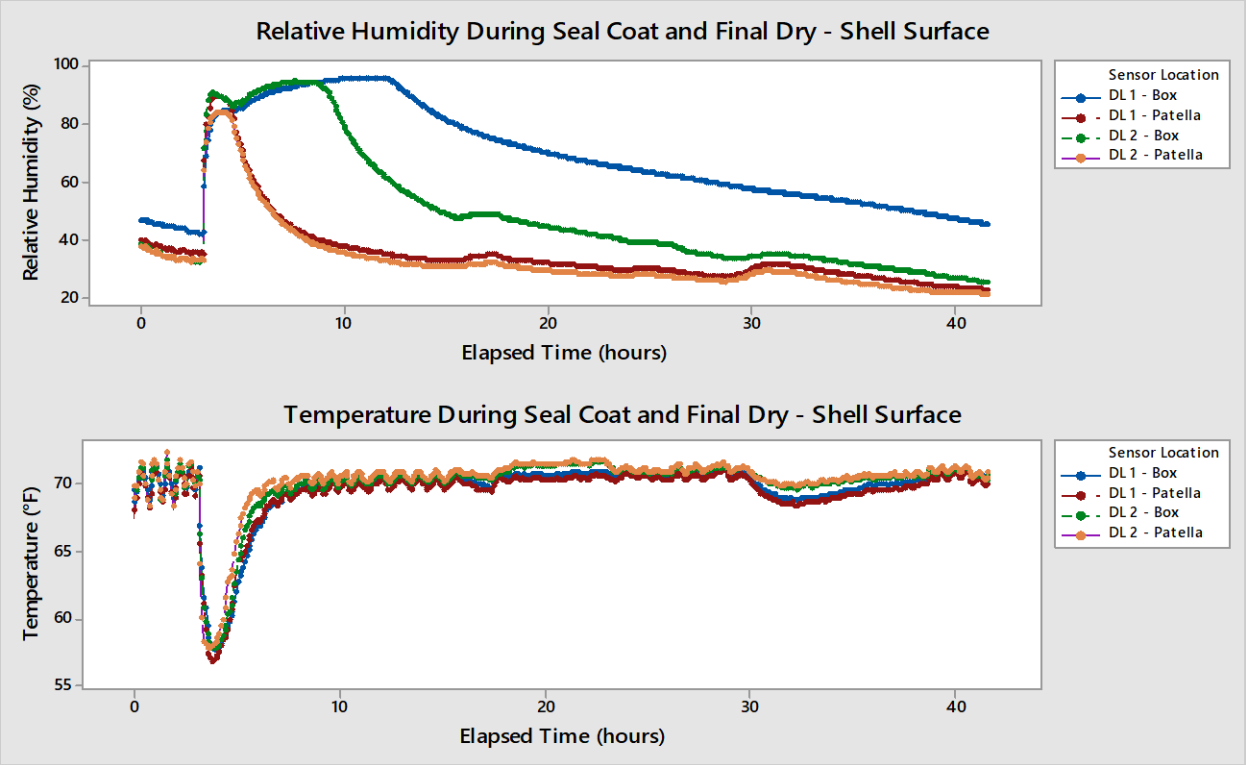

Figure 4. The relative humidity and temperature readings at the shell surface during and after the application of the final coat of slurry, before the installation of the new fans in the final dry room.

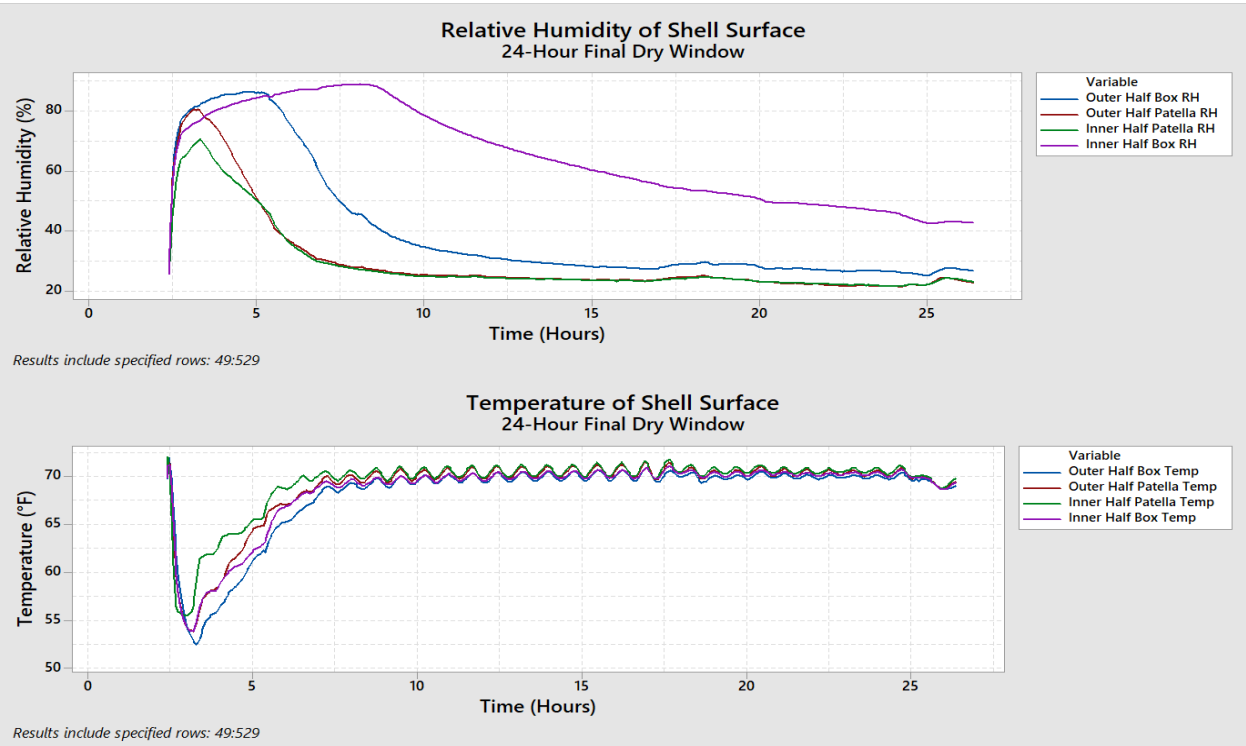

Figure 5. The relative humidity and temperature readings at the shell surface during and after the application of the final coat of slurry, after the installation of the new fans in the final dry room.

The temperature trends of the shell surface show less of a difference than the wax surface after the installation of the new fans according to Figures 4 and 5. Both temperature trends plateau after about 5 hours of being removed from the slurry.

The relative humidity (RH) trends in the shell surface look nearly identical from before and after the installation of the new fans. However, the drop in RH did occur sooner after the installation of the new fans. In both Figures 4 and 5, the RH gets up to about 80-90% after being dipped in slurry. In Figure 5, it takes about 2.5 to 3 hours for the RH of the patella locations to drop to 40%, while this takes about 6 hours in Figure 4 for the same locations. In Figure 5, it takes about 5.5 hours for the box of the outer-half of the mold to reach 40% RH, while Figure 4 shows this takes a little over 20 hours for the same location. For the box location of the inner-half of the mold, it was about an 8-hour improvement to reach 60% RH after the installation of the fans. There is no significance to these 40% and 60% RH targets other than to compare the trends.

It is clear that the addition of the large barrel fans created a positive impact on reducing the dry time for the molds in the final dry room. Big reductions in dry time are evident by the temperature trends on the wax surface as well as the RH trends on the shell surface. However, the disparities amongst the RH readings on the wax surface create some questions about how to determine what the acceptable minimum dry time is for the process. The wax surface RH may not be as significant to that determination, considering the molds get autoclaved afterwards. Possibly, the data to focus on most is the temperature trend of the wax surface, along with the RH trend of the shell surface to see when the final coat of slurry is dry enough. A larger data set, with more concrete and consistent results, will be necessary before making conclusions on when the molds of these parts are adequately dried.

Further Discussions About Drying

W. Snyder, C. Whitehouse, J. Markee

1.0 ABSTRACT

At the 2018 ICI Fall Technical Conference, three foundries presented papers on drying data gathered at their foundries. These papers resulted in a lot of discussion about how the level of dryness impacts shell strength. This year, additional work was planned to continue the discussion around shell drying. In this paper, a mold dryness measurement system was used to provide a more complete understanding of shell properties at various levels of dryness. Three levels of relative shell humidity prior to re-dipping used and a number of shell properties were measured including burst strength, permeability, and the four standard test conditions: green, hot/wet (boiled), fired tested hot and fired cooled to ambient (fired/cold).

On a parallel path, DePuy Synthes gathered additional data around the level of dryness in the mold and correlated this data to casting quality, which will be presented in a separate paper at the 66th Technical Conference. From this data, it is hoped that foundries will be able to better understand how mold dryness impacts shell strength and casting quality.

2.0 BACKGROUND

The level of mold dryness required to make a good casting is a question which is frequently asked by an investment casting foundry. Many papers have addressed different aspects of shell drying over the years. Three papers were presented at last-year's 65th Technical Conference on the topic of drying. Brienza [1] attempted to establish a relationship between shell properties and the degree of dryness. A review of shell temperature, shell relative humidity and electrical conductivity due to the presence of water remaining in the shell was made and compared to shell modulus of rupture data. It was found that the greater the temperature recovery, the higher the green MOR. However, it was pointed out that a relationship between the dryness and the amount of water remaining in the mold was not established. Oyervides [2] studied the dryness of internal passageways also using relative humidity. This paper concluded that there was no apparent impact on shell quality within a range of 60% to 80% relative humidity in the shell. Tella [3] studied shell dryness at the wax surface and exterior shell surface and presented data showing the change in relative humidity from these locations during the DePuy drying cycle.

Many other papers have been presented over the years on drying. Snow [4] shared extensive data on the effect of air temperature, humidity and air velocity upon drying time using shell weight changes due to evaporation as well as the resultant shell strengths. Leyland [5] presented further extensive data on shell drying and suggested that "… water in the gel structure cannot flow freely to the surface" and that the shell pore structure further complicates drying due to with the presence of colloidal gel as the water evaporates.

Markee [6] noted that as the level of complexity of the molds increases, ensuring the inside of the mold is dry enough for the next layer or prior to dewax is critical. This paper indicated that using temperature as a method for measuring mold dryness in the inner passageways may lead to inadequate data. Further, that without proper air movement, the relative humidity of these areas may reach 100%, drying will then stop, and the temperature will begin to climb towards ambient. As a result, % RH was recommended as the best method for measuring mold dryness on the inner passageways of a mold.

3.0 EXPERIMENTAL

3.1 Materials and Equipment

3M™ WDS2 Fused Silica Advanced Shell System, Nalco's small particle 1130 colloidal silica, and 3M™ HP Latex were all sourced for slurry making as shown below in Table 1.

	Wt(g)
WDS2 flour	13500
1130 colloidal	4883
DI-H2O	600
HP Latex	501
Antifoam	10
Total	19494
%SiO2	24.4%
%latex	8.4%

Table 1. Slurry Formula.

Slurry was high sheared for a total of 30 minutes and allowed to cream in overnight (18 hours) in a large rotating Nalgene jug. Slurry creamed in at 20 seconds as measured on a Zahn EZ #5 dip cup.

Mold dryness was measured using Key Process Innovation's KPI-DRI™ system. At the desired location, a digital sensor with a waterproof, breathable membrane measures temperature and relative humidity.

Three levels of shell dryness were used in this study: 75%RH, 60%RH and 45%RH. Once these degrees of dryness were achieved in the shells after each dip, a subsequent dip was applied. Shell conditions were then measured after an 18-hrs final dry time was used. Room temperature and humidity as well as shell temperature and humidity were measured.

3.2 Procedures and Sample Preparation

Standard 1"x 0.25" x 13" steel bars were used for MOR testing. 3/4" schedule 40 inner diameter cold PVC pipes were used for shell building for permeability testing per the method discussed by Snyder [7]. Lastly 4" x 4" x 0.25" wax plates were used to provide data on slurry draining and shell building. Substrates were first coated in Johnson's Paste wax followed by a dip in surfactant and then allowed to dry.

A five-dip shell was made for these tests. First dip in WDS2 was stuccoed with 50x100 fused silica. The second, third and fourth dips were stuccoed in 30x50 fused silica. The last dip was a seal coat.

Shell drying was performed in a small 5'x 8' closed room with its own air conditioning and resistance heating unit. A programmable controller is used to control the temperature while a portable Dri-Eaz Model Revolution LGR dehumidifier is used to control the humidity with use of a setpoint controller. No additional humidifier was used as humidity in eastern Tennessee is typically 50% or greater at the time of year of in which this test was performed. This did result in a slight loss of humidity control one day as an unexpected dry front came through which will be mentioned later. Air is kept turbulent with use of two opposing and wall mounted oscillating fans which provide velocities typically between 100 to 800 ft/ min.

The dry room was controlled to 72±2°F. For consistency, the room humidity was dropped to 40%RH for all shell drying conditions. Cold rolled steel MOR bars 1" x 1/8" x 13" were

used for MOR shell building and for mounting to the KPI-DRI sensor system (shown below in Photos 1 and 2).

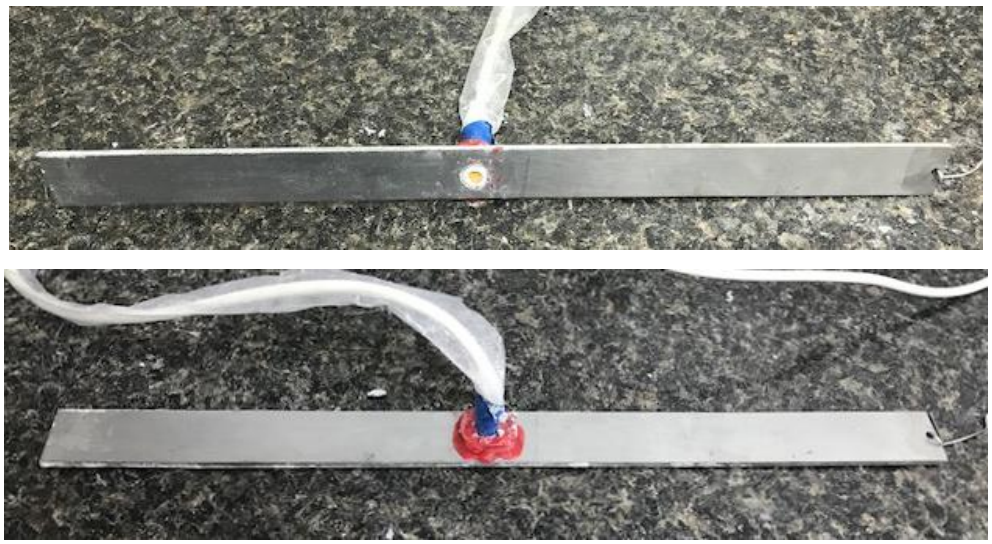

Photo 1. Two Images of MOR Bar Equipped with KPI-DRI Sensor.

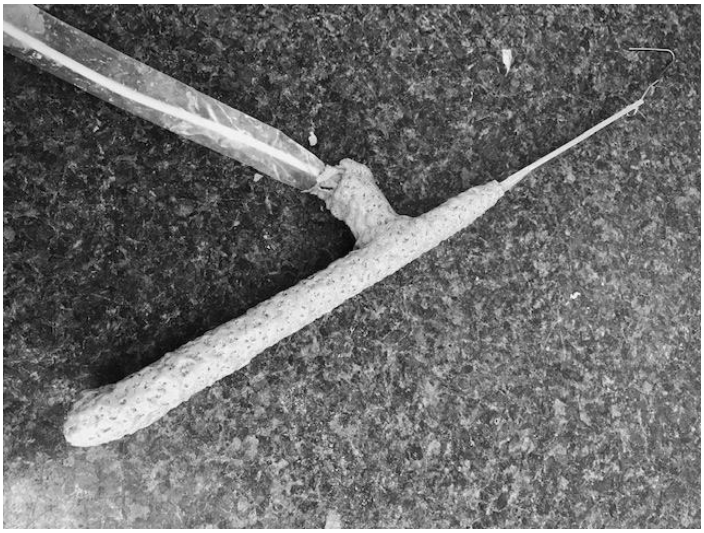

Photo 2. Image of Shelled MOR Bar with KPI-DRI™ Sensor.

The complete shell dryness monitoring system from KPI is shown below in Photo 3.

Photo 3. KPI-DRI™ Shell Dryness Monitoring System.

MOR testing was performed using an Instron 3342 with a 500N/ 112 lbs. load cell. A cross head speed of 0.05”/min along with a two-inch span is used for testing. The thickness of the bar at the break is measured in six locations across the break, three on each side of the break; the width is measured twice and averaged. Shells were removed from the PVC pipes and cut into 6” lengths for permeability and burst testing.

3.0 RESULTS AND DISCUSSION

3.1 Shell Conditions During Drying

The entire shell dry condition for 75%RH is shown below in Fig. 1. Temperature is shown on the left axis in orange and relative humidity is shown on the right axis in blue. Both the room condition and the shell condition for both variables is shown, resulting in four curves total. From the figure it is clear that room temperature condition was well maintained and was steady. Shell temperature (in light orange) was shown to vary with evaporative cooling reaching a minimum of 57-60°F wet-bulb temperature. Humidity in the room started at 50%RH initially but dropped to a steady 40%RH eventually. Shell humidity/ dryness was seen to vary from 60% to 95% as measured with the KPI-DRI™ system.

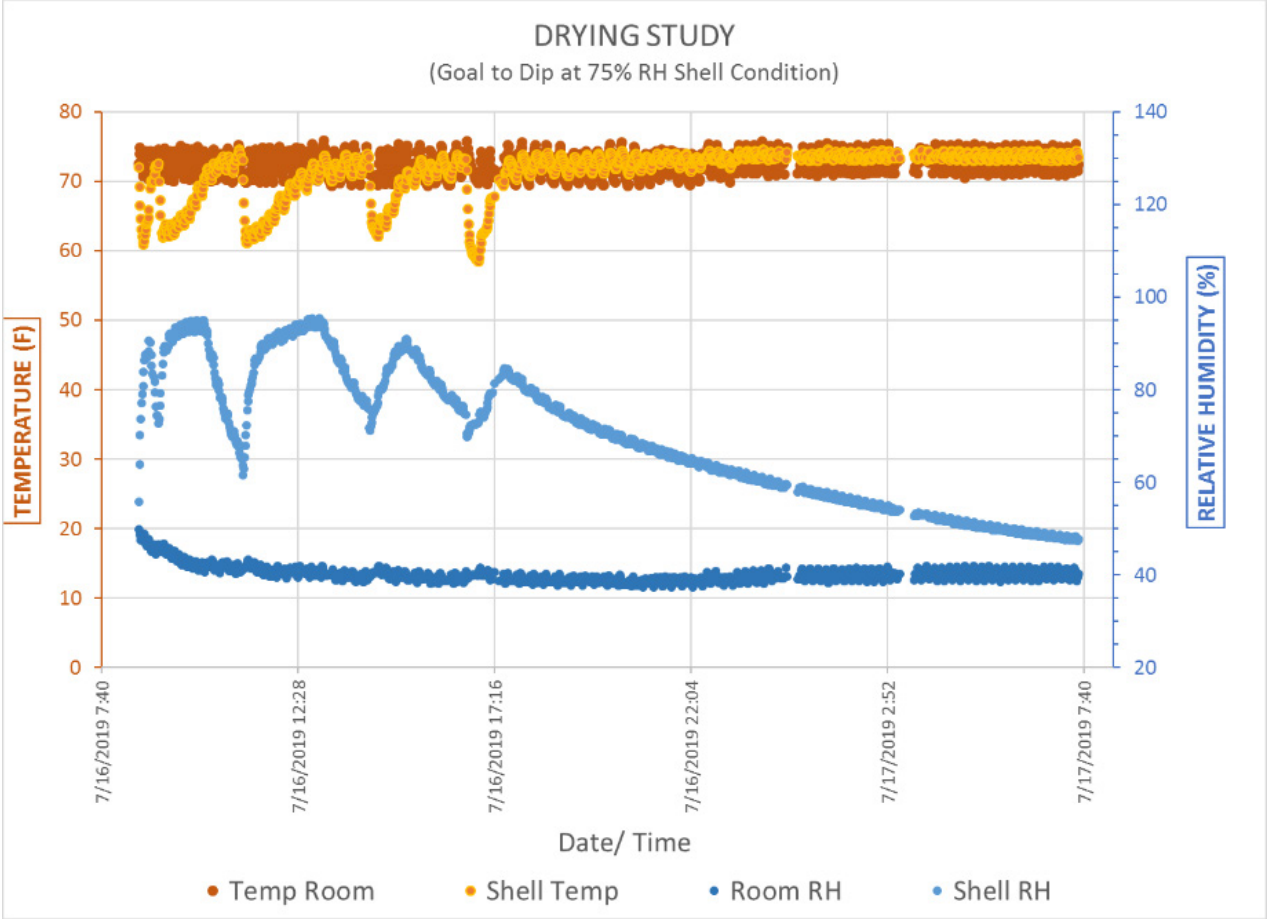

Fig. 1. 75% RH Dryness Level for Dipping.

Below in Fig. 2 the drying condition of shells controlled to 60%RH or higher is shown. Room and shell temperatures are essentially identical to those of the 75% RH condition above. Room humidity was better controlled initially and throughout the entire drying study. Shell humidity/ dryness varied from 60% to 95% between dips.

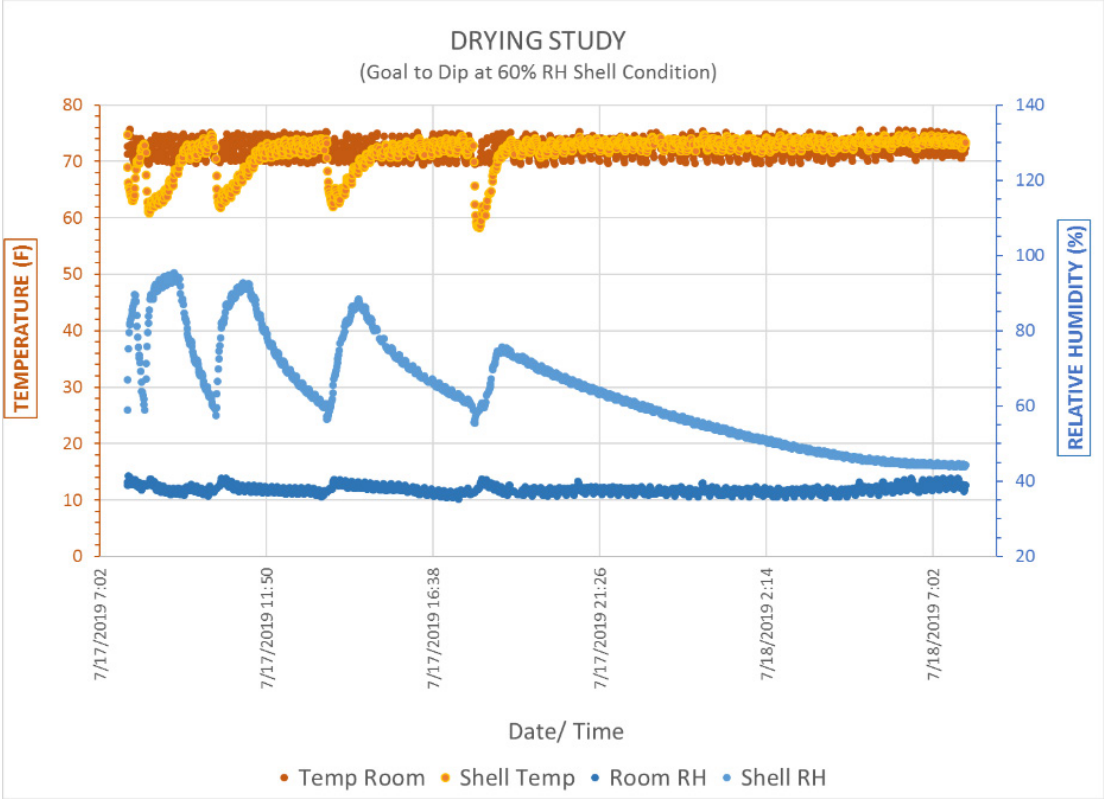

Fig. 2. 60% RH Dryness Level for Dipping.

The most completely dried shell condition is shown below in Fig. 3. Room and shell temperatures were not well controlled during the first day. An unusually dry weather condition rolled through northeast Tennessee which caused much consternation and tweaking to try to maintain the room conditions. As can be seen, it was not terribly successful. However, the temperature and humidity controls were re-established and drying continued as normal. Shell humidity was overall controlled between 45%RH and 95%RH.

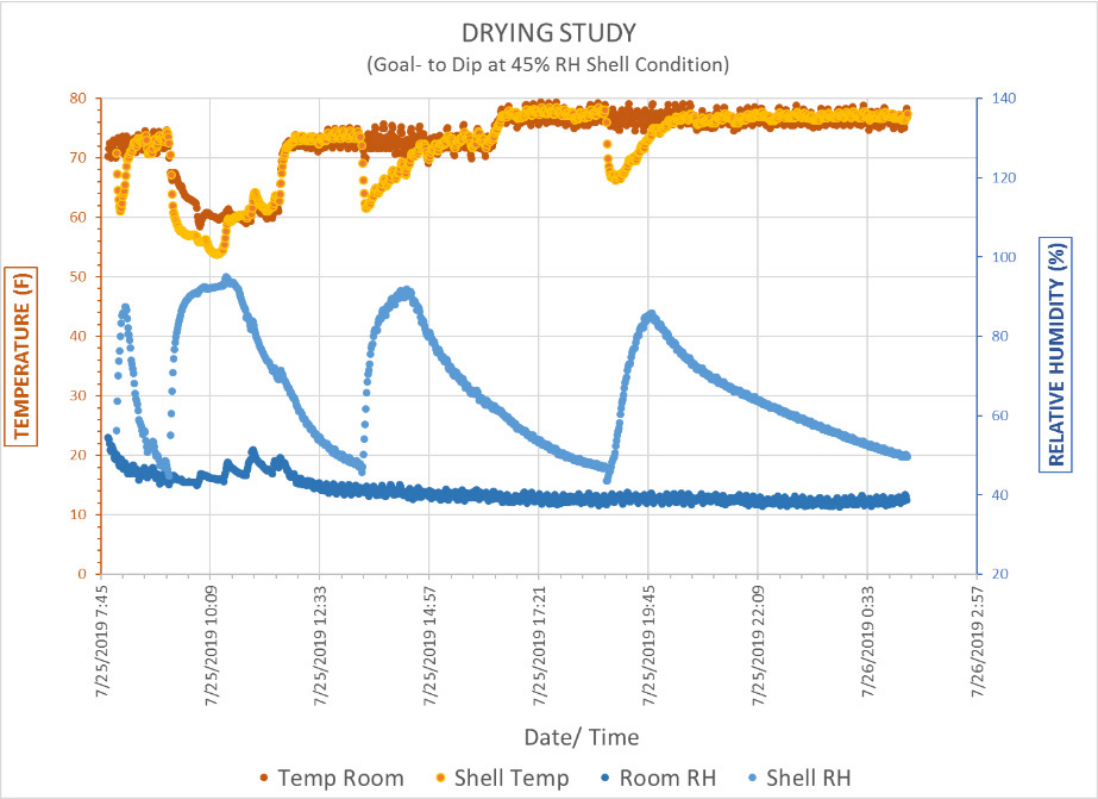

Fig. 3. 45% RH Dryness Level for Dipping.

One interesting point is that even when dipping to 75% RH, the recovery temperature is nearly 100%. This suggests using relative humidity as a dryness indicator on feature-less or simple geometries may not be necessary as it correlates closely with temperature recovery, see Fig. 4 below.

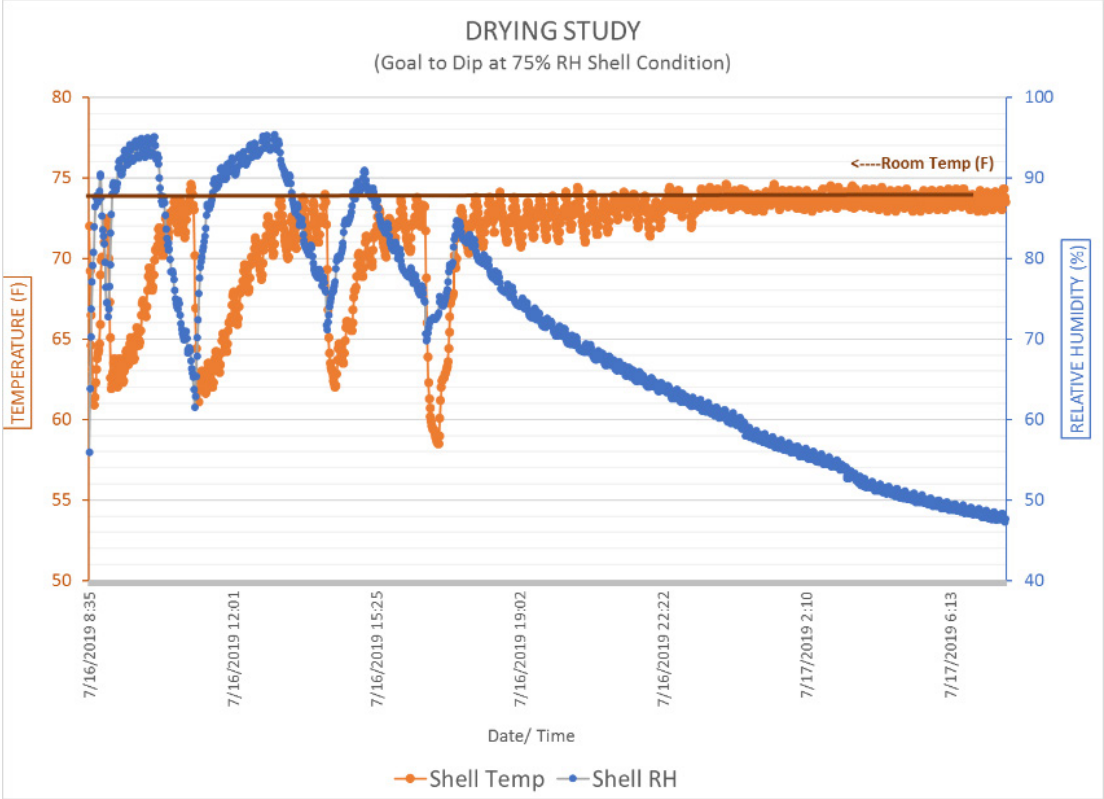

Fig. 4. Shell Temperature and Humidity – 75% RH Condition

3.2 Shell Properties

3.2.1 Shell Thickness

Thickness of shells were measured on both the pipe sections and the MOR bar sections (Figs 5 and 6) and extreme uniformity was seen across all substrates.

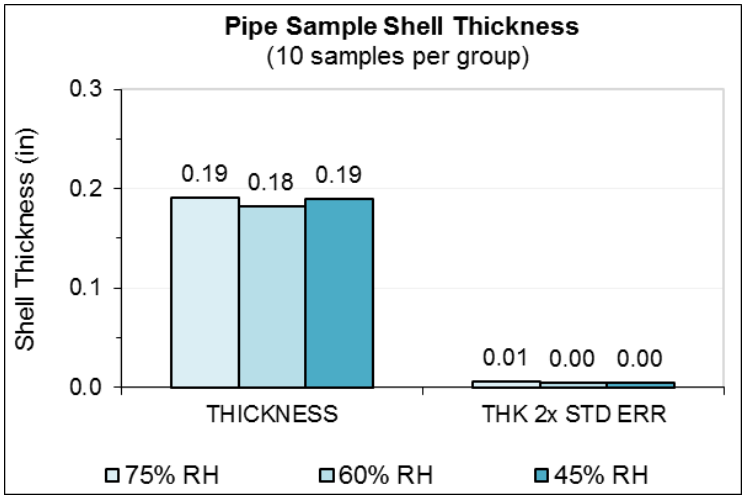

Fig. 5. Shell Thickness Measured from Pipes.

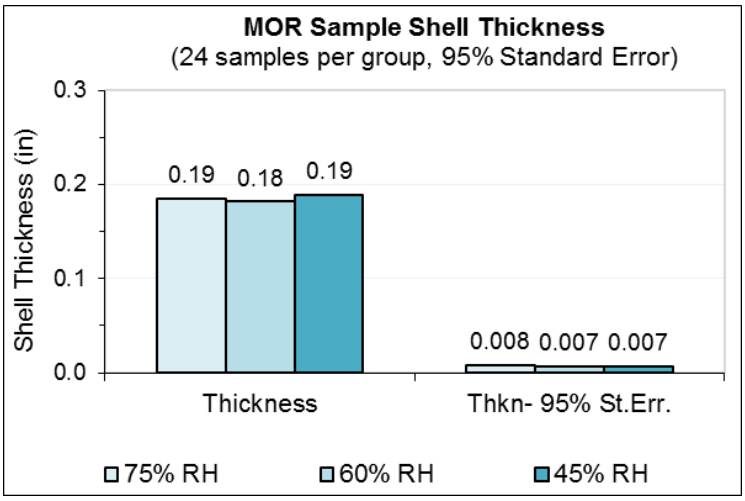

Fig. 6. Shell Thickness Measured from MOR Bars.

4.2.2 Shell Permeability

After pipe sections were measured for thickness, the pipe shells were measured for shell permeability per the Snyder method [7]. Similar to shell thickness performance above, no average discernable difference in permeability was recorded. Results are depicted below in Fig. 7.

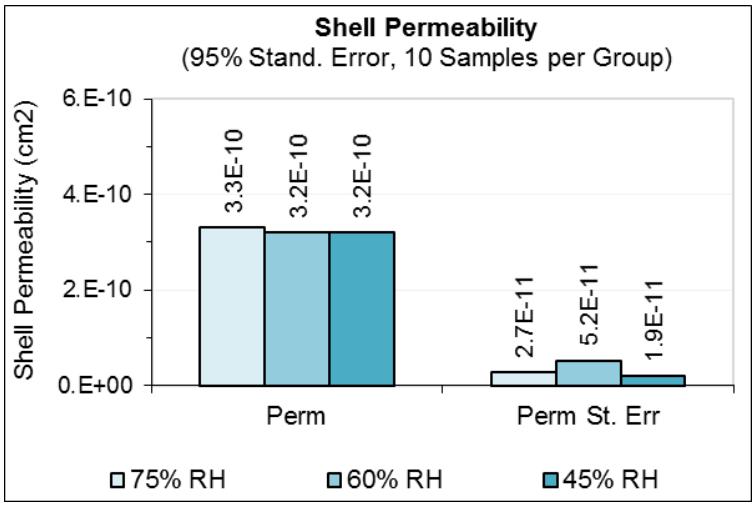

Fig. 7. Shell Permeability Measured in the Green State.

4.2.3 Maximum Tangential Stress Results (Burst Test)

Burst strength of the shell was next measured and is shown below in Fig. 8. Here again, consistent performance was measured with respect to the measured error bars.

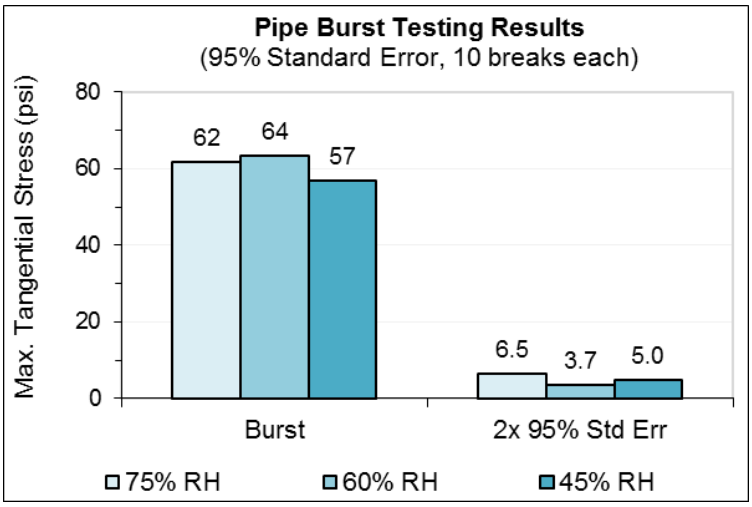

Fig. 8. Shell Maximum Tangential Strength Measured in the Boiled State.

4.2.4 Green Shell Properties

Strength of the shell was measured in the dried, or green state, from MOR bar sections. After the final dry after seal dip of 18 hrs., shells were taken and broken for these results. Strength is depicted below in Fig. 9 where again shell performance was largely unaffected by measured degree of shell dryness. Considering the measured standard error bars, no discernable difference was seen.

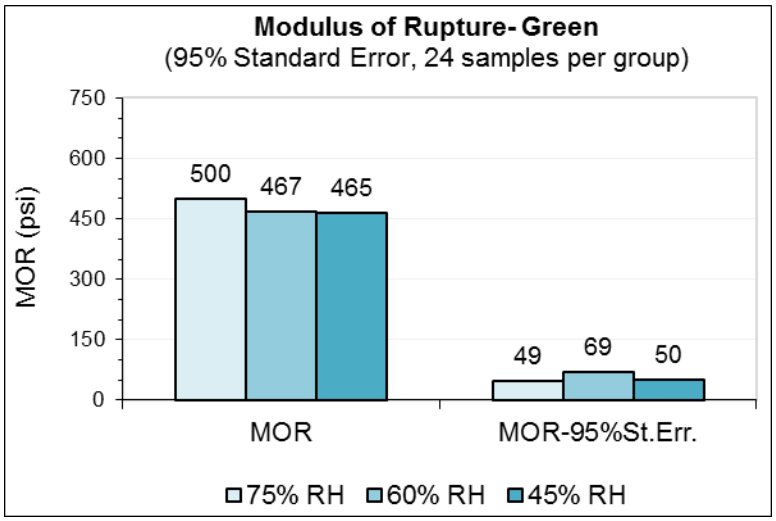

Fig. 9. Green Shell Strength.

Shell rigidity is depicted in Fig. 10 below in the green state. Again, no discernable difference was noted.

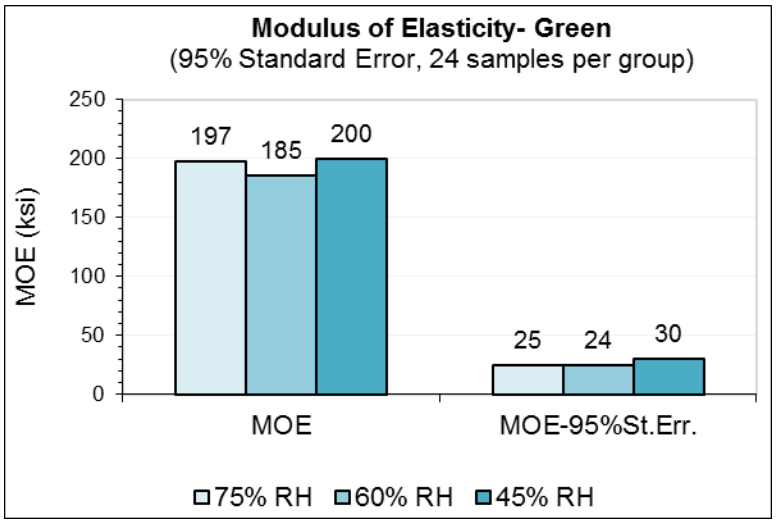

Fig. 10. Green Shell Rigidity.

Load required for shell failure is next depicted below in Fig. 11 where again, respective of the measured errors, no true discernable difference in shell failure loads is seen.

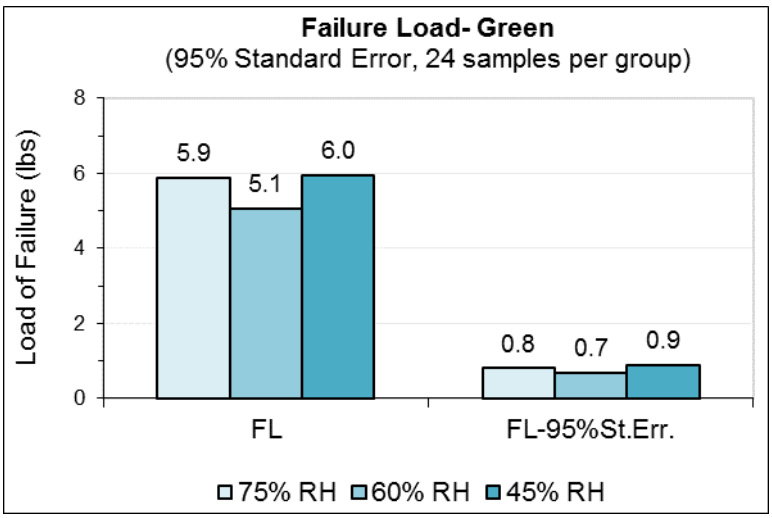

Fig. 11. Green Shell Failure Load.

Lastly, the fracture index in the green state is shown below in Fig. 12. As expected, no trends and no true differences were seen.

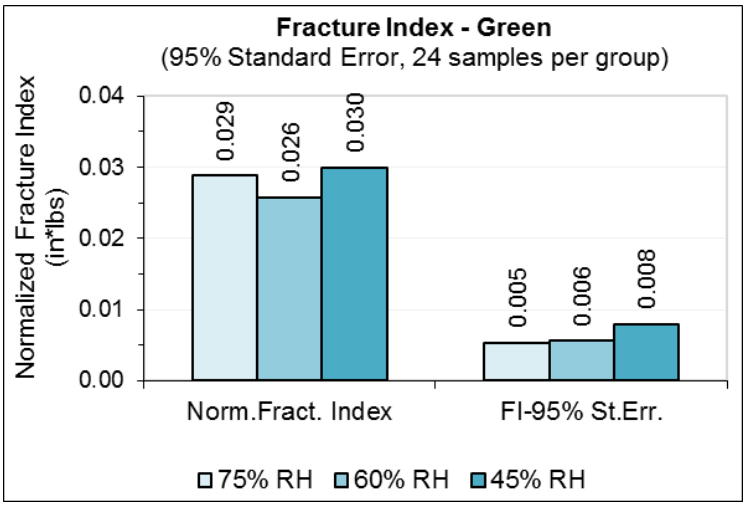

Fig. 12. Green Shell Fracture Index.

4.2.5 Hot/Wet (Boiled) Shell Properties

After a final dry of 18 hrs., shells were boiled for 15 minutes and taken from the water and broken immediately, one break at a time, for these measurements. The 75%RH shells did demonstrate a greater strength than the other two more dried groups. This difference is greater than the measured error bars; however, with no clear trend shown it is difficult to draw any possible conclusions here (Fig. 13).

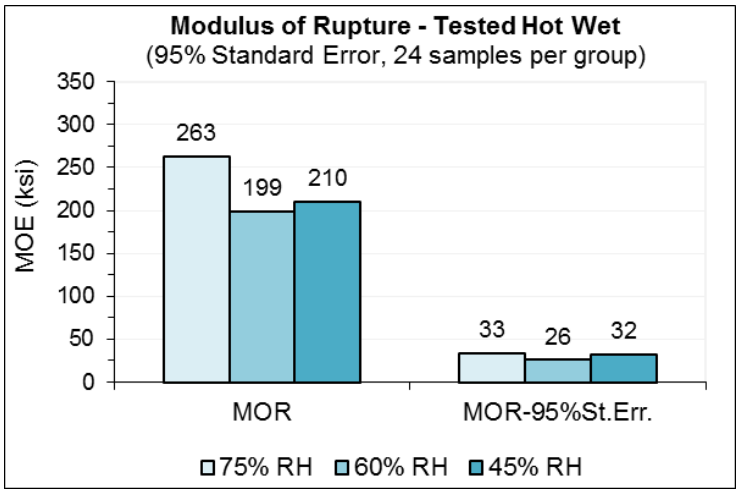

Fig. 13. Hot/wet Shell Strength.

Rigidity of the shells in this boiled and latex softened state is shown below in Fig. 14. Perhaps a slight increasing trend in stiffness is suggested below with a greater degree of shell dryness between dips. No true difference between 75 and 60% RH exists when considering the measured errors, but a numerical trend may exist.

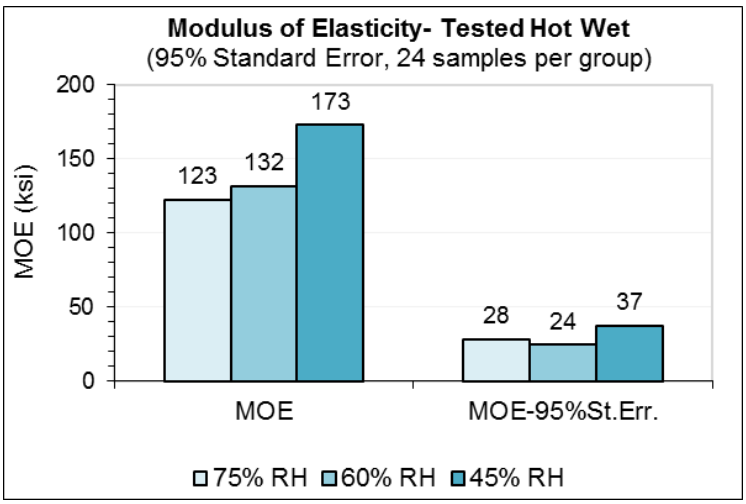

Fig. 14. Hot/wet Shell Rigidity.

Load required for shell breakage in this boiled state is shown below in Fig. 15 where the greatest load was held by the 75% RH sample group. Performance difference here was greater than the measured errors. No difference is shown for the two more dry group averages of 60 and 45% RH.

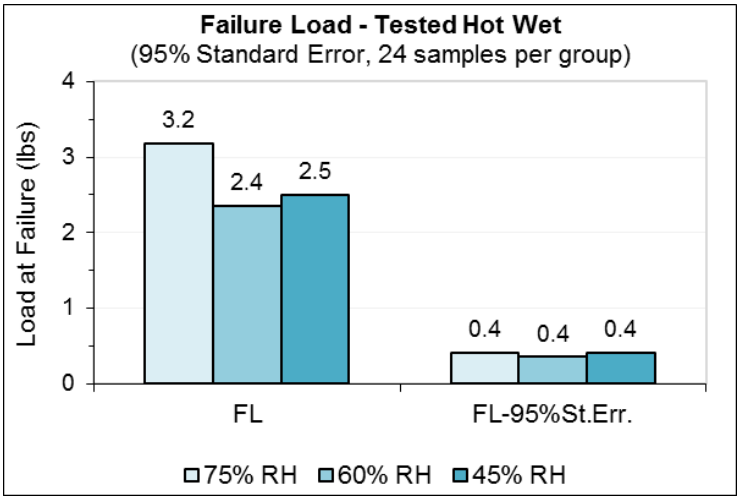

Fig. 15. Load of Fracture in the Hot/wet State.

Fracture index in this state is depicted below in Fig. 16 where again the less dry between dips shell demonstrated best performance. Again, no differnce was realized between the two more dried shell group averages.

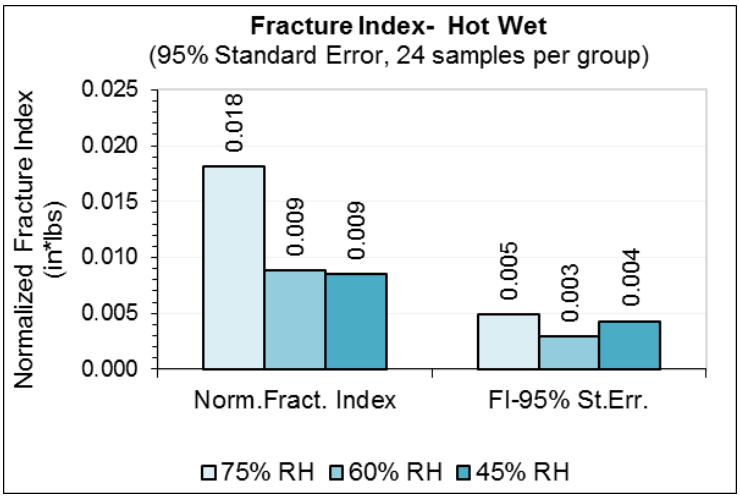

Fig. 16. Fracture Index in the Hot/wet State.

4.2.6 Fired/ Hot Shell Properties

Shell sections were next tested in a fired state where samples were held at 2000°F for a minimum of two hours. One sample at a time was taken out and broken immediately in the Instron while still glowing 'orange/red-hot'. This state is an attempt to duplicate shell condition in the 'metal poured' state. Strength results are shown below in Fig. 17 where no difference was seen between group averages.

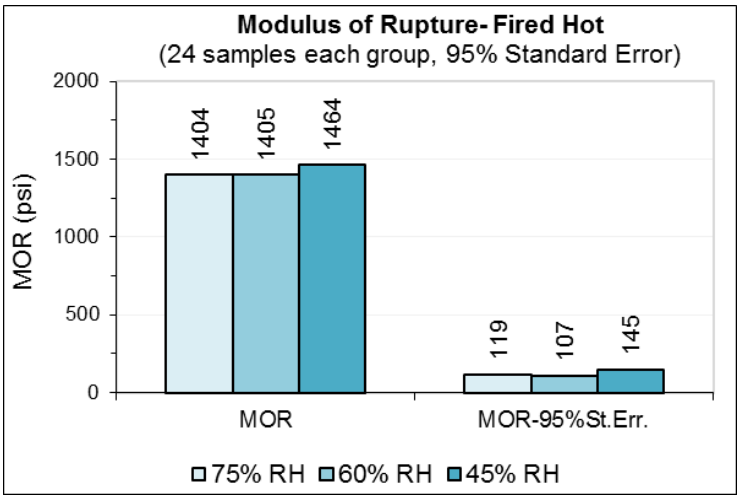

Fig. 17. Shell Strength in Fired and Hot State.

Shell stiffness in this state is shown below in Fig. 18. Shells from the 60% RH group demonstrated the greatest rigidity in this test; however, the high measured error of this

group introduces uncertainty of a true higher value here. All told, little is seen in this test to suggest any trends.

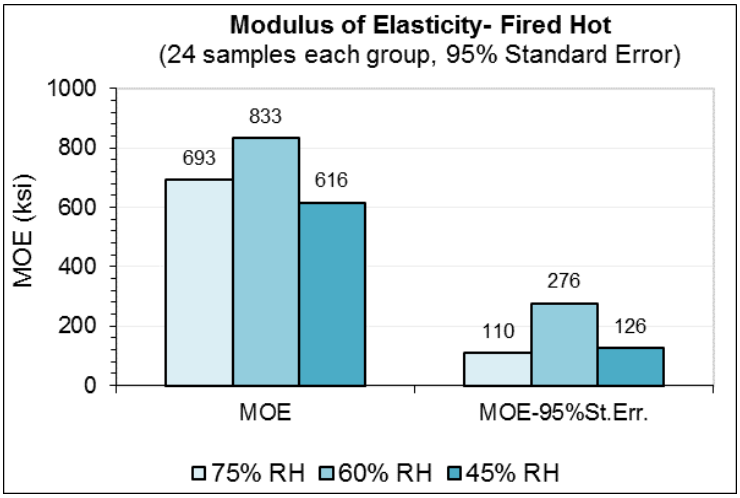

Fig. 18. Shell Rigidity in the Fired and Hot State.

Failure load in this hot state is shown below in Fig. 19 where when considering measured errors, no difference or trend is seen between groups.

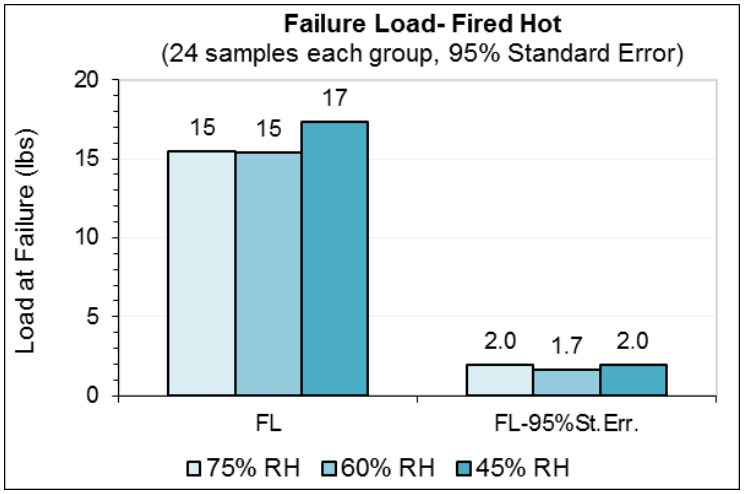

Fig. 19. Shell Load of Failure in the Fired and Hot State.

Shell fracture index was measured and appears below in Fig. 20. Again, differences between groups here is only slighty greater than the measured errors and no trend is seen in these three groups.

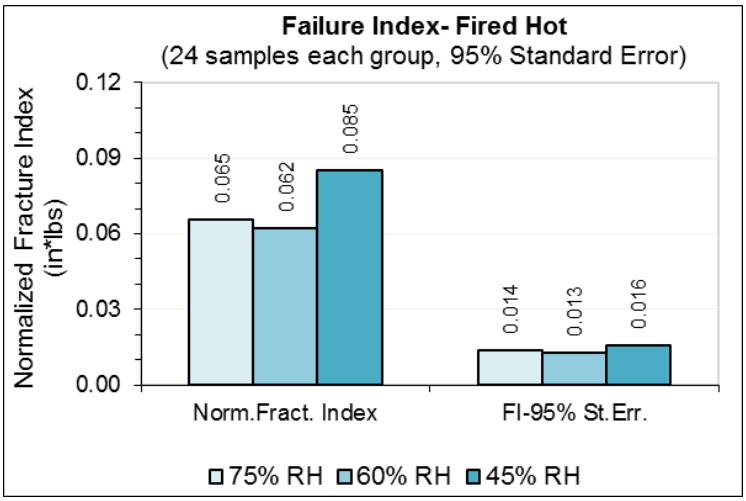

Fig. 20. Fracture Index in the Fired and Hot State.

4.2.7 Fired/ Cold Shell Properties

Shells were tested next in the fired and cooled to ambient state. This best represents the shell 'knock-out' condition where reduced strengths are most desired. Averages of the groups shows the worst performance was recorded for the 75% RH group; however, this group also had the greatest variation in the individual measurements and has the greatest overall standard error. With this factored into the comparison, no difference is realized in this figure below.

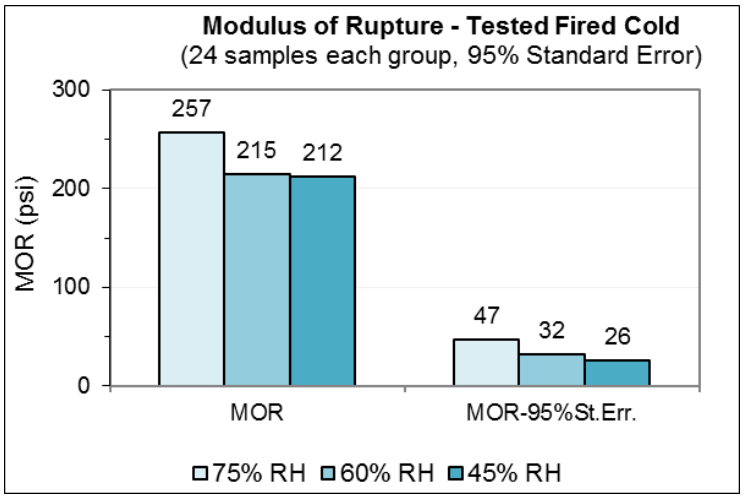

Fig. 21. Fired Measured Cold Shell Strength.

Fired and cold shell rigidity is next shown in Fig. 22 below. The two least dry conditions demonstrate nearly identical performance. The most dry shell group does depict a significant and lower rigidity, especially when considering the error bars.

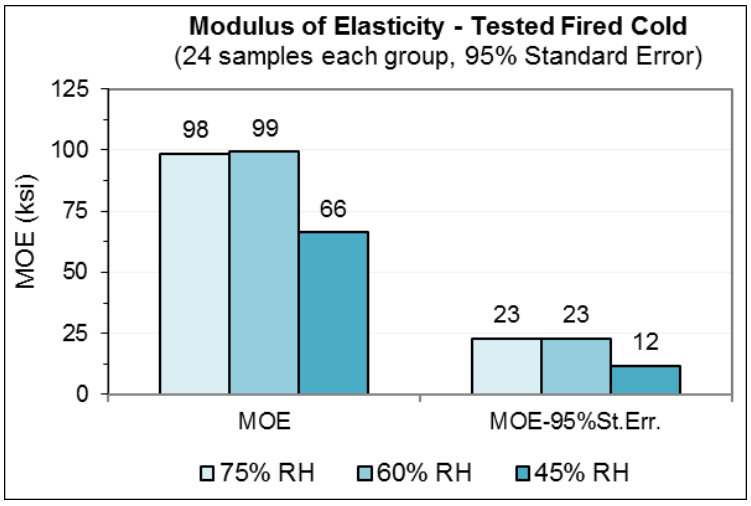

Fig. 22. Fired Measured Cold Shell Rigidity.

Shell load of failure in this knockout state is shown below in Fig. 23. Yet again, differences between group averages is within the measured errors and no trend is apparent.

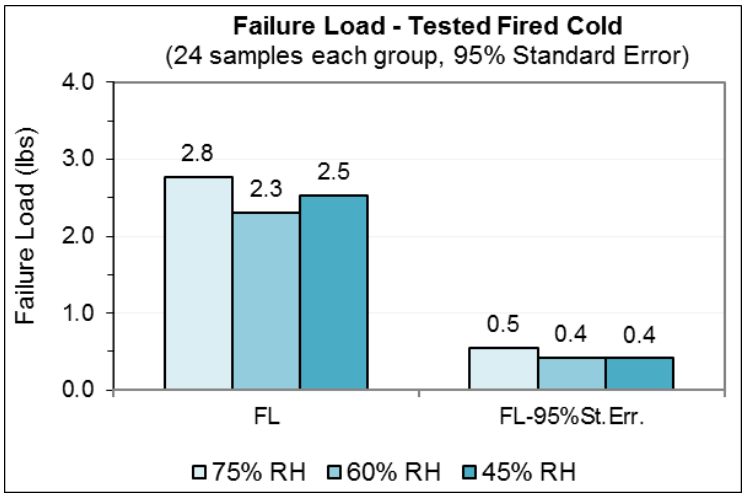

Fig. 23. Fired Measured Cold Shell Failure Load.

Fracture index in this state is shown below in Fig. 24. Measured errors here make any difference between groups here difficult to discern, especially without any apparent trend in the data.

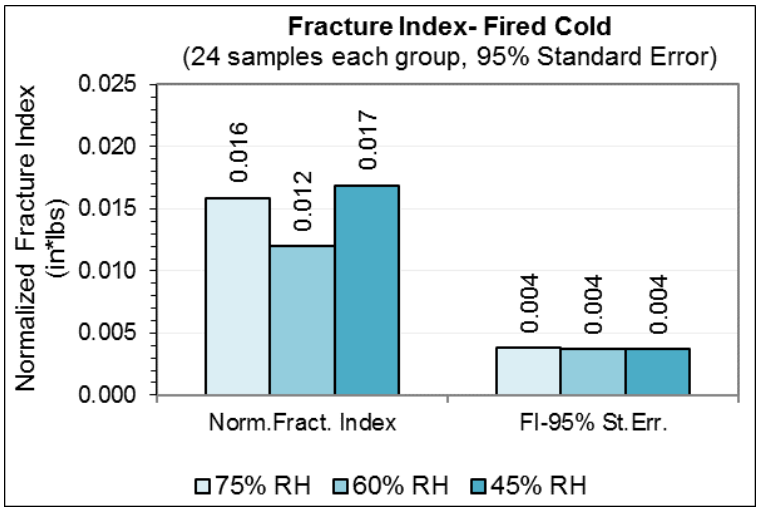

Fig. 24. Fired Measured Cold Shell Fracture Index.

5.0 CONCLUSIONS:

5.1 Differing degrees of shell dryness were achieved but no obvious trends in shell performance in any of the test states were clear.

5.2 This data does show that the temperature reached nearly 100% recovery, even when dipping at 75% RH. Since this is the highest moisture content of the tests, it could be that the data didn't show any differences in shell strength because all molds reached nearly 100% temperature recovery with turbulent air flow.

5.3 Additional tests are being planned to shed more light on shell strength and shell humidity.

6.0 REFERENCES:

1. M. Brienza, et.al. "Intercoat Drying and Shell Properties", 65th Annual Technical Meeting of the Investment Casting Institute, 2018, pp 6:8-20.
2. M. Oyervides, "A Brief Look into MetalTek Wisconsin Investcast's Shell Drying Process", 65th Annual Technical Meeting of the Investment Casting Institute, 2018, pp 6:1-7.
3. R. Tella, et.al. "DePuy Synthes kpi-dry™ Case Study", 65th Annual Technical Meeting of the Investment Casting Institute, 2018, pp 6:21-24.
4. J. Snow, et.al. "Shell Drying- Water Based", 46th Annual Technical Meeting of the Investment Casting Institute, 1998, pp 8:1-30.

5. S. Leyland, et.al. "Implementation of a Water Based shell Mould Investment Casting Process," 9th Annual World Conference on Investment Castings, 1996, pp: 23.
6. J. Markee, "A New Method for Measuring Dryness during the Shell Building Process," 59th Annual Technical Meeting of the Investment Casting Institute, 2012, pp 7:1-9,
7. B. Snyder, et.al. "A New Combination Shell Strength and Permeability Test", 51st Annual Technical Meeting of the Investment Castings Institute, 2003, pp 11:1- 26.

INVESTMENT CASTING INSTITUTE

How It's Made: School of Fish Art Casting

Erich Knoespel
Artcast, Inc.

66TH TECHNICAL CONFERENCE
&
EXPO 2019

Paper № 2

TECHNICAL PAPER

School of Fish, just click print

The process of enlarging sculpture with foundry ready advanced technologies and additive manufacturing methods.

By Erich J. Knoespel, Project Coordinator and Additive Specialist, Artcast Inc.

Introduction

In late 2018, the Royal Botanical Gardens in Burlington, Ontario wanted to create an artwork for their reflecting pond to extend the Dan Lawrie International Sculpture Collection on their grounds. Cobalt Connects, who organized the project, chose Artcast Inc. to complete the project knowing of our experience with enlarging smaller original works into large bronze public sculpture and monuments. The piece that was chosen to be enlarged was *School of Fish* by Kakkee Negeoseak, an Inuit stone carver.

Problem

In the case of *School of Fish,* we had to decide which method of enlargement would work best for the sculpture. At our foundry, we create sculptural enlargements using one of three methods: freehand enlargement, scan-assisted enlargement, and full-digital enlargement. Freehand enlargement is the more traditional method of enlarging a sculpture; however, it is a completely manual process involving potentially inaccurate calculations, human error, and has become more cost-prohibitive unless the artist can do it themselves. The most common technique for us to use is scan-assisted enlargement, which utilizes 3D scanning technology and multi-axis milling equipment. This method does not require a particularly high-resolution scan file as the details can be added with a sculpting medium that is applied to the surface of the milled Styrofoam, typically modelling wax. The manual addition of detail is a labour-intensive process.

Solution

For *School of Fish,* we chose full-digital enlargement. The full-digital method uses a high-resolution 3D scan. A pattern is produced directly from the 3D file. This method allows us to get an accurate wax without the use of rubber molds or additional wax labour. The 3D printed patterns also offer the ability to work with a uniform wall thickness throughout the sculpture, unlike handmade waxes.

Process

Important steps regarding this specific project

Note: The scan file in this case is supplied by the client otherwise it would have been sourced by Artcast Inc.

1. Pricing

   The information available from the 3D scan file allows us to accurately estimate the cost of production as well as plan the project more accurately regarding disassembly for casting and specifics for installation. 3D files offer information such as surface area and volume as well as estimate the final cast weight of the piece in C873 silicon bronze. The use of advanced technologies such as 3D scanning and printing allow the client to save the cost and the storage space required of a rubber mold.

2. Printing

   Material choice in a printed project is critical. For a piece this large and smooth the chosen material was PMMA. The printer used for this project offered a large build volume, modifiable patterns, and excellent burnout properties. Other technologies such as SLA investment casting patterns have excellent surface quality and burnout properties, however, they are not able to be modified to the

same extent as the PMMA patterns and special consideration must be made during shell making and dewax. SLA patterns are a thin shell of plastic with supports on the inside that allow the print to remain rigid until dewax. The thin shell does not allow much material to be removed for modifications and can cause shell cracking during dewax if the shell is not thick enough or if the print has not been punctured to allow pressure from the air tapped in the printed plastic part to escape.

3. Touch Up

Since PMMA is modifiable with standard wax tools we were able to easily add the artist's signature to the top of the piece by carving it into the surface. We also added extra wax around the eyes of the fish to smooth out some faceting that was present due to the original scan resolution.

4. Client Approval and First Looks

The client was able to see a section of the prints that had been tacked together with wax for inspection purposes. With the 3D printed patterns this assembly was not necessary however it was done for documentary purposes. For projects involving handmade waxes, we assemble the wax panels entirely as they are made to ensure that they will fit together properly in the assembly stage later in the process.

5. Gating

Not all printed materials adhere well to our pouring wax. Our pouring wax is the general-purpose wax we use for sprues and making waxes from rubber molds. The pouring wax is reclaimed after steam dewax. For pieces that do not adhere well we use sticky

wax. The PMMA prints do adhere quite easily and no extra care is needed when processing the pieces for gating.

6. Shell Building

School of Fish went through our standard aluminosilicate shell system without any special processing. The prints act exactly as a wax would opposed to other processes such as SLA foundry patterns. SLA patterns are hollow and tend to float during a dip cycle. If the patterns are not adhered well to the gating, then the pattern may detach and float in the slurry tank. Since we hand dip our shells this has not been an issue for us.

7. Dewax

The dewax cycle for our 3D printed patterns varies depending on the material. For instance, the PMMA prints can go through the autoclave with the other 100% wax clusters. The PMMA will not melt out of the shell; however, since it has a negative coefficient of thermal expansion it does not risk destruction of the shell. This allows us to remove any wax used for the gating system as well as the wax used to seal the prints without having to incinerate it. Our preheat/burnout furnaces will incinerate the remaining print material. The incineration of PMMA required higher than average amounts of oxygen in the burn. We remedy this with the addition of air lines directly into the gates and risers of our shells. This addition of air lines was not a new concept for us as it is how we burned out wood for other direct-cast projects.

8. Inspection

Since we had to take special care when dewaxing the printed pieces, we make sure to inspect all of the shells. Normally this means a blast

from the compressed air hose and a visual inspection for any ash or residue.

9. Casting & Chip-off

Pouring metal into shells that once contained 3D printed patterns was not out of the ordinary unless the burn did not successfully incinerate all the remaining PMMA material. If there was still carbon or ash remaining in the shell, we would have had to repair any non-form present on the castings. Otherwise, there is no need to treat these shells any differently.

10. Assembly

The assembly of printed patterns is simple and easy compared to some projects we have worked on where we must make the wax panels by brushing wax into a silicone mold. Handmade waxes often have varying thicknesses and could warp during either the solidification and cooling of the casting or while the piece was assembled for fit in the wax room earlier on in the process. The panels from a printed sculpture may still warp during some stages of the process; however, they are a much closer fit than handmade waxes.

11. Patina

The patina on *School of Fish* is intended to compliment the artist's original sculpture. Often, Inuit sculpture is carved in green or black stone. The patina that was chosen is a combination of a black basecoat with a hand stippled green over top of it. The stippling of the green will give an impression of stone while maintaining the elegant aesthetic of a bronze sculpture.

12. Installation

The cast sculpture itself weighed only 500 pounds. The concrete pedestal it stands on in the reflecting pool is 3000 pounds. The pedestal was lifted into place first, followed by the limestone base, and finally the bronze sculpture.

13. Unveiling

The veil came off the piece, its reflection, enhanced by the setting sun, casting an orange glow on the piece. The sculpture was extremely well-received, and the attendees had nothing but great things to say about the work. Those who were at the unveiling were impressed with how well the sculpture translated from a stone carving into a large bronze fine-art public sculpture. Everyone who was involved in the project, including the artist, was very happy with how the sculpture appears in its final resting place. Although the sculpture was enlarged using advanced technologies, it did not make the final piece any less artistically valid.

Observations

During our pricing process there are calculations we use to estimate how much time is necessary to complete the sculpture. We were impressed with how seamless the process was for *School of Fish* to be cast. The total time in our shop was around two months. The typical timeline for traditional enlargement can be close to six months or more due to the enlarging, texturing, and rubber mold steps necessary to cast the sculpture. This piece has been a proof of concept for ourselves and our clients. The experience of casting enlarged sculpture from printed patterns will play a large role in our planning of large projects in the future.

INVESTMENT CASTING INSTITUTE

How It's Made: Premium Grade Virginia Mullite

Steven Ashlock
Kyanite Mining Corp.

66TH TECHNICAL CONFERENCE
&
EXPO 2019

Paper № 3

How it's Made: Premium Grade Virginia Mullite™

by

Steven Ashlock

Director of Technology and Research

Ceramic Engineer

Kyanite Mining Corporation

Austin Scheer

Ceramic Engineer

Kyanite Mining Corporation

ABSTRACT

The selection of refractory flours and stuccos used in investment casting vary based on the alloy poured, temperature at which they are poured, and the hold time of the alloy at the pour temperature. Within a particular refractory mineral category, deposit characteristics, as well as beneficiation techniques can result in different raw material properties. In addition, varying levels of impurities can greatly differentiate mineral sources among suppliers. Contaminants such as iron (Fe_2O_3) and the alkali/alkaline earths (Na_2O, K_2O, CaO, MgO) can have a dramatic effect on the high temperature performance of investment casting shell molds, impacting casting quality and their as-cast dimensions. For example, impurities in the facecoat can lead to mold-metal reactions that effect the surface finish of the casting (increased rework) and the shell removal. Impurities in the backup layers can lead to decreased strength, increased thermal expansion, and increased creep, which again negatively affect the dimensional stability of castings. Understanding the source of the impurity, the location of impurities in the shell, and their potential impact is crucial to consistent casting quality, yields, finishing labor (rework), and process control

Iron oxide is one of the most problematic impurities in refractories. Iron acts as a flux, causing glassification of the refractory which leads to high temperature creep (shell bulge); ultimately impacting dimensional stability of castings. This paper will focus on the processing of Virginia Mullite™ and how the complex beneficiation process of the ore body produces a consistent raw material with very low iron content. Recent improvements in the purification

process have led to the production of new Premium Grade Virginia Mullite™ which will also be discussed in detail. These process changes have enabled a lowering of the iron oxide content from a maximum of 0.75% to less than 0.2%. Testing was conducted to examine the effects of the lower iron content on the physical properties of the shell. Results indicate that a reduction in iron oxide in the shell refractory leads to increased creep resistance in the shell. This produces a more dimensionally stable casting, improved yields, and help reduce finishing labor costs at the cast house.

INTRODUCTION

Investment casting is the process of creating a complex metal shape by encasing wax in a ceramic refractory shell and removing the wax to create a hollow cavity into which molten metal can be poured. The shell must be able to withstand the high temperatures and pressure of the investment casting process and maintain its constant shape (pattern geometry) in order to produce dimensionally consistent castings. There are many refractory raw materials used in the investment casting industry today; some of these include zircon, alumina, fused silica, and aluminosilicates. Each material has its advantages and disadvantages that must be considered when selecting a mold material. Physical properties, such as maximum usage temperature, creep resistance, strength, thermal expansion, cristobalite formation (health and safety), and the overall relative cost must be considered.

Selecting the proper raw material type is the first step; the second is to compare different sources. The obvious and initial consideration is cost and availability, but the origin of the raw material is of great importance. No two deposits are identical in terms of purity and performance. The naturally occurring purity of the deposit, the amount and type of impurities, mining techniques, and mineral processing techniques can vastly affect how the material will perform in the shell and ultimately impact the scrap rates and the quality of the casting.

A good example of how the differences in natural geology and processing techniques affect the performance of the material can be seen in the aluminosilicates. As the name suggests, aluminosilicates are minerals made up of alumina and silica in various ratios. Pure silica and pure alumina are both very refractory raw materials but have their drawbacks. Pure silica has a high melting point of 3135°F (1723°C).[1] However, impurities in silica act as a flux and drastically reduce the melting point, forming glass. This glass will begin to soften and flow which will affect the dimensional stability of the shell and can cause it to bulge. This can lead to castings that are out of dimensional tolerance. Impurities in a face-coat can result in a glassy phase sticking to the surface of the casting leading to surface defects, scrap, or increased rework. Alumina is also a highly refractory material with a melting temperature of 3730 °F (2054°C).[1] It is one of the pillars in the world if ceramics for its high temperature properties and is more resistant to fluxing than silica. However, pure alumina performs poorly under thermal shock conditions. This can lead to shell cracking and positive metal defects on the as-cast surface.

One way to combat the potential issues of pure silica and/or pure alumina is to mix the two materials together. In Figure 1, you can see the Silica-Alumina phase diagram.[2] There is only one thermodynamically stable intermediate phase in the alumina-silica system: mullite. The ratio of three parts alumina to two parts silica makes stoichiometric mullite with an alumina content of 72 weight percent. While the melting temperature of mullite is lower than alumina, it still exhibits excellent high temperature properties. Mullite has a melting point of 3435°F (1890°C) and is one of the best refractory ceramics for thermal shock resistance.[1]

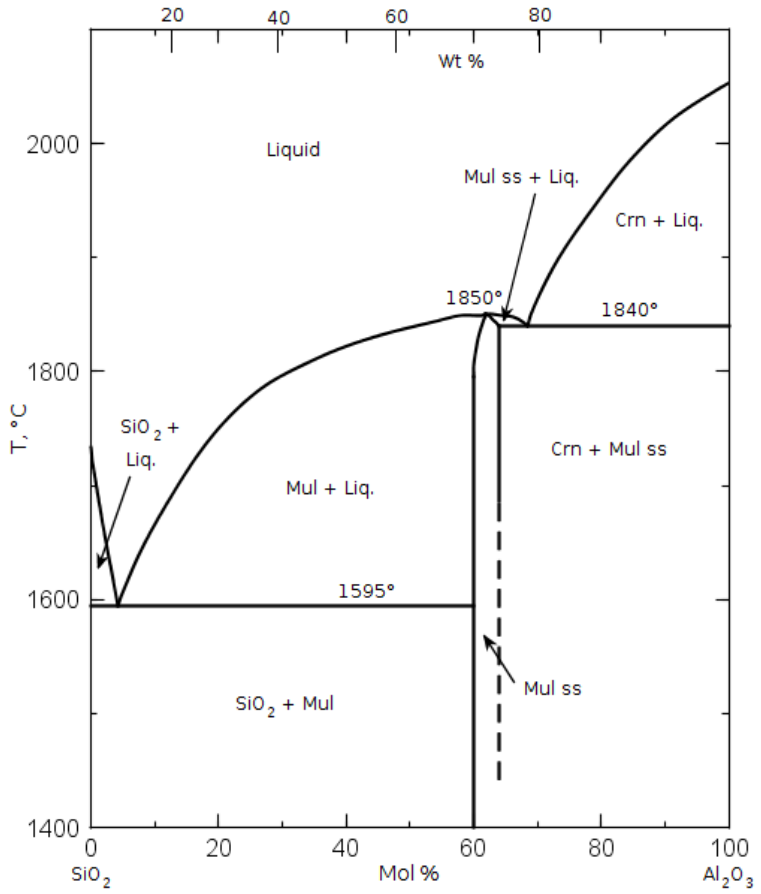

Figure 1: The Alumina-Silica Phase Diagram can be used to determine the hot properties of materials containing different ratios of alumina and silica.

Pure mullite is rarely found in nature due to its high temperature/low pressure formation conditions. The first samples of the 3:2 aluminosilicate were discovered by Bowen and Grieg in the 1920's.[3] They noticed the material in lava flows on the Isle of Mull where clay sediments had come in contact with the hot magma. The new mineral was given the name after the island.[3] Its rarity as a naturally occurring mineral means that it is not mined for industrial purposes. While not stoichiometric mullite, there are many different aluminosilicate minerals. Examples include the clay minerals (kaolin, mica, pyrophyllite, etc) and the sillimanite group of minerals.

Mullite used for industrial purposes must be created using precursor minerals. There are two main methods: in-situ mullite formation and the creation of mullite aggregates. Examples of mullite creation in situ in ceramics go as far back as 1500-1000 BC in Chinese pottery.[3] In situ formation of mullite is a common practice in the ceramics industry to this day.

The investment casting industry uses mullite in both aggregate and powder form. Most of the aggregate mullites in the industry today are made by mixing, extruding/spheredizing, and calcining clay minerals to form the mullite. These aggregates can then be ground to make the flours used in slurries. These mullites are frequently categorized by their overall alumina content. Mullites with alumina contents ranging from 40-70% are commonly found throughout the industry. The major mineral phase of these aluminosilicates is mullite with the remainder comprised of either quartz, cristobalite, or amorphous silica. Selecting the appropriate alumina percentage is critical in order to achieve the desired properties of the mold at temperature. It is commonly believed that the higher the alumina content, the higher the maximum usage temperature of the mullite. While this is generally true, the impurities in mullite can have a greater effect on the usage temperature than the overall alumina content.

While making mullite from clays is the predominate method of obtaining mullite, it is not the only way: industrial grade mullite is also made by calcining the sillimanite family of minerals. The sillimanite family of minerals are aluminosilicates with a 1:1 ratio of alumina and silica. The three industrially important members of the mineral family are kyanite, sillimanite, and andalusite. These three minerals are all polymorphs of the 1:1 chemical composition. The pressure and temperature of formation determines which of the minerals is created. The Pressure-Temperature phase diagram, Figure 2, is shown below.[4]

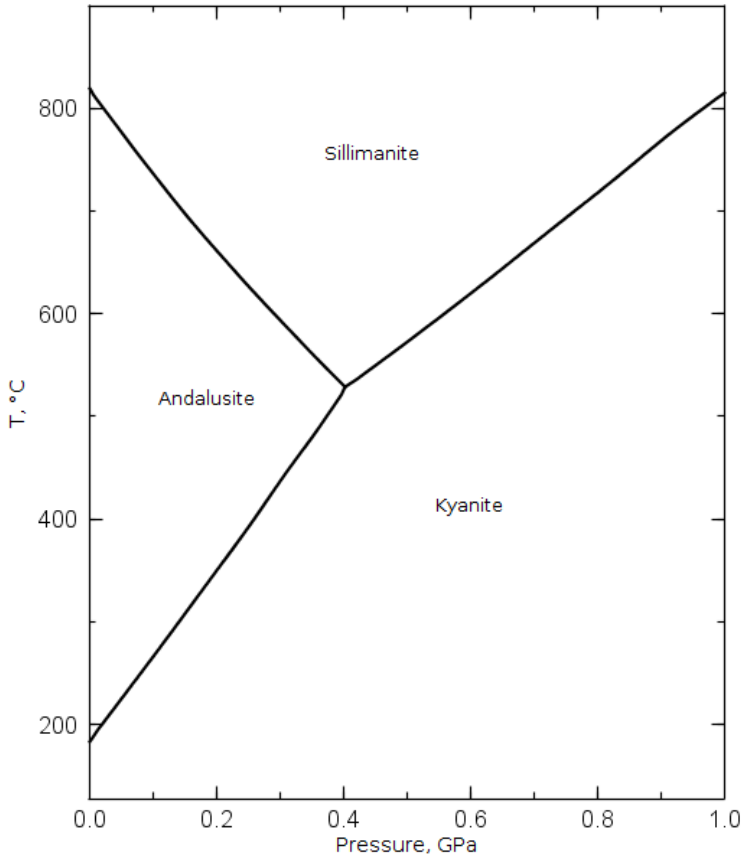

Figure 2: This Pressure-Temperature Phase diagram shows the conditions required to form the different minerals in the sillimanite group.

When heated, the sillimanite group of minerals undergo a phase transformation to mullite plus excess silica. This reaction is shown in Equation 1.

$$3(Al_2SiO_5) \xrightarrow{heat} 3Al_2O_3 \cdot 2SiO_2 + SiO_2 \quad (1)$$

The temperature of this phase transformation differs in each of the three sillimanite minerals.[5] When heat is applied, the Al^{3+} cations change coordination number. This causes the rearranging of the atoms to form the more open crystal structure of mullite. The kyanite crystal structure is the least ordered of the three and thus has the weakest chemical bonding. This means it requires the least heat energy for the phase transformation to begin. Table 1 shows the conversion temperatures and theoretical expansion rates of the three minerals as they convert to mullite.[6] The lower temperature requirement for conversion makes kyanite an ideal candidate for the production of mullite.

Table 1: Conversion characteristics of the sillimanite group minerals.

	Temperature of Full Conversion	Theoretical Expansion
Kyanite	2550°F (1400°C)	17%
Sillimanite	3090°F (1700°C)	6.2%
Andalusite	2910°F (1600°C)	4.1%

VIRGINIA MULLITE™: HOW IT'S MADE

The Deposit

In order to understand how to make Virginia Mullite™, we must first explore how its precursor mineral, Virginia Kyanite™ is made. The first requirement for mining and refining industrial grade kyanite is to find a source mine. Silica and alumina are the two most abundant oxides on planet Earth, making up 59% and 15% of the earth's crust respectively.[7] Yet, finding these two oxides in the correct ratios (that have been subjected to the necessary heat and pressure regimes) to form the sillimanite family of minerals is more uncommon. However, that is not to say that the sillimanite family of minerals are rare. They can be found on almost every continent on the Earth. What is rare, is a deposit that is not only large enough to be economically viable, but one that has a high purity ore body. Pure in this sense typically means not only lacking in impurities but also the other sillimanite minerals. Once such a deposit has been found, the real testing begins. Even if a deposit is large and pure, it does not mean that it will be able to produce industrial grade material. The geology of the deposit and the other minerals present will determine how difficult it is to remove the kyanite from the ore body and its associated minerals-even in trace amounts. When it comes to kyanite, Willis Mountain in Dillwyn, VA is a world-class deposit that is suitable for the production of industrial grade kyanite. The mining and production of industrial grade kyanite (and mullite from kyanite) has taken place at Willis Mountain for over 60 years.

Willis Mountain is located in Central Virginia about seventy miles west of Richmond and fifty miles south of Charlottesville. The Willis Mountain deposit resides in the geological occurrence known as the Whispering Creek Anticline. The deposit is made up of two halves: Willis Mountain itself and East Ridge, which is the other half of the anticline. The deposit was formed around 465 million years ago during the Middle Ordovician Period.[8] The predominant theory is that venting of mineral rich fluids deposited clay minerals. That material was subducted to a depth conducive to form the minerals seen today. The deposit was then thrust upwards to the surface and then truncated which created the exposed east and west legs of the formation.[8] The ore body is made up of kyanite-quartzite rocks.

Willis Mountain rises 475 feet above the surrounding countryside and runs for about 1.75 miles. The ore body contains 20-30% kyanite. The main impurities are quartz, several varieties

of mica, iron oxides, iron sulphides, and a multitude of minor minerals. The deposit runs near vertical through the entire height of the mountain, and is, generally, 120 yards thick through its entire length. Willis Mountain has been continuously worked since the late 1950's, but the majority of this large orebody remains untouched to this day. It is estimated that well over 50% of the Willis Mountain ore remains.

The East Ridge deposit, adjacent to Willis Mountain, also runs for 1.75 miles. The ridge is shorter than the mountain, rising up from the surrounding countryside about 300 feet. The East Ridge deposit contains more impurities than the deposit on Willis Mountain. Higher amounts of iron sulphides and clay minerals are common, and a wider variety of iron oxides and micas are seen. The vein at East Ridge is also thinner than the Willis Mountain vein and runs at a 30° angle instead of vertically. Mining at East Ridge began in the late 1970s, and substantial reserves remain in this part of the orebody also.

The lifetime of these two Virginia deposits is difficult to assess and has never been definitively determined. It is clear that there is enough exploitable ore to continue mining for many generations at current production rates.

Mining and Comminution

Mining is done from both the above-mentioned deposits on a single daylight shift, five days a week. Blasting occurs as needed but typically happens once or twice a month at each deposit. Blasting is done by filling drilled holes (usually roughly 30 feet deep) with a liquid explosive. Rocks that remain too large to move after the blast are broken down by a rock breaker. Loaders pick the material up and put it in the back of haul trucks that bring the material to a single jaw crusher where the ore from various parts of the two quarries is blended together. The average kyanite percentage of the ore runs around 20-25%, which means that roughly 650,000 tons of ore must be mined and processed each year to meet the 100,000 – 120,000 tons of annual demand for the company's purified kyanite and mullite products.

The first step in the comminution process is a large jaw crusher, where rocks weighing several tons each are reduced in size to ones weighing only a few dozen pounds. After this, the material passes through several further stages of crushing (mainly gyratory) and screening to progressively reduce the size of the ore to roughly one inch by down in size.

Wet Processing

After dry comminution, the ore stream is fed into what is called the Float. It is called "the Float" as several of the steps in the wet processing of the material involve froth floatation, but many other size reduction, size sorting, and beneficiation technologies are involved in the removal of impurities in this part of the process. This wet processing, as the name suggests, is very water intensive, using 7,000 – 8,000 gallons per minute, and runs 24 hours a day, usually for five days a week. There are well over twenty steps in this part of the beneficiation circuit (rod

mills, ball mills, hydro-sizers, hydro-cyclones, screens, float cells, spirals, extractors, etc.), and at the end of the elaborate set of mineral purification steps the all the various forms of clay & dirt have been removed, as have almost all of the pyrite and mica. Alkali and alkaline earth oxides have been reduced to less than 0.05% and the titania to around 1.5%. The quartz content has also been reduced to 4-6%. The iron oxides are the only impurity that have been left untouched in this part of the process, and they make up anywhere from 5%-10% of the "float concentrate" at this point in the process. Their removal takes place at the next part of the beneficiation process.

Dry Processing

The removal of the various naturally occurring forms of iron occurs in the dry processing phase of the company's beneficiation circuit. The damp "float concentrate" is dewatered in several steps, and then is fed into a fluid bed dryer, being mixed and blended along the way. The homogenized material falls into the top chamber of heated fluidized bed, similar to those used in stucco application at some foundries, where the material is fully dried. It then makes its way into another chamber of this vessel where it is heated to over 1000°F (540°C) before undergoing a special process to convert all of the various iron oxides into a magnetic form. After which, the kyanite/iron mixture is cooled in a rotary cooler. Once it has cooled down to less than about 250°F (120°C), the material is run through several banks of magnets: some low intensity permanent magnets, some high intensity variable magnets, as well as some rare earth magnets. These banks of magnets bring the total iron content down into the 0.4%-0.6% range. This part of the process runs for extended campaigns 24 hours a day, seven days a week in order to prolong the lifetime of the refractories.

Recently, new processes have been developed in order to further reduce the iron content of a portion of the company's kyanite production. This has allowed for the production of an even lower iron oxide product: Premium Grade Virginia Kyanite™. The iron oxide content in this material is less than 0.2%. It is these new separation techniques that create the lower iron oxide containing kyanite which is the precursor for Premium Grade Virginia Mullite™.

Calcination

The Premium Grade Virginia Kyanite™ is taken by truck to one of our two calcination plants. The kyanite is put through a rotary kiln where it is exposed to temperatures in excess of 2700°F (1480°C). There are three kilns in operation. The heating of the kyanite causes the crystal structure to rearrange and form mullite, as previously discussed. This reaction was shown in Equation 1. The silica produced as a byproduct of the reaction is very fine and amorphous. This amorphous particle is stuck to the side of new mullite crystal blades. When kyanite is converted to mullite it expands seventeen volume percent. The mullite also maintains the very high aspect ratio (acicular or needle shape) of kyanite through the conversion.

Grinding and Sizing

After calcination the Premium Grade Virginia Mullite™ will take one of two routes: screening for stuccos or milling for flours. To make the stuccos, some of the mullite is sent over vibratory sieves. This is a multi-deck sieve stack that creates both the 20x50 and the 50x100 stucco products. The elongated needle shape of the mullite makes this a difficult process to control because the blades can stand on end and pass through the screen. Controlling the feed rate and vibration frequency are very important to maintaining a consistently screened product.

The rest of the Premium Grade Virginia Mullite™ goes to a special ball mill for grinding. This ball mill is lined with granite and uses alumina milling media. Using steel balls or liners would negate the effort put into making a lower iron product. The material exiting the mill passes through an air classifier to send any large particles back to the mill for further grinding.

Testing

Testing throughout the process is vital to make a consistent product. Testing begins at the mill side of the float to determine the kyanite percent of the raw ore. Dozens of tests are done in the flotation building to check on the level of beneficiation of the kyanite from the other minerals. At the dryer, particle size testing is done to check the coarseness of the product. A field XRF unit is also used to monitor the iron removal process. Helium pycnometers are used at the kilns as a field test to check to see if the kyanite was completely converted to mullite during the calcination process.

All material is sent to the main Quality Control Lab for final testing. Each bag of product is tested for particle size distribution, chemistry, and mineralogy. For stuccos, a Ro-Tap is used to screen size the product. For finer meshes, an air sieve is used. Laser light scatter analysis can also be done on the flour products using a Microtrac particle size analyzer. Chemistry is checked on an x-ray fluorescence analyzer. An x-ray diffraction unit is used to check the mullite for any unconverted kyanite and determine the presence of other minerals or compounds of interest, such as cristobalite content.

WHY IT MATTERS

Producing mullite by beneficiating kyanite from the ore body and then calcining is a time consuming and meticulous multi-step process. However, the effort is worth the time and resources spent as this method of mullite production creates a final raw material with some unique and useful properties. There are several differences between mullite made via calcination of kyanite versus mullite made from calcining clay minerals. For one, each individual mullite crystal produced comes from a kyanite crystal instead of an agglomeration of crystals. This allows the mullite particles to have a high aspect ratio. When agglomerated to form an aggregate, the natural aspect ratio of mullite is neutralized by the shape of the aggregate. Kyanite is a blade

shaped mineral. Mullite made from kyanite maintains this aspect ratio throughout calcination. The high aspect ratio of the particles has been shown to increase hot MOR strength, reduce mold splits (cracking), and has led to the reduction of the number of backup coats needed on the mold.

Another difference is the homogeneity of the mullites. Impurities in mullites produced from clay minerals are often well dispersed throughout the entirety of the aggregate. While homogeneity is typically a good thing, this can be a detriment concerning creep resistance. If the impurities are dispersed throughout the material, then the aggregate will creep. Mullite from kyanite, on the other hand, is a single blade particle. The impurities in the material are stuck to the sides of the kyanite/mullite crystal surface and are thus localized. This means that a small area of the grain may creep, but the rest of the crystal, where the impurities are not located, will not. Stacking several of these blades together will spread that creep around and lead greater creep resistance than a typical blended aggregate mullite material.

While mullites generally exhibit excellent creep resistance, the iron content limits the maximum usage temperature before the on-set of creep. Iron oxides act as a flux when combined with silica which drastically lowers the melting and softening point. This forms glass, which is fluid, and allows the shell to creep. It is shell creep (bulge) that can lead to poor dimensional control so castings may be out of tolerance to customer specifications without additional rework. Small changes in iron content can have very large effects on the usage temperature and the stability of the shell. This concept is what led to the production of the Premium Grade Virginia Mullite™. This material has an iron content of less than 0.2% vs the standard Virginia Mullite™ that contains a maximum of 0.75%.

Dilatometer testes were done in order to examine the effect of iron on the creep resistance of various mullites. A listing of these mullites can be found in Table 2. The alumina, silica, iron, and the alkali/alkaline earth oxides contents are shown. Attempts were made to test materials with a wide variety of alumina contents. The dilatometer temperature profile is shown in Table 3.

Table 2: Chemical Analysis of the materials tested.

Name	Al_2O_3	SiO_2	Fe_2O_3	Alkalis/Alkaline Earth
Premium Grade Virginia Mullite™	56.08	43.8	0.18	0.05
Virginia Mullite™	55.25	43.08	0.44	0.06
M 1	66.74	28.40	1.23	0.16
M 2	61.92	33.51	1.27	0.13
M 3	52.38	43.98	0.94	0.17
M 4	48.10	49.79	0.77	0.46

Table 3: Heating profile used during the dilatometer testing.

Segment	Ramp Rate °F/min (°C/min)	Temperature °F (°C)	Dwell Time (min)
1	9 (5)	212 (100)	0
2	36 (20)	2550 (1400)	60
3	36 (20)	77 (25)	100

Figure 3 shows the temperature vs change in length dilatometer curve. The thermal expansion on all samples is very similar up until 2010°F (1100°C). This indicates that all of the sample materials could be used for the same molds due to similar expansion until 2010°F. But after this temperature, performance begins to differentiate among sources. M3 begins to soften and its expansion slows. The next decrease in the thermal expansion occurs in sample M4 at 2280°F (1250°C). It is not surprising that these are the two samples that begin to soften first as they have the lowest alumina contents. The only material that does not show a significant slowing of thermal expansion is the Premium Grade Virginia Mullite™. This can be explained by it having the lowest iron oxide among the samples tested. There is less iron to flux the silica which limits glass formation and extends the maximum usage temperature.

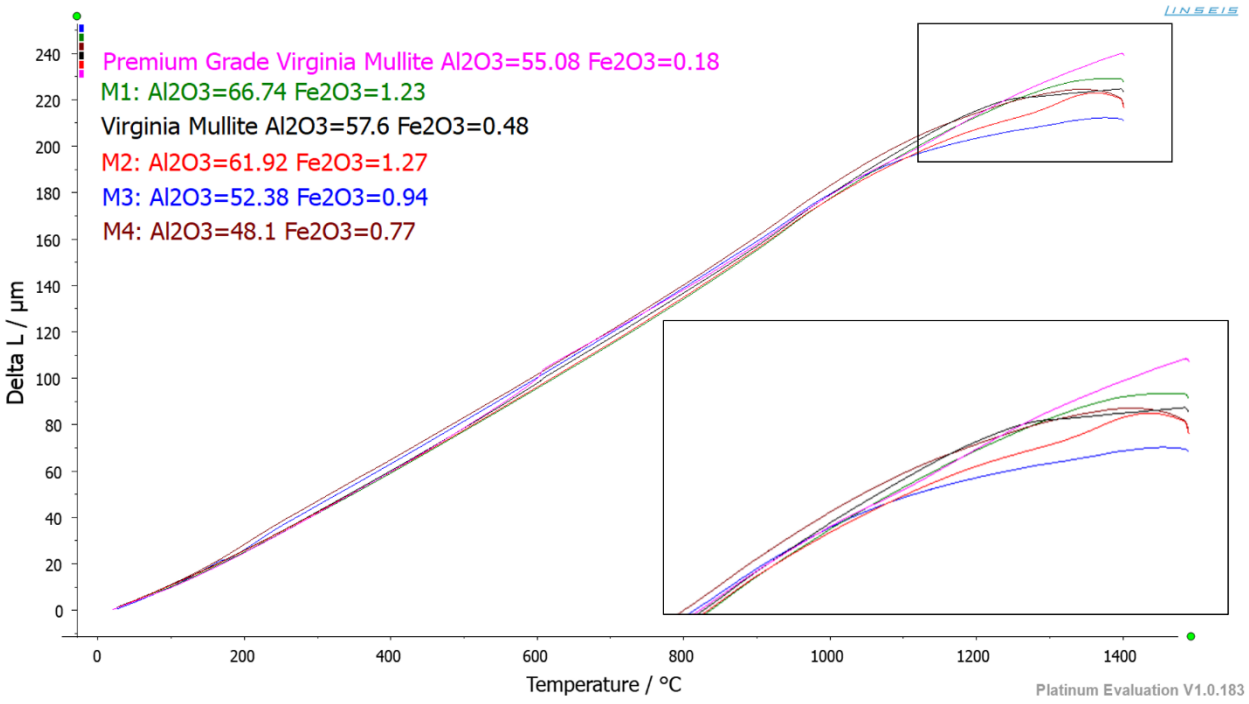

Figure 3: The expansion versus temperature curve is used to determine the thermal expansion of the various mullites.

Changing the x-axis from temperature to time allows for an examination in the creep characteristics of the materials. Each mullite was held at 1400°C for one hour with constant pressure applied by the dilatometer. This, in essence, is a quasi-creep test. Looking at the differences in change in length at the start versus the end of the hold can shed light on the creep resistance of each mullite. The dilatometer curve with this data is shown in Figure 4.

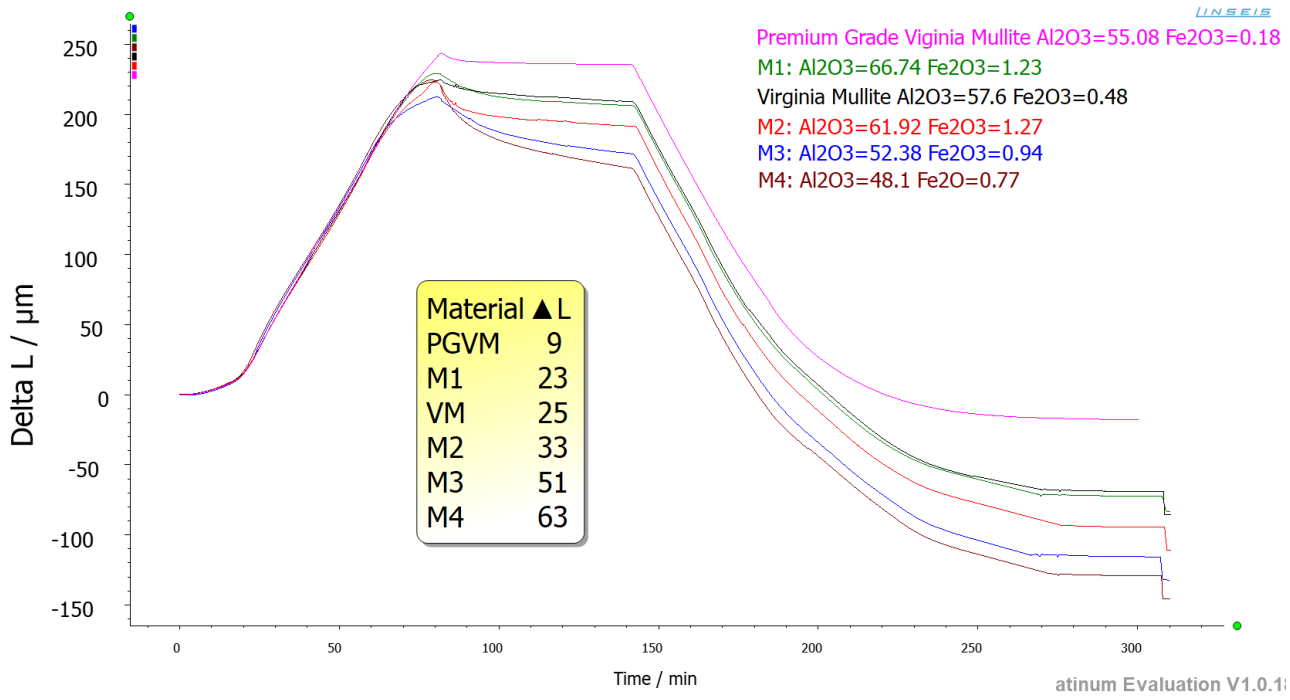

Figure 4: The change in length versus time curve can be used to determine creep resistance.

The Premium Grade Virginia Mullite™ showed the least amount of change through the dwell and thus the most creep resistance. The value of creep for Premium Grade Virginia Mullite™ was significantly less than the second most creep resistant material, M1. This is despite M1 having 9% more alumina. Samples M2 and Virginia Mullite™ also contain more alumina than the Premium Grade Virginia Mullite™ sample yet crept more during the dwell. These results suggest that the iron oxide content affects the creep resistance of the refractory material and that more than just alumina content must be considered when choosing the raw materials. Premium Grade Virginia Mullite™ also had the lowest amount of the alkali/alkaline earth oxides. These also act as fluxes and can lower creep resistance. These oxides might help explain why M1 and M2 show lower creep resistance than Premium Grade Virginia Mullite™. The Virginia Mullite™ products had similar alkali/alkaline earth contents so the difference in creep resistance between these two minerals must be due to the iron content. Samples M3 and

M4 crept the most during the dwell despite having lower iron contents than M1 or M2. This confirms that while iron content is important to consider, high alumina is still required for creep resistance. A large amount of alkali/alkaline earth oxides also negatively affected sample M4. Creep testing suggests that Premium Grade Virginia Mullite™ should be used over the other aluminosilicates tested in molds where dimensional stability of the casting is crucial.

CONCLUSION

The process of mining kyanite-quartzite rock and beneficiating the ore to make an industrially useful kyanite is a very complex process. Over twenty-five steps are used to make a kyanite product with an iron content containing less than 0.2%. This material is then calcined to make Premium Grade Virginia Mullite™. Calcining kyanite to make mullite creates a raw material that exhibits several unique characteristics. The mullite has a low level of impurities that are bound to the crystal surface. This makes the impurities non-homogenous which aids in creep resistance. The high aspect ratio of mullite made from kyanite can be used to increase the strength of the shell, reduce shell splits, and in some cases has led to reduction in the number of backup coats required.

Our studies indicated that all the various mullite sources tested have similar thermal expansion up until 2010 °F (1100°C). At this point the various materials began to soften and their expansion rates decreased. The Premium Grade Virginia Mullite™ was the only raw material to continue expanding at a constant rate until 2550°F (1400°C) and showed the highest creep resistance despite several other samples containing higher alumina contents. This is due to the lower amounts of iron oxide and alkali/alkaline earth oxides present which directly impact creep resistance. This high creep resistance property makes Premium Grade Virginia Mullite™ a great option for shells where high temperature dimensional stability is critical to casting quality and yields.

REFERENCES

1) T. Vert, *Refractory Materials Selection for Steelmaking*. The American Ceramic Society and John Wiley & Sons, 107-113 (2016).
2) S. Aramaki and R. Roy, "Revised Phase Diagram for the System Al2O3—SiO2," *Journal of the American Ceramic Society*, **45** [5] 229-242 (1962).
3) H. Schneider and S. Komarneni, *Mullite*. Wiley-VCH, Weinheim, Germany, 2005.
4) B. Joensson and B. Sundman, *High Temp. Sci.*, **26**, 263-273 (1990).
5) R. Brandt, "The Sillimanite Minerals: Andalusite, Kyanite, and Sillimanite," *Ceramic and Glass Materials,* 41-48 (2008).

6) S. Ashlock, "A Property Comparison of Commercially Available Sillimanite Minerals," *EUROGRESS*, 1-10 (2017).
7) F.W. Clarke and H.S. Washington, *The Composition of the Earth's Crust*. Government Printing Office, Washington, (1924).
8) B. Owens and M. Pasek, "Kyanite Quartzites in the Piedmont Province of Virginia: Evidence for a Possible High-Sulfidation System," *Economic Geology*, **102** [3] 495–509 (2007).

INVESTMENT CASTING INSTITUTE

Analysis of Surface Tension of Materials to Improve Coating Performance of Wax Coating

Gavin Dooley
REMET UK, Ltd.

66TH TECHNICAL CONFERENCE
&
EXPO 2019

Paper № 4

Analysis of Surface Tension of Materials to Improve Coating

Performance of Wax Coating

Gavin Dooley[1.], Alex Spence[1], Manuel Guerra[2] , Azhar Juhari[1]

[1.]REMET UK, Ltd., [2.] REMET PIC Inc.

Submitted to

Investment Casting Institute

Topic Area: Process Improvement – Wax/Shell

ABSTRACT

The surface energy of materials used within the Investment Casting sector is currently not well understood and rarely investigated within the industry. REMET® has acquired and tested the surface tensions of binder materials and their effect on the slurry properties. Shell systems are a blend of many complex ingredients within a tank which can influence the performance of your process. In many cases, attention is paid to the plate weight and/or viscosity as a method of control for the prime slurry on a regular basis. This paper outlines the measurement of the surface tension of the binder as a method of further understanding the wetting properties of the slurry within the process. Analysis of wetting agents, concentrations and effect on the wettability of waxes is completed to understand how this parameter can affect the slurry performance.

Utilizing sessile drop testing within REMET's R&D facility, the raw materials of waxes are also being developed to better understand and increase the affinity of wax to water-based slurries to improve coating performance. Particular attention is being drawn materials to reduce hydrophobicity of wax to slurries.

Furthermore, REMET has also been investigating surface free energies of peripheral materials and their effect on the coating effectiveness. Pattern wash and release agents haves also been investigated as these all impact the final surface area?? of materials. The results show some very interesting correlations between traditional and non-wash release agents.

INTRODUCTION

Surface tension is a key property of materials science which can influence the coating performance of materials during investment casting. REMET® UK has been investigating this phenomenon in recent years with a view to modifying this property to improve coating effectiveness between the slurry and wax during dipping.

LITERATURE REVIEW

There have been papers presented within the area of PIC into surface energies. Bozzo presented work on different surfactants in 1989 [1]. A full review of ionic and non-ionic surfactants is presented, including the difficulty in managing foam generation with the addition of surfactant. This paper outlined the materials used ever since including Victawet™ 12 and Aerosol® OT™. These products allowed a reduction in surface energy of standard DI water from 77.7 mN/mm to 34.4 mN/mm for Aerosol OT® and 31.8 mN/mm for Victawet® 12 respectively.

FOCAST mini conference within the University of Birmingham in 2002 worked briefly on the wax shell interface during de-waxing. A hot drop of wax was placed on a shell surface at different temperatures to assess the ingress into the shell [2]. This exhibited the interactions of both the permeability of the shell and molten wax during de-waxing. This paper showed that the initial wax layer penetrates the shell before it will flow from the shell as per Figure 1.

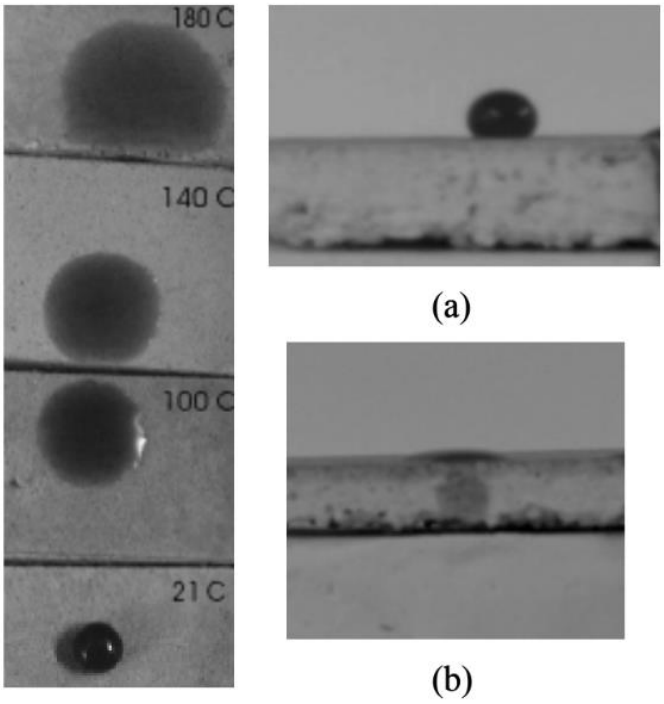

Figure 1 Wax droplet on a shell substrate at different temperatures. [2]

Finally, REMET UK presented work on surface tension in 2017 when it first acquired a Krüss® K6 Tensiometer [3]. Investigation was carried out into the effect of sol particle size on the surface tension of REMET® binders. Results showed no difference between large (10-15 nm) and small (5-8 nm) particle colloidal silicas with the presence of surfactants.

Furthermore, this work included a review of the concentrations of surfactant within a binder to achieve full wetting of the material., This work is presented in Figure 2.

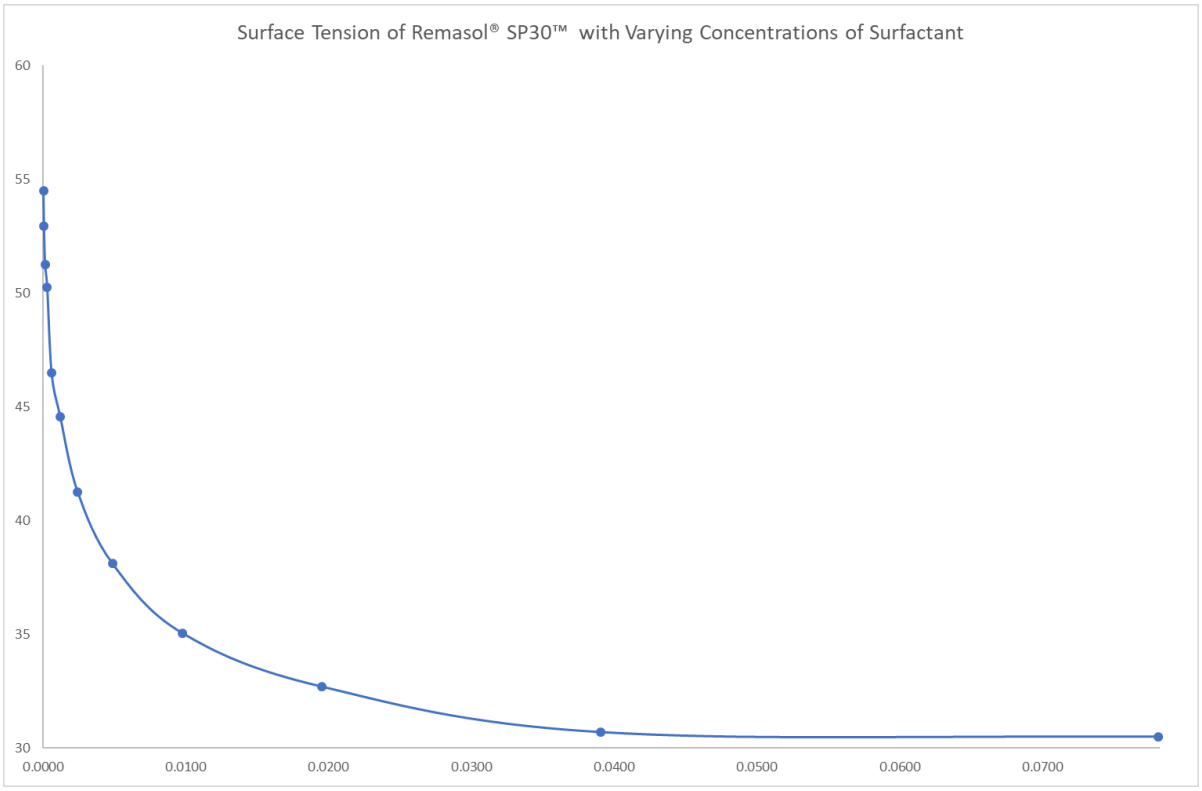

Figure 2 Surface Tension of Remasol® SP30™ with Varying Concentrations of Surfactant

Finally, the effect of these surfactants on the coating effectiveness was produced. As can be seen, the amount of material wetted onto, and retained on a surface of a metal plate for plate weight testing increases with the reduction of surface tension of the binder. These results are presented in Figure 3.

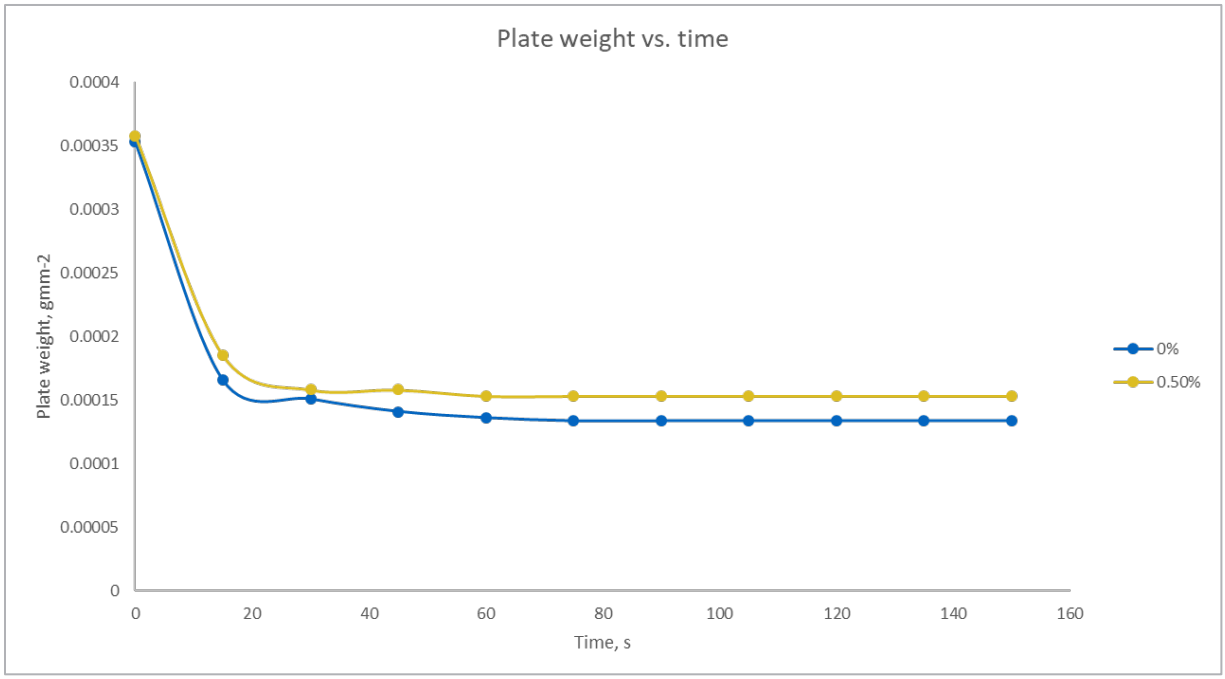

Figure 3 Effect of plate weight on slurry samples with and without surfactant

MATERIALS & METHODS

LIQUID SURFACE TENSION

A Krüss® K6™ Tensiometer was used to assess the surface tension of liquid material. This equipment utilizes the Du Noüy ring method developed in 1925 [4]. The following equation was used to calculate the surface tension.

$$\sigma = \frac{F}{\mathrm{L}.\cos\theta} \qquad \textbf{Equation 1}$$

A platinum iridium ring was removed from the liquid and the force required to remove the ring was recorded. Due to the material used within the ring with an effective contact angle of zero, the force required to remove the ring can be directly measured as surface tension.

SURFACE FREE ENERGY

Surface free energy of solid substrates, including wax was measured using a Krüss® MSA™ (Mobile Surface Analyzer). The equipment allows for rapid measurement of surface energy by applying two drops of liquids of known surface tension onto the solid substrate. The ADVANCE™ software then analyses these surface angle of these drops and calculates the total surface energy including the dispersive and polar energies. Utilizing the sessile drop, the effect of cleaning agent and release agent was reviewed.

To first understand the coating effectiveness of two materials interacting with each other, we must first understand the material surface energies further. Materials are made up of both polar and dispersive surface energies. Polar surface energies are derived from the hydrogen bonding of atoms or molecules within the material. The dispersive surface energy is characterized by the weaker Van der Wahl's forces [5]. Many materials are made up of a mixture of these surface energies or exclusively one or the other. One example of a polar liquid is deionized water.

To calculate the interstitial energy between two surfaces, the following equation is used:

$$\sigma_{12} = \sigma_1 + \sigma_2 - 2\left(\sqrt{\sigma_1^d \sigma_2^d} + \sqrt{\sigma_1^p \sigma_2^p}\right) \qquad \textit{Equation 2}$$

Where *p* and *d* are the polar and dispersive energies between surfaces 1 and 2 respectively. The ideal adhesion between these surfaces occur if the interstitial energies equal zero.

SAMPLE PREPARATION

To measure the surface energy of the pattern wash, samples were poured into a rectangular mold 25 mm x 5 mm x 100 mm. These were then immersed in different pattern wash samples for 30 seconds, rinsed with water and allowed to dry.

To measure the surface energy of release agents, a 5-cavity tool was used to inject samples 25 mm x 5 mm x 250 mm. Each cavity was sprayed with different release agents for a number of injection runs and tested after a 24 hour stability period @ 25 ˚C.

RESULTS AND DISCUSSION

Firstly, we would like to understand where a standard wax surface tension lies currently within investment casting wax.

Table 1 Typical Wax Surface Energy Results

Results	Wax 2 (Unfilled)	Wax 2 (Unfilled)	Wax 3 (Filled)	Wax 4 (Filled)
Total Surface free energy [mN/mm]	22.86	22.72	21.19	27.83
Disperse [mN/mm]	22.29	22.42	20.78	27.54
Polar [mN/mm]	0.57	0.3	0.41	0.28

Based off these results, the polar surface energy of a wax is very low in comparison to the polar energy within the binder. The effect of filler on this property is also negligible. With this in mind, we can investigate the following modifications:

1. Modification of the wax recipe or raw materials
2. Pattern washing of wax
3. Modification of release agent

MODIFICATION OF THE WAX RECIPE OR RAW MATERIALS

This work concentrated on adding polar materials into waxes to increase the affinity of the wax to the binder. At present, this work has resulted in higher polarity within a wax as expected, however, it has a knock-on effect on other properties including viscosity and potentially de-wax properties.

Figure 4 shows the drop melt point of a wax which through Differential Scanning Calorimetry (DSC) testing has been proven to have the same melt point, however during drop melt point testing, the change in surface tension properties causes a shift in when the wax will flow. Linking this finding to the in the work completed by University of Birmingham [2], it is clear this may have a detrimental effect on de-waxing performance and may cause cracking.

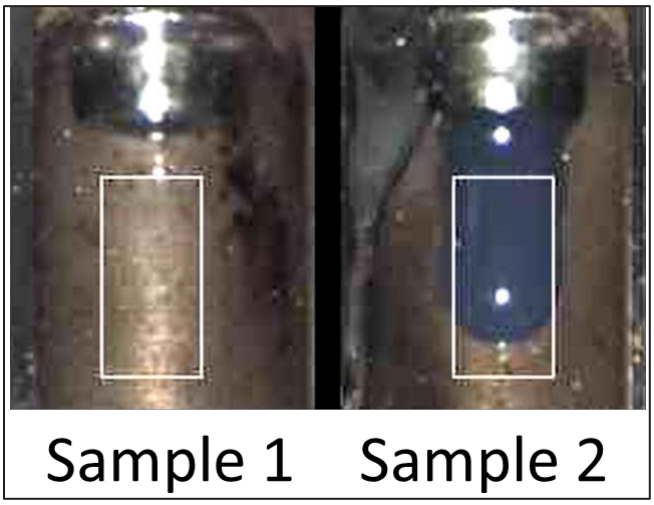

Figure 4 Effect of higher surface tension on flow and drop shape of a standard filled wax within a drop melt point tester

PATTERN WASHING OF WAX

Figure 5 shows the effect of surface energy on a wax after pattern washing on the surface energy of a wax substrate.

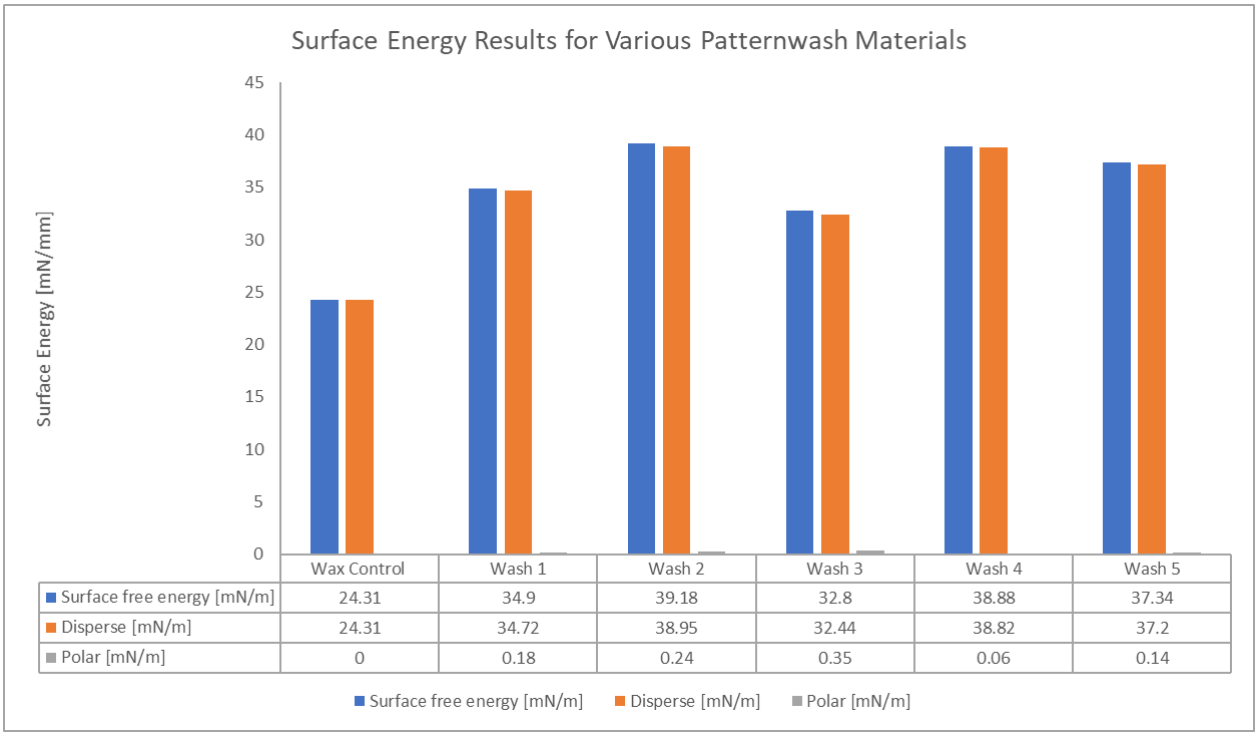

	Wax Control	Wash 1	Wash 2	Wash 3	Wash 4	Wash 5
Surface free energy [mN/m]	24.31	34.9	39.18	32.8	38.88	37.34
Disperse [mN/m]	24.31	34.72	38.95	32.44	38.82	37.2
Polar [mN/m]	0	0.18	0.24	0.35	0.06	0.14

Figure 5 Surface Energy Results for Various Patternwash Materials

As can be seen, there is a change in the surface energies of the wax following washing. Predominantly, the dispersive energy on the surface of the wax increases. However, this may only be half of the story, as the surface modification may happen on a more macro level which also effects the slurry retention level. As can also be seen, the polar energy of the wax remains unchanged at near zero.

RELEASE AGENT ON WAX PARTS

Samples 1-4 show the test results for standard silicone release agents.

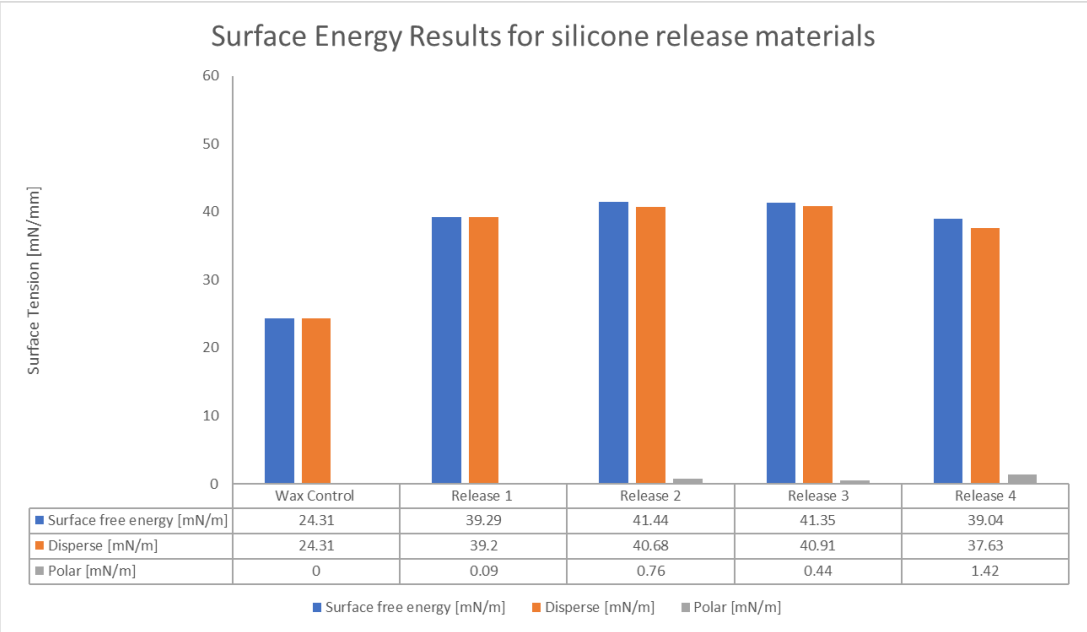

	Wax Control	Release 1	Release 2	Release 3	Release 4
Surface free energy [mN/m]	24.31	39.29	41.44	41.35	39.04
Disperse [mN/m]	24.31	39.2	40.68	40.91	37.63
Polar [mN/m]	0	0.09	0.76	0.44	1.42

Figure 6 Surface Energy Results for silicone release materials

The surface energies of silicone release agent increases the overall surface tension but do little to increase the polarity of the surface, therefore this will increase the interstitial surface energies between the wax and binder material.

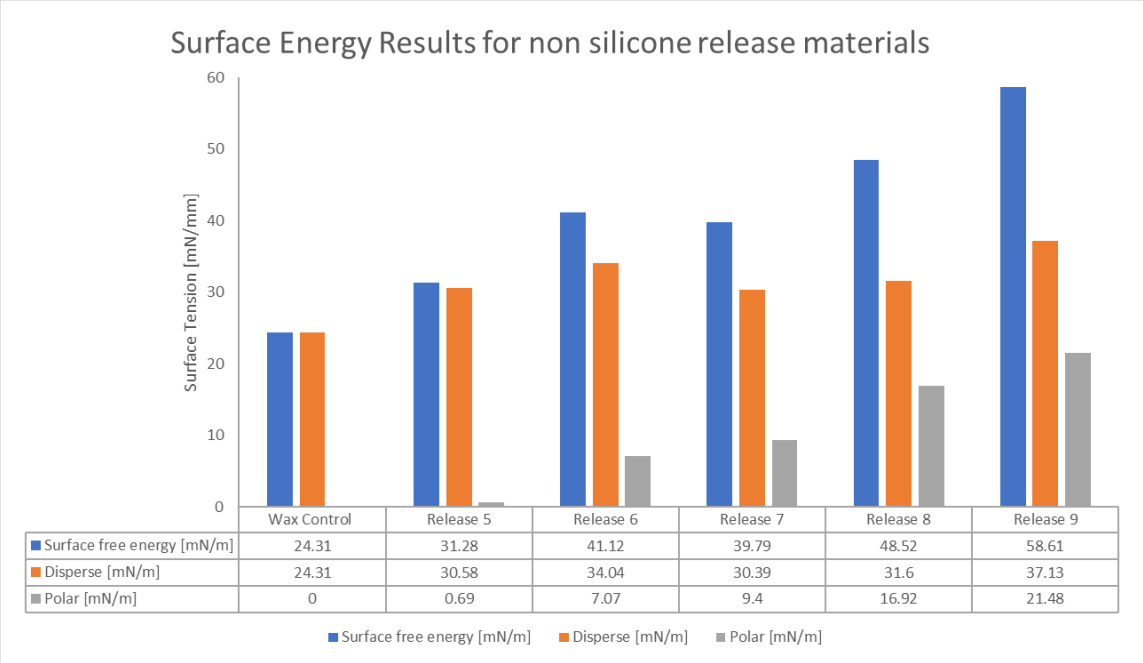

	Wax Control	Release 5	Release 6	Release 7	Release 8	Release 9
Surface free energy [mN/m]	24.31	31.28	41.12	39.79	48.52	58.61
Disperse [mN/m]	24.31	30.58	34.04	30.39	31.6	37.13
Polar [mN/m]	0	0.69	7.07	9.4	16.92	21.48

Figure 7 Surface Energy Results for silicone release materials

Samples 5-9 shows an increase in the polar surface energies. While samples 6 & 7 are commercially available at present within PIC market, samples 8 & 9 are new developments from REMET UK. These products offer a change to reduce the interstitial energies between wax and slurry materials. Reducing the reliance on pattern washing will increase efficiency and decrease consumable costs also.

CONCLUSION & FUTURE WORK

The low polarity surface energy of waxes is an interesting phenomenon which has not been investigated to the full extent at present. To enhance the wax/slurry wetting, the interface between wax and slurry materials can be examined in further detail including the effect of pattern wash and release agent. Future work will assess the coating effectiveness changes on the wax patterns with changing surface properties of the wax. REMET is using this technology to investigate pattern washing and release agents for next generation products.

REFERENCES

[1] Bozzo, A. (1989), “Surfactants, Wetting and Foams”, 37th Annual Technical Meeting, Investment Casting Institute.

[2] Jones, S., Jolly, M.R., (2002) BOILERCLAVE™ Thermal Profiles And The Effect Of moisture Upon Ceramic Shells During The Steam De-wax Process, 3rd FOCAST Mini-Conference, University of Birmingham.

[3] Dooley, G. (2018) “An analysis into the interaction between plate weight and viscosity for prime slurry control - What is the missing link?”, 29th EICF International Conference, Porto.

[4] du Noüy, Pierre Lecomte (1925). "An Interfacial Tensiometer for Universal Use". The Journal of General Physiology. 7 (5): 625–633. doi:10.1085/jgp.7.5.625. PMC 2140742.

[5] Dataphysics, (2019), “Dispersive & polar parts of the surface energy and surface tension”, https://www.dataphysics-instruments.com/knowledge/understanding-interfaces/dispersive-polar-parts/ . accessed 27-August-2019.

INVESTMENT CASTING INSTITUTE

A Comprehensive Analysis of Viscosity Measurements

Sam Duncan
Ransom & Randolph

66TH TECHNICAL CONFERENCE
&
EXPO 2019

Paper № 5

A Comprehensive Analysis of Viscosity Measurements

Michael J. Hendricks, Applications Engineering Director
David Berta, Product and Application Specialist
Sam Duncan, Product and Application Engineer
Ransom & Randolph, Maumee, Ohio USA

Abstract

Viscosity, the measure of a fluid's resistance to flow, is one of the most evaluated and controlled parameters in the shell room. Viscosity is a universally accepted industry test that offers a quick and easy go/no go check to determine if a slurry is fit for use. Using a flow cup, the viscosity measurement is determined by the time it takes for the cup to completely empty after being submerged then extracted from a slurry. Too high of a slurry viscosity could result in insufficient shell coverage in difficult geometries, extended dry times or an increase in shell material usage. If viscosity is too low, the shell may not be strong enough to handle the stresses associated with dewax, burnout and casting.

Viscosity measurement is subject to a great deal of variation based upon equipment and methods used, as well as inconsistencies between operators. This paper will present a comprehensive analysis on the impact these variations have to the accuracy and precision of the viscosity measurement; specifically exploring results from various flow cups, end points, operators and slurry types. From these results, we will conclude best practice methods and equipment for repeatability of viscosity measurements. A correlation of the methods and equipment will also be determined for cross referencing the measurements.

Background

Viscosity is a physical property of fluids; it is a measurement of a material’s resistance to flow (The Editors of Encyclopedia Britannica, 2018). Materials that are thick or do not flow easily have a higher viscosity, whereas materials that are thin and do flow easily

have a lower viscosity. Understanding the viscosity of a material, or how it will flow, is important when determining how to best handle the material. If the viscosity is controlled within a predetermined range, the flow properties can be controlled as well.

The viscosity of a material can be quantified as dynamic or kinematic viscosity. Dynamic viscosity measures the fluid's resistance to flow when an external force is applied to it. Kinematic viscosity represents the ability of a fluid to flow under the weight of gravity (Robert G. McGregor, 2009). The unit of measure for kinematic viscosity is the Stoke (St) or centi-Stoke (cSt). To better comprehend kinematic viscosity, a list of typical liquids and their viscosities is shown in Table 1.

Centistokes (cSt)	Typical Liquid	Centistokes (cSt)	Typical Liquid
1	Water	1100	Glycerin
4	Milk	1735	SAE 50 oil
15.7	No. 4 fuel oil	2200	Honey
20.6	Cream	4500	Glue
43.2	Vegetable oil	6250	Mayonnaise
110	SAE 10 oil	10800	Molasses B
220	Tomato juice	19000	Sour cream
440	SAE 30 oil	19600	SAE 70 oil

Table 1

A common tool used to measure kinematic viscosity (referred to as just viscosity for the remainder of this paper) is a flow cup. A flow cup is a precision instrument that is used to measure the efflux time of a fluid from the cup. Typical flow cups are shown in Figure 1. The distinguishing characteristics of the flow cup are the cup itself and the hole at the bottom of the cup.

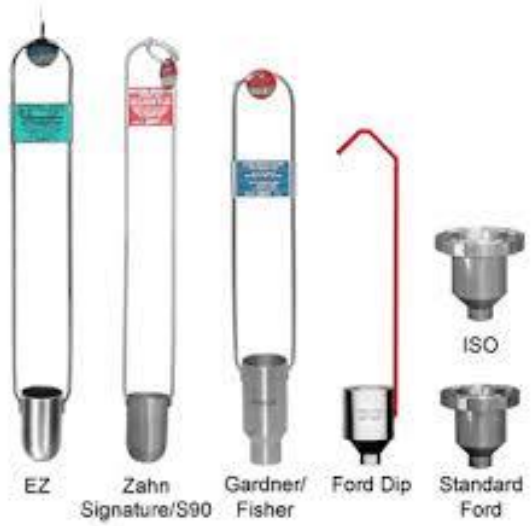

Figure 1 – Flow Cup Examples (Gardco, n.d.)

A typical procedure for determining viscosity with a flow cup is as follows:

1. Insert a clean, dry flow cup into the fluid, filling the cup completely; then empty the cup. This step is often referred to as wetting the cup.
2. Reinsert the cup into the fluid.
3. Extract the cup and as the cup exits the top of the fluid, start a stopwatch.
4. Hold the cup vertically and observe the fluid.
5. Stop the stopwatch when the draining endpoint is reached.
6. Record the time.

This simple procedure is well suited for slurries used in the Precision Investment Casting (PIC) industry, as an operator or technician can simply take the flow cup directly to a slurry tank and easily measure the efflux time. In the PIC industry, the measured efflux time is accepted as representing the viscosity of the material even though it is not a cSt measurement. The viscosity measurement can then be compared to specifications. If viscosity doesn't meet specifications, the slurry can be adjusted back into range. Viscosity measurement is the most widely conducted test in the PIC industry.

In the PIC industry, every shell room is unique with regards to slurry formulations, part geometry, dipping technique and draining procedures. Because of this, it is possible that

every foundry could maintain their viscosity within a range unique to them. The flow cup viscosity test is versatile enough to address all these specificities at a foundry, but universal enough to be a standard test.

There are several brands of standard dip style viscosity cups available, including EZ (Equivalent Zahn), Zahn Signature, Ford and ISO cups. Each of these cups come with various hole sizes in the bottom. For example, the Zahn Signature cups have 5 cups in the range (#1, #2, #3, #4 and #5). A larger number indicates a wider bottom hole diameter. The more viscous the material tested, the larger the hole should be in the cup. It is important to note that cups are not universally sized to a standard. #5 EZ and #5 Signature series cups will not give the same results when used to test the slurry.

In addition to the variation in readings based on the cup type and hole size, the endpoint, or when the stopwatch is stopped, also influences the viscosity reading. There are three endpoints for viscosity testing used in the industry, as shown in Figure 2: through the hole (TTH), one inch below (1 in) and break at the bottom (bottom).

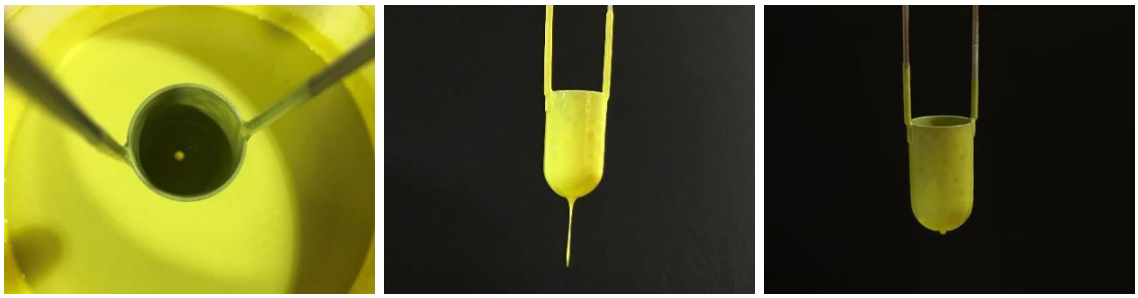

Through the hole One inch below Break at the bottom

Figure 2

When using each of these endpoints, the viscosity is tested using the procedure above, but the endpoint (described in step 5) would be either through the hole, one inch below or break at the bottom. For the through the hole method, the operator looks down into the cup as it drains. Once the hole in the bottom of the cup opens and becomes visible, the endpoint is reached. When using the one inch below method, the stream of slurry exiting from the bottom of the cup is observed. As the cup empties, the stream will change.

When the stream turns from steady to droplets one inch below the cup, the endpoint is reached. The break at the bottom endpoint is reached when the stream of droplets is at the bottom of the cup.

Methodology

In preparation for this experiment, brand new Zahn Signature 5, EZ Zahn 5 and ISO Mini 6 viscosity cups were purchased to ensure the measurements taken would not be affected by an old cup worn down by use.

Two slurries were tested in this experiment: a polymer slurry and a polymer plus fiber slurry. Both slurries were built and maintained in a rotating tank. A detachable propeller mixer was used for two hours to aid in the make-up process. After initial make-up, the tank was covered and allowed to mix over the weekend.

Before beginning the viscosity measurements, ten readings were taken across the surface of the tank to ensure slurry homogeneity throughout. In order to consider a slurry homogeneous, all ten readings must fall within one second of each other. Without the propeller mixer on at a low speed, the slurry had a greater than one second variation between all ten viscosity readings. Because of this, the propeller mixer was running during all testing.

Once a slurry was stabilized, testing began. All readings were taken from the same location. Each operator was only told which viscosity cup and which endpoint to use for that test. The operator started and stopped the stopwatch for each viscosity measurement. However, they only showed the stopwatch to whomever was recording each data point so that they could not bias the readings. After the operator took their ten readings with that cup, they thoroughly washed the cup and the next operator took their measurements. This continued until all four operators had completed one endpoint with the cup, and then the rotation began again with the next endpoint until all for that cup were complete. When one cup was finished, the same process was repeated using a different viscosity cup.

Once all measurements were taken at a given viscosity, a liquid mixture of binder, concentrate and water was added in order to decrease the viscosity in set intervals and then left to mix for at least thirty minutes. This mixture was used in lieu of separate water and binder additions in order to maintain the same ratios in each slurry. Once the viscosity was considered stable again, the next set of viscosity measurements was taken. This process repeated until all five viscosity levels were measured with all cups and endpoints.

Using the Zahn Signature 5, EZ Zahn 5 and ISO Mini 6 cups, a total of 2800 viscosity readings were taken. The testing methods used on the Zahn Signature 5 and EZ Zahn 5 cups were industry accepted methods: through the hole, one inch below and break at the bottom. The only testing method used on the ISO Mini 6 cup was break at the bottom, as this is the only method recommended by the manufacturer. Four operators took ten readings at each loading with each cup and each method, resulting in 70 different variable combinations. This is summarized in Table 2.

Variables	#	**Comments**
Operator	4	
Cup	3	SIG, EZ, ISO
Endpoint	3	TTH, 1 in, bottom
Slurry	2	Polymer, Polymer plus Fiber
Loadings per Slurry	5	L1 (Thickest)…L5 (Thinnest)

Table 2

Results & Discussion

The readings from each variable were evaluated by their standard deviation to determine the precision of each operator, cup and endpoint. The cumulative viscosity reading time for the 2800 readings was nearly thirteen hours, with the fastest test at five seconds and the longest at thirty seconds. The data was used to create an averaged viscosity conversion chart between the three cups, as well as additional correlation charts between the Zahn Signature 5 and EZ Zahn 5 cups based on the endpoint being measured.

Operator

Tables 3 and 4, for polymer and polymer plus fiber slurries, respectively, show the deviation results by operator, cup and endpoint. Each individual operator had a relatively low deviation for their own readings, but the deviation was higher when readings from all four operators were compared. In practice, this would mean if operator 1 takes all readings in a consistent range, but operator 2 takes readings that all are 2-3 seconds higher, the deviation is high even though both operators were consistent on their own. This is the case in Tables 3 and 4 where operator average shows good agreement (precision) among the operators' individual measurements, but overall average of all readings across the operators shows more variation (accuracy).

In a foundry setting, these averages could be interpreted as follows:

- Operator average: One operator takes viscosity at the facility and is only compared to their other measurements
- Overall average: Three different operators take viscosity over three shifts at the facility and the operators are compared to the other operators' measurements

Operator Consistency (STD DEV): Polymer Slurry								
	SIG TTH	**SIG 1 Inch**	**SIG Bottom**	**EZ TTH**	**EZ 1 Inch**	**EZ Bottom**	**ISO Bottom**	**Operator Average STD DEV**
1	0.199	0.242	0.298	0.210	0.357	0.223	0.187	0.245
2	0.165	0.160	0.346	0.209	0.251	0.227	0.138	0.214
3	0.126	0.174	0.218	0.199	0.224	0.208	0.138	0.184
4	0.199	0.199	0.303	0.194	0.320	0.241	0.149	0.229
Polymer	**SIG TTH**	**SIG 1 Inch**	**SIG Bottom**	**EZ TTH**	**EZ 1 Inch**	**EZ Bottom**	**ISO Bottom**	
Operator Average	0.172	0.194	0.291	0.203	0.288	0.225	0.153	
Overall Average	0.232	0.305	0.435	0.342	0.475	0.463	0.222	

Table 3

Operator Consistency (STD DEV): Polymer plus Fiber Slurry								
	SIG TTH	**SIG 1 Inch**	**SIG Bottom**	**EZ TTH**	**EZ 1 Inch**	**EZ Bottom**	**ISO Bottom**	**Operator Average STD DEV**
1	0.353	0.737	0.440	0.365	0.852	0.699	0.241	0.527
2	0.276	0.368	0.373	0.284	0.502	0.409	0.292	0.358
3	0.300	0.456	0.445	0.394	0.496	0.484	0.268	0.406
4	0.315	0.315	0.387	0.600	0.565	0.494	0.258	0.419
Polymer plus Fiber	**SIG TTH**	**SIG 1 Inch**	**SIG Bottom**	**EZ TTH**	**EZ 1 Inch**	**EZ Bottom**	**ISO Bottom**	
Operator Average	0.311	0.469	0.411	0.411	0.604	0.522	0.265	
Overall Average	0.564	0.761	0.506	0.770	1.207	0.602	0.344	

Table 4

Endpoint

The data in Table 5 shows the deviations for all readings using each endpoint for the two slurries. Through the hole and break at the bottom were the most consistent methods tested, due to the definitive endpoint of the tests. The one inch below method has a subjective endpoint, resulting in higher deviations. Through the hole did have some subjectivity, though, but only at the highest viscosities with the polymer plus fiber slurry where the hole took much longer to open.

	Polymer Slurry Average	**Polymer plus Fiber Slurry Average**
TTH DEV	0.287	0.667
1 IN DEV	0.390	0.984
BOTTOM DEV	0.373	0.484

Table 5

For the foundry, this means that using a 1 inch below endpoint for viscosity on a polymer plus fiber slurry could introduce almost six seconds of deviation if viscosity is assumed as a normal distribution. This six second range is wider than the control range that most foundries use.

Cup

The precision of a flow cup is the ability to measure a viscosity consistently, while the accuracy of a flow cup is proximity of all readings to a target. Cup accuracy in this study was measured by the standard deviation of the readings of all operators with a given flow cup.

Table 6 shows the comparison in standard deviation between the polymer slurry and polymer plus fiber slurry across all three flow cups, regardless of operator or endpoint. For the polymer slurry, the readings by all four operators tended to stay much closer together, resulting in a lower overall deviation across cups. In comparison, the readings of the polymer plus fiber slurry were more spread out. The polymer plus fiber slurry was more difficult to determine the endpoint, especially with the one inch below and break at the bottom methods. This was due to the addition of fiber slightly changing the slurry rheology and ultimately affecting how the slurry acted as pressure dropped within the cup as it drained out. As a result, the cups were more accurate on the polymer slurry than the polymer plus fiber slurry.

The deviations for the Zahn Signature 5 and EZ Zahn 5 cups with the polymer plus fiber slurry are roughly double that of the polymer slurry. The ISO Mini 6 cup, however, only showed an increase of about 50%. This means that the ISO Mini 6 cup measurements showed greater accuracy over the other two cups, regardless of slurry type.

	Polymer Slurry Average	**Polymer plus Fiber Slurry Average**
SIG DEV	0.324	0.611
EZ DEV	0.427	0.860
ISO DEV	0.222	0.344

Table 6

For both slurries, there was much more difficulty determining the endpoint when the viscosity was higher. In general, there is a positive correlation between viscosity and deviations where the higher the viscosity, the higher the deviations and vice versa. As an

example of this, Table 7 shows the deviations for the three cups over five loadings of the polymer plus fiber slurry.

	SIG Bottom	EZ Bottom	ISO Bottom
L1	1.061	1.220	0.373
L2	0.457	0.596	0.239
L3	0.493	0.615	0.381
L4	0.307	0.390	0.332
L5	0.214	0.189	0.397

Table 7

The range of deviations from the Zahn Signature 5 and EZ Zahn 5 cups across the loadings is more pronounced than with the ISO Mini 6 cup. Due to this, it will be more difficult to be accurate with the Zahn Signature 5 and EZ Zahn 5 cups at higher viscosities. On the other hand, the ISO Mini 6 cup is more consistent across a broad range, with the only exception being at the lower viscosities tested.

Conclusion

The data confirms industry perceptions that viscosity readings vary by operator, endpoint and cup. This evaluation assigned values, or relative values to variation caused by each of these variables.

In a foundry setting where multiple operators are taking viscosities on slurries, the ISO Mini 6 cup is the best option. It consistently had the lowest deviations amongst operators when compared to other cups. It also maintains a low deviation across the tested viscosity range. The low deviation allows the foundry to hold tighter viscosity because the deviation occupies less of the recommended slurry viscosity range than the other cups, resulting in both consistent and accurate measurements. An ISO Mini 6 cup is roughly 2-3 times more costly than a Zahn Signature 5 or EZ Zahn 5 cup. When a Zahn Signature 5 or EZ Zahn 5 cup is used, variation is reduced by employing the through the hole method.

Data showed a real-world difference between published viscosity equivalency charts and actual slurry viscosity correlations. The published chart is based on tightly controlled and

calibrated oils, while this testing was conducted using ceramic slurries. Using gathered data, we produced more realistic equivalency charts for converting between different flow cups and endpoints. These charts are shown in Tables 8 and 9.

Correlation Charts

Polymer Slurry (seconds)				
SIG TTH	**EZ TTH**	**SIG Bottom**	**EZ Bottom**	**ISO Bottom**
30.00	27.96	30.06	37.54	34.56
29.00	27.52	29.13	36.38	34.01
28.00	27.06	28.20	35.22	33.45
27.00	26.59	27.27	34.06	32.87
26.00	26.10	26.34	32.90	32.27
25.00	25.59	25.41	31.74	31.65
24.00	25.07	24.48	30.57	31.01
23.00	24.51	23.55	29.41	30.34
22.00	23.94	22.63	28.25	29.64
21.00	23.33	21.70	27.09	28.92
20.00	22.70	20.77	25.93	28.16
19.00	22.04	19.84	24.77	27.37
18.00	21.33	18.91	23.61	26.54
17.00	20.59	17.98	22.45	25.67
16.00	19.81	17.05	21.29	24.75
15.00	18.97	16.12	20.12	23.78
14.00	18.08	15.19	18.96	22.75
13.00	17.11	14.26	17.80	21.66
12.00	16.08	13.34	16.64	20.50
11.00	14.95	12.41	15.48	19.25
10.00	13.71	11.48	14.32	17.90

Table 8

Polymer plus Fiber Slurry (seconds)				
SIG TTH	**EZ TTH**	**SIG Bottom**	**EZ Bottom**	**ISO Bottom**
30.00	37.90	31.43	36.07	34.28
29.00	36.66	30.48	35.04	34.34
28.00	35.43	29.53	34.01	34.31
27.00	34.20	28.58	32.97	34.20
26.00	32.97	27.63	31.93	34.01
25.00	31.74	26.67	30.88	33.72
24.00	30.51	25.71	29.83	33.35
23.00	29.28	24.74	28.78	32.89
22.00	28.05	23.77	27.72	32.35
21.00	26.82	22.80	26.65	31.71
20.00	25.58	21.82	25.58	30.97
19.00	24.35	20.83	24.51	30.15
18.00	23.12	19.84	23.43	29.23
17.00	21.89	18.85	22.34	28.21
16.00	20.66	17.85	21.25	27.09
15.00	19.43	16.84	20.15	25.87
14.00	18.20	15.83	19.04	24.55
13.00	16.97	14.81	17.93	23.12
12.00	15.73	13.78	16.80	21.58
11.00	14.50	12.74	15.67	19.92
10.00	13.27	11.69	14.53	18.15

Table 9

References

Gardco. (n.d.). *Viscosity Cup FAQ's*. Retrieved from Gardo: https://gardco.com/pages/viscosity/vi/viscosity_faq.cfm

Robert G. McGregor. (2009, August 1). *Viscosity: The Basics*. Retrieved from Chemical Engineering Essentials for the CPI Professional: https://www.chemengonline.com/viscosity-the-basics/

The Editors of Encyclopedia Britannica. (2018, August 17). *Viscosity.* Retrieved from Encyclopedia Brittanica: https://www.britannica.com/science/viscosity

INVESTMENT CASTING INSTITUTE

Process Control Standards Update

Nip Singh
S&A Consulting Group LLP

66TH TECHNICAL CONFERENCE
&
EXPO 2019

Process Control Standards (PCS)

for Investment Castings:

By

Nipendra (Nip) P. Singh,

Chair, ICI Process Control Standards Core Team

S&A Consulting Group LLP, USA

STATUS REVIEW

As Process Control is very critical to our manufacturing of Investment Castings worldwide, we would like to involve all sectors of Investment Castings in all countries. This paper will present the current status of the Process Control Standards (PCS) and also will detail how casters and suppliers can cooperate.

The task force on PCS, a subgroup under Education Committee, has made considerable strides since our last presentation at ICI 65th Conference in October 2018. Based on the audit forms and other documents, we have planned a beta test in a foundry for October 2019. The details of the test audit will assist the task force to modify the plan and possibly roll out the program in 2020 for all Members of ICI

INVESTMENT CASTING INSTITUTE

Culture & Employment Strategies for Forward Thinking Companies

Aaron Phipps
MPI, Inc.

66TH TECHNICAL CONFERENCE
&
EXPO 2019

Paper № 6

Culture and Employment Strategies for Forward Thinking Companies

Aaron Phipps
MPI, Inc.
aphipps@mpi-systems.com

Abstract:

In today's business climate it is as important as ever to develop and retain a strong workforce. In order to develop and maintain this workforce MPI continually works to develop strategies that support our team and maintains MPI's competitive edge. Some of the strategies MPI has used successfully over the past few years include:

- Paying for an ESL Instructor to develop our non-English speaking employees. This instruction is offered at the workplace weekly. The impact on these employees and the team they work in has been amazing.
- Paying for a sign-language interpreter to assist non-hearing employees during all important company meetings, and trainings.
- Developing relationships with the local colleges to introduce MPI to students planning for internships and after graduation employment.
- Investing in the growth of existing employees by engaging them in guiding and developing our interns on specific projects.
- Joining with other local businesses to develop collaborative development projects that are mutually beneficial to both companies. This provides potential for developing new markets and accelerating our growth in cutting edge technology.

INVESTMENT CASTING INSTITUTE

Eliminating Shrinkage Porosity in a Complex Investment Cast Part

Evan Letourneau
MAGMA Foundry Technologies

66TH TECHNICAL CONFERENCE
&
EXPO 2019

Paper № 7

Eliminating Shrinkage Porosity in a Complex Investment Casting Part

Evan Letourneau
MAGMA Foundry Technologies, Inc. Schaumburg, IL
Gerald Richard
MAGMA Foundry Technologies, Inc. Schaumburg, IL
AJ Menefee
Eagle Precision Cast Parts, Inc. Muskegon, MI

ABSTRACT

Shrinkage porosity continues to plague investment casting foundries resulting in costly repairs and in many cases scrapped castings. Reproducing castings that have been scrapped or reworking parts that can be salvaged are not only costly in terms of additional labor and materials needed, but can also be costly in the damaging effects of poor on time delivery. The damaging effects are then compounded if shrinkage remains in the casting and is found during a machining operation or worse, a failure in service. Reducing the number of shrinkage defects can have an enormous impact on the profitability of a product line, and ultimately, on the profitability of the company. Therefore, it is imperative to the Foundry Engineer to develop tree designs that fulfil the quality requirements that the customer requires despite growing casting complexity and expectations. In this paper, a systematic way of identifying the conditions that lead to shrinkage porosity and the methodology employed to eliminating the porosity will be reviewed using a case study of a complex investment cast part.

Introduction

Shrinkage porosity is an issue that every investment caster deals with, but it can be mitigated identifying concerning areas on a part before it enters production. When liquid metal freezes, its density increases and leaves some of the surrounding volume empty. Parts containing these voids can fail to meet customer's quality requirements due to functional or cosmetic issues. Many times these issues are only discovered when a part goes into production. Scrapping castings and re-cutting tooling to resolve the issue can greatly reduce the profit margins on a casting. Thus, following a robust approach to gating castings before they go into production is mandatory. New casting designs should be evaluated by considering one's objectives, defining potential variables, specifying evaluation criteria, and making a plan to compare production metrics of the resulting design to historical numbers. By considering these steps in advance, unforeseen costs can be mitigated and parts can be made with higher profits, lower lead times, and more consistency.

Porosity

The root cause of metal shrinkage is due to changes in the spacing between atoms at the metal cools. In the liquid state, atoms flow freely throughout the melt. At higher temperatures, atoms stay farther apart from each other. As a result, metal is the least dense when it is first pored. While the liquid metal cools, it shrinks slightly, however this has little effect on the final casting. Because the casting is still fully liquid, volume lost

due to liquid phase shrink does not form voids.

As metal cools, dendrites begin to grow in liquid metal at the liquidus temperature and the metal completely solidifies when it reaches the solidus temperature. Areas that cool more quickly, such as thin sections and the outer edges of the casting, are the first to solidify. Thick sections of the casting hold a lot of heat and tend to cool last. The first sections to solidify will compensate for their loss of volume by drawing additional liquid metal from the areas around them. The last areas to solidify, however, have no liquid metal in their vicinity and no new metal will fill in the shrunken regions. Thus, shrinkage porosity will form in the last areas to solidify.

Shrinkage porosity is one of the most common issues that foundry engineers address. As liquid metal cools it becomes denser, and this loss of volume can create voids in the final casting. While some level of porosity is acceptable in most castings, if it is not properly addressed it can be detrimental to the functionality or appearance of the finished part. Using a large sprue is a common way of removing shrink from investment castings. Instead of the heavy sections of the casting cooling last, the sacrificial sprue will continue to feed the casting until it fully solidifies. This technique makes use of "directional solidification," in which the metal in a thin section is fed additional liquid metal by a heavy section, which is in turn fed by the sprue. This technique is dependent on making sure the gates solidify after the casting so they can continue to feed liquid metal to the casting as it cools.

Not all porosity is worth addressing, however. Attempting to remove all porosity from a part typically requires complex and expensive risering, which makes the casting cost-inefficient. Yet shrink occurs in key functional or visually important area on many parts, and it is important to understand how to effectively address this issue.

Approach

Following a robust and repeatable process is the best way to approach issues with porosity in investment casting. A consistent process can help engineers avoid missing key details and produce quality castings on-time for every project. The first step of this process is to determine what requirements the casting needs to fulfil. Then one considers what designs are possible and what process variables can be adjusted. It is also important to determine the criteria by which one will judge whether a design has fulfilled the objective. Viable designs can then be determined and tested to find the optimal version. Finally, one must implement the solution and then confirm that the solution is working as expected.

1. Set Objectives

Considering objectives in advance keep work on-track and make time is applied efficiently. When making design changes, there are two primary objectives: meeting customer requirements and making the job profitable. The "meeting customer requirements" objective means producing parts that will not be rejected by the customer. If the customer does not specify exactly what they need, requesting further information keeps one from addressing criteria that are not necessary to make a good part. Applied to reducing porosity, this could include knowing whether shrink in

non-machined regions is acceptable and knowing where the machined sections are.

Job profitability is the second major objective for every new part that comes in. Parts that are made at a loss are best to avoid. However, determining whether a part is profitable or not requires an understanding of internal costs. For instance, how much does every square inch of gate cost to cut and then grind? These prices can be difficult to assess and must be estimated from monthly totals, but can give a better sense of which designs need to be improved.

Part designs must meet both the "customer requirements" objective and the "job profitability" objective to be moved into production.

2. Define Variables

When approaching an objective, listing in advance what variables can be changed will keep all possible options available. If one focuses on solving shrink with gating alone, one may lose sight of opportunities to mitigate the issue by changing pouring temperature, changing shell temperature, or adjusting shelling parameters. Additionally, depending on the part and customer, key changes can sometimes be made to the casting design. Adding feed paths, thickening thin areas, or increasing radii can make it far easier to address shrink in difficult features.

Considering what you cannot adjust can also provide valuable constraints for your design. Noting the part orientation required to water blast off shell or where wax would be unable to drain will prevent the creation of new problems while addressing a shrink issue. Having a good sense of constraints and variables before starting a project allows one to consider and compare multiple potential solutions and to be confident that the best solution was reached.

Variables should not be eliminated at this step. Even variables that failed to work on other projects, such as risers, may be valuable to consider and should not be struck from the list.

3. Specify Criteria

Developing evaluation criteria is a way to judge whether the objective has been completed. Criteria should be related to the objectives and measurable. For instance, an objective that states "improve job profitability" could produce the measureable criteria "reduce scrap below 2%" or "reduce weld repair to 5% of parts." Properly defined criteria are used to determine when a gating design for a new part is finished or when a continuous improvement project is complete. Setting a specified end point lets engineers know when to apply their time to a more pressing project.

4. Keep the Task Efficient

An engineer should always seek to reach the best design in the least amount of time. Time spent working on a gating design that turns out not be successful is lost time. To avoid going down a rabbit hole, a few separate ideas should be considered for nearly every project. The exception to this may be a low production or one-off part, where extra designs would be unhelpful. For high production parts, considering more possibilities may save valuable time and resources in the long run.

To gate higher production parts, one may take a few approaches to creating new

types of designs. For instance, three different types of sprue could be considered, each with a different idea for gating design. Additionally, one gate, two gate, and three gate designs could be made. Another part may be approached by choosing multiple orientations and gating in accordingly. These changes each involve a few types of designs to be considered, but the exact sizes of gates are left until further into the design process to be defined. For now, the engineer is simply concerned with creating a few different methods to reach the same aim.

The goal of this step is not to create finished designs, but to come up with more than one way to meet the criteria. This way, the best of multiple designs can be chosen for further revision instead of spending time trying to make a bad design work.

5. Choose a Method

Choosing a sampling plan should be based off of the part's production rate and the number of designs that seem worth investigating.

Determining the number of sample designs to be run is a key part of creating a sampling plan. When sampling for a low production run part, one design for sampling and PPAP may be best. Trying one large gate size may be enough to ensure that scrap is eliminated without wasting resources on sampling. For a larger production part, a larger number of samples allows an engineer to try a variety of gate sizes to optimize yield while still feeding shrink. Sampling is expensive, but becomes more worthwhile on high volume parts where a small design change could save a lot of money.

When using simulation software, many designs can be evaluated without the expense of sampling. The simulations still take time to run, and while their contribution to lead times are shorter, a well-developed project plan can reduce the number of simulations required to meet the objective. Even with simulation, at least one sample must be run of the final design for PPAP and more may be required to hone in process variables. Thus, considering objectives and variables in advance can reduce lead times, reduce sampling costs, and produce high profit castings.

When the sampling or simulating is finished, if the design meets the required criteria, the tooling is ready to be cut.

6. Act and Check Improvements

Once the best design is chosen and put into production, tracking the success of the project can begin. Projects should be monitored for scrap and hold-ups in production as well as customer returns to determine whether the design needs to be revaluated. For projects that addressed an issue with previous production, comparisons can be drawn between new and previous data to justify the improvement. In the case that the new parts are worse than the past design, the design can be reverted back while another solution is tried. Tracking the success of projects determines whether an engineer's work is complete.

Case Study

1. Set Objectives

A stainless steel valve component produced by Eagle Precision, shown in Figure 1, has had a long history of rework. The part is roughly cylindrical with one open end that has four mounting tabs and one closed end that gets drilled by the customer, show in Figure 2. One side of the

part has a ribbed arm that protrudes from the body. 75% of the parts require weld repair at the base of the arm due to visible surface shrink (Figure 3). About 800-900 parts are run per year, each costing $10-12 in weld repair for a total of $8,000-$10,000 in lost revenue annually. Eagle Precision approached MAGMA to assist in eliminating the surface porosity.

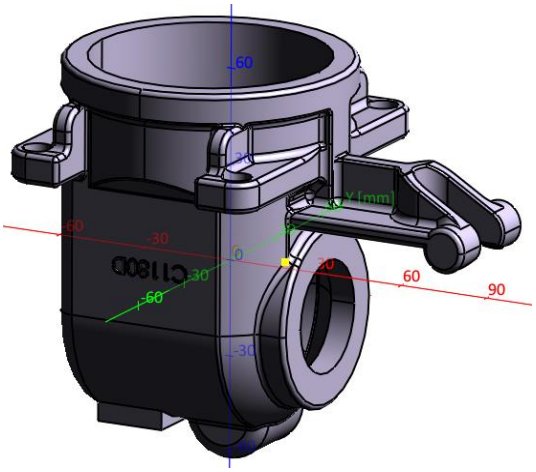

Figure 1. A CAD model of the Eagle Precision part.

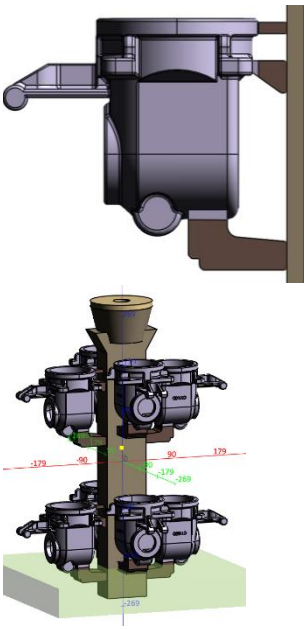

Figure 2. CAD Models of the original gating and assembled sprue.

Figure 3. Welded shrink at the base of the arm.

While the presented goal is to remove the surface porosity and eliminate weld repair, cost is also a major concern. Shrinkage porosity is not hard to remove, but it is hard to remove in a cost-effective way. In the case of this OEM, the casting may have internal shrink but not visible eternal shrink in any locations, as well as be free of shrink in machined locations. These

requirements are less expensive to address than a stringent X-ray requirement, which demonstrates the importance of fully understanding customer requirements. Thus, our solution should maintain the current levels of subsurface porosity to remain cost effective while not creating any new surface shrink. Considering these objectives in advance ensures that the solution addresses the underlying goals of the project.

2. Define Variables

Once the objectives are determined, the potential variables that can be defined. The primary way to address porosity in investment castings is by changing gating design. Within gating modifications, one can alter the shape, size, and number of gates, as well as the gate location and part orientation. There are also the options of adding new features such as preformed holes or blind risers. In this case, the OEM is open to design changes which allows for minor modifications to the part such as adding feed paths or thickening sections. To avoid causing the OEM to reject the design changes, one must avoid interfering with tool paths or requiring additional machining time. Sorting through these variables provides many ideas for potential new designs.

3. Specify Criteria

Setting up evaluation criteria in advance allows one to evaluate whether the new designs fulfill the set objectives. To approach our objective of eliminating surface porosity, our criteria is to reduce weld repair below 10% at the base of the arm. To accomplish this we must have little to no internal porosity. Our second objective, to reduce costs, has many factors that makes it harder to quantify. To meet this goal, yield, grinding time, and subsurface porosity (shown in Figure 4) need to remain relatively constant to ensure that no new issues are created. The final design must meet all of these criteria to be a recognizable improvement over the current gating.

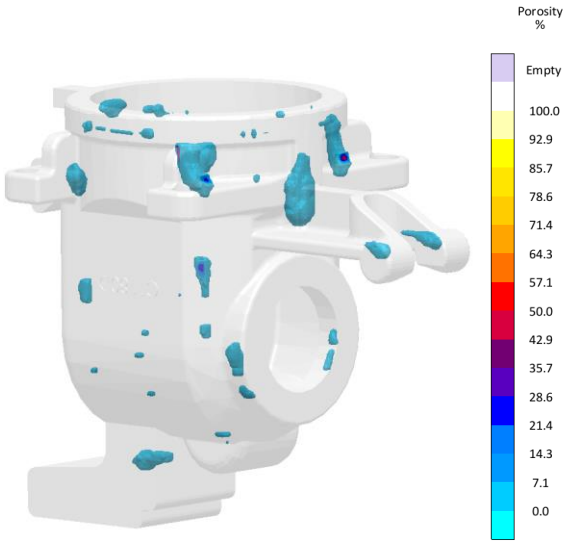

Figure 4. The porosity simulation result for the current gating. The scale shows the percent density of the porosity.

4. Keep the Task Efficient

Considering how the defined variables can be combined to fulfill our criteria keeps the project on track and reduces the number of simulations that need to be run. While it is much less expensive to run simulations than it is to run samples, simulating an excessive number of unlikely designs is not time effective.

A few general approaches to gating were developed based on different part orientations. Each orientation was intended to keep as many hot spots as possible close to the sprue. These designs will be tested in a design of experiments that tests each design independently with varied gate and riser sizes.

The orientation-based approaches are as follows: The first design (Figure 5) consisted of a tilted casting with three gates, one of which reached close to the base of the arm and was connected with a minor feed path. The second design (Figure 6) uses large risers tied back to the sprue to feed hot spots in the bolt tabs and at the base of the arm. This variant requires a large metal addition to the arm, raising the weight of the casing by 0.1 lb but considerably improves the feeding. A large gate on the bottom of the casting feeds a hot spot in a machined area. The third design (Figure 7) is gated into the same arm addition, but base of the casting is oriented towards the sprue. The design uses a spherical blind riser to address the heavy machined section, in an effort to avoid potential shrink. The fourth design (Figure 8) uses the same arm addition and part orientation as the third design, but instead has the hole in the heavy section preformed. Each of these designs appears viable before testing, and are reasonable to sample or simulate.

Figure 5. CAD model of design variation 1.

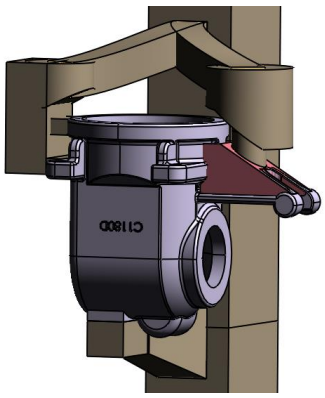

Figure 6. CAD model of design variation 2.

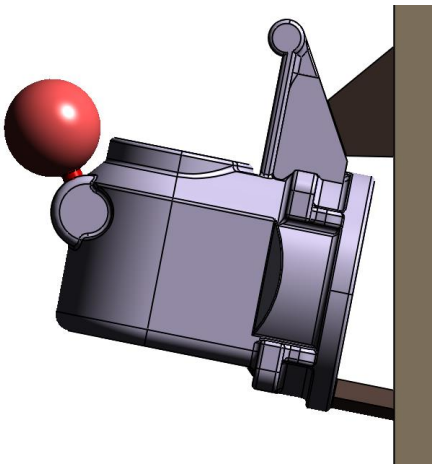

Figure 7. CAD model of design variation 3.

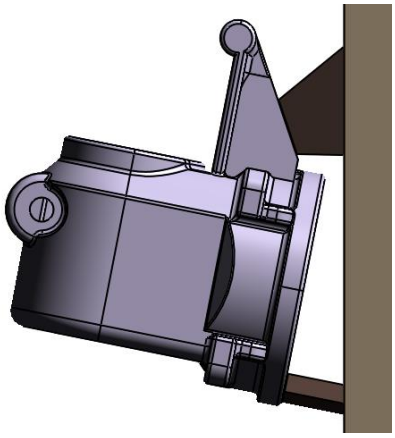

Figure 8. CAD model of design variation 4.

5. Choose a Method

Each part orientation was tested in a separate full factorial design to optimize the

sizing of gates and risers. Because simulation is relatively inexpensive to run and a fair number of parts are to be produced, enough variations of gate and riser sizes were tried in order to find the optimal combination. Once the best version of each design was decided on, they could be compared.

After the designs were simulated (or potentially sampled), they were inspected to see if they met the established criteria. First, porosity at the base of the arm was examined via simulation, but alternately the cross section of a sample could have been cut and polished. All of the designs successfully eliminated shrinkage porosity at the base of the arm.

The parts were then be scrutinized to see if yield, grinding time, and subsurface porosity are better or equivalent to parts produced by the original gating design. Design 1 showed concerning levels of porosity in the mounting tabs (Figure 9), and while the original design had minor porosity, the new design may have issues under process variation. Gate grind was also found to be an issue, as a small overhang on the arm prevented proper grinding of the center gate.

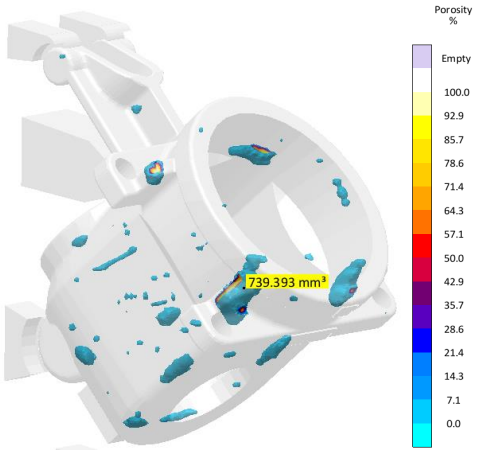

Figure 9. The simulated porosity of design variation 1 in percent density. A 740 mm^3 volume of subsurface porosity is predicted in one of the mounting tabs far from the sprue.

Design 2 had great results for porosity, but the yield was only 30% compared to 38% yield for the original gating, and therefor is likely not the best design.

Design 3 successfully uses the blind riser to avoid problematic porosity in the heavy section (Figure 10) while meeting the same yield as the original gating. Design 4 uses the preformed hole to shift porosity away from the machined section (Figure 11), although it may not survive the process variation inherent in production. Designs 3 and 4 meet the set criteria more effectively than the others, and were set aside for sampling.

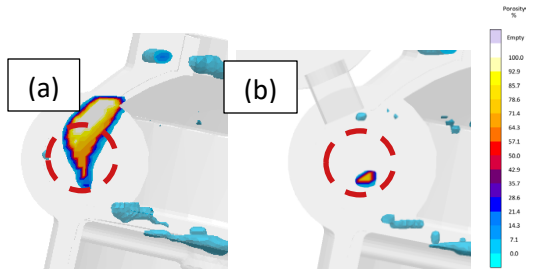

Figure 10. The simulated porosity of (a) the current gating and (b) design variation 3 in percent density. The porosity is mostly eliminated from the drilled hole by a riser in variation 3.

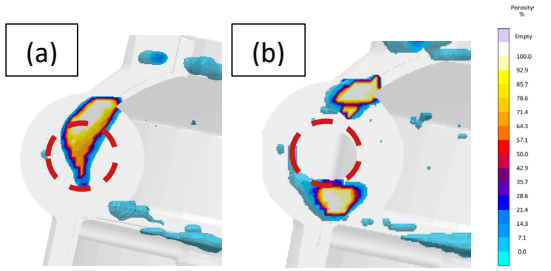

Figure 11. The simulated porosity of (a) the current gating and (b) design variation 4 in percent density. The porosity is moved somewhat away from the drilled hole by preforming the hole in variation 4.

6. Act and Check Improvements

While the project has not yet progressed beyond this point, the two designs are expected to finish sampling soon. From there one final design will be chosen based on whether riser is worthwhile for eliminating shrink compared to the improved yield of the preformed hole version. When the final design is put into production, data will be gathered to see how successful the project truly was and the cost savings will be quantified.

Concluding Remarks

Whether approaching a high-scrap production part or a new job, it is important to follow a set approach. One should set objectives, define variables, set criteria, keep their task efficient, choose their method, and act and check the improvements. Each step helps produce better designs and test them with fewer sampling runs or simulations. By following this process, the engineer can become more efficient in their design process and reach optimal designs faster.

INVESTMENT CASTING INSTITUTE

An Investment Casting Foundry Experience in Improving Degassing & Grain Refining in Molten Aluminum Alloys

Robert Zebick – Atlantic Casting & Engineering
Brian Began - Foseco

66TH TECHNICAL CONFERENCE
&
EXPO 2019

Paper № 8

An Investment Casting Foundry Experience in Improving Degassing and Grain Refining in Molten Aluminum Alloys.

By: Robert Zebick; Atlantic Casting & Engineering & Brian Began; Foseco Foundry Division, Vesuvius PLC

Abstract

The requirements to degas, flux and grain refine molten aluminum alloys for investment casting are well established. The evolution of casting buyer requirements; now requiring larger castings or more complicated geometries than the previous generation, continually require better and more consistent melt treatments for the molten aluminum. Fortunately, several recent technological advancements have allowed degassing, flux and grain refining to be higher performing and more environmentally-friendly than were historically achievable.

This paper will report on the efforts of Atlantic Casting & Engineering (ACE) in Clifton, NJ to implement an improved aluminum alloy treatment process to keep up with the demands of industry. In addition to the process of implementation, this paper will document the rationale and evaluation process for implementing the process improvements. Finally, the paper will discuss the economic, technical and environmental benefits achieved upon complete implementation of the new treatment process.

Keywords: Degassing aluminum alloys, grain refining aluminum alloys, thermal analysis of aluminum alloys, case study, automated treatment of molten aluminum

Introduction

The subject foundry, Atlantic Casting & Engineering, is privately-owned and has been in business for over 80 years. The foundry manufactures high-precision and geometrically complex cast parts, primarily for the aerospace market, but also serves the military, electronics, transportation, medical and various other marketplaces. The operation features two different mold making processes, handling parts up to a 30" cube, and pours approximately 7000 lbs. of aluminum per day. The operation includes various paste and liquid wax injection machines, ranging from 5 to 100 tons. The investment shell area features both automated and manual dipping processes, followed by autoclave dewaxing. Seven electric melting furnaces are used to process approximately 7000 lbs. of metal per day, with up to 15 different aluminum alloys. Finally, the post-casting operation boasts a variety of equipment for finishing, heat treat, and straightening of castings, and a full CNC machine shop.

Incumbent Melt Treatment Procedure

The foundry melts and pours an array of aluminum alloys including 201, A203, A205, C355, A356 and F357. These melts are melted and prepared in one of six electric-resistant crucible furnaces ranging in size from 1200 lbs. to 250 lbs. in capacity. All foundry elemental additions are made into the furnace directly rather than in the hand ladle prior to pouring.

The historical method for treating aluminum in the subject foundry entailed adding metallic-form TiBor (5%Ti, 1%B) pucks into the melt at a rate of .25% the weight of aluminum to be treated. The additions were made prior to the degassing process, which utilized an iron-cross or gear shaped rotary impellor connected to a simple pneumatic drive degassing unit that is raised, lowered and transported via an overhead hoist. High purity argon was the purge gas used during the 30-minute rotary degassing cycles.

In addition to rotary degassing, hexachloroethane degassing pills were used to provide both cleaning and additional degassing of each melt. The hexachloroethane degassing pill treatments were 10 minutes each and were added at a rate of 0.15% the weight of aluminum to be treated.

Only elemental spectroscopy of the Titanium (Ti) levels was historically used to evaluate grain refinement, with a typical target level of 0.15% (+/-0.02%) by weight. A standard reduced pressure test (RPT) was performed to assess degassing efficiency by placing a standard sample cup under a vacuum pressure of 27.5 (+/-.5) inches of Hg for 7 minutes. A picture of the reduced pressure testing apparatus appears in Figure 1.

Figure 1. Picture of the RPT apparatus used to assess degassing efficiency.

Once solidified, the RPT specimens were subjected to the hydrostatic displacement technique, i.e., a ratio of weight in air and a weight in water, to determine the specimen's specific gravity. The minimum threshold specific gravity for each alloy poured appears in **Table 1**.

Table 1. Alloys and specific gravity threshold minimums

Alloy	Specific Gravity Specification Minimum
201	2.70
A203	2.70
A205	2.80
C355	2.65
A356	2.65
F357	2.65

Thermal Analysis Testing

It has been established that grain refinement can beneficially affect feeding, fluidity and mechanical properties in aluminum castings.[1,2] Hence, inadequate grain refinement can yield shrink voids in aluminum castings. Moreover, it is established that too much Sr can cause porosity in aluminum-silicon alloys also resulting in porosity in cast aluminum.[3,4] Accordingly, it was decided to assess the grain refinement and eutectic modification levels to see if an improved practice was possible.

A THERMATEST 5000 NG III thermal analysis (TA) unit was used to assess the grain refinement (or grain fineness) and eutectic modification (or eutectic structure) of the treated melts after they were prepped for pouring. Thermal analysis involves collecting data of temperature versus time of a solidifying melt sample and comparing the curve to a set of known curves algorithmically. A photograph of the subject TA unit is shown in **Figure 2**.

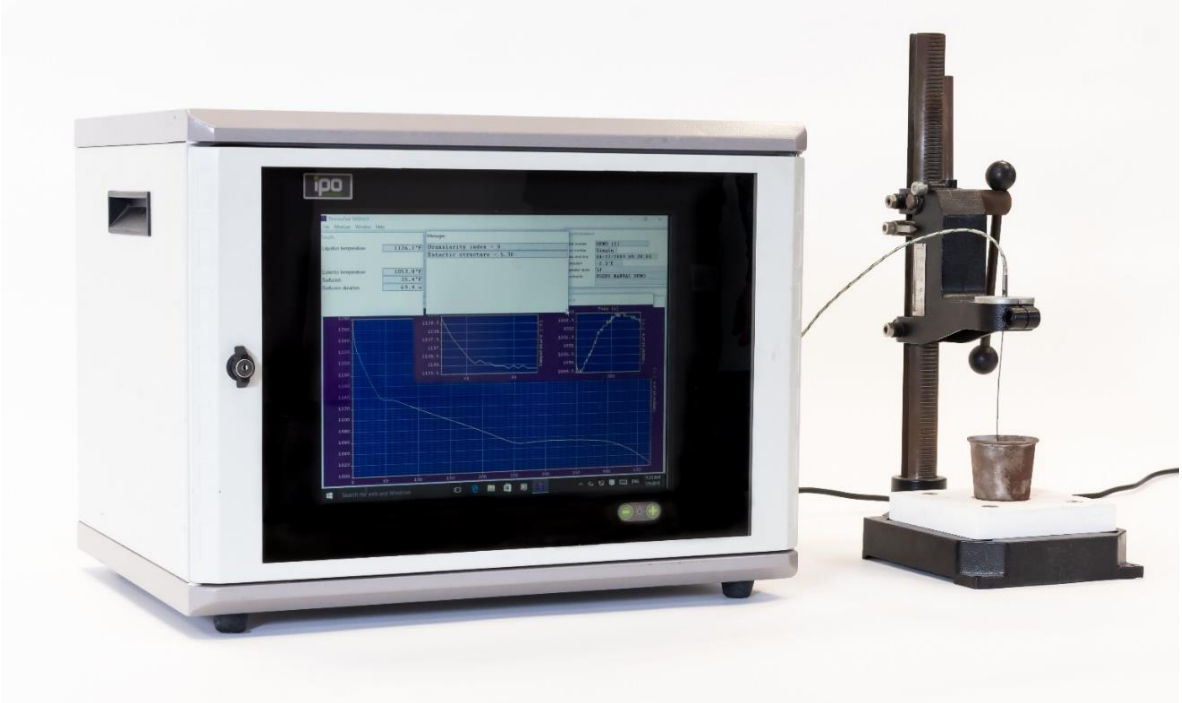

Figure 2. Photograph of the TA unit used in the melt assessment.

The TA algorithm analyzes the sample curve liquidus and computes a score on a scale from 1-9 for evaluating grain fineness (GF). A score of 1 references a curve that compares perfectly with curves exhibiting no grain refining. In contrast, a GF score of 9 is achieved when the sample curve compares with those curves know to have produced "perfect" grain refining of melts with the same alloy composition. A pictorial representation of the subject grain refinement levels is provided in **Figure 3**.

The TA unit is also capable of assessing eutectic modification effectiveness as well. Like with grain refinement, the TA device compares experimentally derived temperature/time curves to known standards and computes a score on a 1-7 scale. The scale for measuring eutectic structure (ES) differs from grain refining in that a score of 7 does not denote perfect modification, but rather a condition in which too much Sr has been added and eutectic shrinkage would be expected. Typically, 356 alloy casters who are intentionally modifying the Si eutectic in their melts target a range of 4 to 5.5 on ES. ES values lower suggest insufficient modification and ES values higher suggest too much Sr modification.

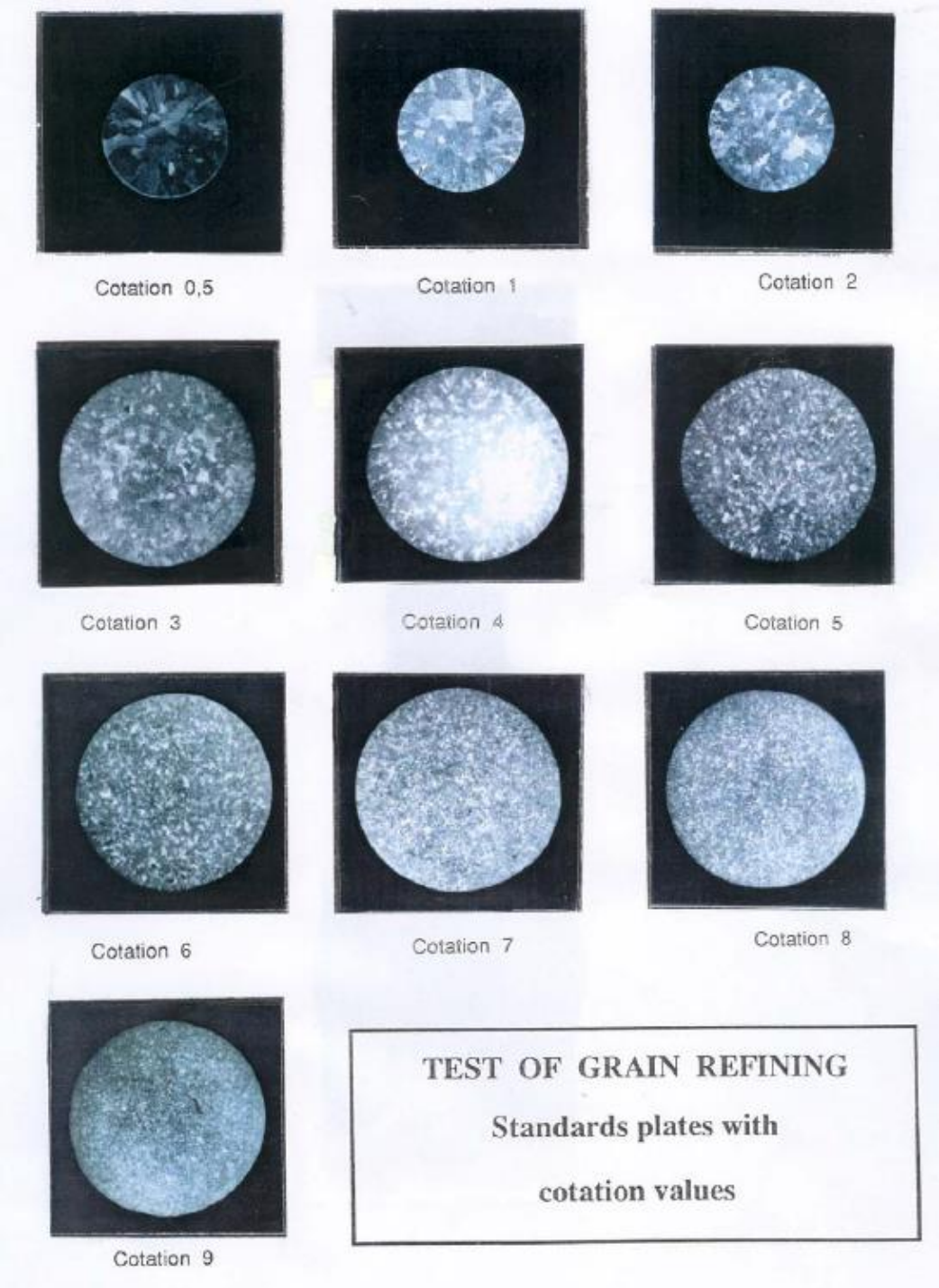

Figure 3. Pictorial representation of the grain refinement levels as measured by the TA.

The results of the TA evaluation of the incumbent process are presented in **Table 2**. It should be noted that no efforts are typically made to intentionally modify the eutectic silicon so a low level of near 1 was expected for the ES. Fortunately, the level of modification was so low that any effects would be negligible and what modification may have been performed should not prove problematic.

Table 2. Results of TA evaluation with incumbent procedure

Alloy	Grain Fineness (GF)	Eutectic Structure (ES)
355	6.9	2.51
356	6.2	1.27
357	7.5	N/A

The results of the TA analysis clearly show an opportunity for improvement in grain refining as the maximum level of 9.0 was not achieved in any of the three alloy (355, 356, 357) melts benchmarked. Hence, a project to improve the grain refining was initiated.

Salt Form Grain Refining

Before there was grain refining with metallic additives such as TiBor, grain refining was predominantly achieved via salt pucks. The salt pucks would decompose and react at the holding temperatures of molten aluminum to form metallic nuclei in situ. Examples of nuclei created from salts include, but are not limited to, $TiAl_3$, TiB_2 and AlB_2. These examples of nuclei were chosen for the listing as they are the same nuclei formed from metallic TiBor. More information on grain refining can be found in the referenced paper authored by Began and Careil.[5]

Unfortunately, salt form grain refining with pucks fell out of favor since the pucks were buoyant in aluminum requiring that they be plunged with a stainless-steel bell jar. The elemental contamination of Fe from the stainless-steel bell jar would yield both chemistry and mechanical property problems in aluminum so an improved grain refining methodology was required. Metallic form TiBor overcame the buoyancy problems of salt form pucks so despite being costlier and largely less effective than grain refining with salt form pucks, it gained widespread adaptation since, for the moment, it resolved the issue of Fe contamination.

More recently, a novel granular salt flux form grain refiner was developed within the past decade to be an improvement over metallic form TiBor. A recent paper documented the success achieved both technically and financially in converting from metallic form TiBor to the reference salt form grain refiner at Littlestown Foundry in Littlestown, PA.[6] The salt form grain refiner can be applied without steel tools so it overcomes the Fe contamination issues associated with the pucks. In contrast to the pucks, the granular flux form grain refiner can be integrated with a Metal Treatment Station (MTS) so that only graphite and inert ceramic components contact the aluminum during its application. The salt form grain refining flux has the additional benefit of being a very strong cleaning flux capable of reacting with oxides to chemically separate them from aluminum.

As previously indicated, the predominant way for reacting the salt form grain refining flux is via a metal treatment station (MTS). In a MTS, a vortex is temporarily created by withdrawing a vortex breaker baffle board and increasing RPM's of the graphite shaft and rotor used in the rotary impellor degassing process. PLC controlled additions of the treatment flux are added into the vortex and mixed to complete reaction prior to the vortex breaker baffle board re-engaging the melt, effectively stopping the vortex. After the vortex has been stopped, the MTS completes a standard rotary degassing process and the treated metal in the ladle or crucible is used for transferring and/or casting.

Experimental Procedure

Degas Modeling

To assist with achieving optimized hydrogen removal, a degassing model was utilized to determine a minimum cycle time.[7] The parameters were plugged in using 357 alloy since it is generally the toughest of the aforementioned alloys to degas in terms of cycle time. The chosen conditions tended towards the extremes where degassing is most difficult, e.g., high temperature and humidity. The parameters for the new procedure model are presented in **Table 3**. A model was prepared as a best estimation of the incumbent process as well with the only change being the rotor design being run at the traditional rpm, flow rate, etc. The results of the model for both the incumbent procedure and the newly proposed procedure are presented in **Figures 4(a)** & **4(b)**, respectively.

Table 3: Parameters for degas modeling

1200 lb Crucible	XSR 220 rotor
357 Alloy	0.50 ml H2 / 100 g Al starting level
1330º F melt temperature (*)	600 s minimum treatment time (*)
60% relative humidity (*)	95° F ambient temperature (*)

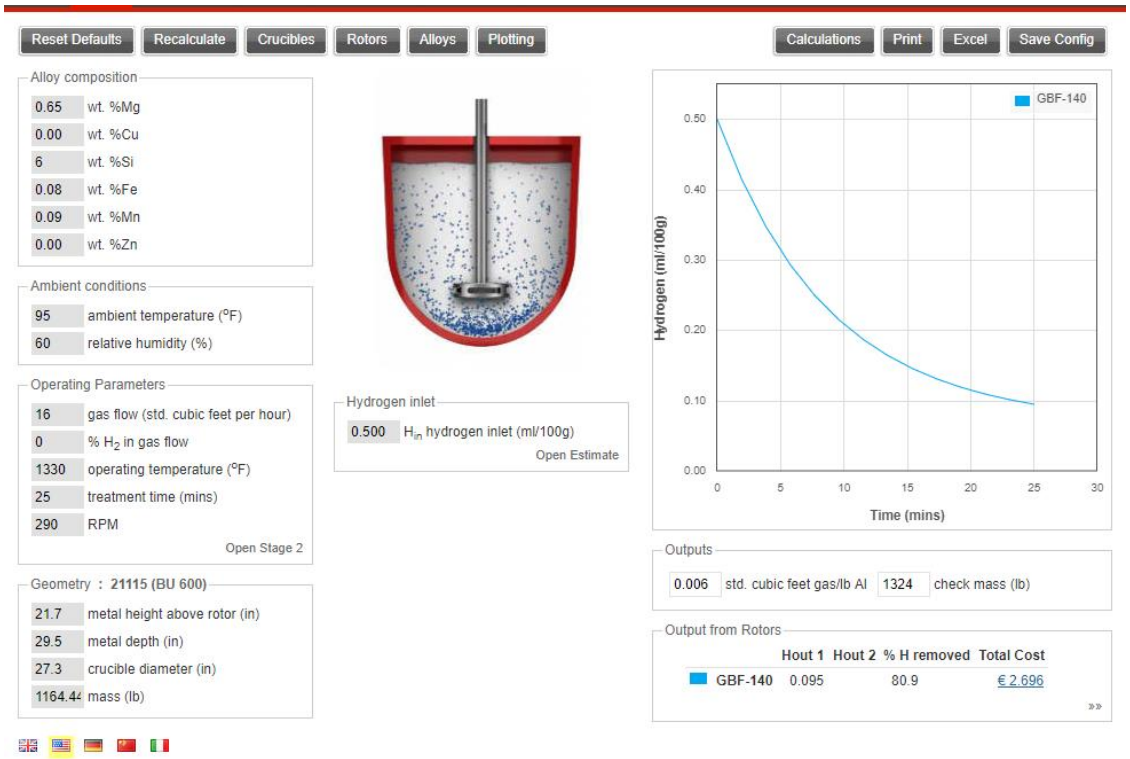

(a) Modelling of incumbent degassing procedure

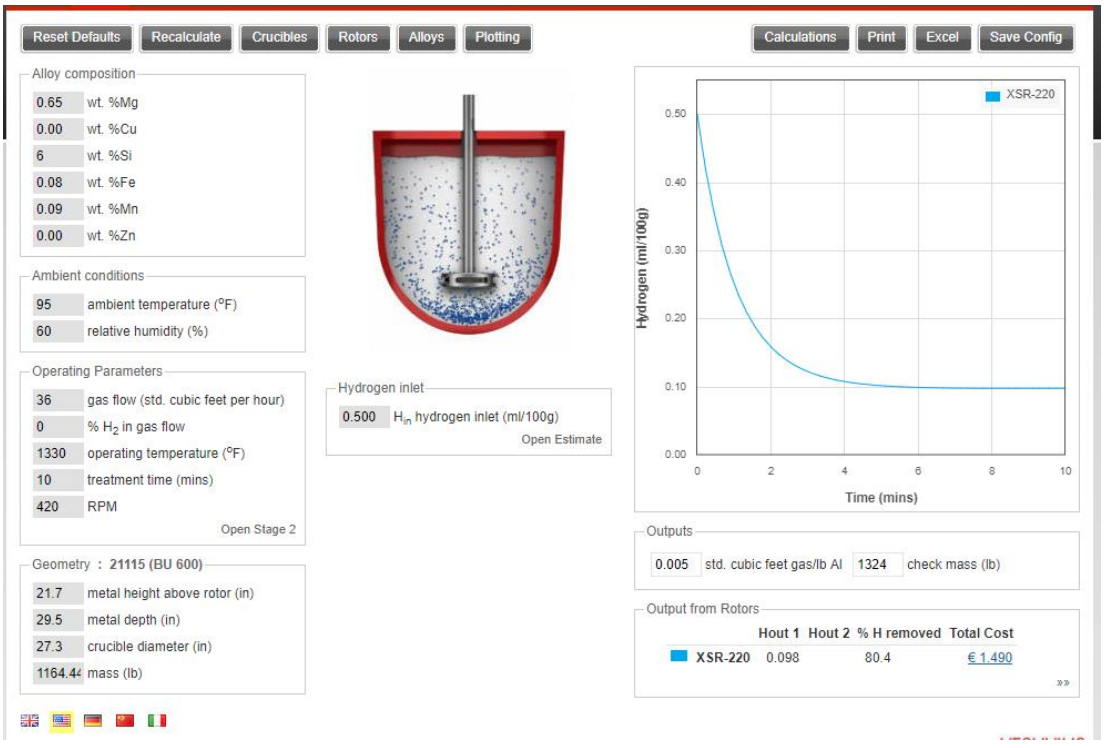

(b) Modelling of proposed degassing procedure

Figure 4. Results of Degas Modelling 357 in 1200 lb. Furnace.

The results of the degas modelling confirmed that in even tough conditions, the new rotor design and unit combination should be able to degas the melt in approximately 6-8 minutes under ideal rotor and baffle plate conditions. A 13-15 minute average cycle should be more than sufficient for when rotor wear, belt wear and perhaps baffle plate wear lead to a slight reduction in degassing performance. The model approximation performed for the incumbent process suggest that 25 minutes are required to degas the same melt in similar conditions; hence, a 30 minute historic degassing time was apropos although experience has shown that when the rotor and/or baffle plate were worn, a repeat cycle was often required.

A dimensional schematic of the MTS degassing unit designed for trials appears in **Figure 5**.

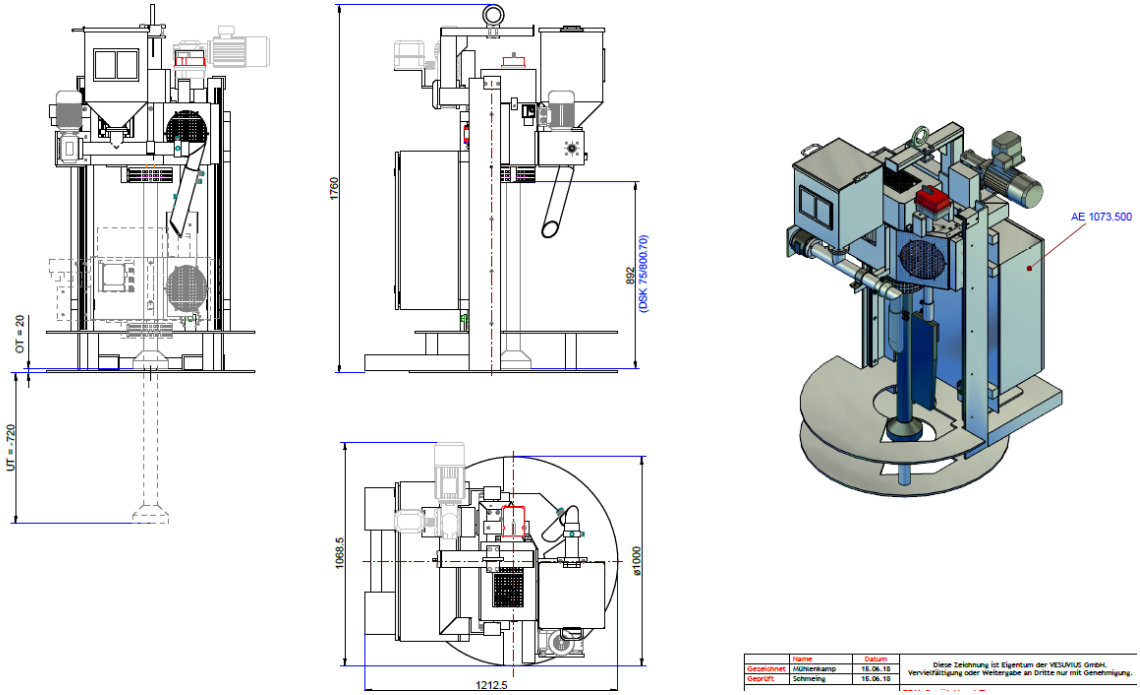

Figure 5. Dimensional Print for the Metal Treatment Station

The unit can be moved into place by either a fork truck or an overhead hoist and operates by being set upon the melt furnace targeted for treatment. The unit employs a retractable carriage that will automatically lower the degassing shaft, rotor and baffle plate into the melt during treatment and automatically withdraw the degassing shaft, rotor and baffle plate at the end of the treatment. The unit is designed to withstand the heat of the melt to be treated and to pass purge gas only during the cycle. The unit is outfitted with a hopper to hold the grain refining flux and an auger drive system to deliver precise amounts of flux each treatment.

The New Melt Treatment Procedure

After completing the modelling, the new melt treatment procedure was tested against the incumbent procedure. Specifics of the newly evaluated procedure follow:

- Treatments with a Hoist Mount MTS unit and an improved pumping rotor design
- Treatment parameters set according to the degas modeling
- Grain refining and cleaning to be performed via the automatic additions of the grain refining flux
- Argon to remain the purge gas
- Treatment cycle will be automated to 10 mins for 600 lb. crucibles and 15 mins for the 1200 lb. crucibles
- Elimination of TiBor and Hexachloroethane pills

Grain Refining

Once the MTS unit was onsite, efforts were taken to verify the effectiveness of the vortexing system with respect to grain refinement. Grain refining flux additions of 0.06% the weight of aluminum melt were added via the MTS to both 600 and 1200 lb. melts. The results of the TA testing results are tabulated in **Table 4**. In every treatment using the grain refining flux, a perfect GF score of 9.0 was achieved.

Table 4: Results of TA Evaluation with grain refining flux

Alloy	Grain Fineness (GF)	Eutectic Structure (ES)
355	9.0	1.69
356	9.0	1.00
357	9.0	N/A
355	9.0	2.98
355	9.0	2.06
357	9.0	N/A

TA curves taken in 356 alloys from the incumbent process (orange) and with the grain refining flux (blue) are overlayed and presented in **Figure 6**. Figure 6(a) shows the entire TA curve and Figure 6(b) shows a blow up view of the liquidus portion of the curve. The liquidus is the portion of the curve where the primary aluminum grain changes from liquid to solid. The TA value for the blue (grain refining flux) line was 9 while the TA value for the orange (incumbent with metallic TiBor) line was 6.2. For reference, these TA values match the readings reported in Table 2 and Table 4 respectively, for 356 alloy.

In Figure 6(b) you can clearly see some the orange line go down and then index slightly back up before indexing back down. This phenomena where the cooling curve indexes up before indexing back down is metallurgically referred to undercooling and indicates

an opportunity to improve grain refining. In contrast, you do not see any undercooling in the blue (grain refining flux) line which indicates there is no opportunity for improving the grain refining in its melt.

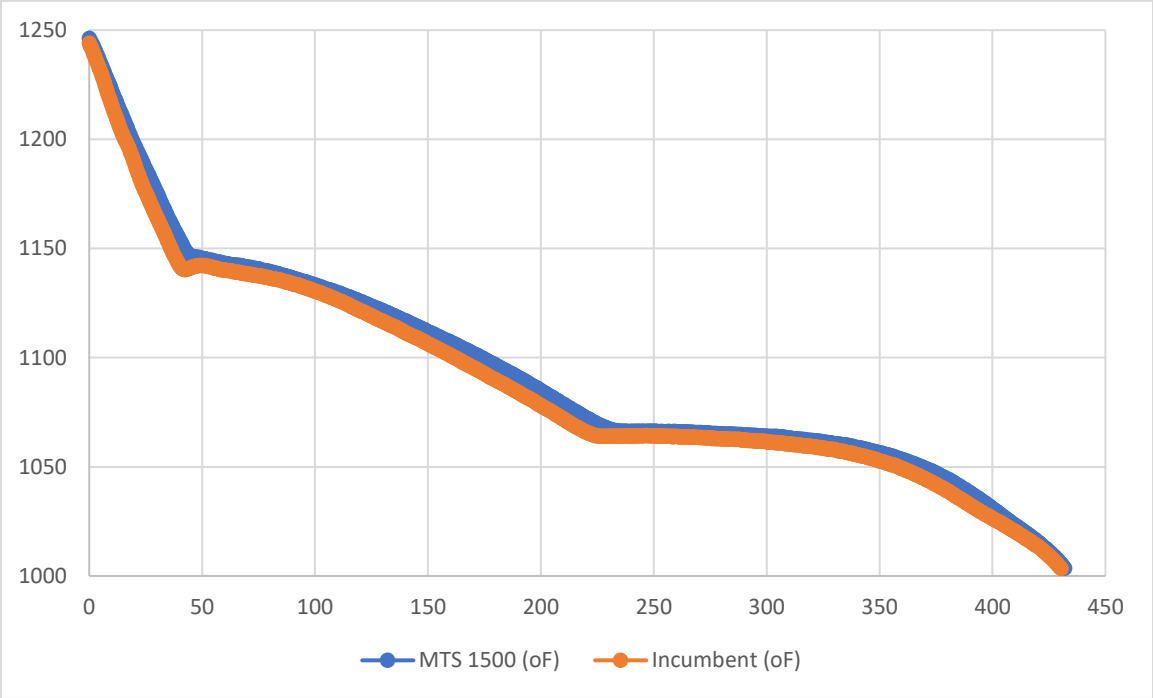

(a) Entire TA overlay of curves for incumbent and flux grain refining

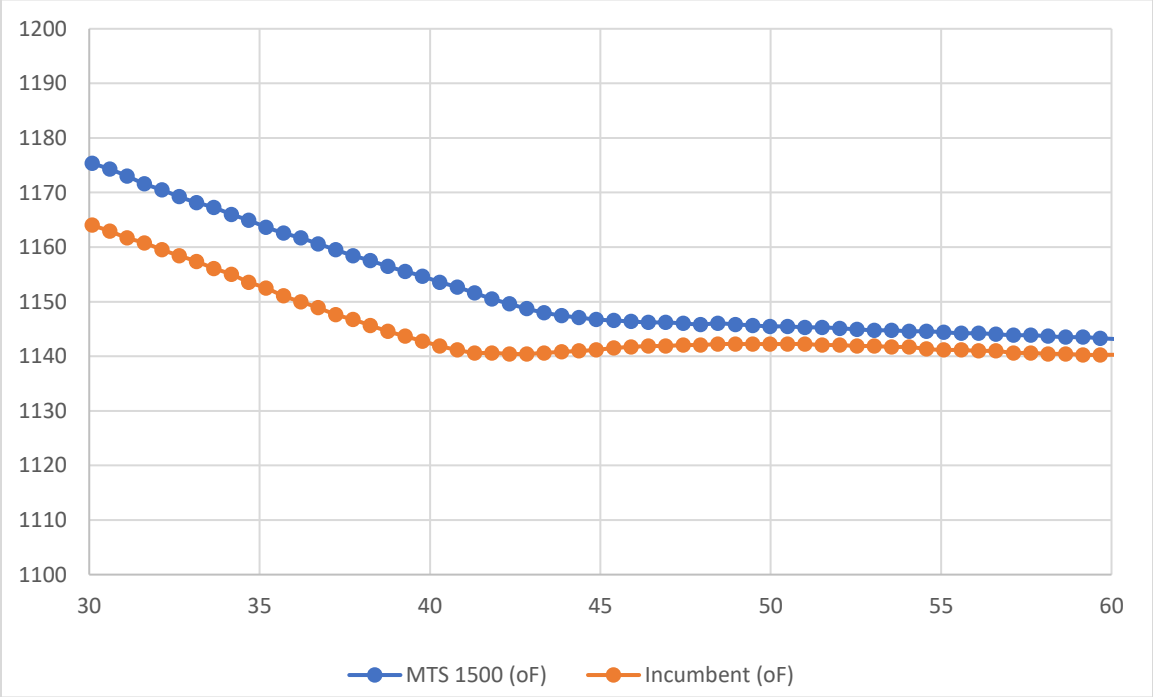

(b) Blowup view of TA curves at liquidus arrest for incumbent and flux grain refining

Figure 6. TA curves taken of both the incumbent and the flux grain refining

Hydrogen Control

Once the effectiveness of grain refining was verified, the evaluation of the hydrogen was completed. The cycle times were lowered from 30 minutes with the incumbent process to a cycle time average of 13 minutes so there was initial concern about matching performance. Fortunately, every cycle tested matched, or exceeded, the threshold specific gravity specification according to the internal RPT protocol. Moreover, a novel in situ hydrogen sensor was used to verify that hydrogen levels were equivalent or better than the incumbent procedure. For more information on the novel hydrogen sensor used to confirm performance, review the content on the work by Fray and co-workers in the referenced paper by Sigworth & Began.[8]

The results of the hydrogen concentrations taken during testing are provided in **Table 5**. The results are concentrations of hydrogen based on the Nernst equation and were taken from two different dates. In contrast to specific gravity where a higher number is preferred, lower values are preferred with hydrogen concentrations. The great news is that even though the new process showed a little bit better hydrogen concentration levels, even the three measurements taken from the incumbent process were strong (favorable) readings.

Table 5: Results of evaluation for hydrogen concentrations

Alloy	Incumbent [ml/100g]	MTS 1500 April 2018 [ml/100g]	MTS 1500 October 2018 [ml/100g]
355	.10	.07 / .05 / .08	N/A
356	.12	.10	.06
357	.08	.08	.04 / .06 / .06

Environmental and Safety Benefits

There are significant environmental and safety benefits available in the elimination of Hexachloroethane degassing pills. Hexachloroethane pills decompose in aluminum aspirating gaseous chlorine ions. These chlorine ions are recognized as toxic, carcinogenic and highly reactive with many materials. Hexachlorethane pills were actively targeted to be phased out of the foundry industry in the United States starting in 1999 because of the array of detrimental side effects when the chlorine ions are aspirated. Even when Hexachloroethane pills do not aspirate chlorine ions, they are dangerous to the touch since they can adsorb to the skin causing a depression to the central nervous system according to Wikipedia.[9]

Results

The original evaluation of the new melt treatment was a success so it was implemented, monitored and verified five months later. A tabularized dataset from the adaptation appears in **Table 6**.

Table 6. Tabularized Dataset of Incumbent and New Procedure

Metric	Incumbent	MTS Process	Comments
Chlorine Cost ($/lb.)	$3.20	0	N/A
Chlorine Usage (per/lb of Al)	0.15%	0	N/A
Chlorine $/day	$28.80	0	100% reduction
Ave Cycle Time (mins)	30	13	56.67% reduction
Ave Total Melts/Day	8	8	N/A
Ave Repeat Cycles	2	0	N/A
Ave Approved Melts/Dav	6	8	N/A
Success rate	75%	100%	N/A
Total Degas Time (mins per day)	338	104	69.2% reduction in degassing time
Melt (lbs./day)	6000	7800	30.00% increase metal poured per day
Tibor% Melt/lbs. per Al	25%	0	N/A
COVERAL MTS 1582	0	0.06%	N/A
Grain Refining Cost/Day	$104.55	$20.13	$84.42 or 80.7% reduction in daily spend
Argon Spend/Melt	$11.05	$6.40	

The successful adaptation of the new process brought about the following technical & productivity benefits:

- Perfect grain refinement every treatment measured with the THERMATEST 5000 NG III unit including 7 more tests run 5 months after implementation as part of the verification process
- Not a single failed specific gravity test since implementation! 25% of the treatments with the incumbent process would fail specific gravity testing allowing for 2 more melts treated and poured per day.
- A 69% reduction in degassing time average per day.
- 30% increase in metal poured per day.
- Effective elimination of hexachloroethane pills (without performance implications) leading to improved safety and environment.

Additionally, the following economic benefits were achieved upon adaptation of the new process:

- Elimination of the $28.80 daily spend on Hexachloroethane pills
- Grain refiner savings of $84.42 per day switching from metallic TiBor to the grain refining flux.
- Argon savings approximating $4.65 per melt.

The adaptation was reviewed for potential drawbacks and other implications it may have caused. It was hoped that the mechanical properties, particularly elongation, may go up due to the improved grain refining (as it had in the referenced paper at Littlestown Foundry); however, the mechanical properties tested before and after the new process adaptation remain unchanged statistically. Viewed from another angle, maintaining mechanical properties without using Hexachloroethane pills is a positive as mechanical properties and cleaning of aluminum melts is the predominant reason some foundries cite for not ceasing their use despite the myriad of health issues they can cause.

The baffle plate is an additional spend item (approximated at $1500 per annum) so these new costs need to be subtracted from the total savings. Finally, the graphite components for the new system cost more per piece than the historic process components but annualized spend is expected to be less since there are shorter cycle and longer usable life of the newer consumables which are thicker and last longer. However, if (or in our case when) the operators accidentally mishandle these components a slight decrease in savings (and potentially an increase in spend) can result and during the first year an increase of graphite spend is estimated to be nearly $1500.

Finally, the biggest difficulty with the new system is the bulkiness of the new unit, which requires a higher-grade overhead hoist and more caution from the operators because it is nearly ten times larger and heavier than the incumbent unit. However, it is unanimously agreed that the benefits of the new system far outweigh those few difficulties that were introduced with the new unit/procedure.

An approximate payback Table appears in **Figure 7**. After all of the cost savings in reduced argon spend, eliminating chlorine pills and lower grain refining costs are offset by the slight increases in spend on graphite and baffle plates, a payback can be calculated and was determined to be approximately 16.5 months.

Saving	Payback Calculation Component Savings	Comment
Argon	$8,462.38	
Chlorine Pills	$7,488.00	
Grain Refining	$21,949.20	
Baffle Plate	-$1,500.00	
Graphite Shafts/rotors	-$1,459.90	
Sum annualized savings	$34,939.68	
Payback (yrs)	1.37	Yrs
Payback (months)	16.50	Months

Figure 7. Payback Calculation Table

Summary

A novel method for applying a combination salt-form grain refining flux and rotary degassing system was implemented at an investment casting operation in Clinton, NJ to great success. The new treatment method resulted in an improved grain refinement practice that lowered spend, increased productivity, improved hydrogen control, delivered environmental & safety benefits and eliminated waste. The calculated payback on a new MTS unit was calculated to be about 16.5 months.

Acknowledgements

The authors would like to thank Jason Allen of Foseco for preparing the TA curve graphics and Ben Groth of Foseco for preparing the optical micrographs. Additionally, the authors would like to thank Joe Spadacinni of Weaver Materiel Services and Vernon Edwards of Atlantic Casting & Engineering for capturing much of the TA data.

References

1. Limmaneevichitr, C., & Eidhed, W. Effect of Flux Compositions on Grain Refinement in Al-Si-Mg Alloy. *TMS Light Metals Proceedings.* p. 1107. San Francisco, CA: TMS (2005)
2. Dahle, A.K., Tondel, P.A., Paradies, C.J., & Arnberg, L. (1996). Effect of Grain Refinement on the Fluidity of Two Commerical Al-Si Foundry Alloys. *Metallurgical and Materials Transactions A,* Vol 27A. pp. 2305-2313 (August 1996*)*
3. Liao, H., Song, W., Wang, Q., Zhao, L., Fan, R., & Jia, F. Effect of Sr Addition on Porosity Formation in Directionally Solidified A356 Alloy. *International Journal of Cast Metals*. Res., 26(4). pp. 201-208. (2013)
4. Bian, X., Zhang, Z, & Liu, X., Effect of Strontium Modification on Hydrogen Content and Porosity Shape of Al-Si Alloys. *Materials Science Forum*. pp. 331-337, 361-366. (2000)
5. Began, B, & Careil, P. Theory and practice of grain refining for aluminum alloys – utilizing COVERAL MTS 1582. *Foseco Foundry Practice Issue 268*. pp 4-11 (2019)
6. Stonesifer, J. & Began, B. Degassing and Flux Grain Refining in a Continuous Treatment Well at Littlestown Foundry. *123rd Metalcasting Congress Proceedings* (pp. 5-7). Atlanta, GA: American Foundry Society. (2019)
7. Simon, R., & Began, B. An Introduction to Self-Monitoring Adaptive Recalculating Treatment Technology (SMARTT) in Degassing Aluminum. *Conference Proceedings.* (pp. 2-7). Newport, KY: Investment Casting Institute. (2017)
8. Sigworth, G., & Began, B. Control and Measurement of Hydrogen in Aluminum. *AFS 116th Metalcasting Congress Proceedings* (pp. 8-9). Columbus, OH: American Foundry Society. (2012)
9. https://en.wikipedia.org/wiki/Hexachloroethane

INVESTMENT CASTING INSTITUTE

Massive Shells & Castings in Reactive Alloys from a Highly Customized Facility...Finally

Will Jeffs
Castings Technology International

66TH TECHNICAL CONFERENCE
&
EXPO 2019

Paper № 9

Matthew Cawood - AMRC Castings
Will Jeffs - Castings Technology International

w.jeffs@castingstechnology.com

Abstract:

Following years of design/manufacture and installation with many a hurdle, the large scale shelling facility, capable of producing shells weighing in excess of 4,000 lbs has finally come to fruition. The initial research into shell selection was conducted by AMRC castings, whilst the practical application and manufacture of real shells and castings was conducted after this initial development by Castings Technology International to supply shells to Western Europe's largest Titanium melting and casting furnace.

The equipment consists of a large scale flood coater for primary coating, two 11 foot diameter slurry tanks for intermediate and back-up layers, plus three 13 foot diameter sand rainers for the three distinct layers. Two 11 foot wide drying pods, each with separately controllable humidity and temperatures for optimum shell build, investigation and results from the detailed drying trials shall also be presented and discussed.

The paper shall detail the initial back-up shell property selection, including detailed test results, control parameters for such massive tanks and footage of this coating process.
Following on from the shell manufacture there will also be details of the structural strength requirements and simulation of the stresses placed on the shell during casting to ensure shell survival during the most arduous conditions when they are spun and can be subjected to forces of 35 G (35 times the force applied when casting statically). This finally resulted in a static casting in Ti 6/4 being poured at 1,805 lbs.

INVESTMENT CASTING INSTITUTE

Improving Thermal Conditions & Reducing Process Costs for Core Setters in Aerospace and IGT Applications

Phil Geers
Blasch Precision Ceramics

66TH TECHNICAL CONFERENCE
&
EXPO 2019

Paper № 10

Improving Thermal Conditions and Reducing Process Costs for Core Setters in Aerospace and IGT Applications

P. Geers, Sr. Metals Market Manager, Molten Metals
Blasch Precision Ceramic, Albany, New York, USA
W. Russell, VP Technical Business Development
Blasch Precision Ceramics, Albany, New York, USA
D. Bacchi, Sr. Principal Engineer
Blasch Precision Ceramics, Albany, New York, USA

In the continuous improvement of investment cast blades for Aerospace and IGT applications, the associated ceramic core technology is also being pushed to new limits. With increased tolerances and intricate geometry, ceramic cores require accurate processing that is consistent and cost effective.

In our previous paper, "Effects and Analysis of Thermal Stresses on Core Setters for Aerospace Applications", we reviewed the benefits of using core setters with matched 3D geometry, to reduce the effects of sintering the ceramic core. We continue with this subject matter as we look at optimal core setter design for thermal consistency, through comparing the thermal profiles for ceramic setters, kiln layout optimization and a discussion of core setter material selection. Our goal is to provide solutions for aerospace foundries and core producers on how to improve yields, generate core consistency, and reduce scrap and energy costs.

Thermal Profiles During Core Sintering and Processes Variances

Having previously reviewed the concepts of sintering (heating) and its effects on ceramic cores; we concluded that these effects can be reduced through the use of a ceramic setter. Additionally, having higher variabilities in the sintering can result in higher stresses and geometric deformation in the ceramic cores, as referenced in Figure 1.

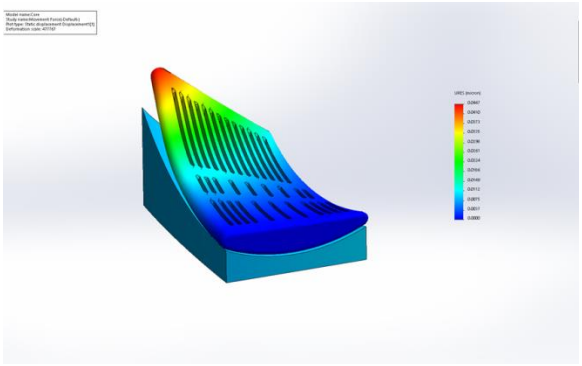

Figure 1: Stress and Deformation of Ceramic Core Under Thermal Load

From this we can theorize that providing more consistent and even heating to the ceramic core during sintering will reduce stresses and improve part consistency.

Our analysis spanned three settering designs: A grog filled sagger, a standard ceramic core setter, and an optimized ceramic core setter.

Figure 2 shows the modelled sagger with grog, representing a simple and common way to set ceramic cores.

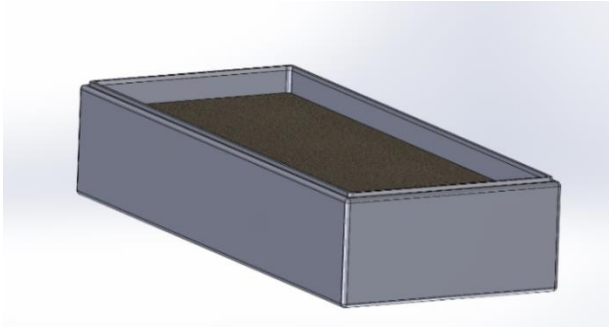

Figure 2: Grog Filled Sagger

Figure 3 models a simple ceramic core setter, a noted improvement over the grog filled sagger, However, this displays an inconsistent wall thickness.

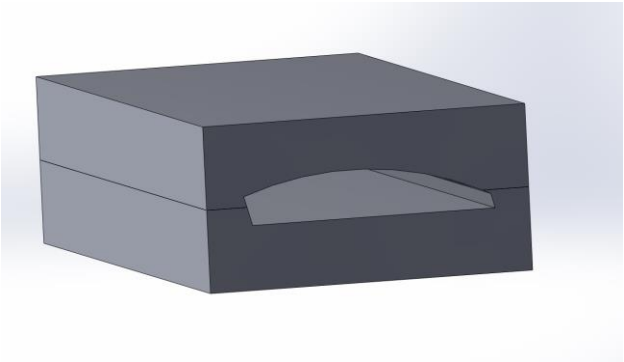

Figure 3: Simple Ceramic Core Setter

Finally, the thermally optimized ceramic core setter is shown in Figure 4, with the thermal mass reduced while still maintaining structural integrity. This allows for a consistency in wall thickness, further aiding in uniform heat transfer.

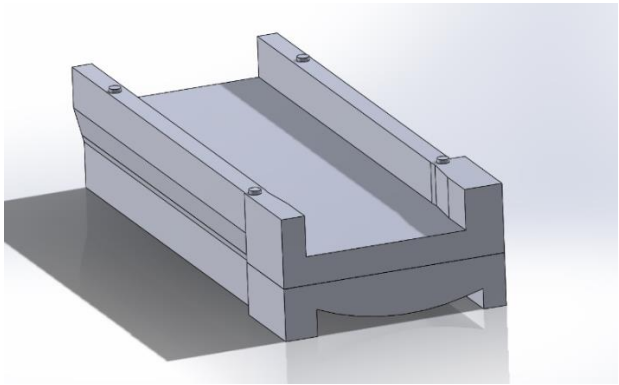

Figure 4: Thermally Optimized Ceramic Core Setter

All three models' overall length, width, height, and material were identical for the studies run.

Using thermal modelling in Solidworks' FEA software, we produced a thermal profile under transient heating for our three models, displayed 820 C in Figure 5.

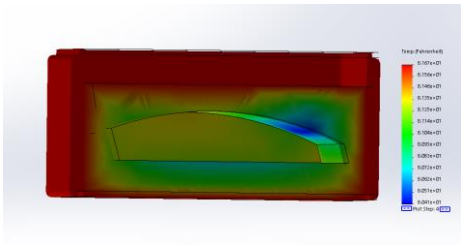

(a)

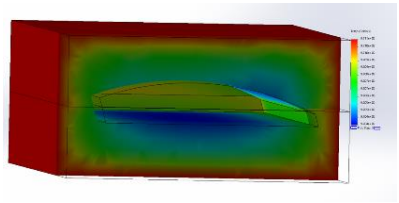

(b)

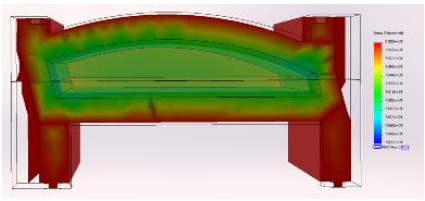

(c)

Figure 5: Thermal Profiles of Three Settering Designs at 820 C

At this temperature the core in a core setter with an optimized wall thickness, Figure 5c, has reached a higher internal temperature sooner. This is due to the reduced total mass, requiring less thermal energy to be heated. Also, we see the more uniform thermal temperature profile of the setter around the core. Conversely, we can see the blue spots in areas around the unoptimized setter, Figure 5b, and in the core in sand, Figure 5a. This variance is caused by the relatively uneven thermal mass of these unoptimized setters, which require more heat (thermal energy) in the thicker areas to bring the core up to the same sintering temperature. It is safe to assume an increase in time might be required to allow the setter and core to heat thoroughly.

From this review, we are showing that having the core set into a thermally optimized ceramic core setter, will provide a more even sintering temperature, along with using less thermal energy to get to that planned sintering temperature.

Kiln Loading Optimization

Now that we have optimized the geometry that we are firing the ceramic core in, we analyzed different organization profiles for improving and optimizing the orientation of setters in the kiln used for sintering.

Though not always the case, we will assume that our kiln is evenly heated with no apparent "dead spots" for heating. An example of this even flow is shown in Figure 6.

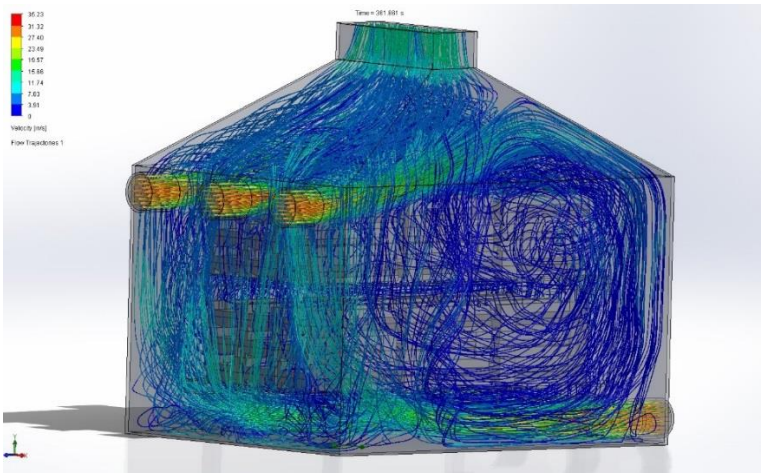

Figure 6: CFD Modeling of Even Flow

Using an evenly heated kiln, we can focus on setting up and arrange setters into the kiln for the best orientation for heating and thermal load optimization.

In Figure 7 we show an example where saggers with sand/grog are set into the kiln tightly packed together.

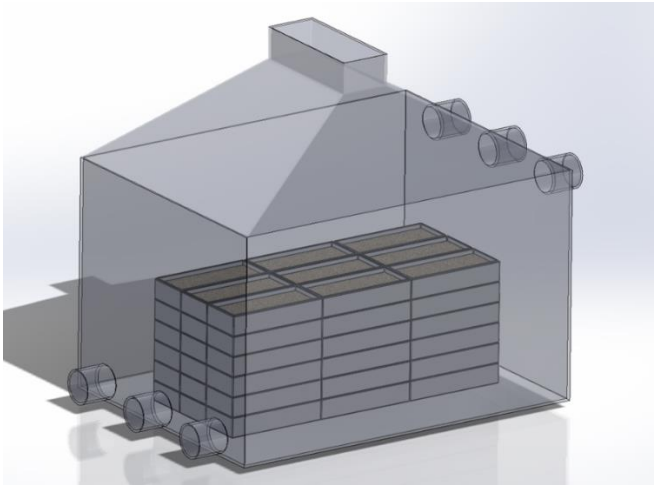

Figure 7: Tightly Packed Grog Saggers in Kiln

With the layout as shown, the heat profile for the large blocks of setters will act as one large object for heating; similar to the thermal model shown for the individual saggars, there are large variants in the temperature distribution and more energy is needed to bring the center saggers up to the required temperature.

Figure 8 shows the kiln load better optimized for heat transfer.

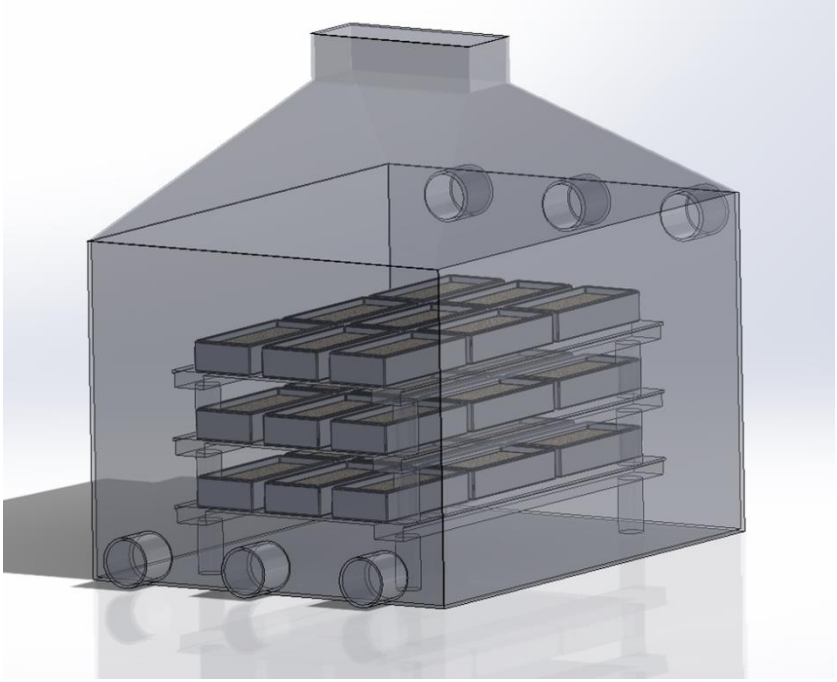

Figure 8: Improved Spacing in Kiln Layout

The saggers are spaced with gaps around them. This is done by using kiln furniture interlocking beams and plates. The kiln furniture structure allows this orientation, and in addition is made from a thermally conductive ceramic with assists in heat transfer.

In this next example, Figure 9 and Figure 10, we show a similar stacked kiln orientation, but now with the optimized ceramic core setter.

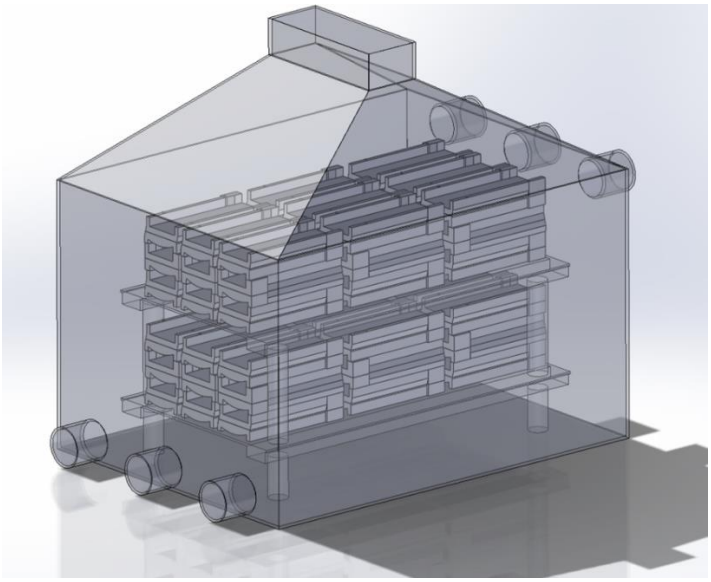

Figure 9: Isometric view of Kiln with Optimized Setters with Optimal Layout

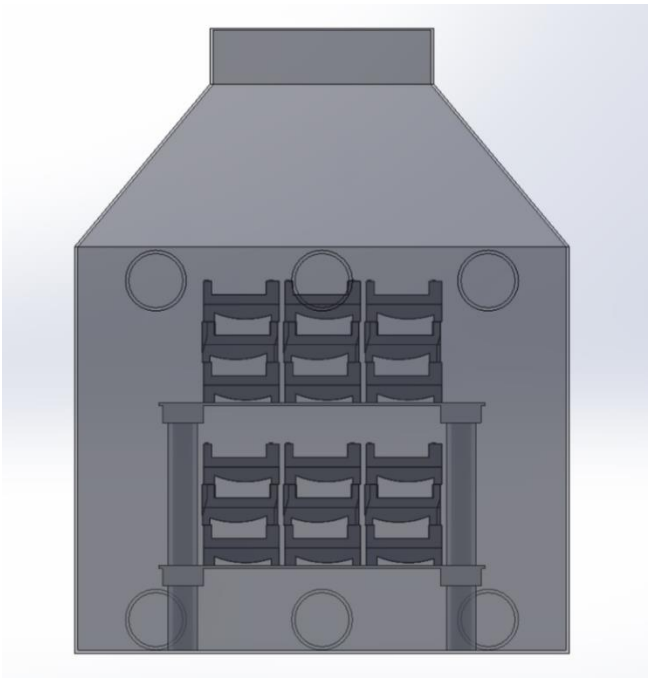

Figure 10: Front view of Optimal Layout

As shown, using the optimized ceramic core setter design, we have integrated stacking capability into the core setter which allows increased heat transfer around the setter and reduces the amount of kiln furniture required to accomplish this. Even spacing can also be accomplished with or to assist with automatic loading and unloading systems.

We see that organizing the kiln using a planned kiln furnace layout and even spacing of setters will allow the ceramic cores to have more uniform heating and allow better thermal profiles for sintering no matter what type of core firing technique is used. Adding design features into the core setter can optimize the thermal profiles even further.

Core Setter Material Selection

Core setter material also plays a vital role in the sintering and consistency of the finished part. Material characteristics that are most crucial to settering include: thermal shock resistance, part geometry tolerance, and ceramic creep resistance.

Thermal Shock Resistance:

The environment of the kiln sintering process requires heat cycling from ambient temperature to 1,200C, so the ceramic must be highly resistant to thermal cycling, called thermal shock.

Part Geometry Tolerance:

As the design of aerospace blades continues to evolve, the cores necessary are increasing in complication and complexity. To provide a matched 3D designed core setter to properly hold the core, high as-cast tolerances are required for the setter to function properly. Cast part tolerances near the range of .005" per inch are needed in the core setter and the forming process for the ceramic core needs to provide for this.

Ceramic Creep Resistance:

As the ceramic core setter thermally cycles potentially hundreds of times, the ceramic needs to resist any movement or change in tolerance through these cycles. This phenomenon can be tested by a three-point bend creep test, Figure 11. In this test, a single point weight is placed on a test bar of material, and is heated for the predetermined cycle. Once cooled the test bar is then measured for movement.

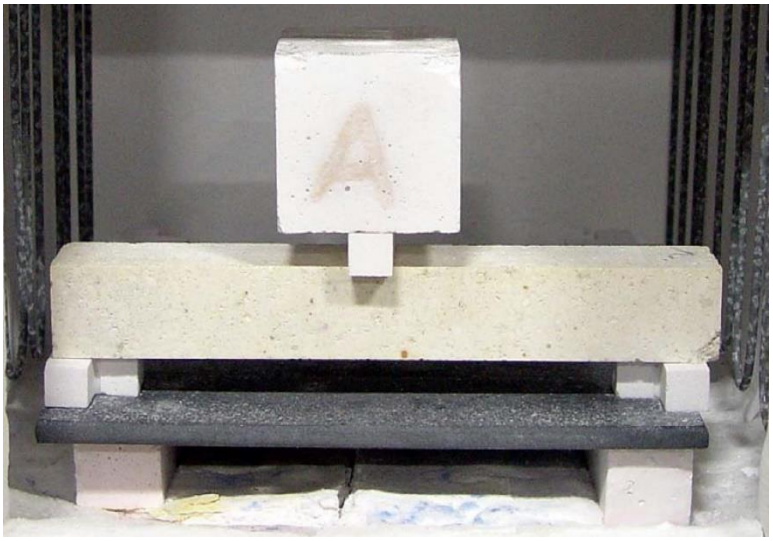

Figure 11: 3-Point Bend Creep Test Setup

As we develop materials for core setters, the creep test is a great developmental tool. Blasch recently developed a new material which was creep tested along with two other materials for reference as shown in Figure 12.

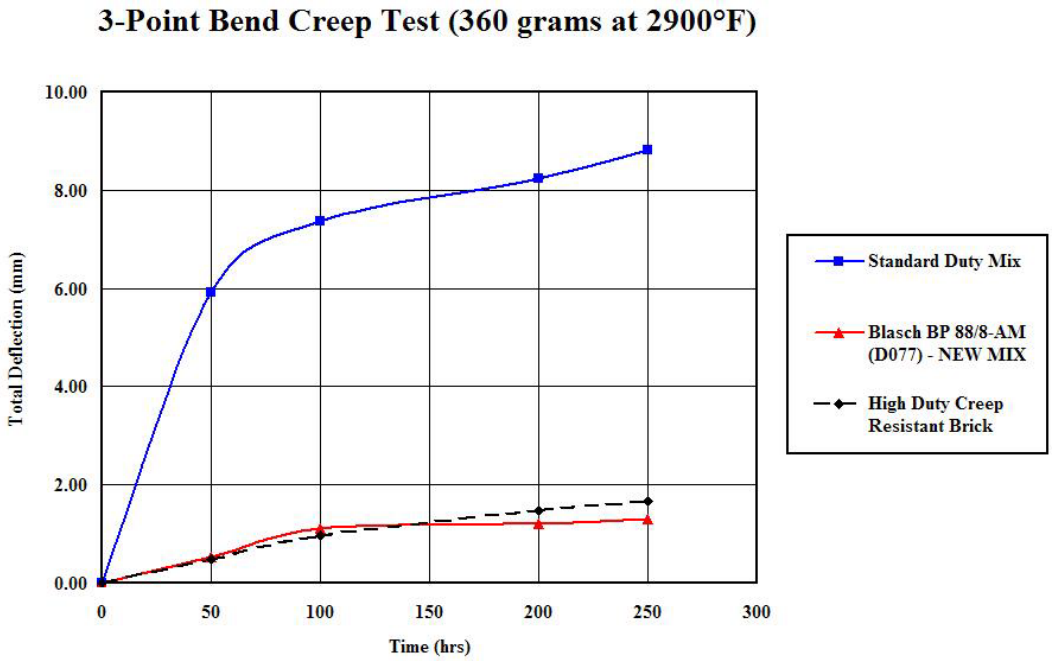

Figure 12: Results of 3-Point Bend Creep Test for Three Materials

We tested three materials: a standard refractory material, an industry standard high duty creep resistant brick material, and a new Blasch developed material. Displayed by total deflection over time (less deflection being better) this newly developed material showed a substantial improvement over a current industry standard creep resistant brick material. Improvement has also been noted in core setter life and tolerance stability over repeated firings with this new material.

The optimal conditions for sintering complex cores are as such: a uniform spaced kiln layout utilizing thermally optimize core setters made from high tolerance, thermal shock and creep resistant material. Blasch has over 40 years in ceramic materials and processes to help improve your foundries core sintering process.

INVESTMENT CASTING INSTITUTE

Analysis of 17-4 AND 15-5 Alloy Data from Investment Casting Trials

Victor Okhuysen
Cal Poly Pomona University

66TH TECHNICAL CONFERENCE
&
EXPO 2019

Paper № 11

ANALYSIS OF 17-4 AND 15-5 ALLOY DATA FROM INVESTMENT CASTING TRIALS

Victor Okhuysen, PhD

Professor, Cal Poly Pomona University

Dika Handayani, PhD

Assistant Professor, Cal Poly Pomona University

ABSTRACT:

Investment castings have a penalty in design parameters vis-à-vis wrought products for aerospace applications. An extensive study with over 1000 specimens from 14 investment casters in 17-4 PH and 15-5 PH was conducted. Tensile properties were analyzed for comparison between producers from a benchmarking point of view.

MOTIVATION:

This study is a benchmarking study to compare potential capabilities of alloys produced by different foundries using an existing data set. Two areas were looked at: Average performance and variability within foundries.

SPECIMEN PREPARATION AND TESTING PROCEDURE:

The tensile specimens were made by one injection house and sent to 14 participating foundries. The specimens originated from plate and externally cast bars. Foundries produced molds according to their practice and materials and followed their internal melting and pouring procedures as well. The heat treatment was performed at one heat treatment house and the tensile testing at one laboratory following the ASTM E8 standard.

DATA ANALYSIS PROCEDURE:

A subset of the entire data set was analyzed for this purpose. The alloys were 15-5 PH aged at 935 F and 1000 F and 17-4 PH aged at 1000 F and 1100 F. The properties reviewed were Ultimate Tensile Strength, Yield Strength, Percent Elongation and Percent Reduction in Area.

Averages and standard deviations for each foundry/alloy/aging treatment/property were calculated. Then probability plots for each of these averages and standard deviations were made to identify outliers on the top side and pand 17-4 1000 Fotentially look at best practices.

Table 1: Foundries and number of specimens tested per condition.

Foundry	15-5 PH 935 F	15-5 PH 1000 F	17-4 PH 1000 F	17-4 PH 1100 F
A	11	10	-	-
B	14	11	14	11
D	7	13	8	10
E	14	13	14	12
H	10	12	6	11
J	12	9	15	12

K	-	9	11	8
L	11	7	11	8
M	11	9	11	12
P	9	9	9	10
R	11	9	10	9
S	10	8	10	8
T	12	9	11	8
U	10	13	12	7
Total	142	141	142	126

RESULTS AND DISCUSSION SUMMARY:

This section is organized by looking at each property in turn for all alloys. That is, UTS for all alloys, followed by yield strength for all alloys, etc. In each alloy/property combination four plots were generated. General comments on the properties and representative plots of the characteristics in question will be presented. All of the charts are available in the appendix.

Ultimate Tensile Strength (UTS):

For the most part, the UTS values were above the standard minimums. However, the 15-5 935 F and 17-4 1000 F had several instances below the standard (figure 1). Foundry "B" also had data points that went below standard values in other alloys, though this appears to be a variability issue as the average was clearly above the minimum. In terms of some foundries performing significantly better than others, the normal probability plots for UTS indicate that the variation can be explained by normal variation. However, the variability of results (standard deviation) it can be seen that some foundries have significant larger variation as indicated by the point outside of the normal range (figure 2).

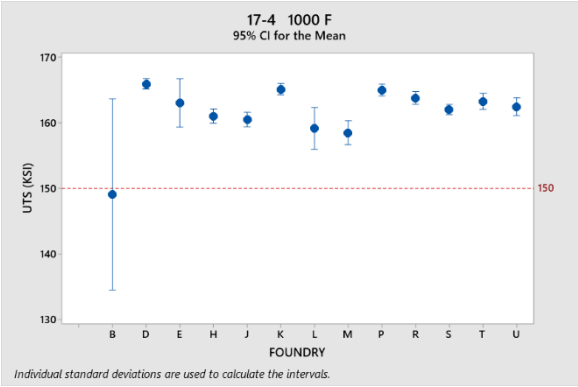

Figure 1A: UTS Confidence intervals. Note some intervals going below the minimum limit.

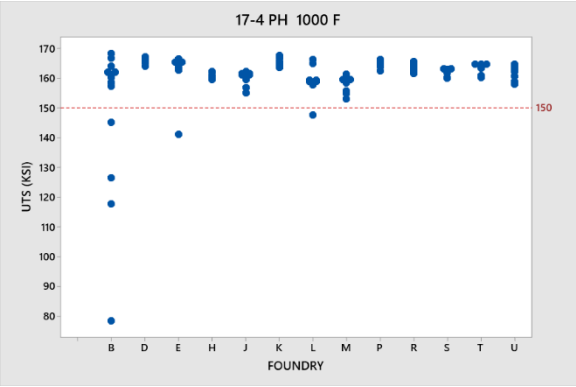

Figure 1B: UTS Individual data plot. Note that generally the values below the specification appear to be outliers, except for foundry B, where large variation is present.

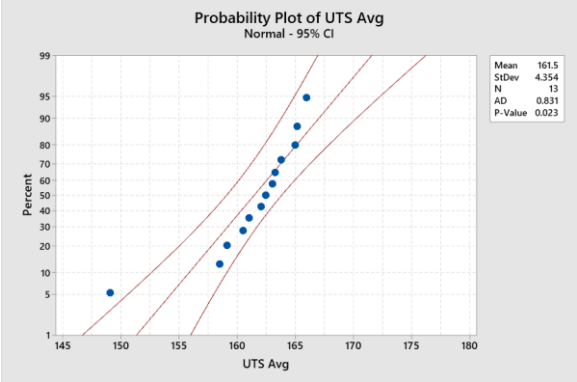

Figure 2A: Probability plot of UTS averages for each foundry 17-4, 1000 F. One significant outliers beyond normal variation, however, below desired value.

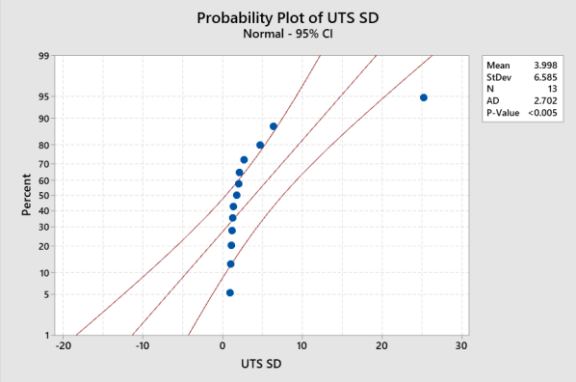

Figure 2B: Probability plot of UTS standard deviations by foundry 17-4, 1000 F. One significant outliers beyond normal variation indicating one instance with more variation between foundries than anticipated.

Yield Strength (YS):

Only two data points were below the minimum value for the entire data set of over 120 points. Thus, the YS minimums were easily met. In terms of variability, the yield strengths were more consistent from foundry to foundry than the UTS. In figure 3 this can be seen.

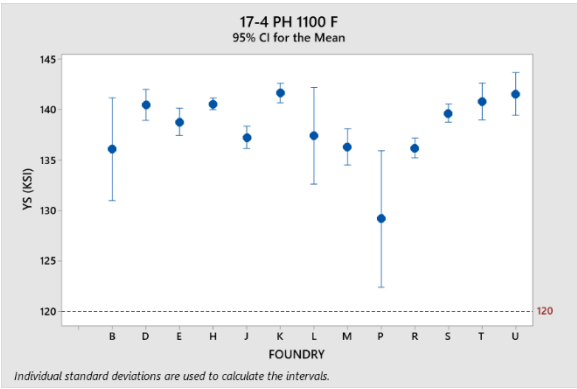

Figure 3A: Yield strength confidence intervals.

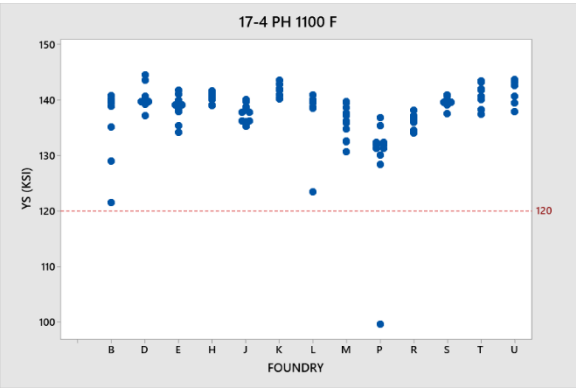

Figure 3B: Yield strength individual plot.

Percent Elongation (%EL):

The percent elongation data for each alloy shows that average values meet the minimum requirements. The variability though typically results in the confidence interval for several (1 to 4 per alloy) foundries extending below the minimum limit. However, looking at the individual data plot in all instance at least 8 foundries had points below the minimum (figure 4). Also note the wide variability in the data, this is one area where results can be obtained, but reducing the variability would provide the best benefit.

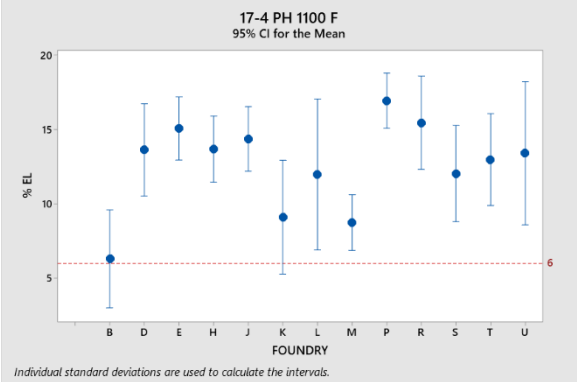

Figure 4A: Percent elongation confidence intervals. Note some intervals going below the minimum limit.

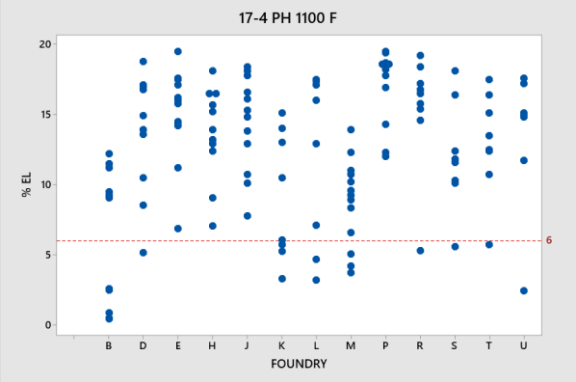

Figure 4B: Percent elongation individual plot. Note many data points below standard.

Percent Reduction in area (%RA):

The %RA follows similar but improved characteristics as the %EL. That is, the averages are significantly higher than the minimum requirements, though some confidence intervals extend below the minimum requirement. High variability is the issue here. See figure 5.

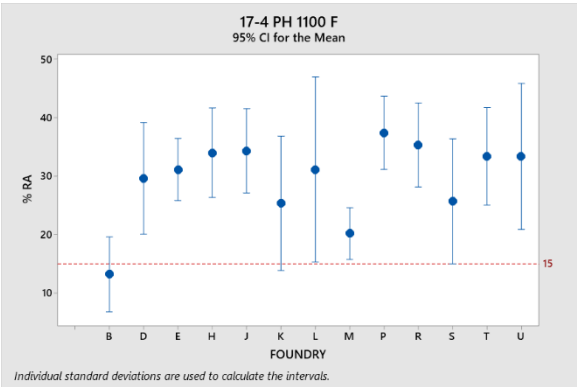

Figure 5A: Percent reduction in area confidence intervals. Note some intervals going below the minimum limit.

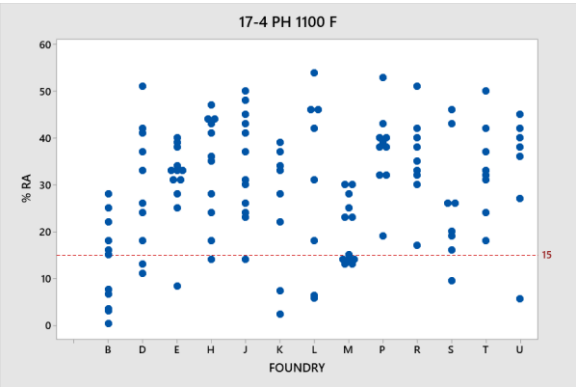

Figure 5B: Percent reduction in area individual plot. Note many data points below standard.

CONCLUSIONS:

Generally, the average UTS, YS, %EL and %RA are well above the minimum requirements. In the case of %EL and %RA high variability can lead to individual values below the minimum requirements. In terms of looking for difference between foundries from a benchmarking standpoint, most of the results can be explained by anticipated normal variation between foundries. The exception to this would be that some foundries perform worse (lower averages and/or more variability). However, on the top end for higher averages and/or less variability there were no clear differences.

This does not mean that there are no improvements to be made. Foundries can strive to improve their processes to attain the top range of values and lower variability if they are not already there.

APPENDIX

This section is written to be read in the following manner:

Each alloy and treatment are done separately. Then each mechanical property is presented with four graphs. The first graph shows the 95% confidence interval of the property by foundry. The objective here is to present statistical soundness to the analysis. However, as this may mask some features of the data, the second plot is the raw data points by foundry. In both of these plots, it is possible to benchmark differences in values and variation. In order to further identify significant differences between foundries in both mean and standard deviation values, normal probability plots were used on the foundry averages for mean and standard deviations. The interpretation here is to find the outliers with higher properties (top of average/mean chart) and lower variability (bottom of standard deviation chart).

Figures 1A-P: 15-5 PH, 935 F Age Confidence intervals, individual data plots, and normal probability plots for average and standard deviation of properties for each UTS, yield strength, percent elongation and percent reduction in area.

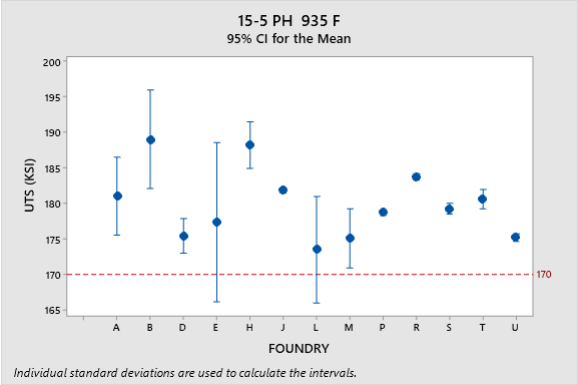

A: UTS Confidence intervals. Note some intervals going below the minimum limit.

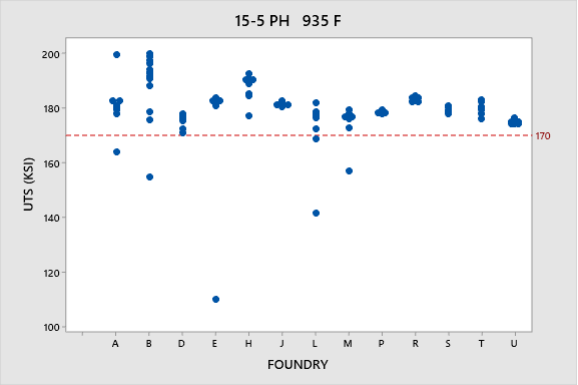

B: UTS Individual data plot. Note that generally the values below the specification appear to be outliers.

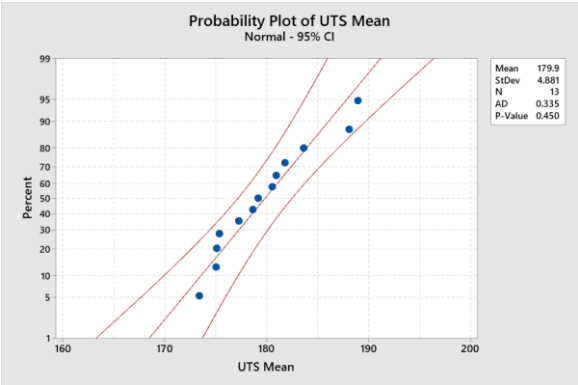

C: Probability plot of UTS averages for each foundry. No significant outliers beyond normal variation.

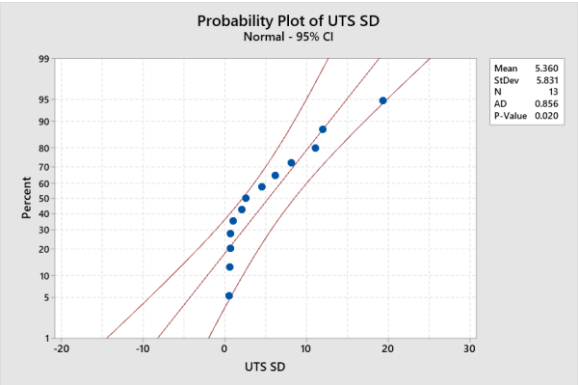

D: Probability plot of UTS standard deviations by foundry. No significant outliers beyond normal variation. The skewness is anomalous.

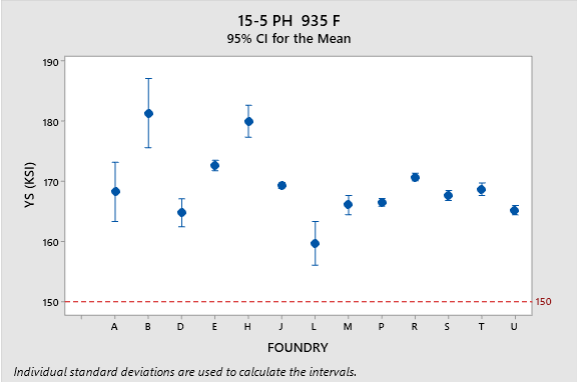

E: Yield strength confidence intervals. Note some intervals going below the minimum limit.

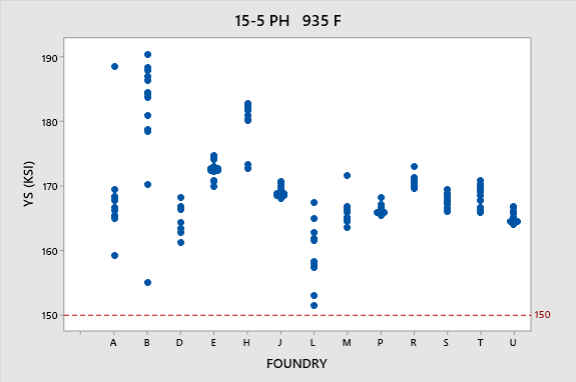

F: Yield strength individual plot. Note differences in variation.

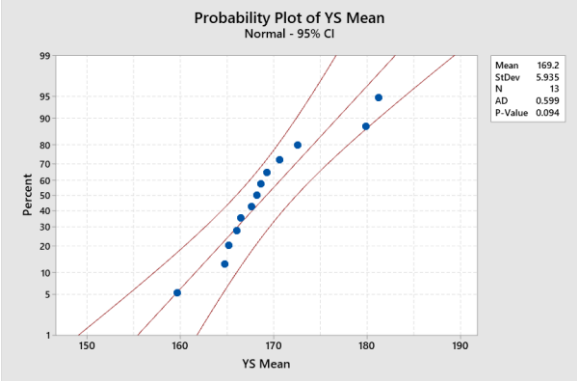

G: Probability plot of yield strength averages for each foundry. No significant outliers beyond normal variation.

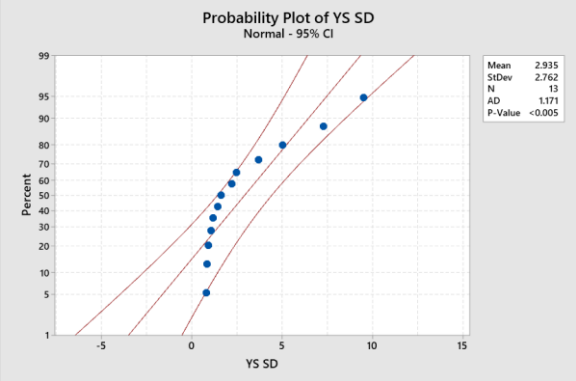

H: Probability plot of yield strength standard deviations by foundry. No significant outliers beyond normal variation. The skewness is anomalous.

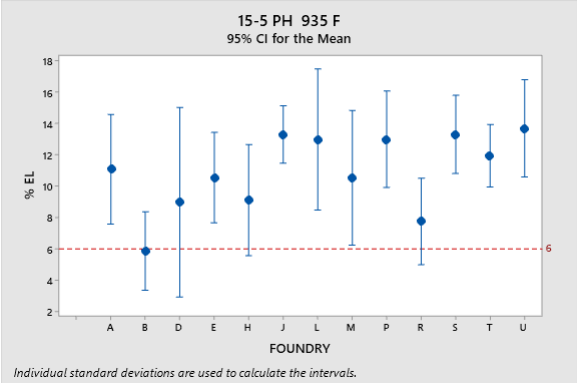

I: Percent elongation confidence intervals. Note some intervals going below the minimum limit.

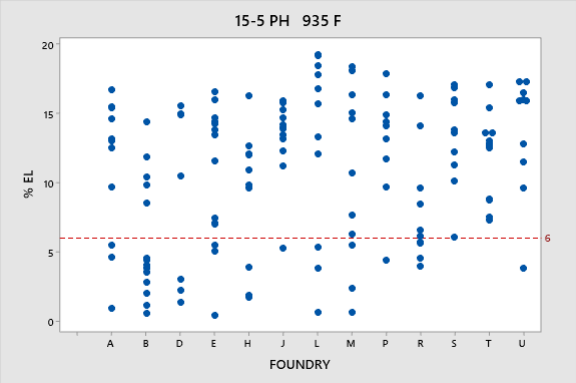

J: Percent elongation individual plot. Note many data points below standard.

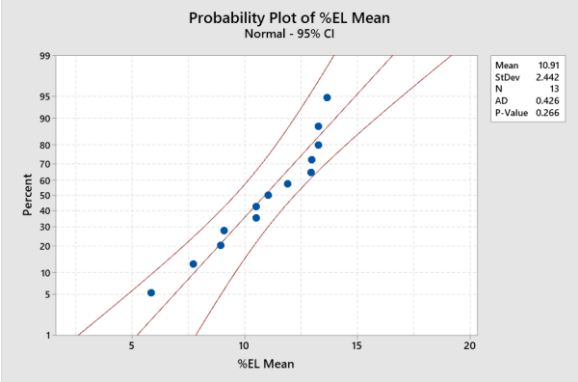

K: Probability plot of percent elongation averages for each foundry. No significant outliers beyond normal variation.

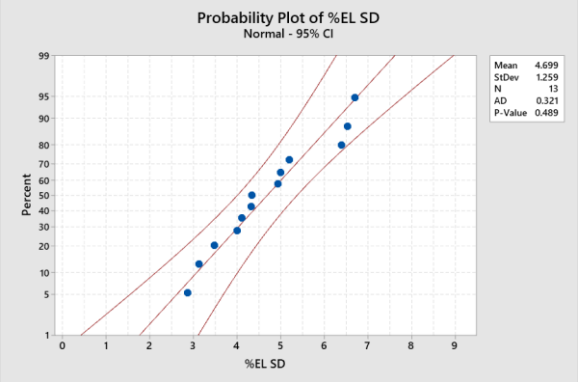

L: Probability plot of percent elongation standard deviations by foundry. No significant outliers beyond normal variation.

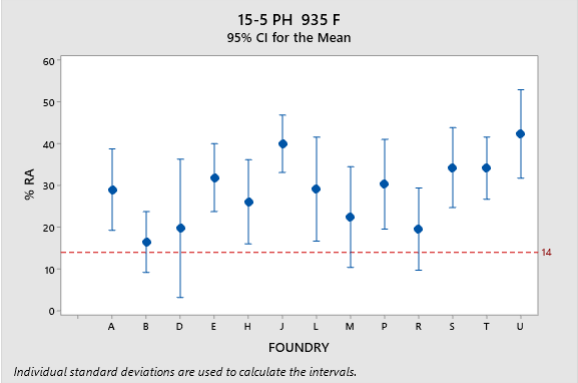

I: Percent reduction in area confidence intervals. Note some intervals going below the minimum limit.

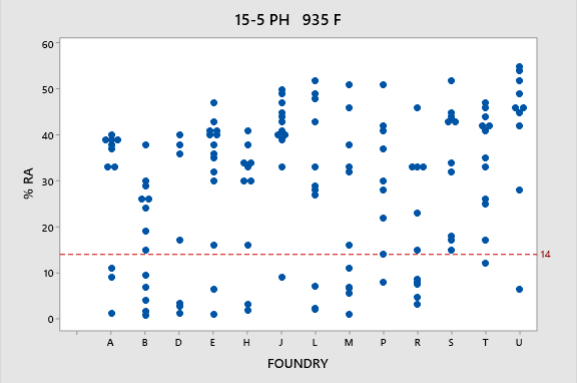

J: Percent reduction in area individual plot. Note many data points below standard.

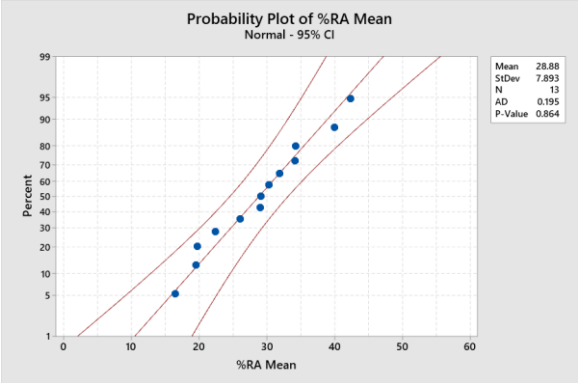

K: Probability plot of percent reduction in area averages for each foundry. No significant outliers beyond normal variation.

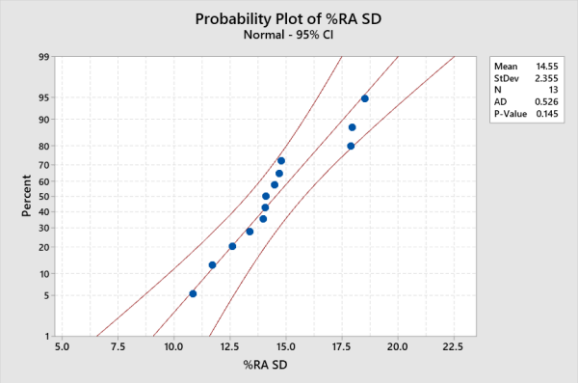

L: Probability plot of percent reduction in area standard deviations by foundry. No significant outliers beyond normal variation.

Figures 2A-P: 15-5 PH, 1000 F Age Confidence intervals, individual data plots, and normal probability plots for average and standard deviation of properties for each UTS, yield strength, percent elongation and percent reduction in area.

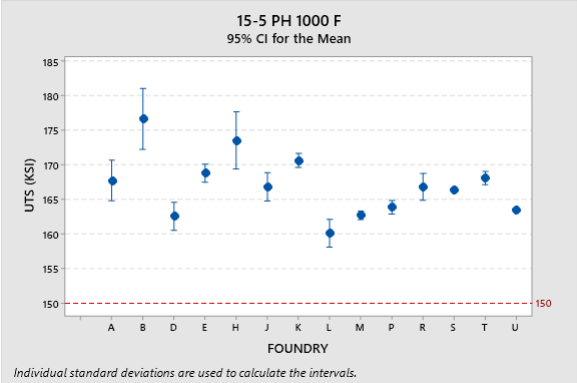

A: UTS Confidence intervals.

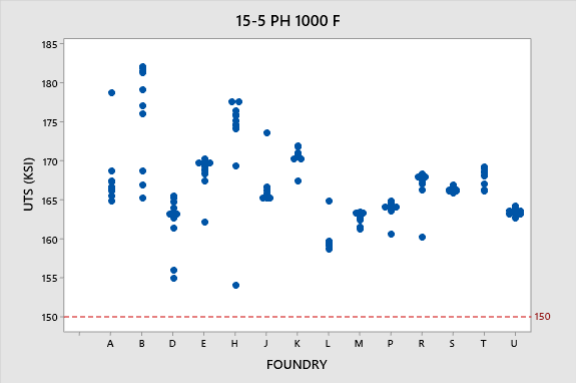

B: UTS Individual data plot.

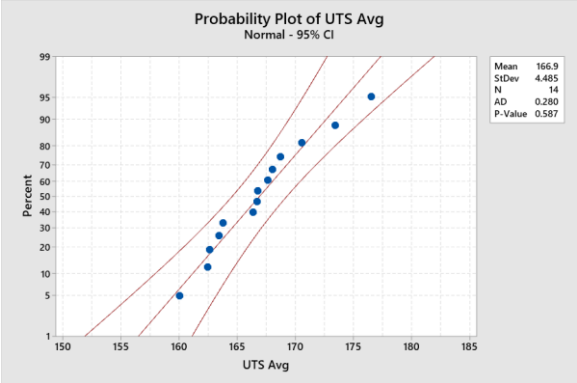

C: Probability plot of UTS averages for each foundry. No significant outliers beyond normal variation.

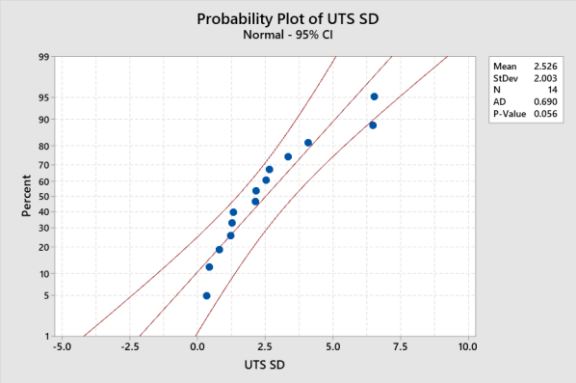

D: Probability plot of UTS standard deviations by foundry. No significant outliers beyond normal variation. The skewness is anomalous.

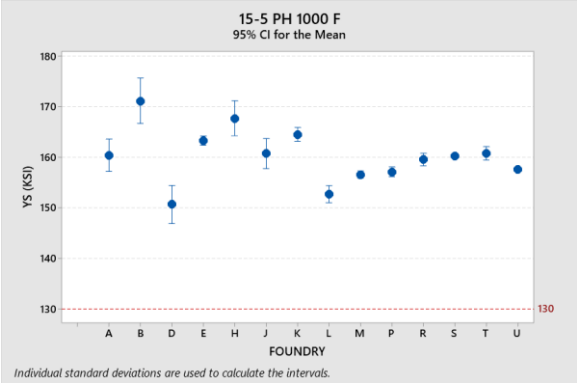

E: Yield strength confidence intervals.

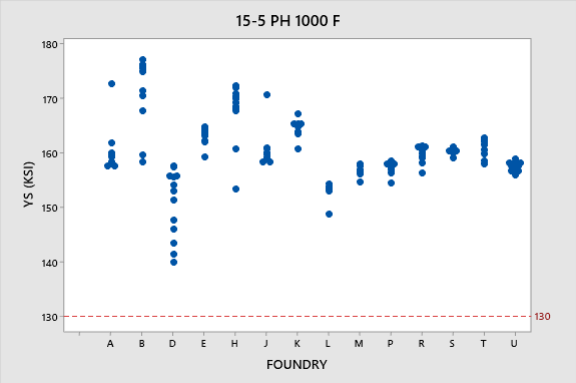

F: Yield strength individual plot. Note differences in variation.

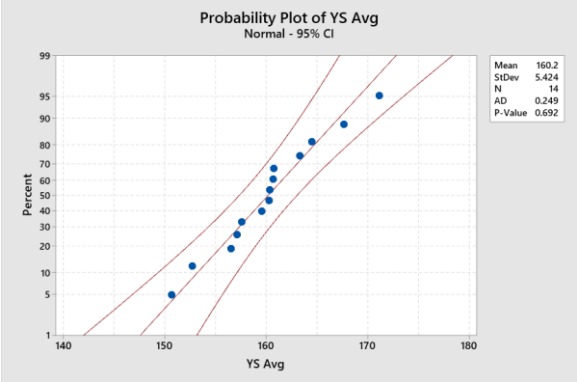

G: Probability plot of yield strength averages for each foundry. No significant outliers beyond normal variation. The skewness is anomalous.

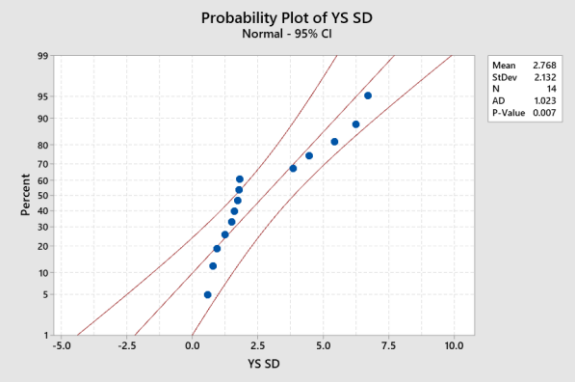

H: Probability plot of yield strength standard deviations by foundry. No significant outliers beyond normal variation.

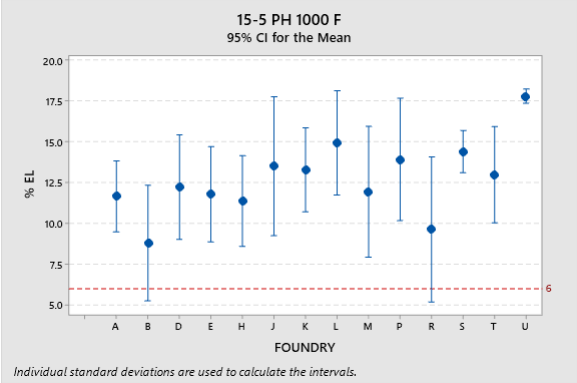

I: Percent elongation confidence intervals. Note some intervals going below the minimum limit.

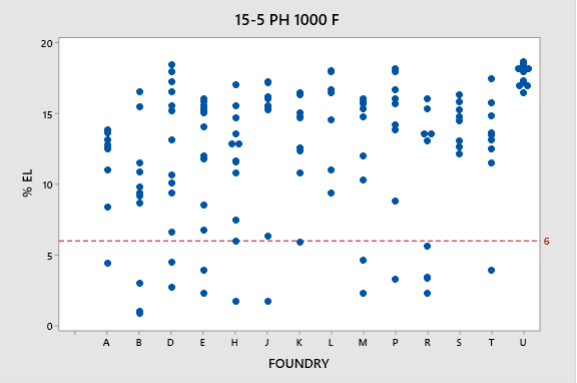

J: Percent elongation individual plot. Note many data points below standard.

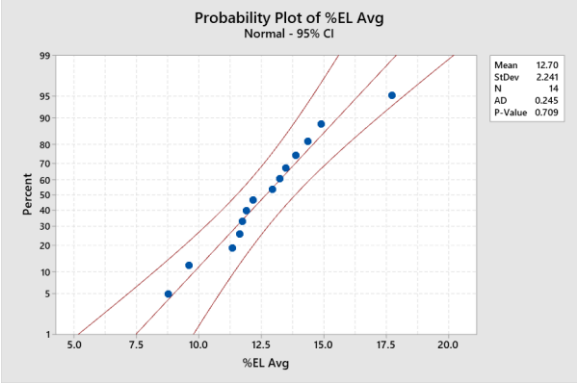

K: Probability plot of percent elongation averages for each foundry. No significant outliers beyond normal variation.

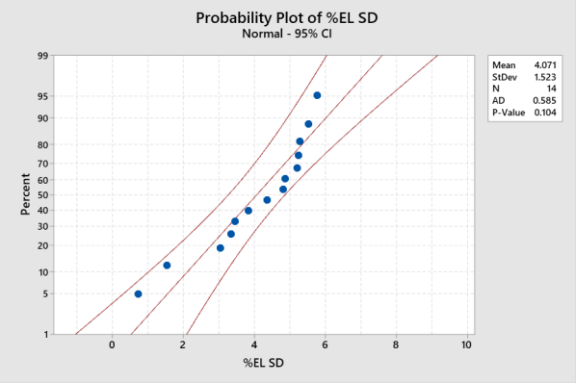

L: Probability plot of percent elongation standard deviations by foundry. No significant outliers beyond normal variation.

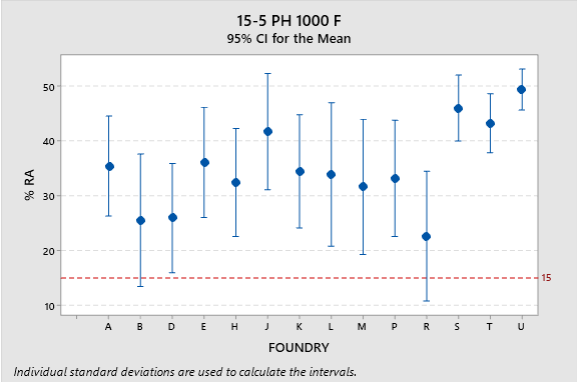

I: Percent reduction in area confidence intervals. Note some intervals going below the minimum limit.

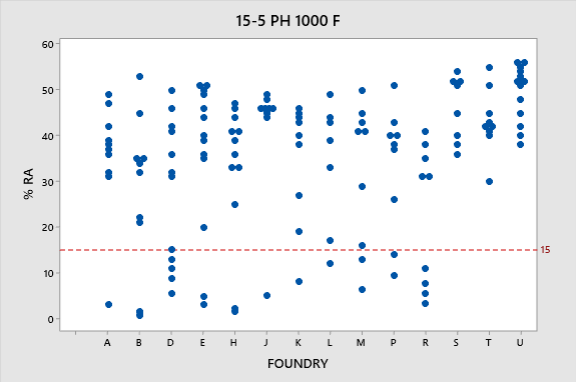

J: Percent reduction in area individual plot. Note many data points below standard.

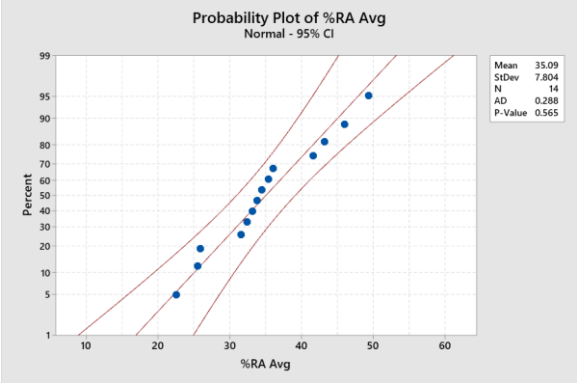

K: Probability plot of percent reduction in area averages for each foundry. No significant outliers beyond normal variation.

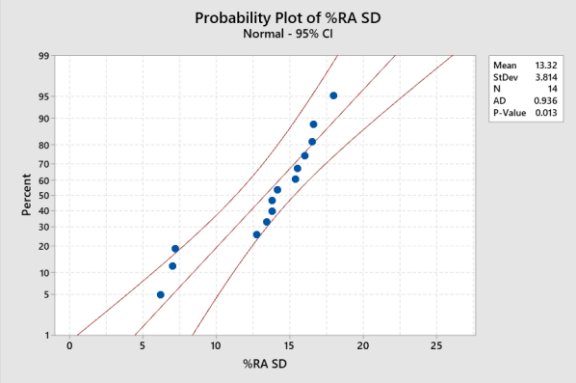

L: Probability plot of percent reduction in area standard deviations by foundry. Data is skewed, but no useful identifiable outliers.

Figures 3A-P: 17-4 PH, 1000 F Age Confidence intervals, individual data plots, and normal probability plots for average and standard deviation of properties for each UTS, yield strength, percent elongation and percent reduction in area.

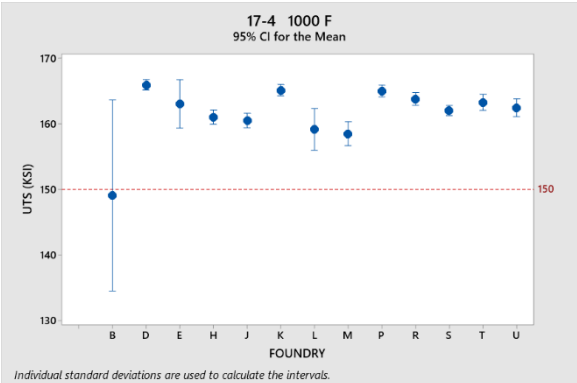

A: UTS Confidence intervals. Note some intervals going below the minimum limit.

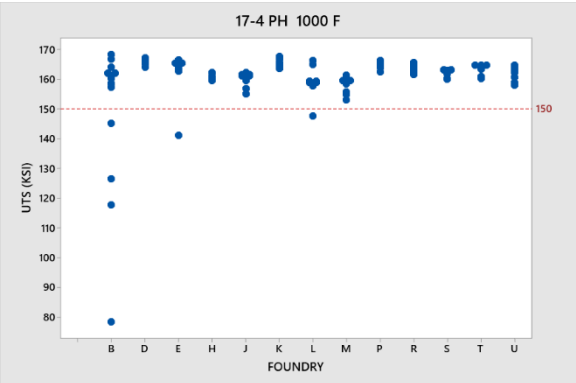

B: UTS Individual data plot. Note that generally the values below the specification appear to be outliers.

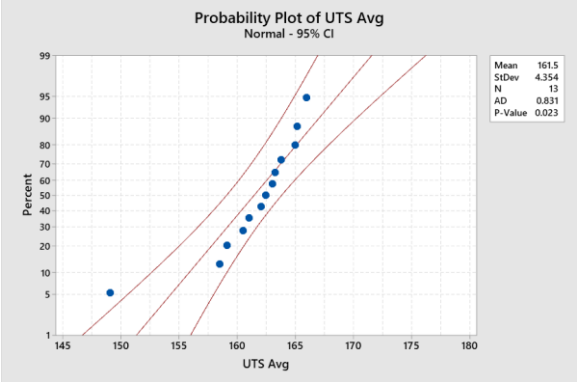

C: Probability plot of UTS averages for each foundry. One significant outliers beyond normal variation, however, below desired value.

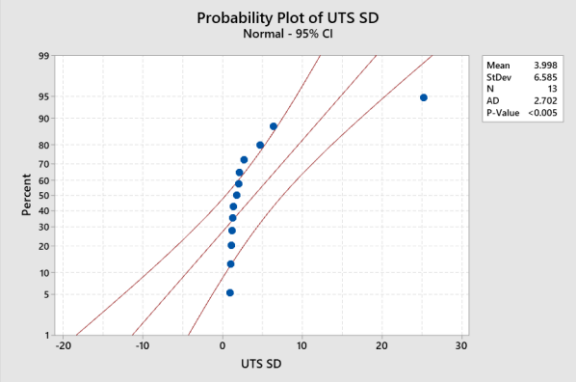

D: Probability plot of UTS standard deviations by foundry. One significant outliers beyond normal variation indicating more variation than anticipated.

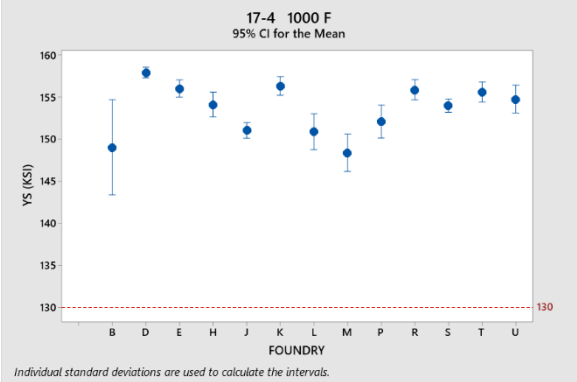

E: Yield strength confidence intervals.

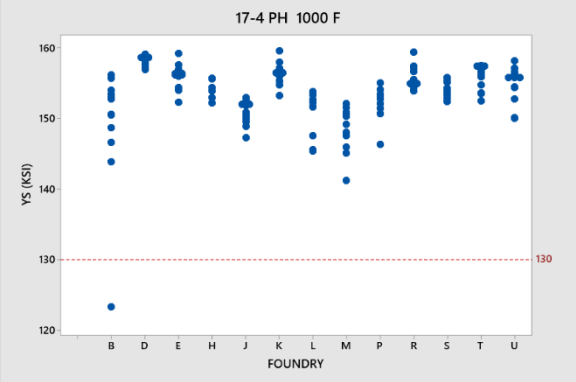

F: Yield strength individual plot. Note variation is quite uniform.

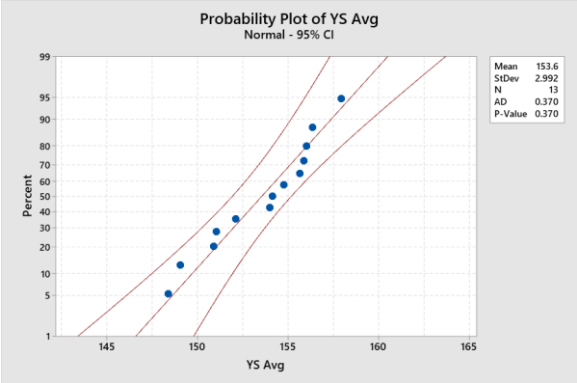

G: Probability plot of yield strength averages for each foundry. No significant outliers beyond normal variation.

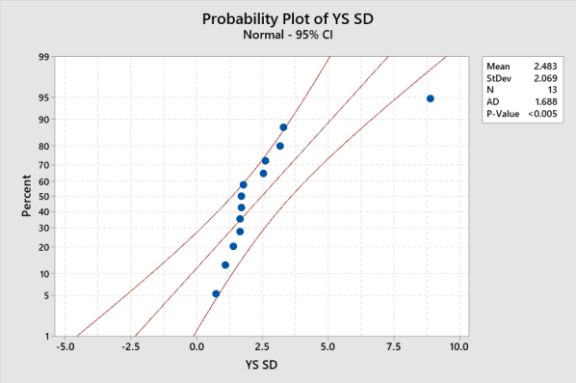

H: Probability plot of yield strength standard deviations by foundry. One significant outliers beyond normal variation indicating more variation than anticipated.

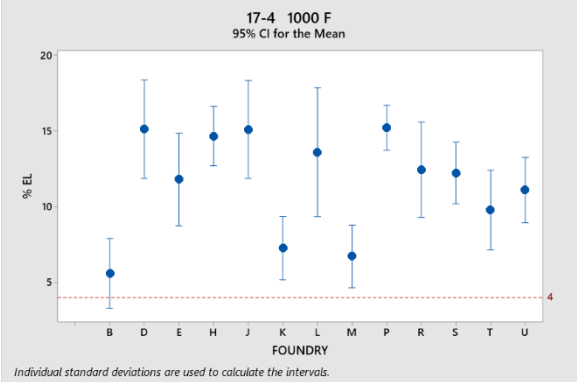

I: Percent elongation confidence intervals. Note some intervals going below the minimum limit.

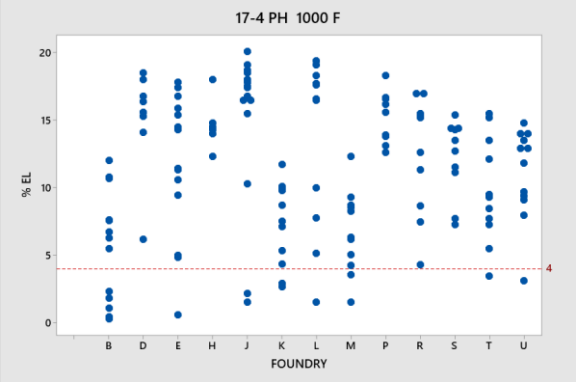

J: Percent elongation individual plot. Note many data points below standard.

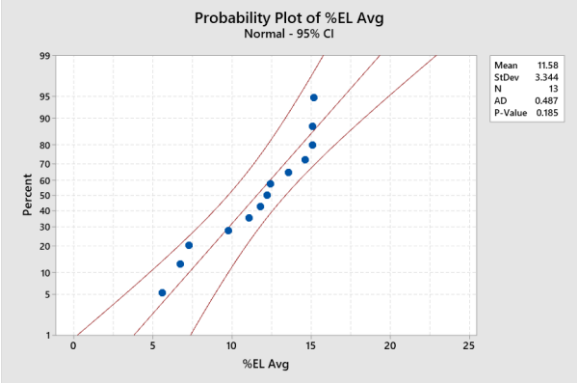

K: Probability plot of percent elongation averages for each foundry. No significant outliers beyond normal variation.

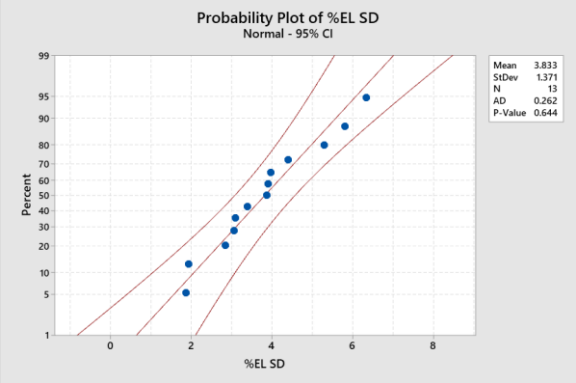

L: Probability plot of percent elongation standard deviations by foundry. No significant outliers beyond normal variation.

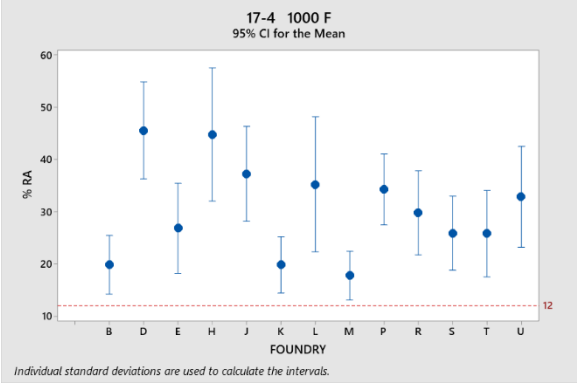

I: Percent reduction in area confidence intervals. Note no intervals going below the minimum limit but many values in the next graph.

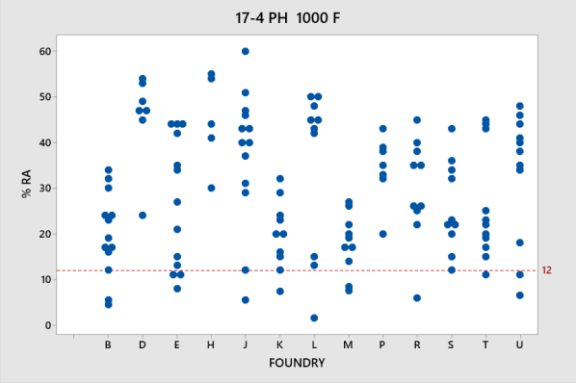

J: Percent reduction in area individual plot. Note many data points below standard.

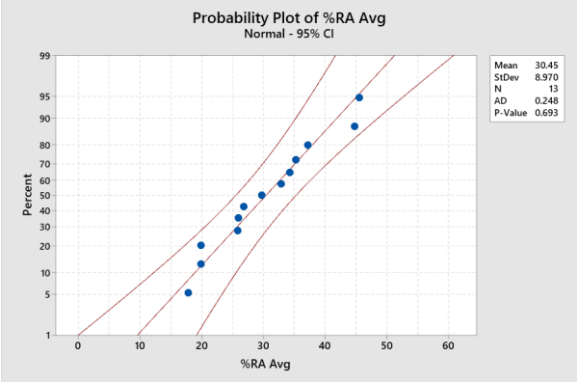

K: Probability plot of percent reduction in area averages for each foundry. No significant outliers beyond normal variation.

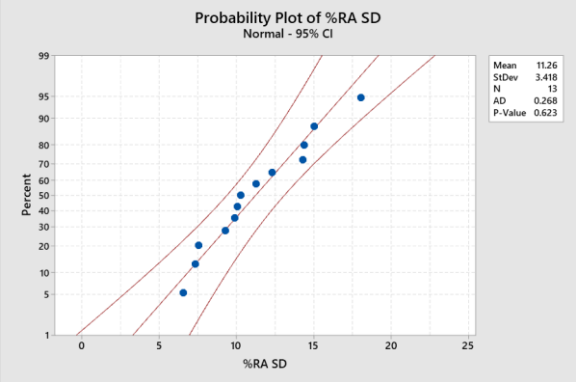

L: Probability plot of percent reduction in area standard deviations by foundry. No significant outliers beyond normal variation.

Figures 4A-P: 17-4 PH, 1100 F Age Confidence intervals, individual data plots, and normal probability plots for average and standard deviation of properties for each UTS, yield strength, percent elongation and percent reduction in area.

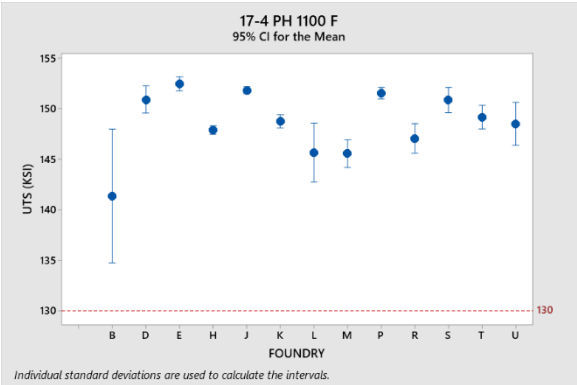

A: UTS Confidence intervals.

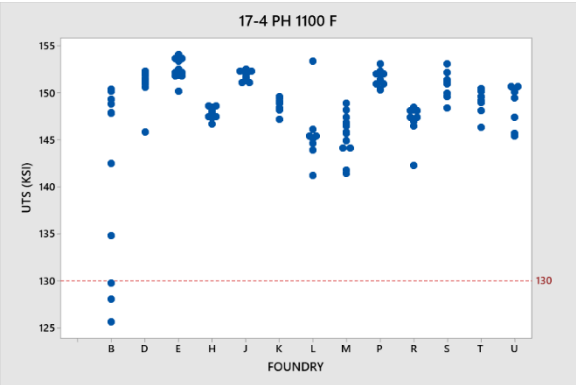

B: UTS Individual data plot. Note that one foundry has very wide variation.

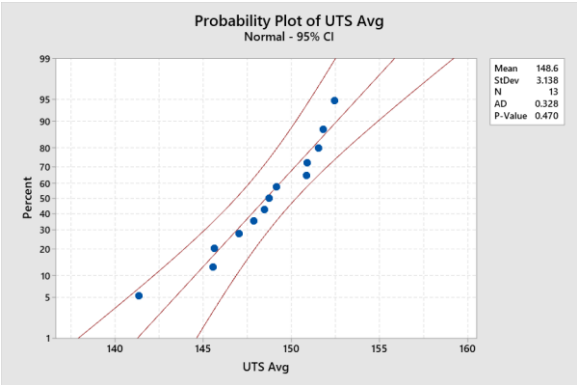

C: Probability plot of UTS averages for each foundry. No significant outliers beyond normal variation.

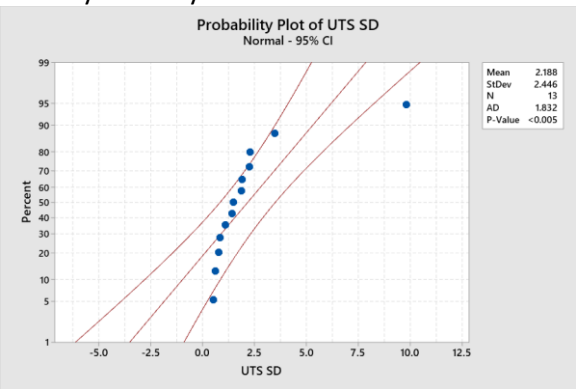

D: Probability plot of UTS standard deviations by foundry. One significant outliers beyond normal variation indicating more variation than anticipated compared to other foundries.

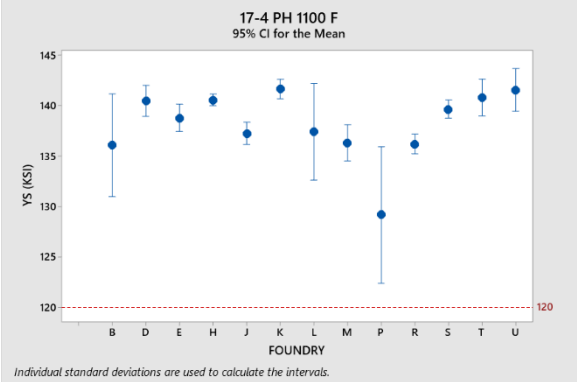

E: Yield strength confidence intervals.

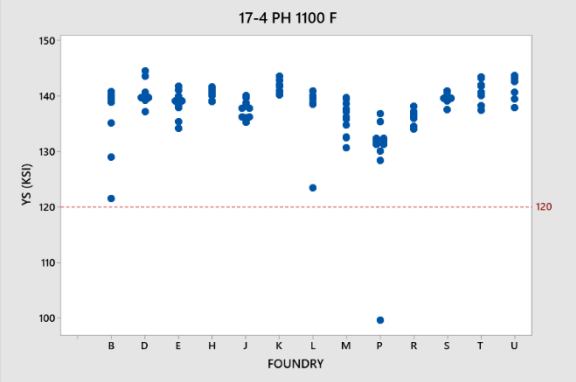

F: Yield strength individual plot.

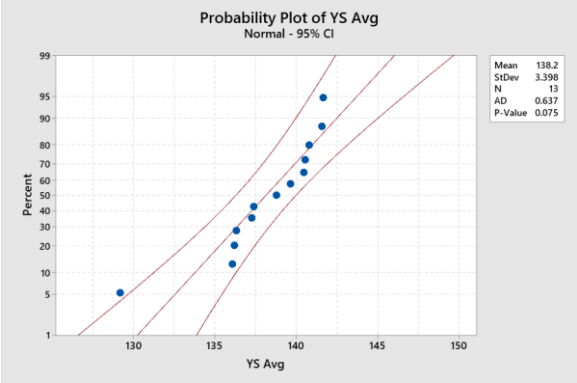

G: Probability plot of yield strength averages for each foundry. One significant outliers beyond normal variation on the low end.

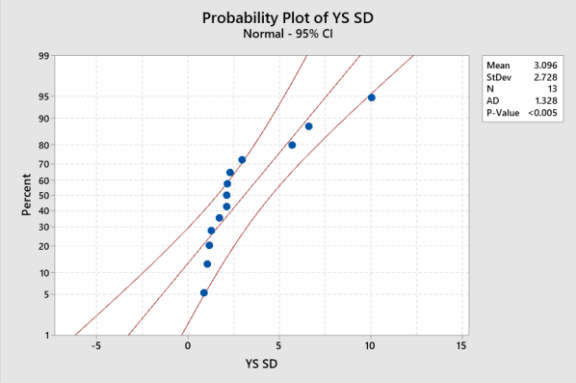

H: Probability plot of yield strength standard deviations by foundry. One significant outlier with higher normal variation than expected from peer foundries.

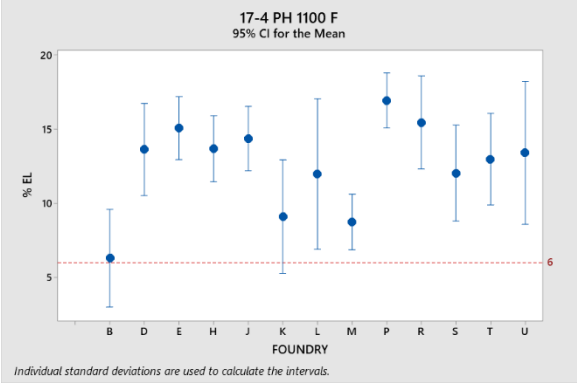

I: Percent elongation confidence intervals. Note some intervals going below the minimum limit.

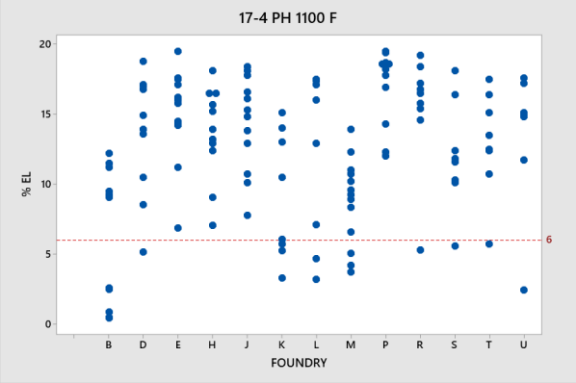

J: Percent elongation individual plot. Note many data points below standard.

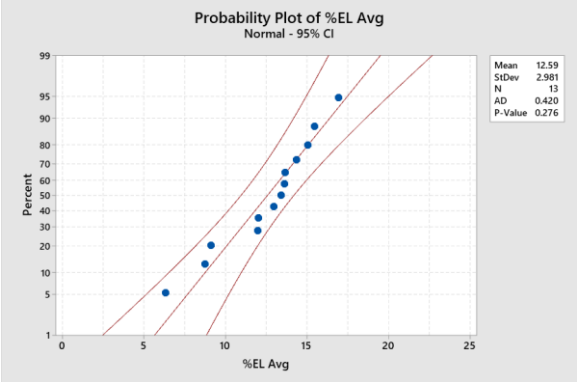

K: Probability plot of percent elongation averages for each foundry. No significant outliers beyond normal variation.

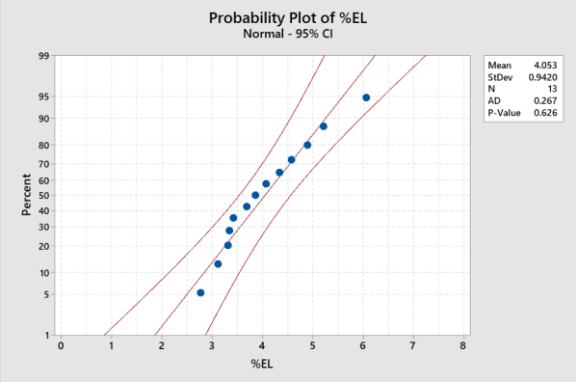

L: Probability plot of percent elongation standard deviations by foundry. No significant outliers beyond normal variation.

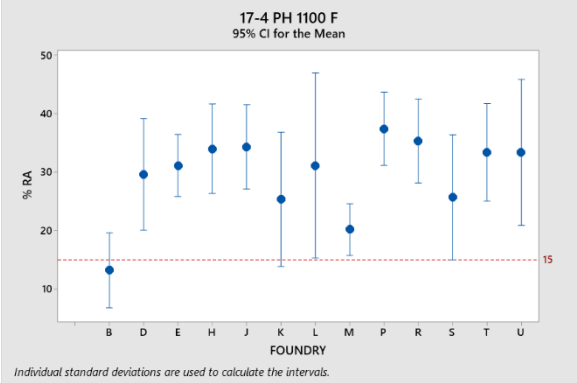

I: Percent reduction in area confidence intervals. Note some intervals going below the minimum limit.

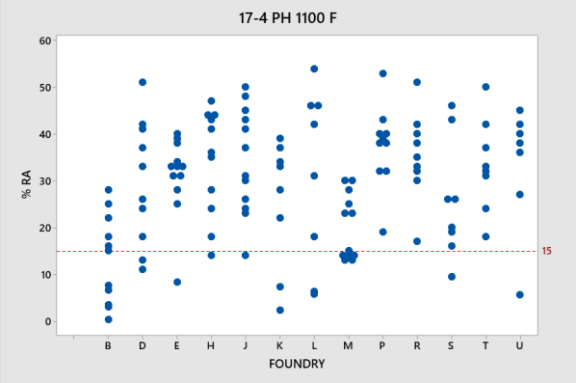

J: Percent reduction in area individual plot. Note many data points below standard.

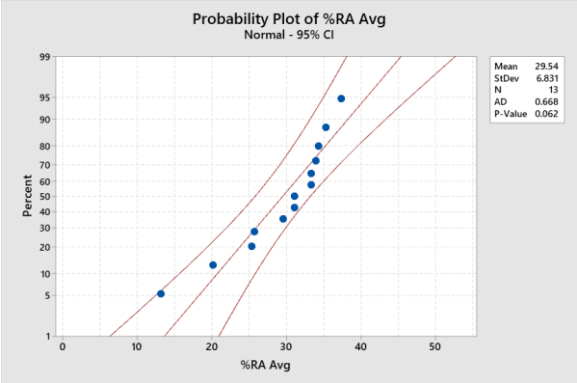

K: Probability plot of percent reduction in area averages for each foundry. No significant outliers beyond normal variation.

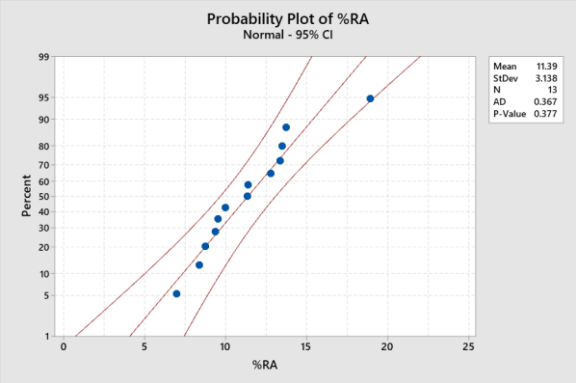

L: Probability plot of percent reduction in area standard deviations by foundry. No significant outliers beyond normal variation.

INVESTMENT CASTING INSTITUTE

Enhanced Investment Casting Quality Using 3D-Printed Ceramic Filters

Dan Z. Sokol
Renaissance Services – PERFECT – 3D Division

66TH TECHNICAL CONFERENCE & EXPO 2019

Paper № 12

PERFECT 3D
A Division of Renaissance Services Inc.

Enhanced Investment Casting Quality Using 3D-Printed Ceramic Filters

Why Use Filters

As the market for castings has grown and evolved over the years, the demands for quality and precision have increased as well. This has resulted in the need to maintain finer control over the quality of the source material filling the molds. Ceramic filters are a key element in providing this control over the metal flow system in investment casting.

Filters serve a twofold purpose: first, they capture non-metallic inclusions as well as other contaminants (typically referred to as dross or slag) present in the molten metal; second, they regulate the rate of molten metal flowing into the casting mold. These functions are intended to both ensure product performance of the casting and reduce impurities that can lead to scrap. Filters are used with many different metals, including steel, nickel, aluminum, and iron. Today, many investment casting foundries use ceramic filters in one form or another.

- Improve yield and reduce cost by:
  - Removing metal contaminants
  - Avoiding non-metallic inclusions
- Source of inclusions:
  - Foundry contaminants
  - Sprues, runners, molds
  - Ladle refractories
  - Oxidation
  - Ceramic filters

Conventional Ceramic Filter vs. Engineered 3D-Printed Filter

Ceramic Filters – Purpose & Background

Filters provide the ability to remove contaminants from the molten metal by using one, two, or all three of these processes depicted below.

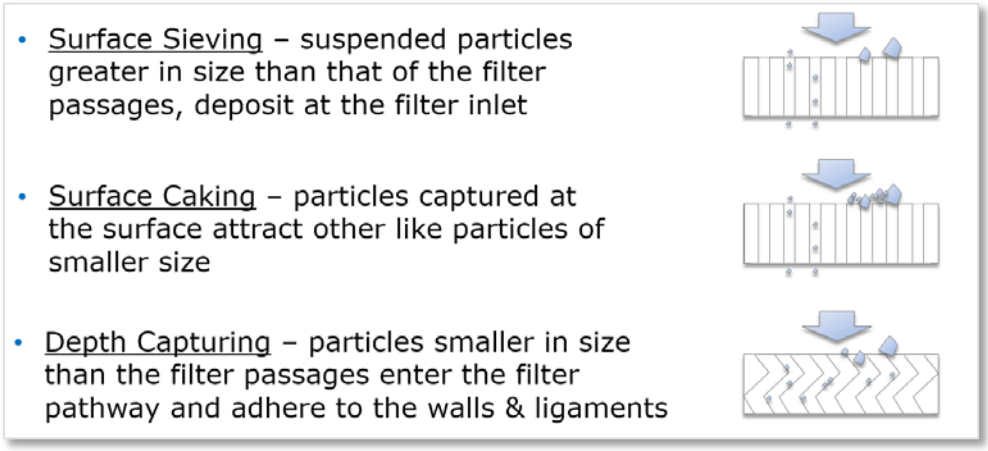

Processes that enable a filter to remove undesirable elements from metal flow

Filters are typically used in investment casting in these three areas in the mold tree as shown below. The pour cup filter is inserted into the bottom of the pour cup while the gate filter is located in the runner nearest the gating of the individual molds.

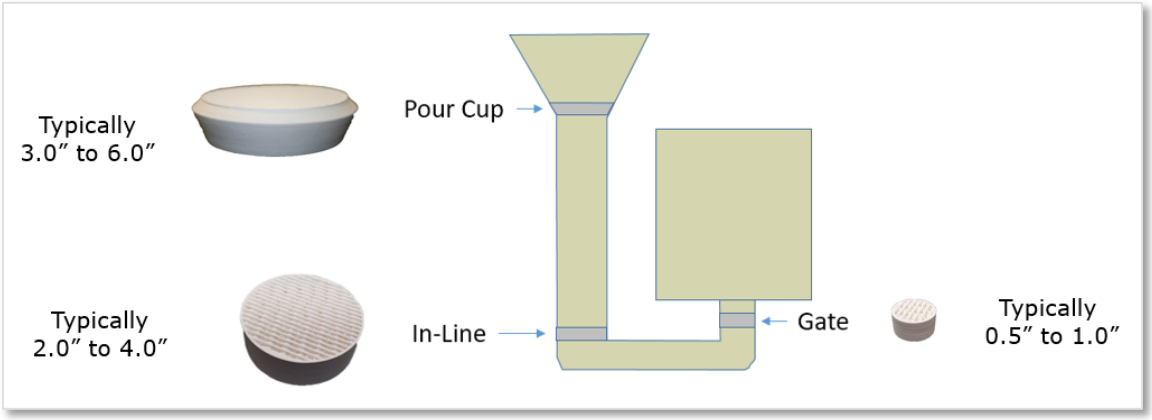

General Definition of Filter Types for Investment Casting

Casting suppliers started adopting the use of ceramic filters in the 1970s when foundries discovered that filters could help improve quality by reducing contamination in the molten metal.

The first generation of ceramic filters are based on a straight-through extruded honeycomb design, which operates predominantly on the principle of surface sieving to remove the contaminants. The second-generation filters are based on an amorphous reticulated foam, which introduced the use of depth capturing with the torturous pathway through the filter body to improve the removal of undesirable particles.

The graphic below illustrates the evolution of filters including the more sophisticated torturous pathway of the 3D-printed filter.

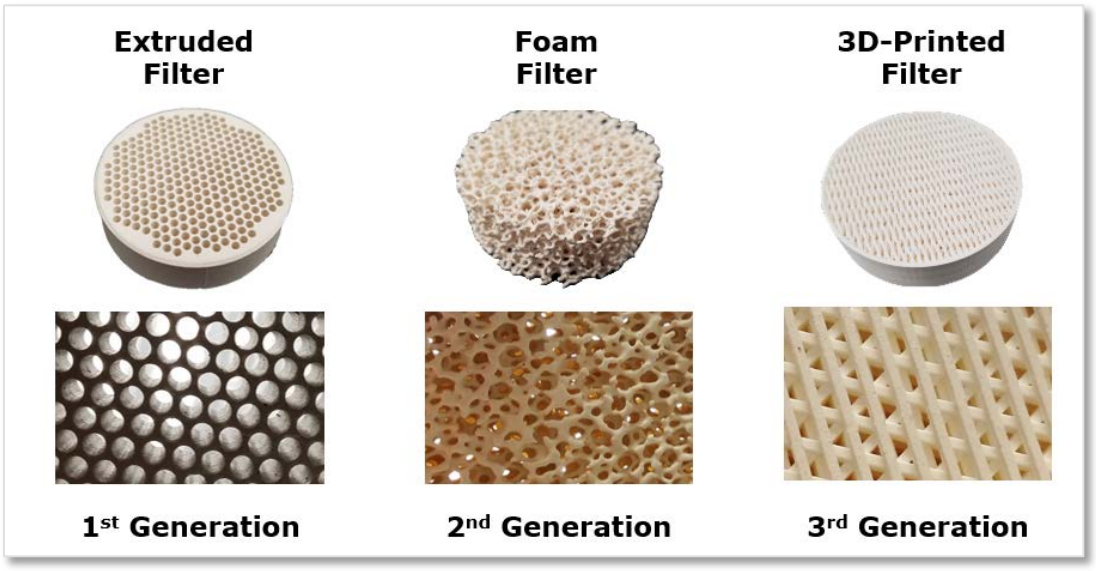

The Generations of Ceramic Filters for Investment Casting

Filters are often treated as a commodity by foundry purchasing departments, which select filters based only on the lowest price. The actual use of filters on specific mold trees is typically a decision for the process engineer. The evaluation approach is often not very analytical as reflected by this quote from a foundry engineer:

"If we have a problem in making a casting, we'll throw a filter on the mold tree… or if we already have a filter, we'll remove it and pour without a filter".

Problems with Earlier Generation Filters

During the last decade, foundries started discovering some of the short-comings of the first- and second-generation filters, which includes the inability to capture enough of the undesirable constituents and – even worse – the introduction of inclusions from

splintering or fracturing filters. This has resulted in the introduction of the third, and latest generation of filters, which is based on ceramic additive manufacturing (also known as 3D-printing). Ceramic 3D-printing enables the production of a very precise filtering structure that provides the ability for a much more deterministic method for capturing contaminants, as well as a more resilient structure to withstand the mechanical forces of pouring hot metal.

Current standard foam filters are essentially ceramic sponges, which do not consistently control the metal flow rate and can be a secondary source of contamination as very small pieces of the filter material sometimes break loose and enter the molten metal flow stream.

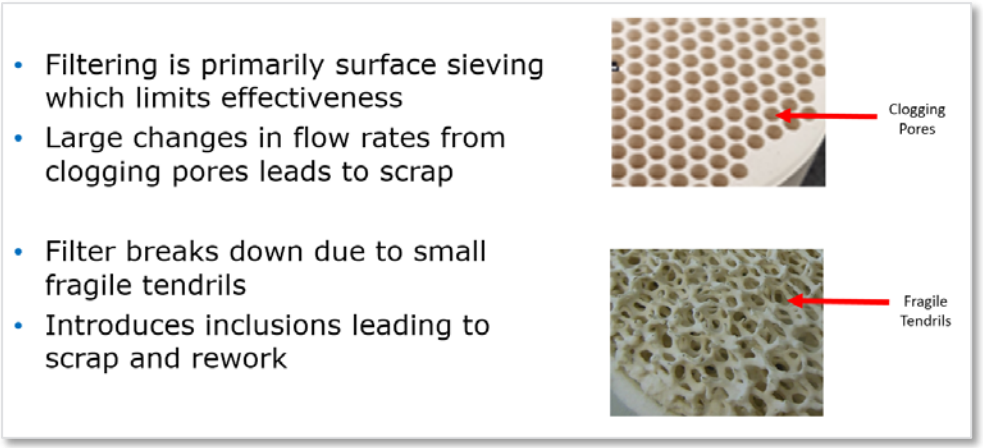

Summary of Problems with Earlier Generation Filters

Filter Performance Metrics

In late 2015, a variety of foundries that were pursuing improved filtering became aware of Renaissance Services' capabilities in custom ceramic 3D-printing. These foundries expressed an interest in better filters, and Renaissance began working with the foundries to research the application of its 3D-printing technology to the production of filters. The initial step involved the definition of a more definitive set of objective and measurable criteria to evaluate filter capability:

1. **Capturing** - Ensuring the capture of contaminants. The filter needs to provide various stages of sieving and cleaning to help remove inclusions and undesirable constituents.
2. **Flowing** - Providing consistent metal flow rates. The filter needs to provide a deterministic structure that ensures the same metal fill rate from one pour to the next.
3. **Containing** - Avoiding any breakdown of the ceramic filter. The filter itself needs to maintain structural integrity such that it does not introduce inclusions into the casting.
4. **Smoothing** - Providing a smooth laminar flow of metal. The filter needs to ensure that the molten metal is not exiting in waves that is erosive to the ceramic gating system.

In addition to defining suitable performance criteria, Renaissance Services identified and developed detailed testing methods for each of the metrics. For example, for Capturing, the team developed a testing apparatus and detailed process for evaluating a filter's capability to apprehend contaminants. For Flowing, the Renaissance team developed a specialized digital apparatus to consistently measure the flow rate of liquids through the filters.

Objective	Testing/Evaluation Methods
1. Capturing	Controlled testing in casting apparatus
2. Flowing	Flow rate testing machine
3. Containing	Material mass & temperature impact testing
4. Smoothing	High speed videography during flow testing

Methods of Testing & Evaluating Filter Performance Metrics

The subsections that follow provide some of the specific insights gained by the rigorous testing of conventional filters and 3D-printed filters.

Capturing

This metric addresses the ability to capture contaminants in the molten metal. The filter needs to provide various stages of sieving and cleaning to help remove inclusions and undesirable constituents.

- Foam filters are created by a non-deterministic process that creates random passages for the filtering structure
- A torturous path through the filter body is the fundamental basis for capturing contaminants
- A 3D-printed engineered filter can be crafted to create pre-determined torturous passages through the filter body

Cutaway of 3D-Printed Filter

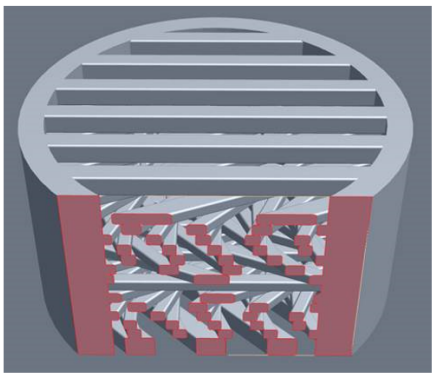

Explanation of Capturing Performance for Conventional Filter vs 3D-Printed Filter

As part of a US Air Force contract, the Renaissance team tested 3D-printed engineered filters relative to conventional foam filters. During trials producing nickel-based castings in the foundry, 40% of the tested foam filters allowed impurities into the casting. By contrast, the 3D-printed filters stopped the impurities from reaching the casting—none of them allowed any inclusions past the filter.

Flowing

This metric involves the need to provide consistent metal flow rates. The filter needs to provide a deterministic structure that ensures the same metal fill rate from one pour to the next. The graphic below illustrates the far superior performance of 3D-printed filters versus conventional foam filters.

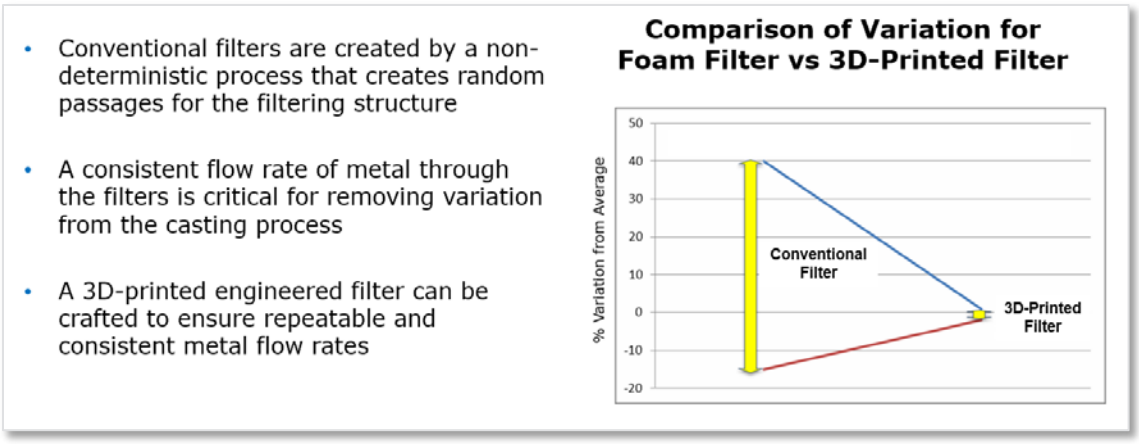

Explanation of Flowing Performance for Conventional Filter vs 3D-Printed Filter

The conventional foam filter flow rates deviated from their average by as much as 40%. Meanwhile, the 3D-printed filters experience variation of +/-2%, demonstrating the ability to precisely control metal flow into the casting.

Containing

This metric addresses the avoidance of any breakdown in the ceramic filter. The filter itself needs to maintain structural integrity such that it does not introduce inclusions into the casting. The graphic below shows the comparison between foam filters and 3D-printed filters.

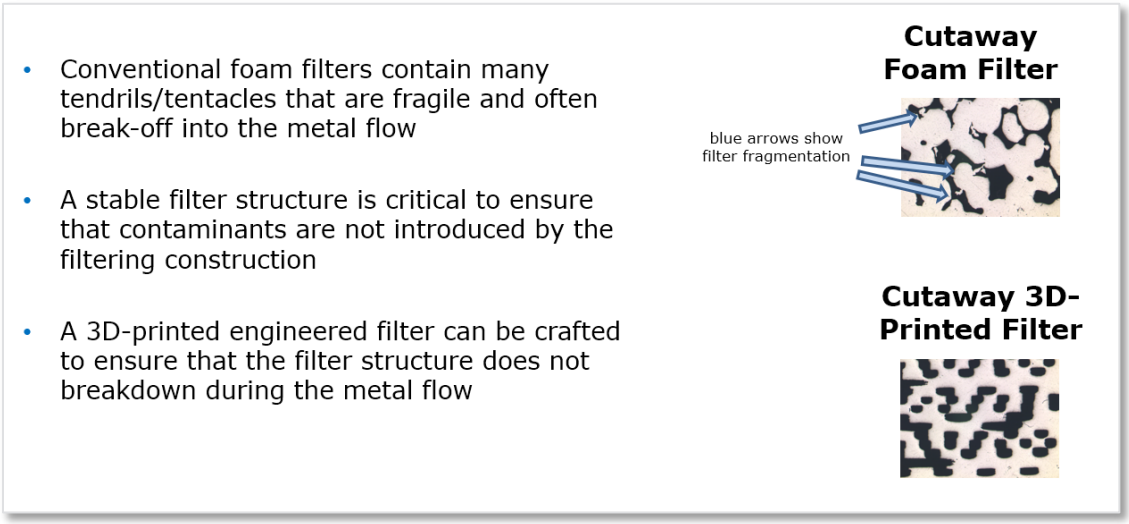

Explanation of Containing Performance for Conventional Filter vs 3D-Printed Filter

The photo below shows the results of testing filters in a high-temperature vacuum pour of an aerospace nickel alloy at POK Castings. The traditional extruded filter experienced a catastrophic failure that resulted in scrapped castings.

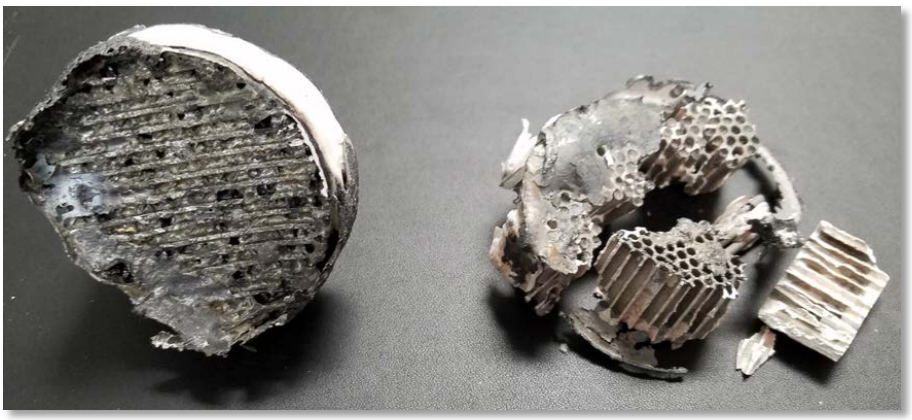

3D-Printed Filter (left) and Crushed Extruded Filter (right)

Smoothing

This metric addresses the need for the filter to provide a smooth laminar flow of metal in the exit stream. The filter needs to ensure that the molten metal is not exiting in waves that is erosive to the ceramic gating system. The graphic below illustrates how the 3D-printed filter designed by the Renaissance team enables a tight laminar flow of liquid as it exits the filter.

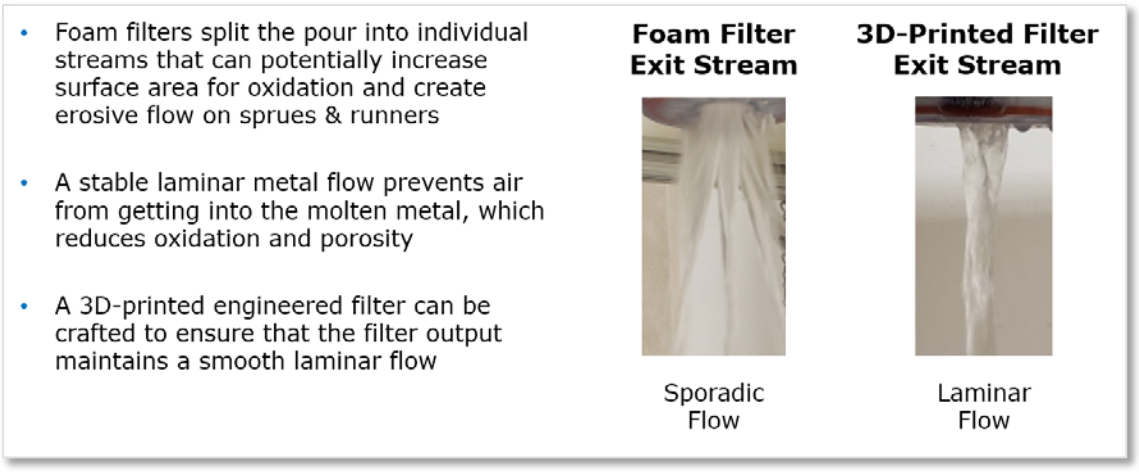

Explanation of Smoothing Performance for Conventional Filter vs 3D-Printed Filter

Design Parameters for Engineered Ceramic Filters

The graphic below highlights the design principles adopted by the Renaissance team in the development of 3D-printed ceramic filters.

Objective	Design Features
1. Capturing	Consistent torturous pathways through the filter
2. Flowing	Well-defined and consistent filter passages
3. Containing	Resilient multi-stage levels and ligaments
4. Smoothing	Guided ligaments to vector output from filter exits

Key Design Features to Provide Improved Filters

The early 3D-printed filter designs were evaluated with test pours at POK Castings. The foundry was able to provide essential feedback about the filters and the performance metrics based on the results in an actual production environment.

3D-printed filters have thus far proven to address the performance metrics in a very positive manner, enabling consistent and repeatable metal flow rates without becoming a secondary source of contamination. These engineered ceramic filters can be designed and produced on-demand to tightly control metal flow as well as to eliminate secondary contamination of the metal.

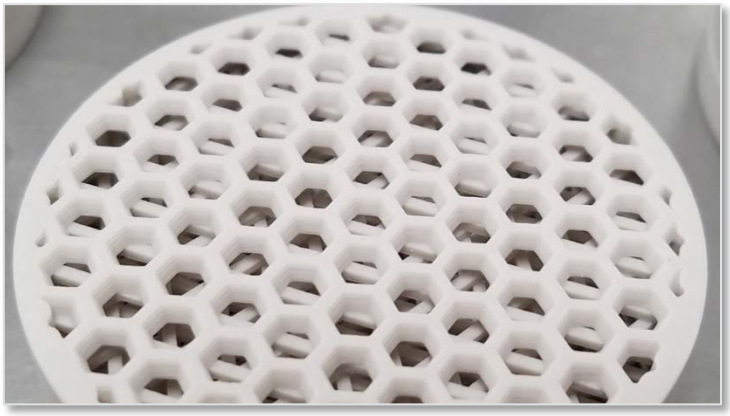

Close-up of PERFECT-3D Ceramic Filter

Based on a comparison to conventional filters (using the defined filter performance metrics), there are definitive advantages in using 3D-printed ceramic filters. The implications of 3D-printed filters for the casting industry are significant. Not only can they be designed to meet the specific needs of the foundry, they can have a profound effect on reduction of potential scrap.

References

1. "A New Source for Production of Ceramic Filters", A.C.Carvalho, et al., Materials Letters, 2015.

2. "Advances on Ceramic Filters Fabrication Process", Vânia R. Salvini, Francisco A. R. Rojas, et al., EESC-USP, Sao Carlos, SP, Brazil, 2015.

3. "An Investigation on Permeability of Ceramic Foam Filters", Robert Fritzsch, Norwegian University of Science and Technology, February 2015.

4. "Casting Alloy Filtration", Jaromír Roucka, Czech Foundry Society, 2000.

5. "Casting Alloy Filtration with Ceramic Foam Filter", Ehsaan-Reza Bagherian, University of Dundee, December 2014.

6. "Ceramic HEPA Filter Program", M. A. Mitchell, Lawrence Livermore National Lab, International Society for Nuclear Air Treatment Technologies, May 2012.

7. "Characterization of Ceramic Foam Filters Used for Liquid Metal Filtration", Mark William Kennedy, et al., The Minerals, Metals & Materials Society and ASM International, 2013.

8. "Efficiency of Solid Inclusion Removal from the Steel Melt by Ceramic Foam Filter: Design and Experimental Validation", Soumava Chakraborty, et al., AFS Metalcasting Congress, 2018.

9. "Efficiency and Performance of Industrial Filtration Systems", W.Schneider, et al., VAW Aluminium AG, 2000.

10. "Effect of the Pressed Ceramic Filters on the Re-Oxidation Process", Marek Bruna, et al., MATEC Web of Conferences, 2017.

11. "Filling System for Investment Cast Ni-Base Turbine Blades", DZ Li, Journal of Materials Processing Technology, Volume 148, Issue 3, 30 May 2004, Pages 310–316.

12. "Global Ceramic Filters Market by Product and by Application", Grand View Research, Inc. 2012, http://www.grandviewresearch.com/industry-analysis/ceramic-filters-market

13. "Measurement of Filtration Performance, Filtration Theory and Practical Applications of Ceramic Foam Filters", Steven Ray, et al., Aluminium Cast House Technology, 2005.

14. "Metal Flow through A Filter System", A. Habibollah Zadeh, AFS Transactions, American Foundry Society, 2002.

15. "Numerical Simulation on Flow Dynamics and Pressure Variation in Porous Ceramic Filter", Kazuhiro Yamamoto, Nagoya University, Chikusa Japan, 2018.

16. "Wetting Behavior of Aluminium and Filtration with Al2O3 and Sic Ceramic Foam Filters", Sarina Bao, et al., Transaction of the Nonferrous Metals Society China, 2018.

PERFECT 3D

A Division of Renaissance Services Inc.

INVESTMENT CASTING INSTITUTE

Innovation & The Race To Space

Michael Kugelgen
MK Technology Gmbh

66TH TECHNICAL CONFERENCE
&
EXPO 2019

Paper № 13

Innovation and the Race to Space

Investment Casting is one of the oldest primary forming technologies, around 5000 years old. During the last 5 decades there have been a lot of improvements in respect of better materials and process. But is this enough to face the challenge of other technologies, which seems to be more fresh and sexy? To be competitive against modern production processes like 7-axis high speed milling or 3D-metal printing? Let's talk straight: Investment Casting is an archaic process, quite complex with many intermediate steps and a high risk to fail. The only chance we have to survive and not to share the fate of other technologies, which are now nostalgic history, is to think out of the box. To be really innovative and optimise speed, output and quality.

But what is the difference between development, improvement, innovation and real breaktroughs. And are there something like a golden rule for innovations?

In my following paper I would like to summarize some ideas and show a few short and interesting videos.

1. Be willing to do it [Video]
2. Aim for breakthroughs [Video]
3. Take risks [Video]
4. Have confidence in nonsence
5. Accept to have failures
6. Keep it simple - KISS
7. Right Timing
8. Bad times lead to breakthroughs

Someone who followed these rules, at least most of them, is Elon Musk. He is the founder of Tesla, Solar City, Hyperloop and SpaceX. He is always aiming for the latest and most advanced technology and therefore he is not only using all kind of 3D-Printing technologies, he has also his own Investment Casting Facility to be fast and independent. And beside his creativity and enormous knowledge and understanding of technology, he has one big strength, which separates him from other people:
"He never gives up – never".

At the end of this paper I would like to show a short video, proving, that keeping the 8 rules in mind and having the ultimate will to do it, will finally lead to great success. It is the launch of Falcon 9, after 3 others failed, and the first successful reversed landing. (Video)

INVESTMENT CASTING INSTITUTE

3D Printed Inserts & Mold Cavities That Can Be Used for Producing Wax Patterns

Jacob Lehman
Pittsburg State University

66TH TECHNICAL CONFERENCE
&
EXPO 2019

Paper № 14

3D Printed Inserts and Mold Cavities That Can Be Used for Producing Wax Patterns

Jacob Lehman
Associate Professor
Pittsburg State University
Summer 2019

ABSTRACT:

Traditional investment casting wax tooling is often expensive to produce and time consuming to design and manufacture. This paper will explore the use of inexpensive 3D printed tooling to produce wax patterns for investment casting. Printed mold cavities can be produced very quickly using additive manufacturing compared to traditional methods for mold and die manufacturing. This investigation examines both printed mold cavities and inserts produced on an inexpensive 3d printer as a supplement to traditional tooling, especially for low volume production runs.

Table of Contents

Introduction

This project is an investigation into utilizing inexpensive 3D printed tooling components for making wax patterns to be used in investment casting applications. Currently, 3D printing technology is most often used for making investment patterns themselves, which may be useful in prototyping or small production run applications. Producing traditional metal tooling by machining can be very expensive Thus, for small to mid-sized production runs the tooling costs can be very high, significantly impacting the viability of the project and its economics. Since 3D printing technologies are widely available and inexpensive, the possibility of printed tooling and tooling components is being examined in this project. There may be several advantages to printing the tooling itself, rather than simply printing patterns which are consumed in the investment casting process. Some of the possibilities are: reduced lead times, reduced tooling costs, tooling design freedom, etc. Although there are many different 3D printing technologies currently used in various industries, this investigation is only utilizing low costs FDM technology. These printers and their build materials are very inexpensive to obtain and print parts.

Equipment

As noted in the introduction, this investigation only utilized inexpensive FDM print technology, and did not explore the variety of printing technologies available today. Since there are many metal 3D print technologies already on the market, the concept of printed tooling is not difficult to envision. These metal printing technologies could easily print dies and die components. Using printed metal tooling, however, often may exceed the cost of traditional machined tooling and requires very expensive printers.

For this project, the primary printer is an “Ender-3 3D Printer” purchased online for around $200. There are many FDM printers on the market which will likely produce similar results. Since this project primarily is a “proof of concept” investigation into inexpensive printed tooling, this printer’s performance was sufficient. The printer’s capabilities and part quality may be eluded to, however, that was not the primary focus of the project. For the build material, PLA (Polylactic Acid) was utilized since it is a very common and inexpensive printer filament. During the course of the project, an insert was printed using ABS (Acrylonitrile Butadiene Styrene) to see if the performance was different, however the results were similar to the PLA parts. Further research may need to be done to determine which build material has better performance as tooling components.

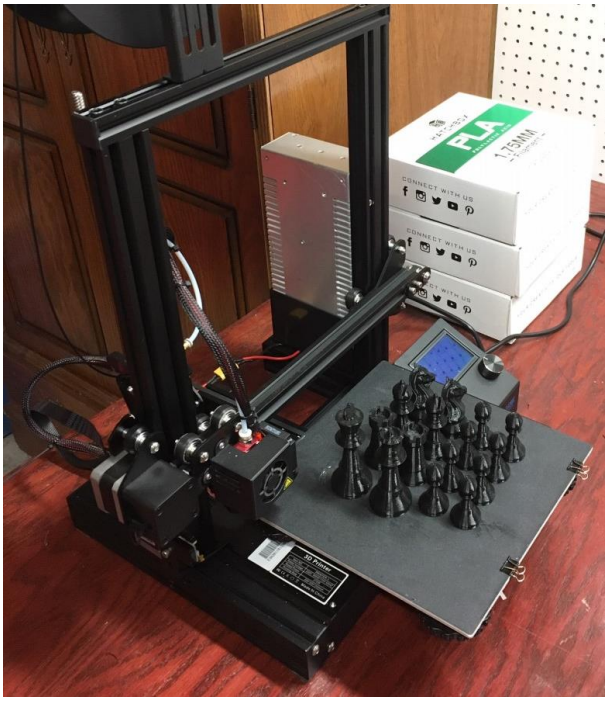

The Ender-3 3D Printer is a very inexpensive FDM printer designed for the DIY or hobby individual. Although this machine is not necessarily designed for industrial applications, the parts produced utilizing this small machine were of satisfactory quality. For the PLA prints, the build table was heated to 60 degree C, the nozzle set to 200 degrees C, and layer thicknesses were set to 0.2 millimeter.

Figure 1 Printer

Printed Tooling Inserts

The first printed tooling component in this investigation was a small printed insert that fits into an aluminum die. The die selected has two cavities, both with removable inserts that may be changed, allowing the user to vary to text and/or logo on the wax patterns. As noted in Figure 2, an aluminum insert was replaced with a printed (PLA) insert in the die. The second cavity was left with a traditional machined aluminum insert, allowing for a "side by side" comparison.

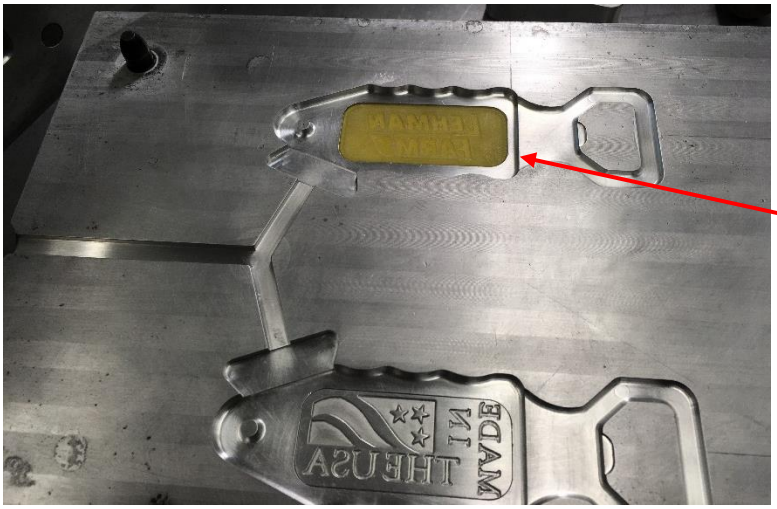

A printed PLA insert was a located in the existing insert position. It was designed to be the same size and shape as an aluminum insert, even including threaded holes in the back side for fastening in the die.

Figure 2 Multi cavity die with a printed insert

As for the wax injection process parameters, they remained essentially unchanged (from the parameters used without the printed insert). Figure 3 shows the two wax patterns produced by the die during the initial trial. Although a part was produced in both cavities, there were several issues with the process and the wax pattern quality produced. The wax had a tendency to stick to the insert side of the die, likely due to the "textured" surface left by the printing process. This made it more difficult to remove and did not allow for the automatic ejection features already designed in the die. Further research could be done on techniques to smooth the surface of the printed insert either mechanically (sanding), chemically, or through a coating.

Another common defect occurred when the pattern was removed from the die before it was fully solidified. Since the PLA insert has a drastically different heat transfer coefficient than the aluminum insert, it took considerably longer for the pattern in that side of the die to solidify. Coupled with the textured surface that created sticking in the die, this was a likely defect. To avoid this defect, the die had to remain closed longer before an attempting to remove the part. Depending on the size of the printed insert, the available surface area, and the amount of heat needed to remove, this process parameter will vary from one die to the next. For this particular part, leaving the die closed for an additional 30 seconds seemed to allow enough cooling to remove the part.

The wax pattern produced with the printed insert was more difficult to remove from the die than wax produced with the aluminum insert. This slowed the process and created some notable defects in the resulting wax pattern.

Figure 3 Wax patterns prior to gating removal

A common defect on the wax pattern resulted when removing the part too early. Because the PLA insert insulated the part rather than cooling the wax, it had to remain in the die longer before it was solid enough for removal. The pattern above avoided this particular defect by leaving it in the closed die additional time, however still was difficult to remove from the insert.

Figure 4 Wax patterns with defects

Printed Die Cavities

The second printed die component investigated was a simple cavity. Since this is a "proof of concept" investigation rather than a specific production part, the cavities chosen were simple, flat-backed part designs. This would require for only one side of the die to be printed, reducing the build material and print time needed. Figure 5 shows the basic test part used for the proof of concept. It is a basic rectangular cavity that is 2 1/2" by 1 1/8" and is 3/8" deep. To make the part easier to remove from the cavity, 5 degrees of draft angle was added to the walls of the cavity, and basic text was also added to the floor of the cavity.

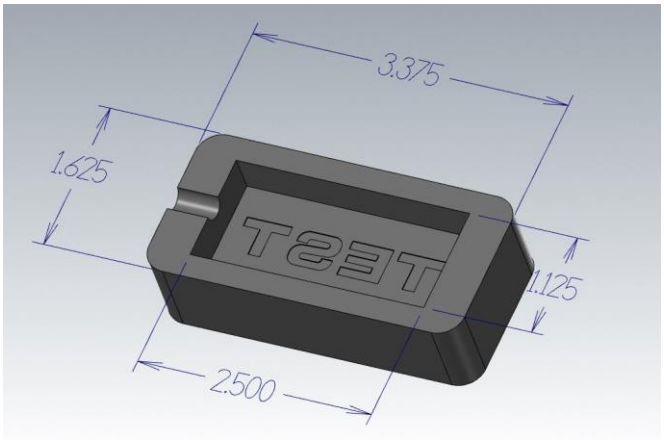

The first trial printed cavity was a simple rectangular "Test" block. This cavity was printed using PLA, with 80% infill and a layer height of 0.2mm.

Figure 5 "Test Block" cavity design

A basic mold base needed to be machined that could hold the cavities during the mold process. The mold base, in Figure 6, is an aluminum die with a pocket to accept printed cavities. This allows a variety of printed cavities to be tested using the same mold base and also provides the strength needed to withstand the clamping forces of the wax injection press. A through hole in the bottom of the pocket allows the cavity inserts to be removed, either by pressing out with a dowel pin or with compressed air.

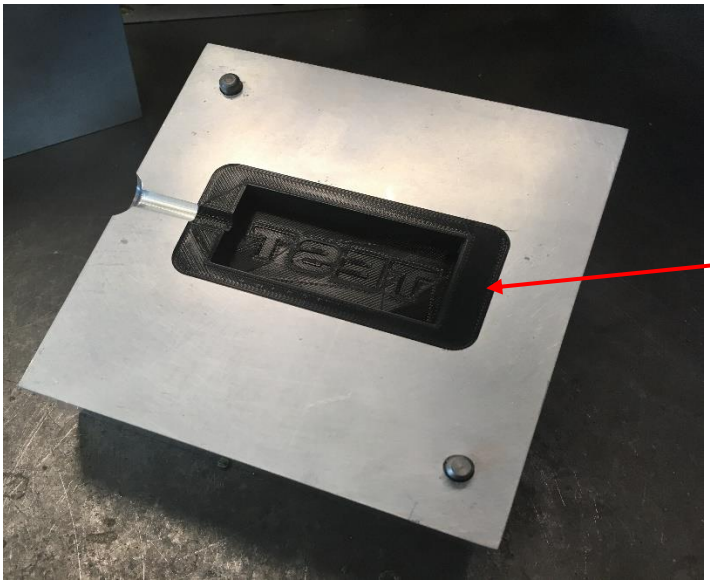

An aluminum mold base was machined to accept the printed cavities. The first "test block" cavity is shown here installed in the mold base. To ensure a close fit, the cavity was printed the same size as the pocket (no clearance) and the lightly sanded to press fit. The surface finish of the cavity was "as printed" and a light coat of Stoner® Wax Pattern Release was applied to the surface.

Figure 6 Aluminum die with printed cavity installed

The first trial run of the test block cavity produced a part. It's easily to notice that the surface finish reproduced the texture of the printed cavity. Even though the surface was textured, the 5 degree draft allowed it to be removed easily from the cavity with a blast of compressed air.

Figure 7 Wax Test Block

Small Production Run – Domino Set

With early success in trial test of the printed cavities, a part was designed to run as a small production run and continue testing the concept of printed cavities and inserts. To utilize the same mold base, the cavity insert was designed to fit into the pocket and was also a simple flat back part. The part selected was a simple domino, which when produced as a set, would utilize both a printed cavity and interchangeable printed inserts. To produce a double-six set of dominos, a total of 28 different wax patterns would have to be molded. The design is essentially a family of parts, one standard cavity with different combinations of parts that could be produced by replacing removable inserts. As can be seen in Figure 8, a single die cavity was designed, with 28 different interchangeable printed inserts that could produce all the different dominos needed for the complete set. The cavity was designed to include gating, which was angled such that patterns would assemble easily on a sprue. Some holes in the bottom of the cavity were included to allow for removal of the inserts.

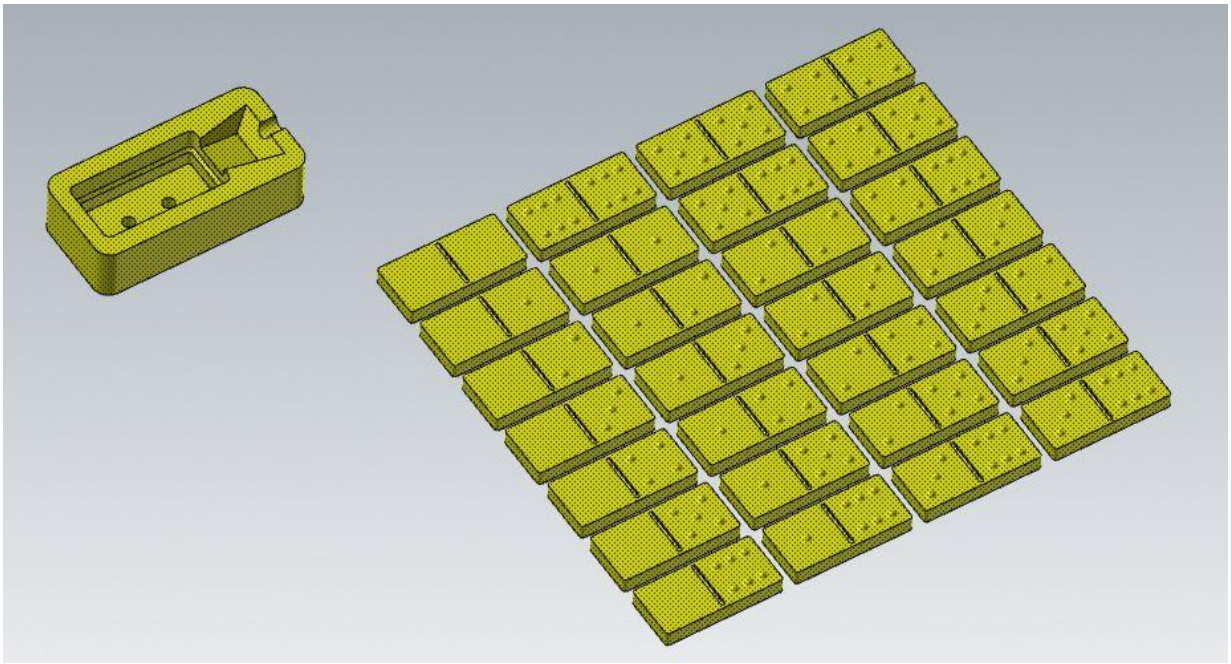

Figure 8 A Single Cavity designed with 28 interchangeable inserts to produce a full Double-Six domino set

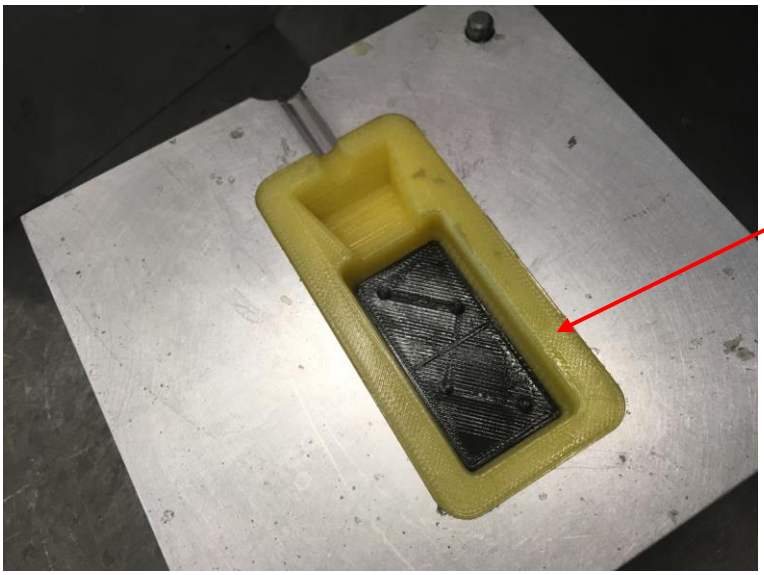

The printed domino cavity (yellow PLA) shown here is installed in the mold base with a "Double 2" domino printed insert (black PLA). The domino inserts pressed very tightly into the pocket of the printed cavity, however, could be easily removed by blowing compressed air through the holes in be back side of the tool and then replaced with a different domino insert.

Figure 9 Mold base with printed domino cavity and insert

The printed domino cavity, shown assembled in the mold base in Figure 9, was coated in wax pattern release and filled with the wax injection press. No special process adjustments were made to the injection press, however, as noted earlier, the solidification times were slow due to the insulating properties of the printed material. Since there are no ejector pins in this design, the part was removed by blowing compressed air along the edge of the part and under the gate once solidified. There was

some trial and error in determining the wait time before removal, as the part needed to be fully solidified prior to removal. As can be seen in Figure 10, the domino shape was able to be produced, and the wax reproduced the surface finish left by the printed tooling. Some black specks can be seen on the surface, due to contamination in the reclaimed wax being used during the trials.

The first part has a few wax related defects, however, it successfully produced the shape. There was some flash along the parting line that was easily removable. The surface finish (parallel lines) are a result of the as printed surface of the cavity/insert.

Figure 10 First wax pattern produced with the printed domino tooling

The design included draft angle (1 degree) on the walls of the cavity, which allowed for removal of the wax patterns by blowing compressed air between the wax and printed cavity. Surprisingly, the patterns removed reasonably easily, especially considering the layer texture along the sidewalls of the cavity.

To speed up production, a total of 3 cavity dies were printed that could all be used with the 28 different domino inserts. This allowed two wax patterns to be cooling while a third was being molded on the injection press. By the time the third cavity was molded, the first was pattern was ready to be removed. Blowing air along the edge of the wax allowed for removal from the printed cavity. The yellow PLA components were printed at 60% infill, while the black were printed at 80% infill. There wasn't a notable difference in the performance of the two different infill percentages on these part.

Figure 11 Three printed cavities were used to speed up production

As production continued, the printed cavity began to warm, which further increased the solidification times. To maintain a steady pace, additional cavities were printed (See Figure 11). After one cavity was

filled with wax, the entire printed cavity insert was removed from the mold base and set in a bucket of ice, to avoid warming of the printed cavities during the production run and to increase the cooling rate. Next, the second cavity was filled, and so on until all were filled with wax. By the time the last cavity was filled, the first wax pattern was ready to be removed, and thus the rotation continued. Figure 12 shows a tray of wax patterns produced during the trial run.

After 4-5 patterns were molded for a particular domino, the insert was changed and production of the next domino in the series began. Since this was a trial run, only a small number of each domino was produced. The patterns shown in this tray still have some flash that needs to be removed.

Figure 12 Tray of domino wax patterns

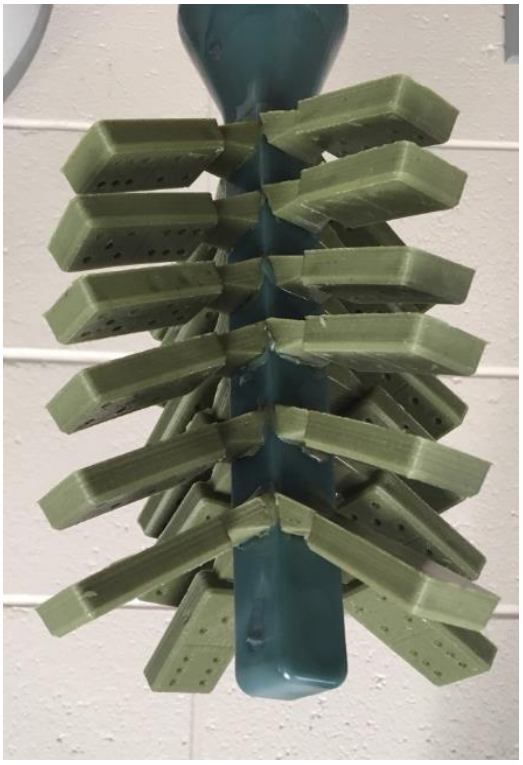

After the production run of parts, the dominos were assembled onto sprues. Since the gating was already molded with the part the parts assembled very quickly onto the sprue. The gating itself was designed and molded at an angle to improve dewaxing of the shells. With careful placement, an entire set of double-six dominos can fit onto a single sprue.

Figure 13 Sprue with dominos attached

Economic Analysis

This was primarily a "proof of concept" project, rather than an economic feasibility study, into printed die cavities and inserts. That being said, the expenditures for this project were essentially the printer and the build material for the printed components. Overhead, utilities, time, etc. are not considered in this economic analysis. The wax press used was already in service and the wax used was reclaimed, thus those costs are not part of the consideration either. The aluminum mold base, which consisted of two 6"x6"x"1.5" aluminum plates, were machined in house (using material already on hand). Here is a simple breakdown of the material costs for the printed components.

Ender-3 3D Printer – purchase price (online, included shipping) = $193.49
PLA build material - $21.49 per 1 kg spool of filament
Breakdown for the Domino Project:

> Each cavity used approximately 52 grams of PLA build material, thus a material cost of $1.12 per cavity. Since there were 3 cavities produced, a total of $3.36 for the build material for the prints.
>
> Each domino insert used approximately 6.2 grams of PLA build material, thus a material cost of $0.14 per insert. Since there were 28 inserts needed to produce a full set, a total build material cost of $3.92 for the printed inserts.

Total expenditures - $193.49 (printer) + $3.36 (PLA for cavities) + $3.92 (PLA for inserts) = $200.77

Conclusion

As a proof of concept, this project illustrated that it is possible to produce a small production run of wax patterns using inexpensive 3D printed wax injection tooling. The printed inserts were able to function in the existing tooling to produce a part, however, the cooling rate was much slower and the part surface finish had definite limitations due to the printing process (layer thickness and nozzle size). This inherent process limitation will also limit the level of detail achievable when producing inserts. In the case of this tool for this project, most of the inserts include text and/or logos and there is a need for fine details that would be difficult to produce with this print technology. The surface finish was also less desirable, because of the "texture" left by the 3D prints. Further research could be done to determine if there are smoothing methods to improve the surface finish when using printed tooling. For this particular die, the aluminum inserts are far superior in their performance and actually take less time to produce.

As for the small production run using printed cavities, this seems more promising application for print technology in certain applications. Although the domino part was quite simple geometry, it demonstrated that the printed cavities could produce wax patterns and even a small production run of them. The concept of a "universal" mold base in which a variety of printed cavities could be interchanged with the same mold base has real possibility, especially for educational uses, prototyping and small production run applications. While it is not a replacement for traditional tooling methods, it can be a viable method of producing tooling in certain applications.

Economics was not the primary focus of this investigation, but when considering the feasibility of a process, it's worth noting that these technologies have become very inexpensive. Further research needs to be done, but in many cases it there may be a significant economic benefit to printing tooling rather than machining dies or simply printing patterns for investment castings.

INVESTMENT CASTING INSTITUTE

Autonomous Quality Control: The Future is Now

Rahul Alreja
VJ Technologies, Inc.

66TH TECHNICAL CONFERENCE
&
EXPO 2019

Paper № 15

The Future of Quality Control
Intelligent and Autonomous

By Rahul Alreja

"The bitterness of poor quality remains long after the sweetness of low price is forgotten" – Ben Franklin.

This quote is still very much prevalent today and can be applied to all companies, especially those that must continuously improve the quality of their product, especially in the fast-paced technological society we live in today. How has quality control evolved over time and what will it look like in the future?

History of Quality Control

Before the early 20th century, the principal focus of mass production was focused on quantity, rather than quality. During this time, quality control was a means of improving upon the machinery and technology to increase productivity while using less human energy. However, by the 1920s, the focus shifted from quantity to quality of the product due to an increase in demand. There was an increase in emphasis to ensure that quality was consistent. Manufacturers required cheaper and more efficient work in order to increase output per machine, per person per hour. It became clear that working longer and harder did not produce maximum efficiency. This understanding demonstrated that working smarter and employing quality control measurements was the way to yield the most profits.

Today, there are two important quality assurance methods that is used in a wide variety of industries that produce products: Six Sigma and Lean Manufacturing. Both methods are aimed at reducing waste and creating efficient processes, but they take a different approach on how to accomplish this.

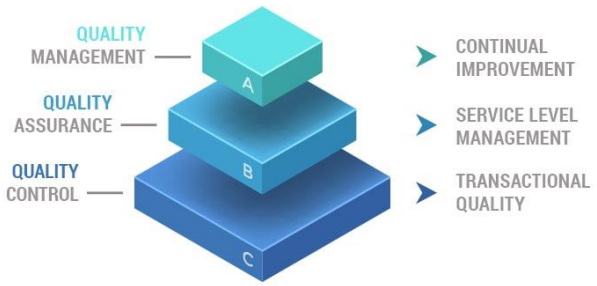

Figure 1 Quality Assurance

The goal of six sigma is to reduce variation and defect rates in production processes through statistical analysis. Essentially, six sigma uses two methodologies: DMAIC and DMADV.

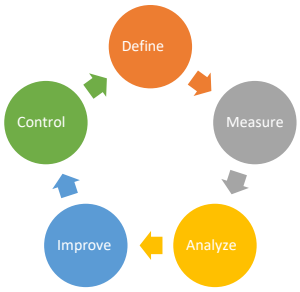

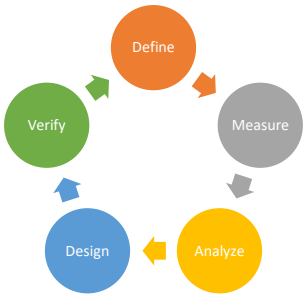

The DMAIC and DMADV methodologies may seem similar but they have different use cases. The DMAIC methodology is used for existing processes or products that aren't meeting customer's needs or performing to standards. When a business needs to develop a process that doesn't exist or when a product has been optimized but falls short of standards, DMADV is used.

Lean manufacturing on the other hand focuses on analyzing the workflow and eliminates waste. It tries to maximize value to the customer while using as few resources as possible.

Ultimately, both quality assurance methods improve a company's manufacturing efficiency while reducing waste and maximizing profit. But what if there is a way to take it one step further? What does the future of Quality Control look like? But, before we talk about that, a general understanding of Industry 4.0 is required.

Industry 4.0

Look at the graphic below. How many of these concepts do you know or have heard of? I'll go so far as to say all of them.

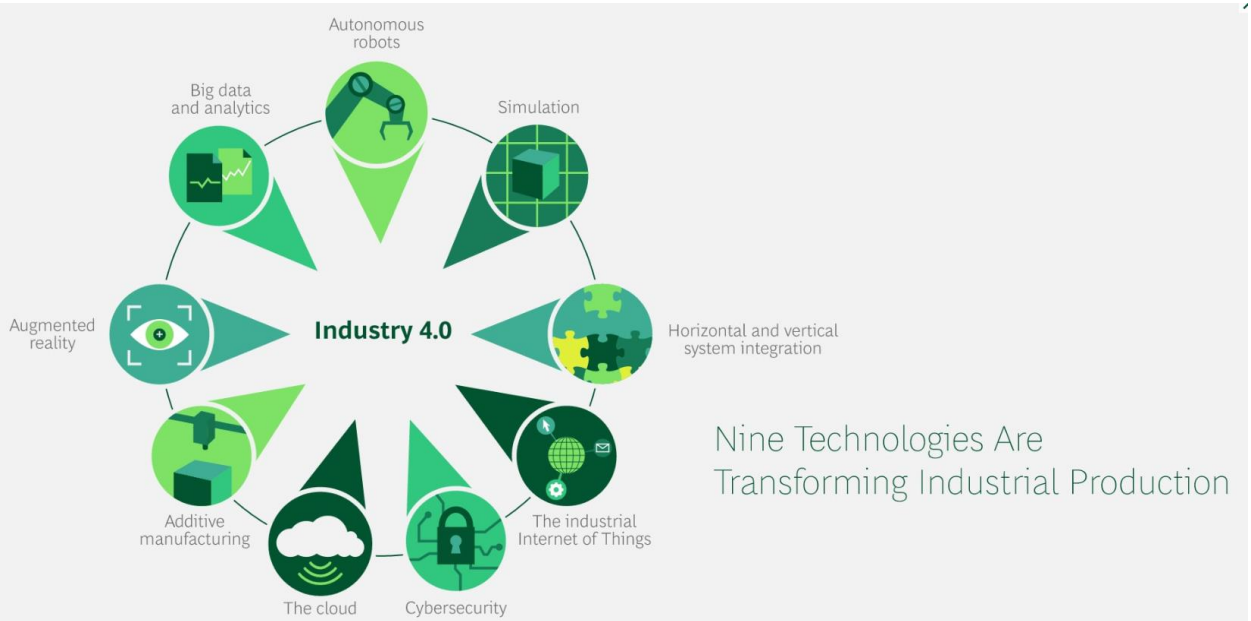

Industry 4.0 began with the rise if IoT and cybersecurity systems only made possible to the technological advancements in computing power. These 9 technologies are the enablers of industry 4.0 and allow for manufacturing processes to be completely automated with the help of autonomous robots, cloud storage systems and IoT. Previously unexplored territories due to limitations in technology can finally be revealed with things like simulations, big data and analytics, machine learning, augmented reality and additive manufacturing. Industry 4.0, when applied to factories will turn them into SMART factories and when applied to robots, make them work faster and better than ever before.

One example is Audi's Smart Factory. If you search on Youtube: Audi Smart Factory – Future of Audi production, you'll see something that might just make your jaw drop. Self-driving vehicles that move heavy cargo, modular robot arms that perform assembly, drones that carry steering wheels, and more… all in a factory.

Industry 4.0 allows existing quality control methods to evolve and improve.

What is the Cost associated with a lack in Quality Control?

What happens when a company neglects quality control in favor of profitability? One example that instantly comes to mind is the Boeing 737 debacle. All that time used for training and development simply went to waste. All the cost associated with it used for equipment, maintenance, personnel and more. In the end, Boeing lost close to $50 billion in market cap in the span of 4 months. Was it worth it?

At first, the cost of good quality control is expensive, as companies need to invest in cyber security systems, robots, and more. But the question comes down to, will it provide you more value than what you initially invested with? One can argue that the benefits of Industry 4.0 technology are limitless in the long run and sooner or later every company will have to jump on board due to increased competition.

Advanced System Designs Today

The graphic below shows what an advanced system looks like today with I4.0.

How many of these steps can be done through automation and Artificial Intelligence? That's right. All of them. What's more is that in some instances, software can enhance the image of the part it inspects and is able to characterize it using different metrology and inspection measurements. As shown below, software can take a Raw image, enhance it with an Automatic Defect Enhancement Filter and process it even further to reduce the noise if required (ADE-N). All of this can be done within a matter of seconds from taking the image.

Raw ADE ADE-N

Along with image enhancement, software can recognize defects in an image given certain criteria and mark whether that part will pass or fail the inspection.

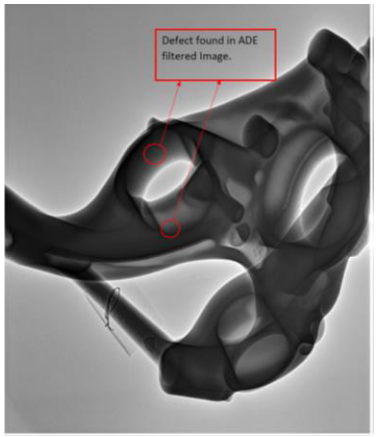

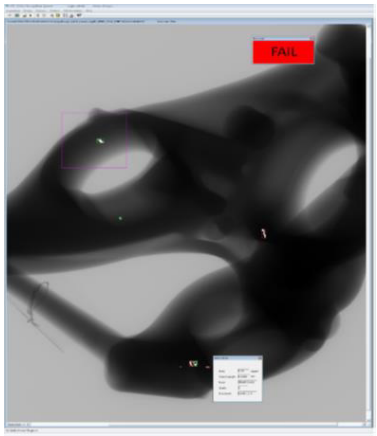

By automating the inspection process and having a consistent way of measuring failed or passed parts, a company can drastically increase production and value. Another way companies increase their value is by providing various metrologies such as Porosity Analysis, Nominal-Actual Comparison, Wall thickness and even oxide detection.

Nominal Actual Correction:

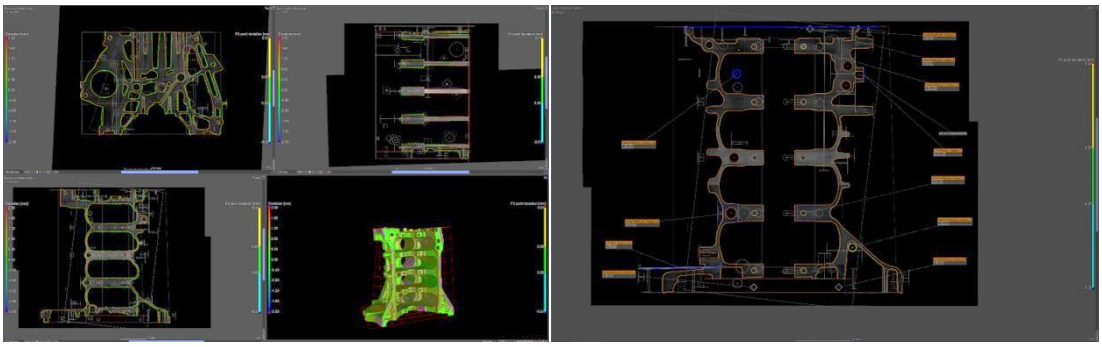

Porosity Analysis:

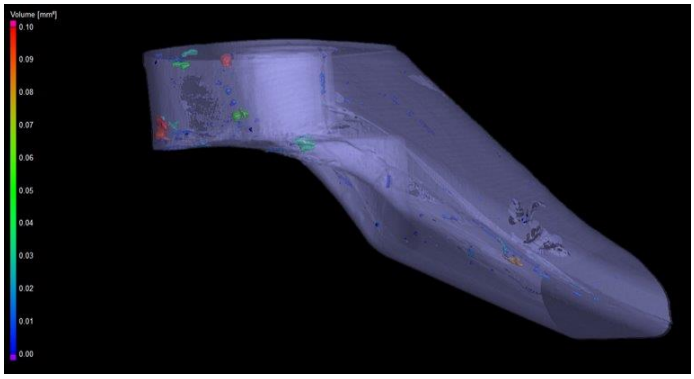

Wall Thickness:

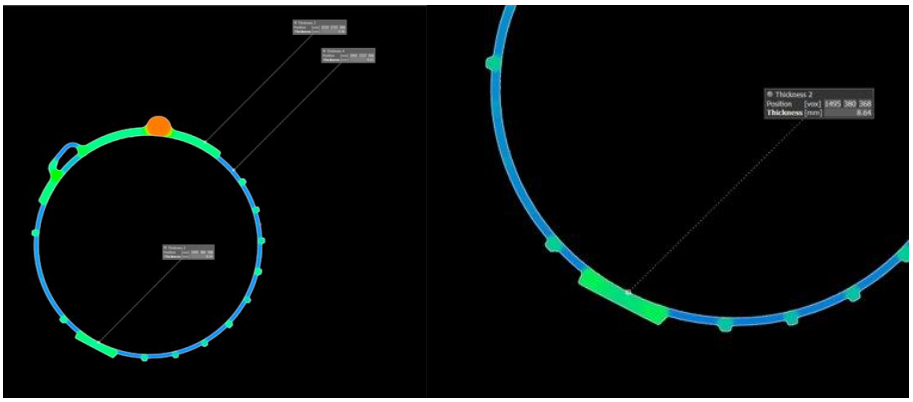

Oxide Detection:

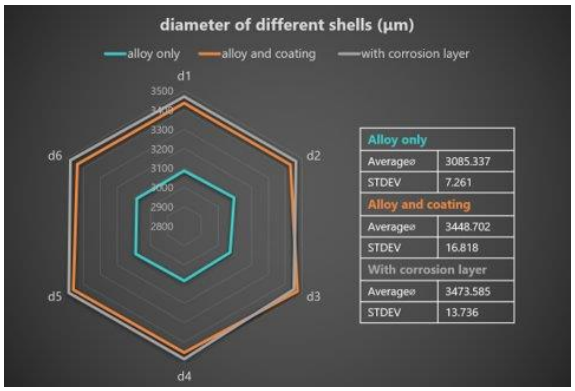

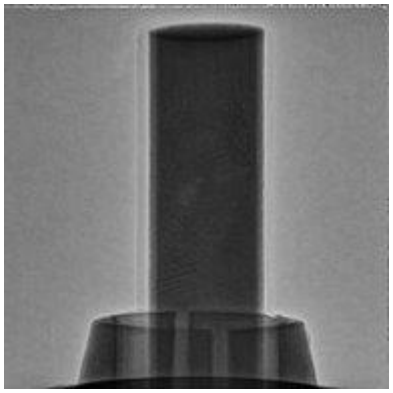

Currently, these kinds of metrology require an operator to input certain criteria and values to enable the software to output the analysis. In the future, AI will be able to detect and learn what criteria and values to input and the operator only needs to push a button that will do the desired metrology. Quality Control will become

Future of Quality Control

Now, what does the future of Quality Control look like if it's already good? Currently humans are still driving the "ship" with the help of these advanced technologies. However, AI will soon take the drivers seat and humans will be the passenger. AI will eventually be able to learn how to use six sigma and lean manufacturing overtime when given enough data and has run enough processes. It can point to certain robotic movements and limit movement inefficiencies that it may notice to reduce the time it takes the robot to move a part. It can suggest factory set up improvements overtime to maximize production rates even.

Soon enough, companies will be able to share their data on the Cloud and with the emergence of blockchain and be able to track certain information companies need. Perhaps all the data around the world will eventually be shared in a unified data repository and companies can leverage that data in their own companies.

These are the kinds of Quality Control methods that can be made possible and eventually this process itself will be completely intelligent and autonomous.

INVESTMENT CASTING INSTITUTE

An Evaluation of Using a Low-Cost 3D Printer for Prototype Investment Casting Patterns

Aaron Meyer
Wisconsin Precision Casting Corporation

66TH TECHNICAL CONFERENCE
&
EXPO 2019

Paper № 16

An Evaluation of Using a Low-Cost Printer for Prototype Investment Casting Patterns

Aaron Meyer, Wisconsin Precision Casting Corporation

Tom Mueller, Mueller AMS

Introduction

Wisconsin Precision has used printed patterns for many years to create prototype and low volume production castings. This has been a key element of their marketing strategy, allowing WPCC to provide rapid prototype investment castings for current customer R&D as well as provide investment castings to companies that would previously have not considered using investment castings. As a result, approximately 10% of their revenues are from castings created with printed patterns. The use of printed patterns has allowed them to satisfy their customers need for rapid prototypes and often-times is used as a stepping stone while production injection tooling is being manufactured.

Except for a short experiment with a Thermojet printer many years ago, they have not been tempted to bring in 3D printing capability to build printed patterns. The printers commonly used for printing investment casting patterns were too expensive, and they were reluctant to spend that much money on equipment that would only service 10% of their revenues. The prototype market also tends to be cyclical, leaving expensive machines idle for extended periods of time or backlogged causing lead times to be extended. They would get much better returns spending capital on equipment or information systems to continue to support and grow their production revenue.

In addition, there were several service providers who, in most cases, could deliver quality patterns in the time frame needed. However, because of the cyclical nature of prototyping mentioned above, these suppliers could get busy and then could not provide patterns in the time frame needed. The purchase price of a printed pattern is also a significant amount of the cost of a prototype casting.

Earlier this year, Ultimaker offered WPC an opportunity to evaluate a small printer for pattern printing applications. The offer was interesting for three reasons:

- It would give them better control over the timing of patterns. They would not be affected by supplier backlogs.

- Because both the price of the printer and materials were significantly less than traditional methods of printing investment casting patterns, there was a good possibility they could print patterns for much less than it would cost to buy them.

- It would eliminate the need to wait for suppliers to quote a job before they could quote their customers as well as eliminate the delay in purchasing patterns. These delays are sometimes the difference between getting the order and losing it to a competitor.

Areas of investigation

To replace patterns from suppliers with patterns built in house, they would have to be able to create acceptable castings from those patterns. To do that, there were certain criteria that would have to be met.

- **Build envelope** - The build envelope would have to be large enough to handle approximately 50% or more of the geometries they cast. Larger patterns would still be outsourced.
- **Build Speed** - The printer must be fast enough to provide the patterns in a timely basis. If it takes too long, it would not be worth much to them.
- **Build Cost** - The cost to build patterns must be better than the cost to buy them
- **Dimensional accuracy** - The patterns would have to be within their normal casting tolerances. In general, if the pattern tolerance is 50% or less than our casting tolerance, they will have enough tolerance left to reliably provide castings within tolerance
- **Surface finish** - The surface finish must be good enough to provide an acceptable casting
- **Casting process** – the process required to obtain an acceptable casting must be no more difficult than that required for QuickCast patterns and ideally would be easier than QuickCast

WPCC has been using the Ultimaker printers and Polycast filament since May of 2019 and have made approximately 50 castings. The following are the results of that experience.

Build Envelope

The build envelope of the S5 printer being used is 330 x 240 x 300 mm (13 x 9,4 x 11.8 in). WPCC certainly casts parts larger than the build envelope but estimates that 60-70% of the patterns they cast would fit. To date, they have seen a significant reduction in outsourced printed patterns.

Build speed

WPCC doesn't have experience with other types of printers to compare to the speed of this machine, but it seems to be fast enough for their needs, at least for now. A couple of examples:

This pattern built in 21 hours with a build volume of 6" x 5" x 8".

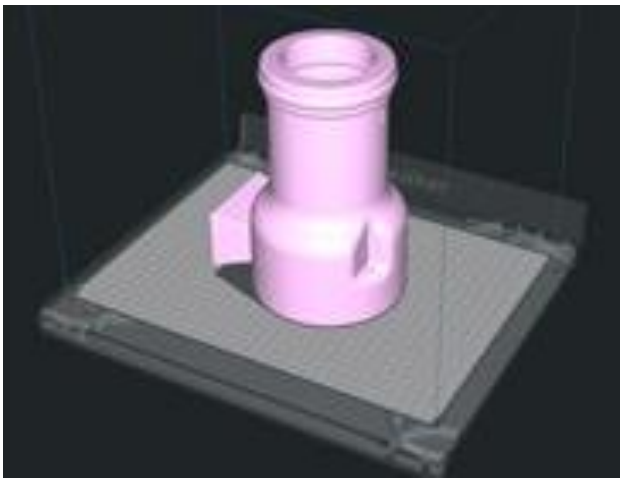

This pattern built in 7 hours with a build volume of 7” x 6” x 3”.

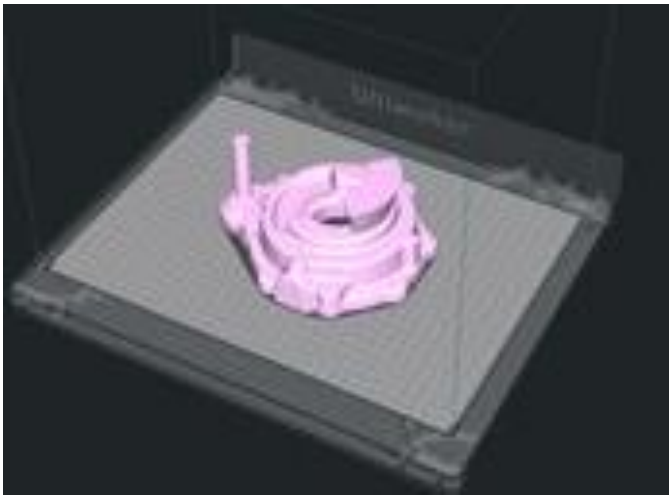

The build speed is enhanced for investment casting patterns because they are built hollow.

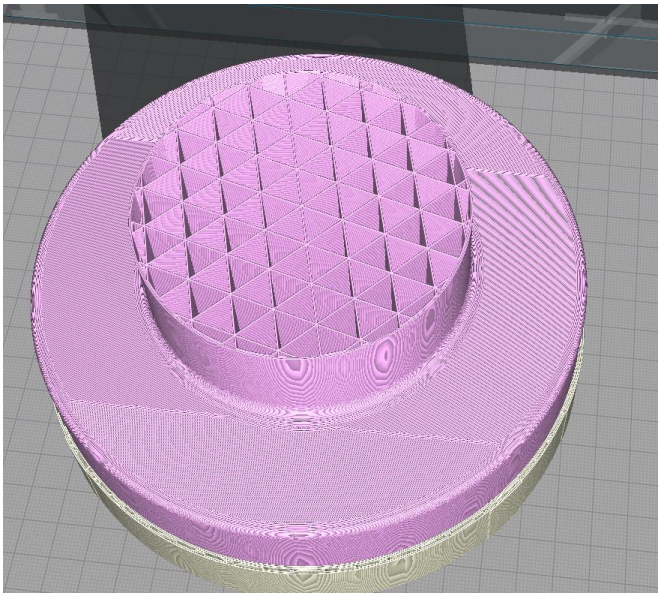

To estimate an average build speed, the total volume of each pattern built as well as the total build time for that run was recorded. Dividing the build volume by the build time gives us the cubic inches per hour for that run. Averaging build speed for a larger number of runs provides a good estimate of the average build speed for the printer.

Twelve geometries were built with volumes ranging from 13 to 185 cubic inches. Build speed averaged 2.76 cubic inches per hour (ranging from 0.86 to 5.60 cubic inches per hour). This average likely underestimates the true average build speed since only one part per platform was considered and in many if not most cases, more than one part will be built at a time.

Compared to the average build speeds determined in Mueller's 2016 comparison of the four leading methods of printing investment casting patterns[i], it is more than three times as fast as an inkjet wax printer but slower than the other three technologies (PMMA, QuickCast and SLS).

With the low price of these printers, if a faster build rate is required for orders with multiple patterns, additional printers can be purchased. Running fewer patterns on multiple machines will result in a significant decrease in build time.

Build Cost

Following the model developed by the author in a previous study, three of the four major costs of a printed pattern: (depreciation, maintenance, and material cost) were calculated. The fourth major cost is labor and is more difficult to quantify.

Depreciation Cost - The cost of the printer is $6000. Using a 7-year straight line depreciation, the monthly depreciation cost is $71.43. The monthly production volume, assuming 80 hours of printing per week, or 320 hours per month is 884.66 cubic inches (multiplying average build rate times 320 hours. The depreciation cost per cubic inch of pattern is then $71.43/884.66, or $0.081 per cubic inch of pattern built.

Maintenance Cost - Ultimaker offers an extended maintenance plan which costs approximately $1200 per year or $100 per month. The monthly maintenance cost is divided by the production per month to obtain the maintenance cost per cubic inch of pattern built. The result is $0.113 per cubic inch.

Material cost - There are two materials used in the printing process; the pattern material and support material. All the support material is removed and discarded after the build is complete.

The prep software, Cura, calculates both the cost of pattern material and support material for each build. Dividing the material cost for a run by the volume of pattern built yields the cost per cubic inch for that run. Averaging that number over the 12 geometries yields a material cost of $0.502 per cubic inch

The total of these three costs is $0.696 per cubic inch. This is less than one-third the cost of the least expensive build cost of the four methods covered in the 2016 comparison[ii].

Dimensional accuracy

In general, the accuracy is pretty good and, in most cases, will meet prototype casting requirements. These are the observations regarding dimensional errors:

- Circular sections tended to be slightly oval; the diameter in one direction is slightly longer than the diameter in the perpendicular direction.
- Rectangular cross-sections appear to print as expected with no discernable difference in the X or Y direction.
- Significant errors were not observed in the Z or vertical direction. This direction has the least amount of machine variables and is therefore the most stable direction.
- Cura allows for a high degree of control over the printing parameters, and small changes to the parameters can have a large effect on the dimensional accuracy.

- The filament also moves slightly as it cools on the build plate. The geometry of the part and the way in which the pattern is constructed can also impact the dimensional accuracy.

The overall dimensional accuracy of the printed patterns falls within the accuracy of an injected wax pattern. At times, Quickcast patterns can be *too* accurate, especially when used as a fill-in before production injection tooling is complete. Having printed patterns with a dimensional accuracy similar to injected wax patterns will allow for a smoother transition from prototype to production.

Surface finish

The layer lines are fairly pronounced as the pattern comes out of the printer. The thickness of the layers is controllable in Cura, however, the greater the number of layers, the greater the build time. Finishing the patterns is a three-step process:

1. Remove the support material
    a. The support material used is water soluble. Removing as much support material beforehand via mechanical means will greatly reduce the amount of time needed to soak the patterns in water to completely remove the support material
2. Mechanically remove layer lines
    a. The material is capable of being finished using mechanical means (sanding, scraping, etc.). Removing heavy layer lines via mechanical means will decrease the time required and enhance the results in the final finishing step.

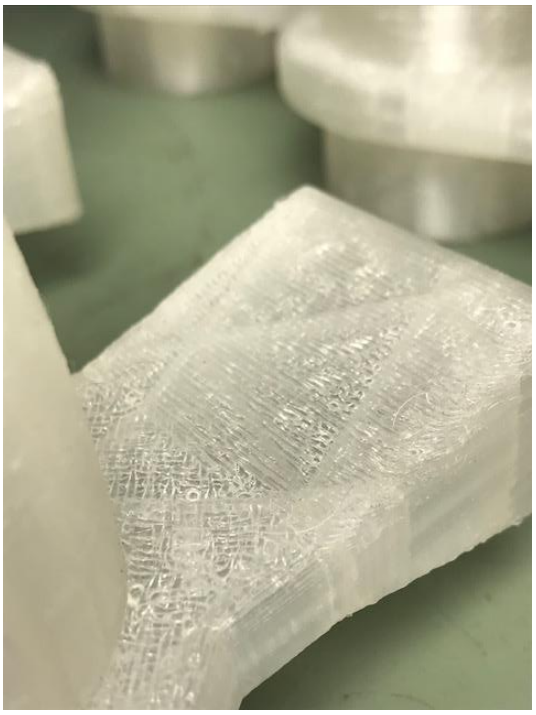

3. Polishing and sealing
    a. Because the material is a thermoplastic, as opposed to the thermoset materials used for QuickCast patterns, patterns can be smoothed with a vapor polishing

process. WPCC bought a low-cost system to polish the patterns they printed. They simply put the printed pattern in the chamber, turn on the machine and in 15 minutes it was significantly smoother. This process also seals the pattern to make it watertight. The polisher uses denatured alcohol, a low-cost consumable. It does, however, affect detail resolution. It might not be advisable to use it on patterns with tiny lettering or to leave the patterns in the machine for an extended period of time. Patterns can also be sprayed with or dipped in denatured alcohol. Doing either of these methods will decrease the aggressiveness of the polishing effect, but will still seal the pattern. Patterns too large to fit in the polishing machine are either sprayed or dipped.

QuickCast Casting Process

The majority of the patterns that Wisconsin Precision used in the past were QuickCast patterns. Over the years, a casting process was developed that reliably produced acceptable castings. There were several variations from the casting process used for injected wax patterns. Those differences included:

- **Adding vents in the assembly process** - Vents must be added for two reasons. First, to allow steam to enter the pattern immediately during pressurization in the autoclave. The steam softens the internal QuickCast structure and allows the pattern to collapse as it expands with heat. Secondly, it provides a means for airflow through the shell during burnout. At least one vent is added to each mold on the assembly. If the patterns are large, more than one vent is often required.

- **Additional 2-3 dips on Quickcast patterns** - The additional dips are to strengthen the shell to resist the expansion of the pattern during the autoclave step.
- **Opening vents prior to autoclave** - The vents must be opened before the shell is autoclaved to allow steam to enter the pattern.
- **Burning out the pattern in an oven** – The shell is placed in an oven to remove the pattern material. Typically, the shell is burned out at 1800 degrees Fahrenheit.
- **Cooling the shell after burnout** - After burnout, the shell is removed from the oven and allowed to cool so that it can be handled.
- **Rinsing ash out of the shell** - Once the shell is cooled, any ash remaining in the shell is rinsed out.
- **Patching vents** – At this point the vents are patched

Compared to the process used for injected wax patterns, these variations add significant cost because of the additional labor required. In addition, they add significantly to the time required to ship the casting. These additions to the process can add several days to the lead time.

Not only are these variations expensive, it makes running a mix of printed and injected patterns very difficult. Printed pattern shells need to be kept track of and handled differently from injected wax shells.

WPCC found that they could use a much simpler process to cast the Polycast patterns created on the Ultimaker printer.

Ultimaker Pattern Casting Process

Assembly

Assembling patterns onto wax sprues is straightforward. They used exactly the same process that was used for injected wax patterns. The patterns were not vented.

Shell building

WPCC used one additional dip compared to the shell for injected wax patterns. It may be possible to use the same number of dips, but to be on the safe side they use one additional. Further testing will be needed in order to use the same number of dips as injected wax patterns.

WPCC did not observe any problems with shell adhesion.

Autoclave

WPCC uses their normal autoclave cycle. They found that the Polycast material will soften and start to run out of the shell. It is not quite liquid, it is a very thick goop.

WPCC didn't want this plastic to mix in with their reclaim wax and were concerned about it clogging up valves and piping in the autoclave plumbing. To combat this, a pan was put under the shell to collect any plastic that melts out of the shell. Some of the pattern remains in the shell and will be burned out later.

No shell cracking has been observed as a result of pattern expansion when the patterns were built in a similar manner as QuickCast patterns. Polycast patterns built with extremely thick

walls and/or dense infill have experienced shell cracking due to expansion. These were early experiments while learning the properties of the material.

It does appear that the Polycast patterns have much less tendency to crack shells than QuickCast patterns. One of the test patterns that was used was a closed impeller. Closed impellers have been notoriously difficult for WPCC to get through the autoclave without cracking the shell. QuickCast patterns required several vents to allow steam to get inside the pattern and soften the internal structure so that it could collapse. The Polycast pattern showed no cracking at all and had no venting.

Burnout and preheat

Patterns were burned out at their normal preheat temperature, 1800 degrees Fahrenheit for the normal time, 2 hours. Shells were not cooled or cleaned out after burnout. They went right to pouring.

In the several castings done to date, there has not been evidence of excessive ash or other defects in the castings.

There was no excessive smoke during burnout.

Casting

No change from process for wax patterns

Summary of WPCC Results

- Accuracy was similar to injected wax, which is acceptable for the vast majority of WPCC castings
- Surface finish was acceptable after mechanical finishing and vapor polishing
- Build speed is marginally adequate but can be easily improved with additional printers
- Build Cost is significantly lower than competing technologies
- Casting process is significantly easier than for QuickCast patterns. The only changes from injected wax are:
    - 1 additional coat on the shell
    - Pan under the shell during autoclave
- Not having to perform additional operations saves several days in the casting process

Conclusions

1. Patterns printed using the Ultimaker S5 running the PolyCast material
    - Create acceptable castings
    - Are less expensive to print than purchased printed patterns
    - Are less expensive to cast than purchased printed patterns
    - Are faster to cast than purchased printed patterns
2. Even though the printer is slower than leading methods, the purchase price is low enough that multiple printers can be purchased to improve build speed.

[i] . "A Comparison of 3D Printing Technologies Used to Make Investment Casting Patterns", Thomas J. Mueller, Presented at the 2016 ICI Fall Technical Conference, October 2016

[ii] Ibid.

INVESTMENT CASTING INSTITUTE

Digitization & Automation of the Process of Printing Patterns for Investment Casting

Ben Wynne
Intrepid Automation

66TH TECHNICAL CONFERENCE
&
EXPO 2019

Paper № 17

Digitization & Automation of The Process of Printing Patterns for Investment Casting

Ben Wynne – CEO

September 2019

Background

Founded in late 2017, Intrepid started with the mission of applying new manufacturing methods and technologies to customer use cases to enable a faster, cheaper and more JIT and digital a manufacturing flow to be realized. Intrepid believes this will enable significant cost and time savings across a supply chain for OEMs, allow a faster time to market and empower more optimal designs to be realized.

We believe these technologies in aggregate, applied to a Hybrid IC approach will future proof the IC industry as methods like generative design, customization, topology optimization and 3D metal printing become more mainstream in the very industries we serve (e.g. aerospace, automotive, medical).

At Intrepid, we are focusing on the following core disruption areas:

1. **New 3D Printing Technologies** – speed, quality, cost, consistency "no snowflakes"
2. **Material Innovations** – "castability of wax, with the handleability of resin"
3. **Automation of Processes** – Removing humans to make consistent parts with lower cost overhead.
4. **Control and Auditability though Industrial Internet of Things (IIOT)** – Create a data trail for part auditability and use data to optimize downstream process steps.

This paper aims to go over these disruptions at a high level, share some of our learnings and open up the discussion to the wider Investment Casting community.

The Elephant in the room! Metal Printing

Why 3D Printing and Investment Casting? **Why not just metal print the parts directly?**

A large marketing push is focused on 3D printed metal today. I won't re-iterate here, but refer to the fantastic body of work by Tom Mueller in the past analyzing the costs per part for metal printing vs a Hybrid IC approach. (Mueller, web.investmentcasting.org, 2017)

But to touch on a number of key points:

- Speed – very slow process
- Scalability – very expensive
- Cost per part – powder costs are orders of magnitude higher than standard casting ingots
- Post Processing / Support Removal (see **Figure 1**)
- Material selection is limited vs Investment Casting
- Directional Solidification and Super-Alloys are not yet possible.
- Safety / Powder Handling / Facility Requirements

***Figure 1**. Metal Print + Support*

Most importantly, the realization that final part properties can vary vs castings and failure modes are difficult to spot.

What does this mean? Short answer is **RISK**:

In the orthopedic implant market, insurance companies such as Blue Cross Blue Shield are setting policies of non-coverage for direct 3d printed implants due to the early stage of the technology. (*Refer to Section 520(b) of the Food, Drug and Cosmetic Act*). Further details with examples are outlined in (Blue Cross Blue Shield, 2019)

In conclusion, metal printing is an amazing new technology but has many obstacles to overcome in order to displace standard or Hybrid IC methods for anything but extremely low volume production or prototyping. Medical, Aerospace and Automotive are all interesting areas for use, but until more direct metal printed parts are produced and tested in real world use cases, the risks remain extreme.

Hybrid IC Today

Please see the fantastic article series from the ICI's INCAST magazine by Tom Mueller from March, April and June of 2017 (Mueller, A Comparison of 3D Printing Technologies Used to Make Investment Casting Patterns, 2017) for a detailed comparison of printed pattern technologies today, their pros / cons and costs.

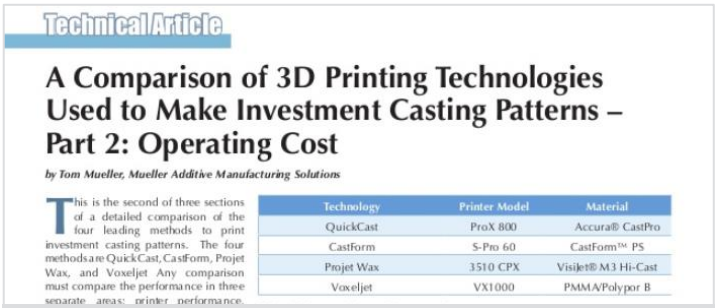
Technical Article

A Comparison of 3D Printing Technologies Used to Make Investment Casting Patterns – Part 2: Operating Cost

by Tom Mueller, Mueller Additive Manufacturing Solutions

This is the second of three sections of a detailed comparison of the four leading methods to print investment casting patterns. The four methods are QuickCast, CastForm, Projet Wax, and Voxeljet. Any comparison must compare the performance in three separate areas: printer performance,

Technology	Printer Model	Material
QuickCast	ProX 800	Accura® CastPro
CastForm	S-Pro 60	CastForm™ PS
Projet Wax	3510 CPX	Visijet® M3 Hi-Cast
Voxeljet	VX1000	PMMA/Polypor B

***Figure 2**. 2x Knee Implant Patterns – Time ~44 min*

New 3D Printing Technologies

***Figure 3**. 2x Knee Implant Patterns – Time ~44 min*

As far as analogies go, I like to compare 3D printing to that of **single vs multi-core processors**: Initially, having a single "processor" was hugely novel. It allowed fundamentally new ways of controlling things and processing data, then, as time went on, faster and faster CPU clock speeds were obtained, until a physical limit was reached.

Development didn't stop there, and in order to realize faster processing throughput, parallel architectures were developed. Single computer systems with many "processor cores".

I like to think of 3D printing as going through a similar evolution: prototyping and short run 3D printers are similar to the super-computers of old.

Another major issue with printing patterns with multiple printers is that of unit-to-unit and part-to-part variations. Using closed-loop approaches at every step of the manufacturing process enable consistent parts to be produced.

As shown in **Figure 3** above, new printing technologies are enabling much faster print speeds for investment casting pattern production, however in order to really enable true production the speed needed **has to be much faster than 2 parts in 44 minutes** shown above! Why do printers need automation if a print takes many hours to complete?

As per the analogy above, we tested the notion of parallelizing the print process enabling a staggered printing approach realizing an **effective print speed of 8 minutes and 38 seconds per pair of knee patterns** (see **Figure 4** below).

Why is this important? Production is only going to be as fast as the slowest component in the manufacturing flow. We believe that one of the targets for Hybrid IC is to have a print system that produces patterns, ready to be assembled on a tree with no post processing at the same cadence as the foundry shell building cycle.

This is not as trivial as it may initially seem. A holistic approach is required to take into account all necessary steps to get a 'ready to cast' part.

This includes the following:

- Multiple high-speed print engines.
- New resin developments.
- Automated Part Handling.
- Automated Resin Handling.
- Automated Post Processing.
- Automated QA.
- An Additive Centric Workflow Management System.

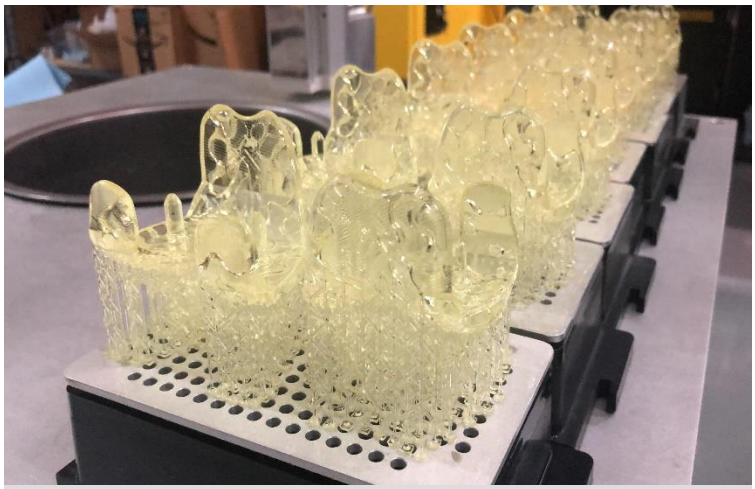

***Figure 4**. 14 Knee Implant Patterns – Staggered prints result in a tray every 8 minutes 48 seconds*

Material Innovations

Conventional printed patterns is a proven method for prototypes or short production runs but have a number of issues: Printed wax can be very delicate when support material is removed, this makes them tricky to measure with accuracy defects only evident after casting. Resin patterns have great handleability but are normally difficult to burn out.

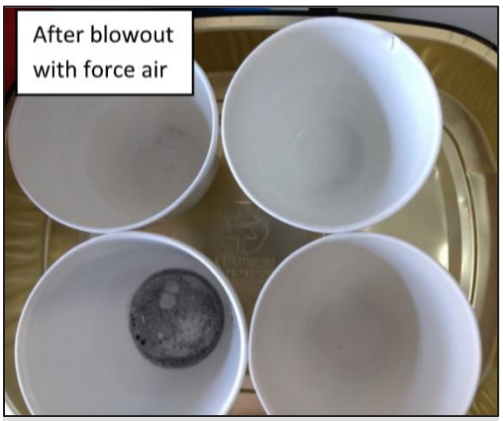

***Figure 5**. Multiple burn out tests showing residue vs clean*

Intrepid has been able to create a happy medium between these needs and has demonstrated promise with a new material for investment casting that is accurate, durable and antimony free. When paired with burn out improvements (as described in the technical paper by Tom Mueller – ICI 2019) it can enable significantly cleaner and faster burnout for 3D printed patterns.

We started with existing available materials and the result is shown in the bottom left crucible of **(Figure 5)**. After a few iterations we developed a material that resulted in the results on top right.

Reults are further validated by real castings **(Figure 6).** Notice the stark difference between the complete and incomplete burn out.

As per "Stereolithography and other RP&M Technologies author Dr Paul F. Jacobs" – *"cross-linked photopolymers NEVER melt. They may weaken at elevated temperatures, but they do not melt, although of course, at sufficiently high temperatures they will burn."*

Our formulations are based on fundamental understanding of polymer "structure property relationships" (SPRs) for specific material sets. The SPRs are very important to establish the optimal interplay between physical strength and mechanical properties under burnout conditions. (**Figure 6a-c** demonstrate the result from one such test).

***Figure 6**. Clean shells vs Residue*

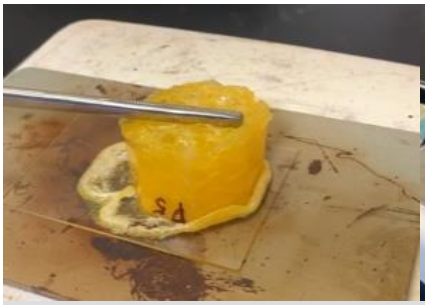

***Figure 7a**. 1 minute*

***Figure 7b**. 3 minutes*

***Figure 7c.** 5 minutes*

Automation of Processes

Batch vs Continuous printing is a complex topic, with specific part geometry, build orientation and part size all playing a role in build rate and ultimately per part cost. For production, an optimum balance is required between all these factors to make true production real.

Intrepid believes a continuous, automated solution is required that closes the loop on part quality during the printing **AND** post processing.

It starts with automatic part layout, and geometry pre-processing followed by the assignment to a trackable, robotically interfaced manufacturing fixture. That fixture follows the part(s) not only through the digital to physical steps but post-processing, inspection, and final packaging too. This allows normally manual steps such as measurement, support removal and other secondary and tertiary processes to be automated.

It also creates a break away from current 3D Printing limitations, printing can run continuously with little down time vs the current 'overnight' printing approaches prevalent today. Parts that **could** be affixed to trees and cast aren't 'trapped' inside a large batch-based printer. Unstaffed hours can now be productive too.

Control and Auditability though IIOT

The manufacturing fixture described previously has unprecedented auditability throughout the whole process (even manual steps). But it doesn't stop there.

The same closed loop trackable approach is used for downstream processes too.

Imagine for example, a shell building system or burnout oven with many key controls and parameters that have a direct impact on casting quality. What if any one of these systems changes? Or fails slightly?

"What if the slurry tank stirring rate falls by 10%?"

"What if the temperature of the slurry changes affecting viscosity?"

"What if oxygen content or temperature in the burn out oven is not optimal?"

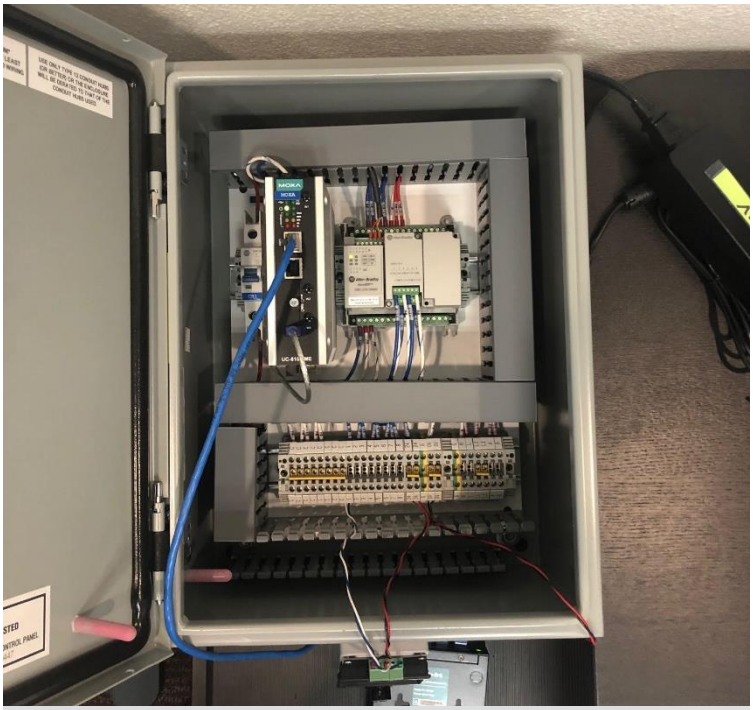

***Figure 8**. Element Box, Industrial Components for gaining telemetry on other factory systems.*

These potential variations led Intrepid to develop small system that enables us to "make dumb equipment smart". Internally we call this asset "element" (see Figure 8).

Element was developed for internal use in order to create a data stream from anything that could have an effect on part quality.

Ambient temperature in the factory? Relative humidity? Air pressure in the factory? Duty cycle of compressors? etc.

Element allows us to quantify these variances and build an audit trail that ultimately links these potential variations to a particular part produced by the factory.

The ultimate aim here is to use data as a tool to optimize process steps enabling faster cycle times and decreased cost per part. It also can enable failure prediction reducing the chance of "line down" issues. Things get especially interesting when "element" can be used to control systems too (instead of just consuming data).

Conclusion and Next Steps

In order for Hybrid IC to become more prevalent, multiple complex innovations are required across many disciplines in order to solve the key pain points of 3D patterns. From print speed, to post processing as well as developing a more wax like flow. Please see (**Figure 9**) for reference. Of particular note here is the combined "**Burnout and Pre-Heat**" step that could significantly close the gap between conventional and 3D printed wax, and resin or thermoplastic type patterns. (Please see Tom Mueller's Paper from ICI Conference 2019 on Air Injection for Fast Burnout).

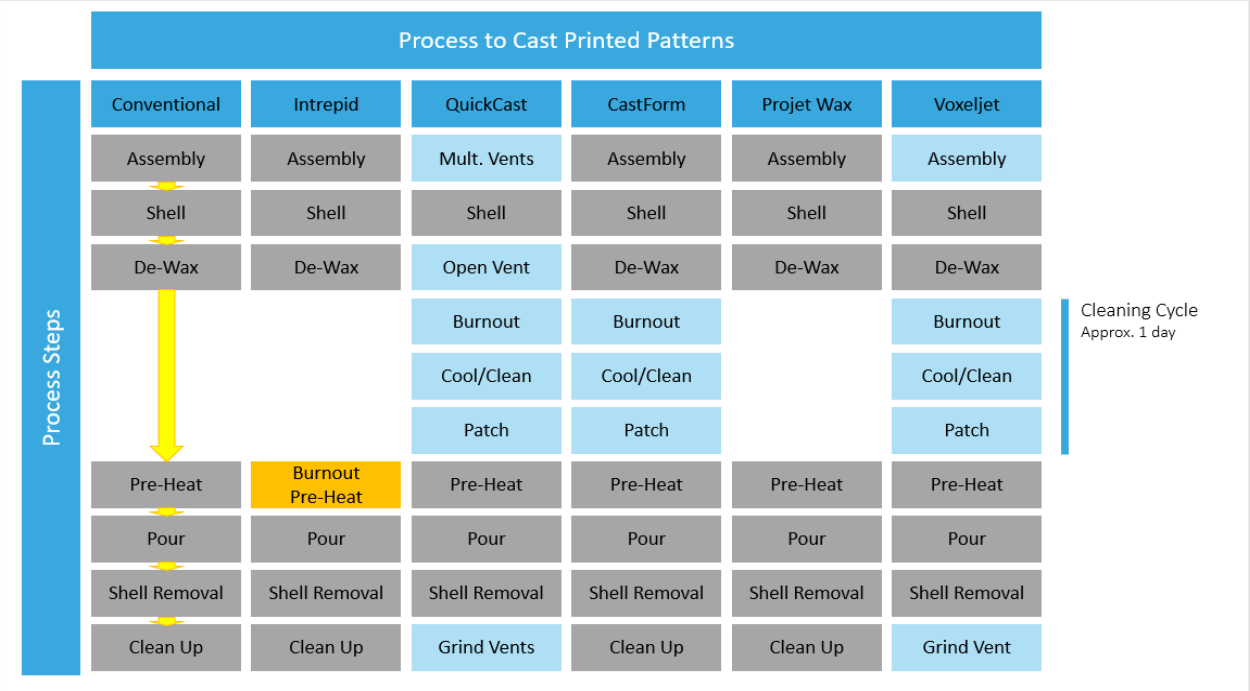

Figure 9. *Variations to the normal investment casting process required for printed patterns.*

Further cost and time savings are possible by applying full automation to the steps outlined in **Figure 9** in combination with IIOT methods and a data driven workflows to enable custom and optimized paths through the process to be defined.

Intrepid has immensely enjoyed interfacing with the ICI, their foundry members and other affiliate partners and looks forward to continuing along the path of disruption to enable new ways of making things to become mainstream. We'd especially like to thank Sonny Tran from Fenico Precision Castings and the whole ICI family for their continued support and encouragement over the last few years.

Bibliography

Blue Cross Blue Shield. (2019, February). Retrieved from https://www.bluecrossnc.com/sites/default/files/document/attachment/services/public/pdfs/medicalpolicy/three_dimensional_printed_orthopedic_implants.pdf

Mueller, T. (2017, June 28). *A Comparison of 3D Printing Technologies Used to Make Investment Casting Patterns.* Retrieved from Linkedin: https://www.linkedin.com/pulse/part-3-comparison-3d-printing-technologies-used-make-tom-mueller/

Mueller, T. (2017). *web.investmentcasting.org.* Retrieved from http://web.investmentcasting.org/External/WCPages/WCWebContent/WebContentPage.aspx?ContentID=422

INVESTMENT CASTING INSTITUTE

Improvements in the Burnout Process For Printed Patterns

Tom Mueller
Mueller Additive Manufacturing Solutions

66TH TECHNICAL CONFERENCE
&
EXPO 2019

Paper № 18

Improvements in the Burnout Process for Printed Patterns

Tom Mueller, Mueller AMS
Chris Tanner, Intrepid Automation
Sonny Tran, Fenico Precision Casting

Background

The first printed patterns and the majority available today are made from materials that will not melt out in an autoclave. They are either thermosets (like those from SLA or DLP printers) or thermoplastic materials with melting points above those normally encountered in an autoclave (SLS, or FDM printers).

The solution proposed by printer manufacturers and those companies trying to sell printed patterns was to simply burn out the pattern in the pre-heat furnace prior to pouring. However, foundries soon found out that burnout was not so straightforward.

Preheat furnaces are designed to heat shells prior to pouring, not support combustion. As a result, most preheat furnaces have insufficient oxygen to provide complete combustion of printed patterns. Attempts to burn out patterns typically were far less than successful. Material remaining in the mold resulted in significant defects in the castings.

Foundries attempted to increase the oxygen content in the furnace atmosphere by pumping in plant compressed air. However, shells in preheat are typically positioned upside down resting on the pouring cup which effectively shuts off any potential flow of the pumped in plant air into the shell. Even with a grooved furnace floor, the area available for air to flow into the shell was minimal. Little improvement was shown from that step alone.

Access to furnace air could be increased by setting the pouring cup on a couple bricks separated to allow airflow into the shell. However, the shell is a closed volume and flow into the shells would be minimal.

Several years ago, some foundries tried adding vents to each mold to allow air to flow through the mold. This change greatly improved the combustion of printed patterns. Flames would shoot out of the vents like a blow torch, and air would be drawn in between the bricks and into the pouring cup. Now printed patterns could typically be completely combusted. However, ash remaining in the shell still resulted in ash related defects in the castings.

To remove the ash, foundries found they could cool the shell to room temperature and blow out or rinse out the shell. It also gave them a chance to patch the vents added to provide airflow. Cooling the shell created another problem, however. Most foundries use a fused silica shell system and burning out the patterns at 1800F or above resulted in a great deal of cristobalite being created in the shell. When the shell was cooled, cracking occurred in the cristobalite, weakening the shell and creating potential shell failures when the shell was reheated and poured.

To avoid that risk, foundries typically lowered the preheat temperature to 1500F or less during burnout to avoid cristobalite conversion.

Now the industry had a process for burning out printed patterns that could reliably provide acceptable castings. This is the process used by most foundries who cast printed patterns. However, this process has several disadvantages:

- It requires additional labor to cast the pattern including adding the vents, opening the vents prior to burnout, rinsing the shell, and patching the vents.
- Cooling down the shell, rinsing out the ash and patching vents adds at least a day and often two to the casting process.
- While the oven temperature is lowered to avoid cristobalite conversion, it cannot be used to pre-heat normal production shells. To avoid delaying production while burning out patterns, the burnout is typically moved to a time when the furnace is not needed for normal production. That may add as much as another day to the casting process.

These disadvantages are significant but are tolerable to make prototype castings. Being able to provide prototype castings without the time and cost of wax pattern tooling makes

the process well worthwhile for prototype and very low volume production castings. For most foundries, prototype castings are a few shells a week and those can be fairly easily walked through the variations in the casting process.

However, the variations required for a clean burnout make it unpractical for any significant production use. It would be extremely difficult to keep track of which shells use the printed pattern process and which use the molded wax pattern process, especially if printed patterns were 20% or more of total production.

If the investment casting industry is going to be competitive in the emerging market for complex geometries (generative design or topology optimized designs which can't be molded), it will be important to be able to use printed patterns for normal production. Normal production will require a much better burnout process.

Proposed Burnout Process

The major disadvantages of the current burnout procedure detailed above are the result of having to cool the shell to room temperature. The shell must be cooled to remove ash and patch the vents. If it were possible to avoid cooling the shell, there would be no change to the furnace temperature, no disruption of production because the furnace temperature was lowered, and it would save at least a day in the casting process.

To avoid having to cool the shell, we need to be sure that:

a. There will be enough oxygen to completely combust the pattern
b. Any ash will be eliminated from the mold in the burnout process
c. There is no need to patch vents before pouring.

With that in mind, we devised a method that might be able to accomplish all the above requirements. The method consisted of two features:

1. **Air injection into pouring cup** – Rather than trying to increase the oxygen content in the furnace atmosphere, air injected directly into the pouring cup will force air with the necessary oxygen directly to the molds where it is needed for

combustion. This forced airflow will hopefully carry out any ash produced during combustion.

2. **Venting Change** - the venting system is changed to one that goes back to the pouring cup as shown in Figure 1. This venting style is commonly used to ensure that no air is trapped in the mold preventing a complete fill. The advantage of this type of venting is that it does not need to be patched prior to pouring.

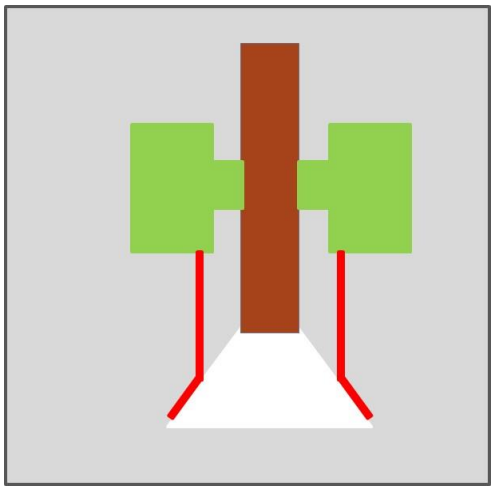

Figure 1, Venting to the underside of the pouring cup.

Testing the Proposed Process

To test our theory, we ran a test of the proposed burnout process in the foundry. Specific tasks included:

1. **Design and build a test fixture** – A test fixture was designed to direct the air stream into the pouring cup. An image of the fixture design is shown in Figure 2. It is designed to allow two shells to be burned out at a time. It was important to introduce some turbulence into the airstream to help flush any ash out of the mold. In addition, we wanted to make sure that any material dropping down from the sprue would not clog the air outlet. Consequently, the air outlet is

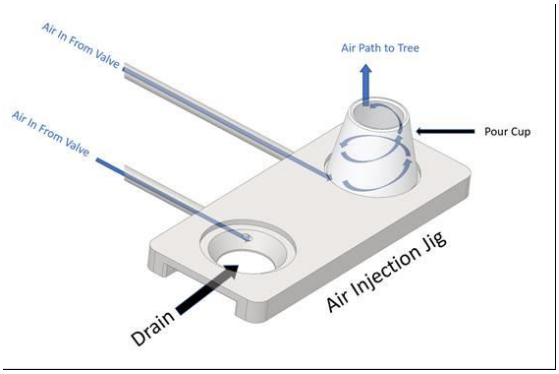

Figure 2, Fixture Design

Figure 3. Completed Fixture

recessed and tangentially to the pouring cup to induce a circular flow. Figure 3 shows the completed fixture. Stainless tubing extended outside the furnace and was connected to air pressure regulators fed with plant compressed air. The fixture was placed in the preheat oven and allowed to come to temperature.

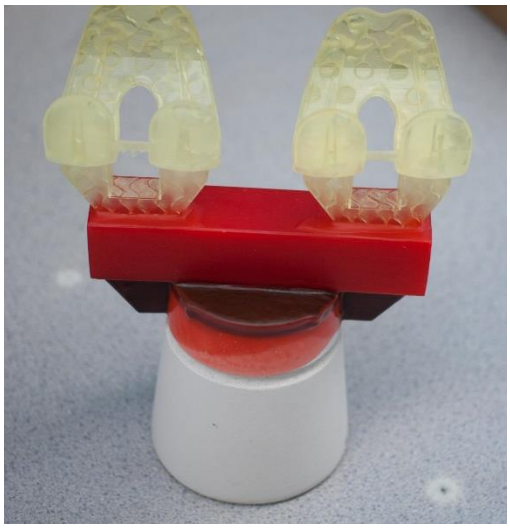

Figure 4. Completed assembly

2. **Select a test pattern** – It was important not to use a test pattern that was too easy nor too difficult to burn out. We also wanted a realistic investment cast component that was not too 2large. We chose an artificial knee geometry. The geometry is relatively complex and has some small columns that will be a challenge to burn out cleanly.

3. **Create Test Shells** – Intrepid Automation created 16 test patterns plus extras for spares. Those were sent to Fenico to assemble and shell. When the shells were complete, the test could begin. A completed assembly is shown in Figure 4. Vents were not added due to a miscommunication, but we went ahead with the test since the shells were all completed.

4. **Burnout Test** – We weren't sure what air flow would be required to both provide enough oxygen for combustion and to carry out any ash created, so we burned out four pairs of shells, each at a different regulator pressure. The pressures used were 0, 5,10 and 20 psi. For each test:
    a. A pair of shells were placed on the fixture in an 1800F oven as shown in Figure 5.
    b. The regulator was adjusted to the desired pressure.
    c. The shells remained in the furnace with airflow for 30 minutes.

d. One shell was removed from the furnace and immediately poured as shown in Figure 6.
e. The remaining shell was removed from the furnace and allowed to cool.

Figure 5. Shells placed on the fixture in the oven.

5. **Identification** – The empty shell was marked with the air pressure used. The poured shell was allowed to cool, the shell was removed and the casting blasted. The casting was marked with the pressure used.

6. **Evaluation of the empty shell** – The shell was cut apart to see if there was any evidence of incomplete combustion. Previous testing had shown a great deal of soot in the shell when there was incomplete combustion. We did not see soot in the Fenico testing.

7. **Evaluation of the casting** – the casting was inspected for surface defects indicating either incomplete combustion or excessive ash.

Figure 6. Pouring the mold.

Results

1. 0 PSI (no airflow)

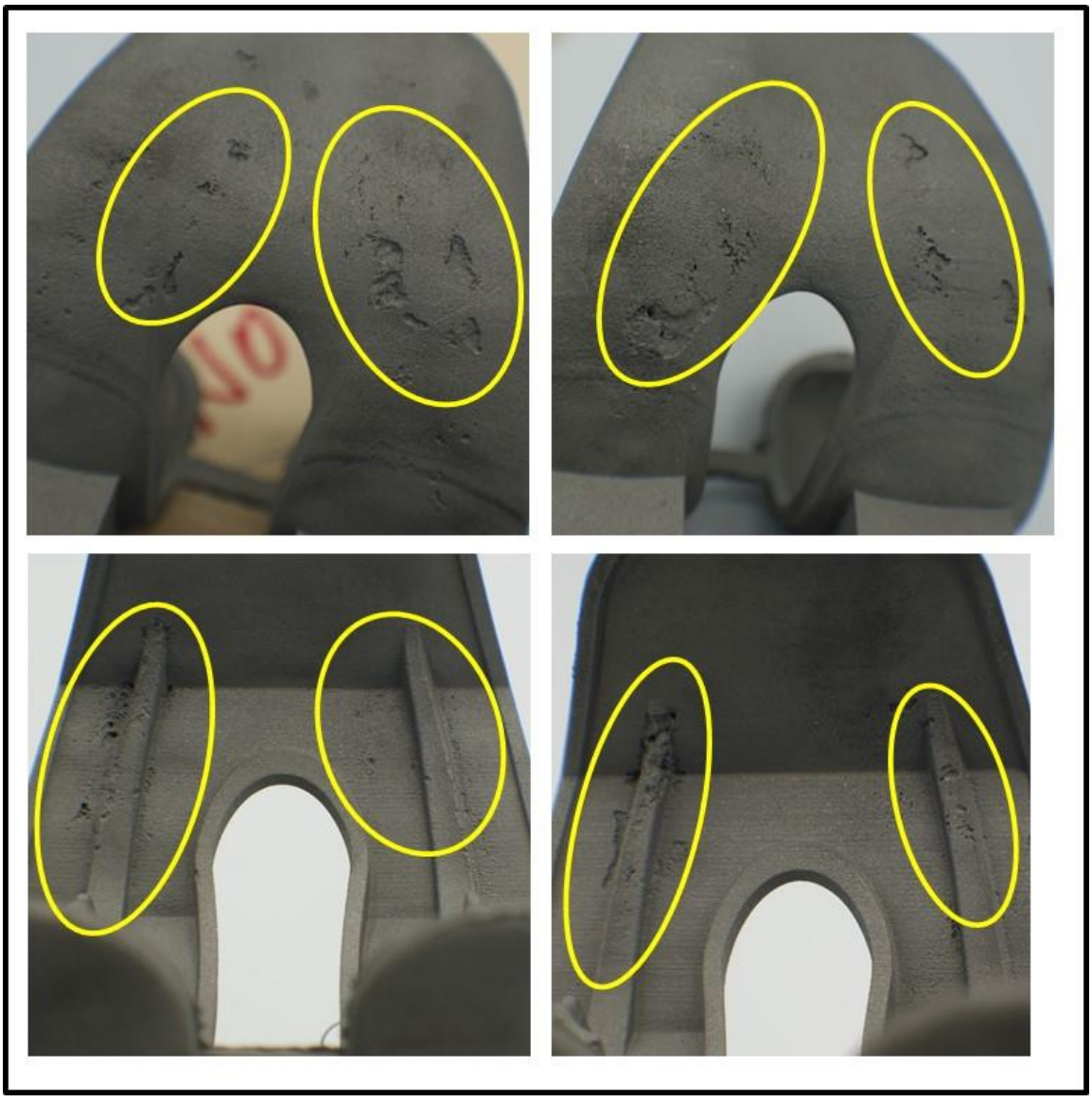

Figure 7. Castings with no airflow.

Clearly there are numerous defects in the castings that would render these unacceptable.

2. 5 PSI

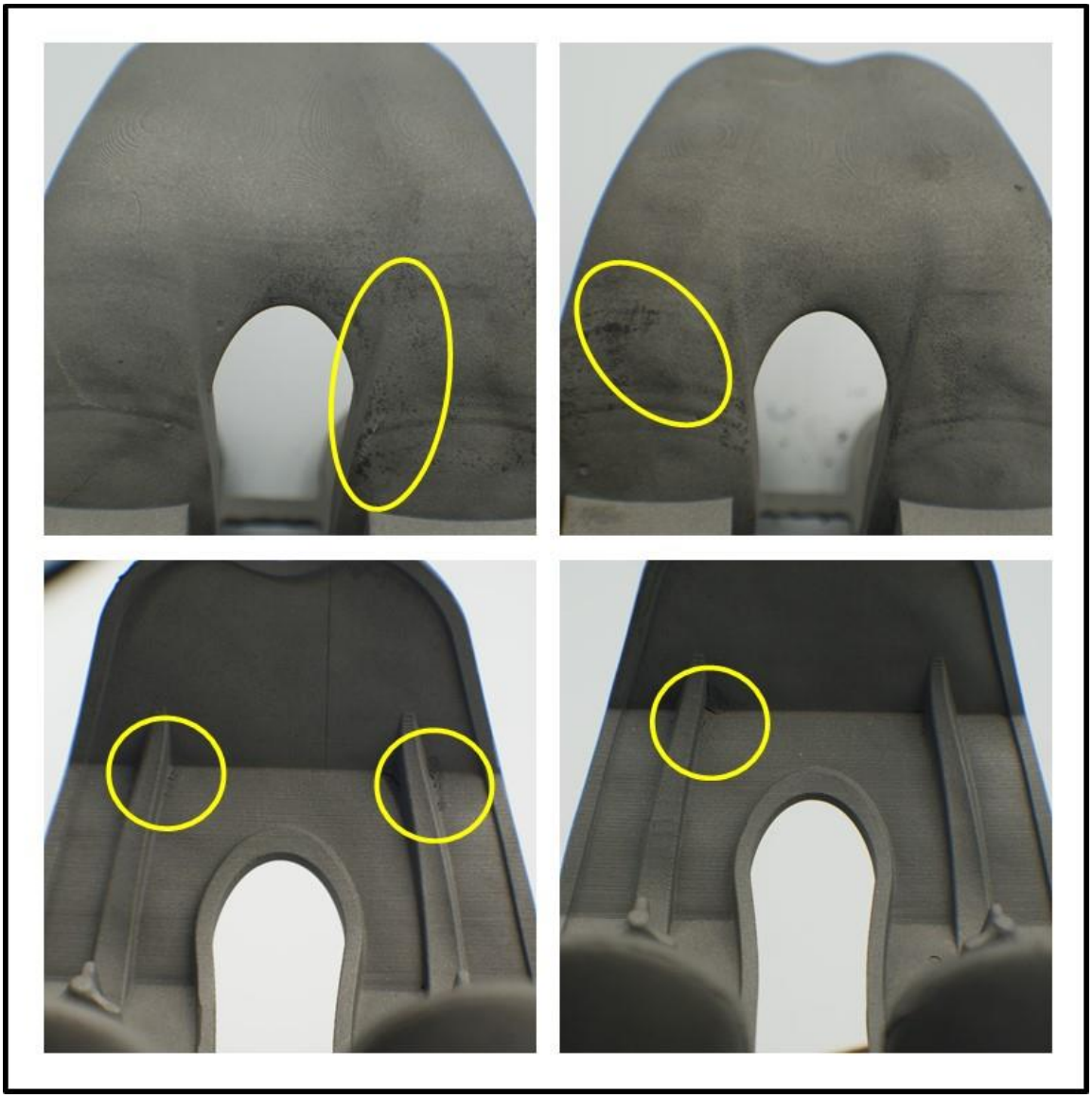

Figure 8, Castings with 5 psi pressure airflow.

Even at this low airflow, there is a significant reduction in the number of defects observed. These castings would require repair and could be marginally acceptable depending on the application.

3. 10 PSI

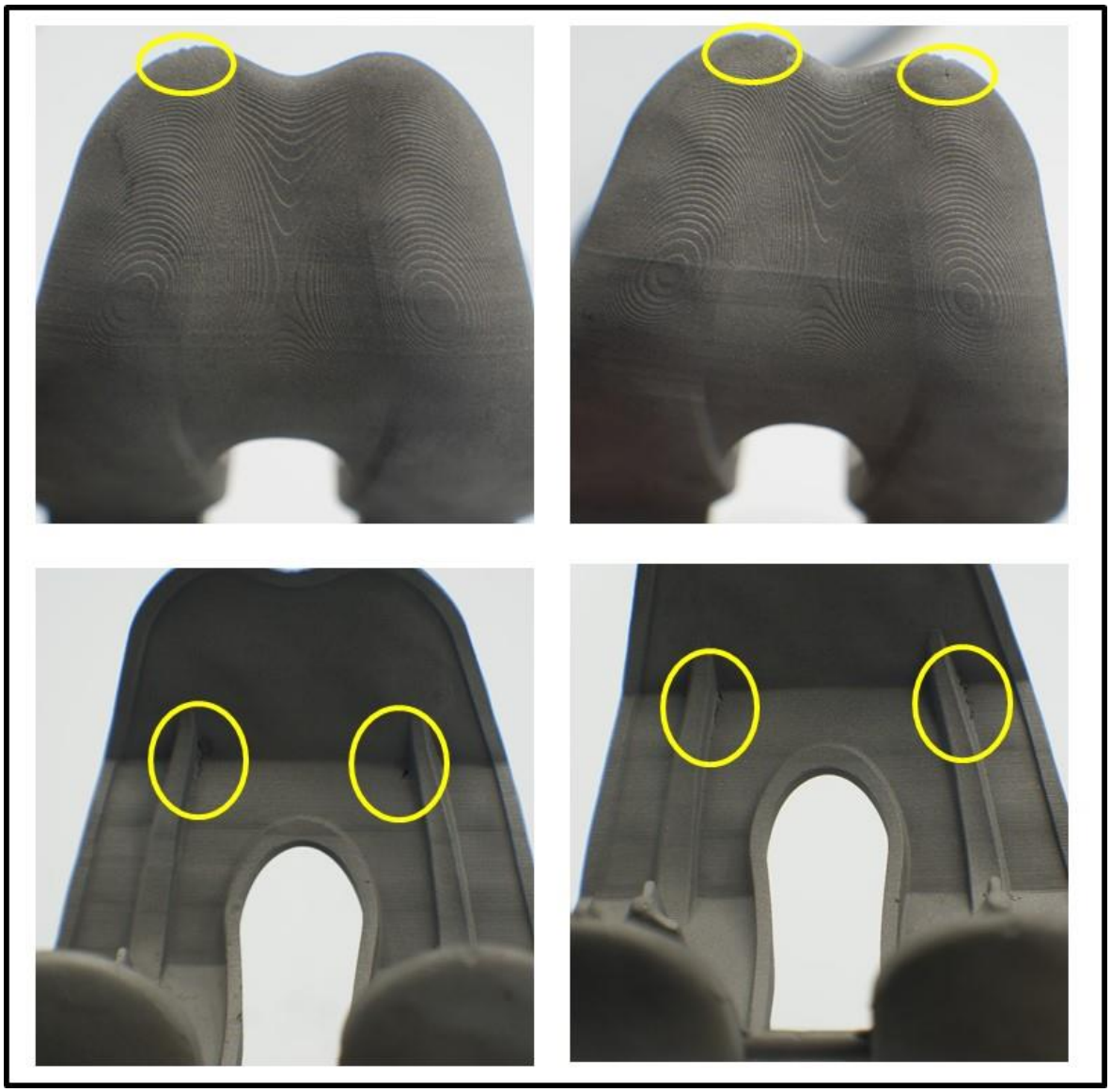

Figure 9. Castings at 10 psi airflow.

There is improvement from the 5 psi. All defects here are relatively minor and depending on the application, might be acceptable.

4. 20 PSI

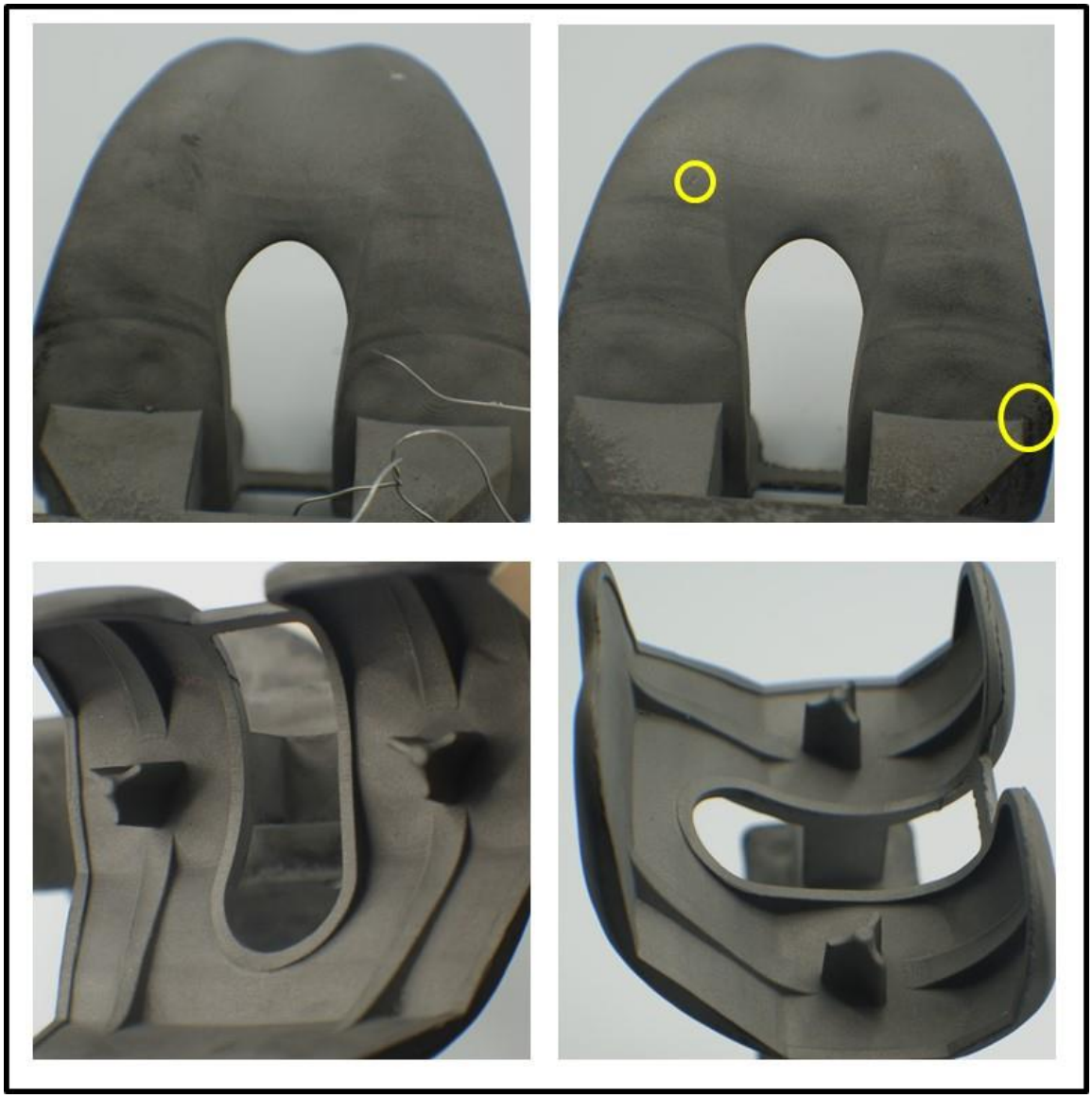

Figure 10. Castings at 20 psi airflow.

It was difficult to find any defects on these castings. They would be acceptable for most applications.

Figure 11 summarizes the results below.

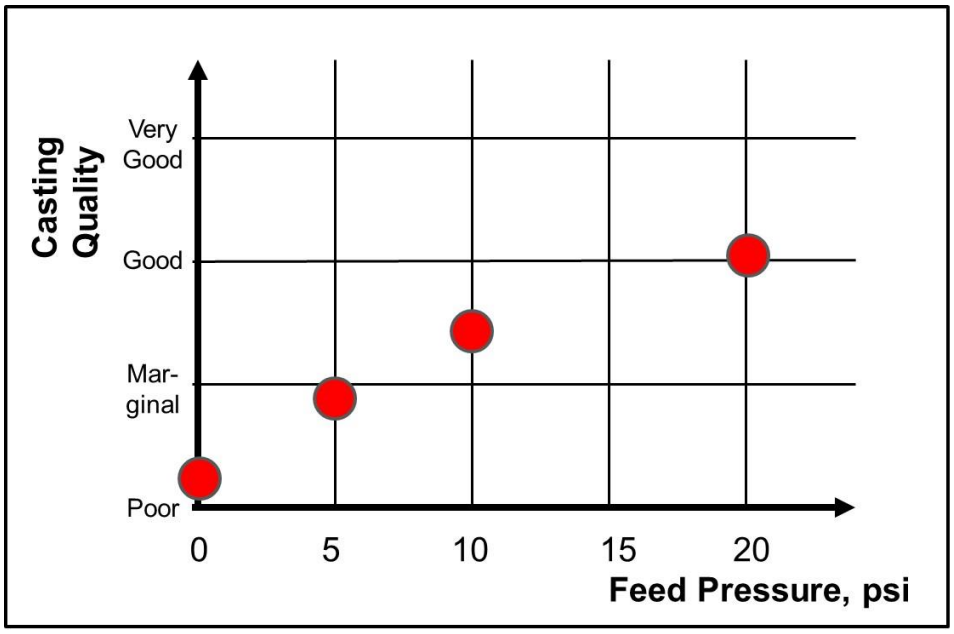

Figure 11, Subjective casting quality vs. feed pressure.

Conclusions

1. At least for this printing process, pattern geometry, resin, and assembly configuration, it is possible to obtain good castings without cooling the shell to remove ash and patch vents.

2. This process saves at least a day in the casting process, avoids production disruptions due to furnace temperature changes and reduces labor required to cast printed patterns.

3. These results show promise for extending the process to other printing processes, pattern materials, and pattern geometries.

4. Except for positioning the shell on the fixture during preheat, the same process can be used to cast these patterns as is used for molded wax patterns, making it much easier to use printed patterns for production runs.

Recommendations

1. Fenico recommended increasing the burnout time to at least 1 hour. That may help to get more complete combustion and reduce ash even more. Since preheat times are generally longer, that will not be an issue in practice.

2. There is some concern that the airflow through the shell is cooling the shell and preventing the shell from reaching the desired preheat temperature. It may be well worthwhile to stop the airflow after a period of time and allowing the shell to come up to furnace temperature. For example, if the normal preheat cycle is two hours, the air could be turned on for the first hour, and then stopped. The remaining hour would bring the shell to desired temperature.

Future Work

While these results are only for this one situation, we believe that we will see similar results for other printing technologies (such as QuickCast, Voxeljet, and a variety of FDM processes), other pattern materials, and a wide range of pattern geometries. However, that is yet to be proven. We will be doing testing to evaluate the process for other situations and will especially be looking at venting configurations, airflow requirements and burnout times.

Based on the results obtained here, we have filed a patent application on the process.